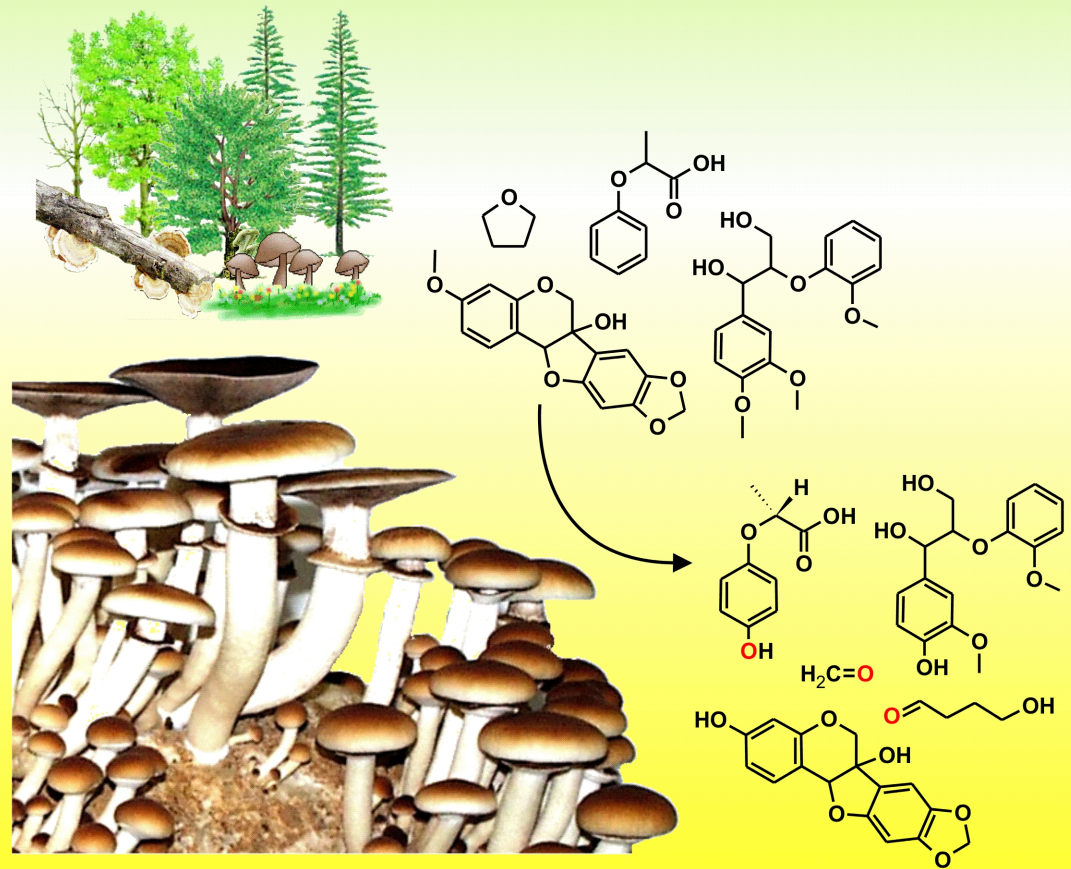


# The extracellular peroxygenase of the agaric fungus *Agrocybe aegerita*: catalytic properties and physiological background with particular emphasis on ether cleavage

The peroxygenase of *Agrocybe aegerita*: catalytic properties and physiological background

Matthias Kinne



**The extracellular peroxygenase of the agaric fungus *Agrocybe aegerita*: catalytic properties and physiological background with particular emphasis on ether cleavage**

**„Die extrazelluläre Peroxygenase des Lammellenpilzes *Agrocybe aegerita*: Katalytische Eigenschaften und physiologischer Hintergrund unter besonderer Berücksichtigung der Etherspaltung“**

Vom Institutsrat des Internationalen Hochschulinstitutes Zittau  
genehmigte

Dissertation

zur Erlangung des akademischen Grades  
doctor rerum naturalium  
(Dr. rer. nat.)

vorgelegt

von Matthias Kinne B.Sc (Biotechnologie), M.Sc (pharmazeutische Analytik)  
geboren am 18. Juni 1980 in Görlitz (Deutschland)

Gutachter: Herr Prof. Dr. Martin Hofrichter (IHI Zittau)  
Herr Prof. Dr. Kenneth Hammel (*University of Madison*, USA)  
Frau Prof. Dr. Katrin Scheibner (Hochschule Lausitz)

Tag der Verteidigung: 22 Oktober 2010



**The extracellular peroxygenase of the agaric fungus *Agrocybe aegerita*: catalytic properties and physiological background with particular emphasis on ether cleavage**

Approved by the Council of International Graduate School of Zittau

**Academic Dissertation**

Doctor rerum naturalium

(Dr. rer. nat.)

by Matthias Kinne, B.Sc. (biotechnology), M.Sc. (pharmaceutical analysis)  
born on June 18, 1980 in Görlitz, Germany

Reviewers:           Herr Prof. Dr. Martin Hofrichter (IHI Zittau)  
                          Herr Prof. Dr. Kenneth Hammel (University of Madison, USA)  
                          Frau Prof. Dr. Katrin Scheibner (Hochschule Lausitz)

Day of defense: October 22, 2010







---

# Contents

<b>Contents</b> .....	<b>I</b>
<b>List of Abbreviations</b> .....	<b>V</b>
<b>Zusammenfassung</b> .....	<b>VI</b>
<b>Thesis summary</b> .....	<b>VII</b>
<b>1. Introduction</b> .....	<b>1</b>
1.1 Heme proteins.....	3
1.1.1 Cytochrome P450 monooxygenases.....	5
1.1.1.1 Cytochrome P450-catalyzed reactions.....	6
1.1.1.2 Reaction mechanism.....	7
1.1.2 Fungal heme peroxidases.....	9
1.1.2.1 Peroxidase-catalyzed reactions.....	11
1.1.2.2 Reaction mechanism.....	13
1.1.2.3 Lignin peroxidases (LiPs).....	14
1.1.2.4 Manganese Peroxidases (MnPs).....	15
1.1.2.5 Versatile Peroxidases (VPs).....	15
1.1.2.6 DyP-type Peroxidases (DyPs).....	16
1.1.2.7 Peroxidase from <i>Coprinopsis cinerea</i> (CiP).....	16
1.1.3 Heme proteins with peroxygenase activity.....	17
1.1.3.1 Plant seed peroxygenases.....	17
1.1.3.2 Peroxide “shunt” of P450s.....	18
1.1.3.3 Peroxygenase activity of Chloroperoxidase ( <i>CfuCPO</i> ).....	18
1.1.3.4 Engineered peroxygenases.....	19
1.1.3.5 Extracellular fungal aromatic peroxygenases (APOs).....	19
1.2 Aims and objectives.....	21
<b>2. Materials and Methods</b> .....	<b>23</b>
2.1 Reactants.....	23
2.1.1 Methyl 3,4-dimethoxybenzyl ether.....	23
2.1.2 Methyl 4-nitrobenzyl ether.....	24
2.1.3 1-Methoxy-4-trideuteromethoxybenzene.....	24
2.1.4 PEG terminated 4-nitrophenyl ether.....	24
2.1.5 4-Hydroxybutanal 2,4-dinitrophenylhydrazone.....	24
2.1.6 Arylglycerol <i>beta</i> -aryl ethers.....	25

## CONTENTS

---

2.1.7 Milled pine and poplar wood .....	25
2.2 Enzyme preparations .....	25
2.3 UV-Vis Spectroscopy .....	27
2.4 Standard reaction conditions .....	28
2.5 Product identification .....	28
2.5.1 HPLC-Method .....	28
2.5.2 HPLC-MS Method I .....	28
2.5.3 HPLC-MS Method II .....	29
2.5.4 Aliphatic aldehydes or ketones .....	29
2.5.5 4-Nitrobenzaldehyde .....	29
2.5.6 Ethanol, 2-propanol and <i>tert</i> -butanol .....	30
2.5.7 Methanol.....	30
2.5.8 4-nitrophenyl-terminated PEG .....	30
2.5.9 ( <i>R</i> ) and ( <i>S</i> )-2-(4-hydroxyphenoxy)propionic acid.....	30
2.5.10 Milled wood and DHP.....	31
2.5.11 Amines .....	31
2.6 Stoichiometrical analyses .....	31
2.7 Enzyme kinetics.....	31
2.7.1 1,4-dimethoxybenzene .....	31
2.7.2 Tetrahydrofuran.....	32
2.7.3 Methyl 3,4-dimethoxybenzyl ether .....	32
2.8 Experiments with <sup>18</sup> O-isotopes .....	32
2.8.1 Methyl 4-nitrobenzyl ether.....	32
2.8.2 Aromatic substrates .....	33
2.8.3 Arylglycerol <i>beta</i> -aryl ethers .....	33
2.8.4 2-Phenoxypropionic acid.....	33
2.9 Deuterium isotope effect experiment .....	33
2.10 Experiments with <sup>14</sup> C-labeled compounds .....	34
2.11 Experiments with milled wood.....	34
2.12 <i>In vivo</i> -incubation experiments .....	34
<b>3. Results .....</b>	<b>35</b>
3.1 UV-Vis spectrophotometric features of <i>Aae</i> APO .....	35
3.1.1 Ligands of <i>Aae</i> APO .....	35
3.1.2 Difference spectrophotometry.....	36

---

3.2 Oxidation of ethers .....	38
3.2.1 Aromatic ethers .....	38
3.2.2 Aliphatic ethers .....	42
3.2.3 Stoichiometry of ether cleavage .....	44
3.2.4 pH-Optimum of ether cleavage.....	46
3.2.5 Bisubstrate kinetics .....	46
3.2.6 Source of the oxygen introduced during ether cleavage.....	47
3.2.7 Deuterium isotope effect experiments .....	48
3.2.8 Arylglycerol <i>beta</i> -aryl ether.....	49
3.2.9 Scope of ether cleavage .....	53
3.3 Ring hydroxylation of aromatic compounds.....	54
3.3.1 Nitroaromatics .....	55
3.3.2 Regio-and stereoselective hydroxylations .....	57
3.3.2.1 2-Phenoxypropionic acid.....	57
3.3.2.2 Propranolol .....	59
3.3.2.3 Diclofenac.....	61
3.3.2.3 Acetanilide.....	62
3.4 Benzylic oxygenation.....	63
3.5 Further oxidation reactions .....	66
3.5.1 Phenol oxidation .....	66
3.5.2 Dehalogenation .....	67
3.5.3 <i>N</i> -dealkylation.....	69
3.5.4 Halogenation.....	69
<b>4. Discussion .....</b>	<b>71</b>
4.1 Reaction mechanisms of <i>Aae</i> APO-catalyzed reactions .....	71
4.1.1 General mechanistic aspects .....	71
4.1.1.1 <i>Aae</i> APO shares spectrophotometric features with heme-thiolate proteins ..	71
4.1.1.2 The substrate range of <i>Aae</i> APO resembles that of heme-thiolate proteins ..	72
4.1.1.3 Reactions exhibit an equimolar stoichiometry .....	73
4.1.1.4 Bisubstrate kinetics suggest a ping-pong mechanism .....	73
4.1.1.5 Oxygen introduced into reaction product derives from the peroxide.....	74
4.1.1.6 High deuterium isotope effect points to a hydrogen abstraction.....	75
4.1.1.7 <i>Aae</i> APO active site fails to accommodate polymers.....	76
4.1.2 The hypothetical reaction cycle .....	77



## CONTENTS

---

4.1.3 <i>Aae</i> APO an enzyme of a new sub-sub class?.....	81
4.1.4 Ether cleavage .....	81
4.1.4.1 Cleavage of arylglycerol <i>beta</i> -aryl ethers .....	84
4.1.5 Aromatic hydroxylation .....	86
4.1.6 Benzylic oxygenation.....	87
4.1.7 Further oxidation reaction catalyzed by <i>Aae</i> APO.....	89
4.1.7.1 Oxidation of the phenolic moiety .....	89
4.1.7.2 Dehalogenation .....	91
4.1.7.3 <i>N</i> -Dealkylation.....	91
4.1.7.4 Halogenation.....	92
4.2 Physiological role of <i>Aae</i> APO.....	92
4.3 Potential applications of <i>Aae</i> APO-catalyzed reactions .....	97
4.4 Key findings .....	99
4.5 Outlook .....	101
<b>5 References.....</b>	<b>102</b>
<b>6 Appendix.....</b>	<b>116</b>

## List of Abbreviations

ABTS	2,2'-azino-bis(3-ethylbenzthiazoline-6-sulphonic acid)
<i>Aae</i>	<i>Agrocybe aegerita</i>
APO	Aromatic Peroxygenase
APx-CcP	Hybrid Ascorbate-Cytochrome c Peroxidase
Apx	Ascorbate Peroxidases
Cam	Camphor
CcP	Cytochrome c Peroxidases
<i>Cfu</i>	<i>Caldariomyces fumago</i>
Ci	Curie
CiP	<i>Coprinus cinereus</i> Peroxidase
CPO	Chloroperoxidase
<i>Cra</i>	<i>Coprinellus radians</i> ,
<i>Cve</i>	<i>Coprinopsis verticillata</i>
CYP	Cytochrome P450
DHP	Dehydrogenase Polymer
DNPH	2,4-Dinitrophenylhydrazine (Brady's reagent)
dpm	disintegrations per minute
DyP	Dye-decolorizing Peroxidases
E	Enzyme
EC	Enzyme Commission
ESI	Electrospray Ionization
GC	Gas Chromatography
<i>gem</i>	<i>geminal</i>
IEF	Isoelectric Focussing
HPLC	High Performance Liquid Chromatography
HPOPA	2-(4-Hydroxyphenoxy)propionic acid
HrP	Horseradish Peroxidase
$k_{cat}$	turnover number
$k_{cat}/K_m$	catalytic efficiency
$(k_H/k_D)$	intrinsic deuterium isotope effect
$[(k_H/k_D)_{obs}]$	observed deuterium isotope effect
kDA	kilo Dalton
$K_m$	Michaelis-Menten-(Henri) constant
LiP	Lignin Peroxidase
LRET	Long-Range Electron Transfer
Mb	Myoglobin
MnP	Manganese Peroxidase
MP	Microperoxidase
MS	Mass Spectrometry
MTBE	Methyl Tertiary Butyl Ether
NIH	National Institutes of Health
NADH	Nicotinamide Adenine Dinucleotide
NADPH	Nicotinamide Adenine Dinucleotide Phosphate
P	Product
P450	Cytochrome P450 Monooxygenase
P450cam	Camphor 5-Monooxygenase
PAHS	Polyaromatic Hydrocarbons
PEG	Poly Ethylene Glycol
POPA	2-Phenoxypropionic acid
<i>Pch</i>	<i>Phanerochaete chrysosporium</i>
SEC	Size Exclusion Chromatography
SbP	Soybean Peroxidase
UV	Ultraviolet
Vis	Visible
VP	Versatile Peroxidase

## Zusammenfassung

Die Peroxygenase des Südlichen Ackerling (*Agrocybe aegerita*, *AaeAPO*) wurde gereinigt, ihr Katalysepotential ermittelt und ein allgemeiner Reaktionsmechanismus postuliert. Die *AaeAPO* katalysiert sowohl  $\text{H}_2\text{O}_2$ -abhängige Monooxygenierungen (Zwei-Elektron-Oxidationen) wie (a) die Spaltung aliphatischer und aromatischer Ether, (b) die regio- und enantioselektive Hydroxylierung von Aromaten, (c) die schrittweise Monooxygenierung von Toluolderivaten, (d) die *N*-Dealkylierung sekundärer Amine und (e) die Dehalogenierung chlorierter Aliphaten als auch typische Reaktionen bekannter Peroxidasen (vermutlich Ein-Elektron-Oxidation) unter anderem (f) die Oxidation/ Polymerisierung von Phenolen und (g) die Halogenierung von Aromaten. Polymere Verbindungen wie Polyethylenglycol (PEG) werden nicht oxidiert.

Mechanistische Untersuchungen zur Etherspaltung am Beispiel der *AaeAPO* haben Einblick in den generellen Reaktionsmechanismus dieses neuen Enzymtyps ermöglicht: (1) die Stöchiometrie der Spaltung von Tetrahydrofuran entspricht der einer zwei-Elektron-Oxidation, (2) die Spaltung von Methyl-3,4-Dimethoxybenzylether zu 4-Dimethoxybenzaldehyd und Methanol ergaben parallele Verläufe für die ermittelten Ausgleichsgeraden in der doppelt reziproken Darstellung, was einem „Ping-Pong“-Reaktionsmechanismus entspricht (3) die Monooxygenierungen haben stets den Einbau eines aus dem Peroxid ( $\text{H}_2\text{O}_2$ ) stammenden Sauerstoffatoms in das Produkt zur Folge, (4) die *O*-Dealkylierung von 1-Methoxy-4-Trideuteriummethoxybenzol zeigt einen ausgeprägten Deuterium Isotopen Effekt, was auf die primäre Abspaltung eines Wasserstoffatoms vom Substratmolekül hindeutet. Demnach verläuft die Peroxygenase-katalysierte Monooxygenierung über Wasserstoffabstraktion und eine unmittelbar anschließende Sauerstoffrückbindung (*hydrogen abstraction - oxygen rebound mechanism*). Diese Reaktionsabfolge ähnelt dem sogenannten *peroxide "shunt" pathway*, der von einer Reihe Cytochrom-P450-abhängiger Monooxygenasen her bekannt ist.

Die physiologische Funktion der *AaeAPO* besteht möglicherweise in der extrazellulären Transformation und Detoxifikation niedermolekularer Pflanzeninhaltsstoffe, mikrobieller Metabolite und anthropogener Xenobiotika. Aufgrund der Stabilität und Unabhängigkeit der *AaeAPO* von teuren Kofaktoren ergeben sich vielversprechende biotechnologische Möglichkeiten zum Einsatz isolierter Biokatalysatoren in selektiven (bio)chemischen Synthesen monooxygener Metabolite.

## Thesis summary

Litter-decay fungi have recently been shown to secrete heme-thiolate peroxygenases that oxidize various organic chemicals, but little is known about the physiological role or the mechanism of these enzymes. The aromatic peroxygenase of *Agrocybe aegerita* (*Aae*APO) was purified and catalytically characterized. An overall reaction mechanism was proposed. The results show that *Aae*APO catalyzed diverse H<sub>2</sub>O<sub>2</sub>-dependent monooxygenations (two-electron oxidations) including (a) the cleavage of aliphatic and aromatic ethers, (b) the regio- and enantioselective hydroxylation of aromatic compounds, (c) the stepwise oxygenation of benzylic compounds, (d) the *N*-dealkylation of secondary amines and (e) the dehalogenation of halogenated aliphatic compounds as well as typical peroxidase reactions (suggested to involve one-electron oxidation) such as (f) oxidation and polymerization of phenols and (g) halogenations. The enzyme failed to oxidize polymers such as polyethylene glycol (PEG). Mechanistic studies with several model substrates provided information about the reaction cycle of *Aae*APO: (1) stoichiometry of tetrahydrofuran cleavage showed that the reaction was a two-electron oxidation that generated one aldehyde group and one alcohol group, yielding the ring-opened product 4-hydroxybutanal, (2) steady-state kinetics results with methyl 3,4-dimethoxybenzyl ether, which was oxidized to 3,4-dimethoxybenzaldehyde, gave parallel double reciprocal plots suggestive of a ping-pong mechanism, (3) the cleavage of methyl 4-nitrobenzyl ether, the hydroxylation of aromatics such as diclofenac and nitrophenol and the oxygenation of benzylic compounds, resulted in incorporation of <sup>18</sup>O into the reaction product in the presence of H<sub>2</sub><sup>18</sup>O<sub>2</sub>, and (4) the demethylation of 1-methoxy-4-trideuteromethoxybenzene showed a distinct observed intramolecular deuterium isotope effect. These results support a mechanism similar to that envisaged for the peroxygenase activity of P450s in which the enzyme heme is oxidized by H<sub>2</sub>O<sub>2</sub> to give an iron species that carries one of the peroxide oxygen. This intermediate then abstracts a hydrogen from the substrate, which is followed by rebound of an •OH equivalent to produce the monooxygenated reaction product (hydrogen abstraction and oxygen rebound mechanism). *Aae*APO may accordingly have a role in the biodegradation of natural and anthropogenic low molecular weight compounds in soils and plant litter. Moreover, the results raise the possibility that fungal peroxygenases may be useful for versatile, cost-effective, and scalable syntheses of drug metabolites and herbicide precursors.



# 1. Introduction

The biomass on earth is the biochemical synthesized matter that consists of living organisms and the biological material derived from it with a photoautotrophic primary production of about 105 billion tonnes of carbon per year (Field et al. 1998). Lignocellulose is the major component of polymeric biomass, comprising around half of the photo mass and the majority of ether structures in the biosphere (Sanchez 2009). Almost all terrestrial fixed carbon consists of lignocellulose, the principal structural component of vascular plants (Hammel and Cullen 2008).

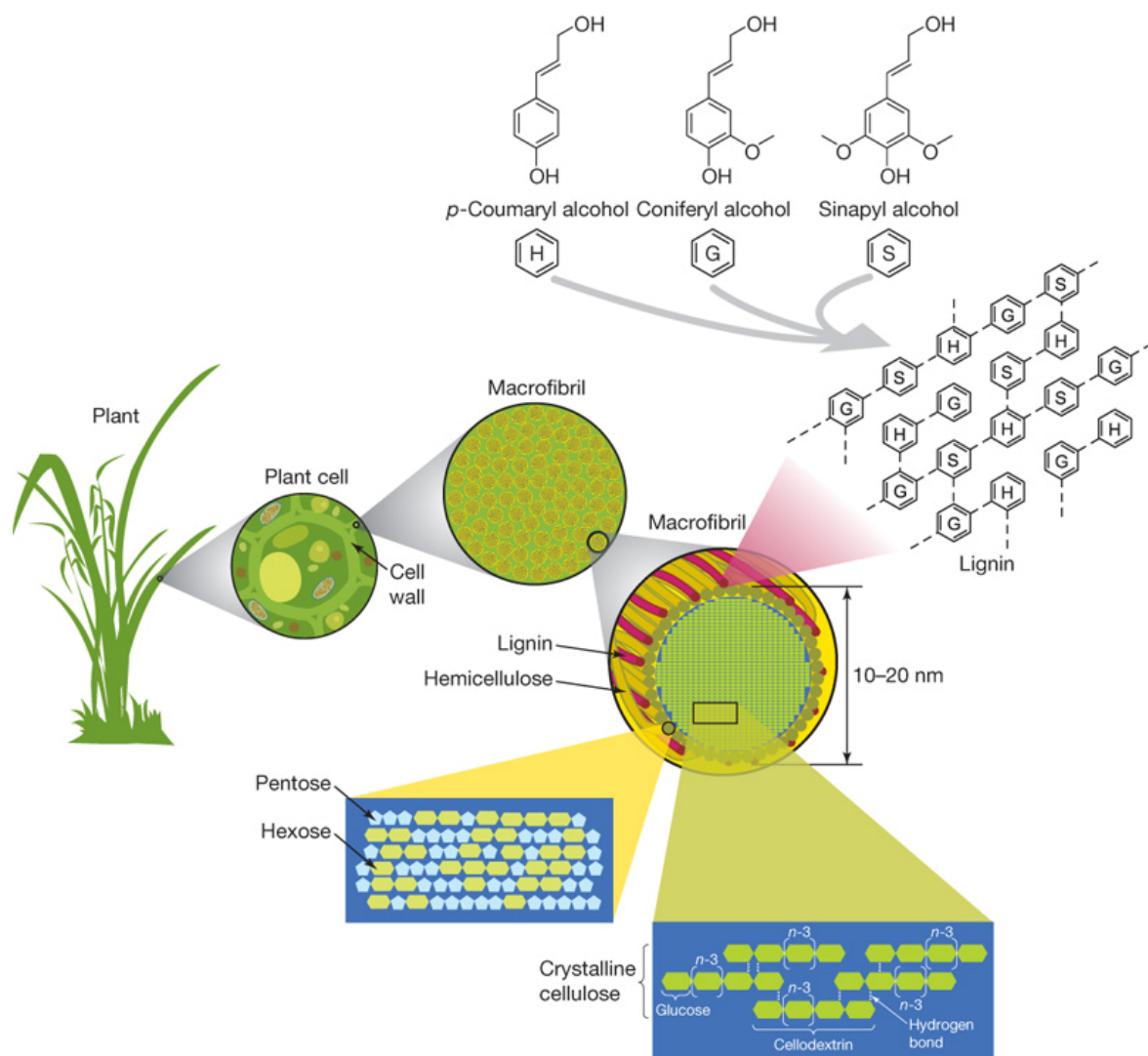


Figure 1 The lignocellulose complex (Rubin 2008).

It is composed of three biopolymers: cellulose, hemicellulose and lignin (Latin *lignum*, wood), forming structures named microfibrils, which are organized into macrofibrils that mediate structural stability in plant cell walls (Sarkar et al. 2009). The cellulose is a *beta*-(1-

4) linked chain of glucose molecules embedded and protected within a heteropolymeric three-dimensional lignin-hemicellulose matrix (Jürgen et al. 2008). Hemicellulose is composed of different 5- and 6-carbon sugars such as galactose, arabinose, mannose, glucose and xylose (Liu et al. 2006, Kumar et al. 2009). The microfibrils are cross-linked together by homopolymers of hemicellulose. The complex lignin polymer consists of three major phenolic components, *para*-coumaryl alcohol (H), coniferyl alcohol (G) and sinapyl alcohol (S) (Rubin 2008). These phenols are bonded via inter-monomer ether bridges that contribute to the recalcitrance of this polymer, increasing stability and protecting the plant against biochemical degradation (Kirk and Farrell 1987). The lignin is tightly linked to the hemicellulose via ether bonds between the *alpha*-positions of the lignin side chains and the carbons of sugar residues (Sun and Sun 2002).

The ecological balance is a result of equal formation and degradation of biomass. Microorganisms, predominantly filamentous fungi for the initial lignocellulose degradation, play an essential role in biomass recycling because: (a) their high genetic diversity and mutability enable them to occupy nearly all ecological niches, (b) they carry a high enzymatic diversity that can be rapidly induced, (c) they have a high active cell surface/ cell volume ratio and (d) they exhibit high rates of cell division. Without these (primary) decomposers, carbon and nutrients would be locked in organic molecules that cannot be metabolized by plants or animals.

Like all organisms, these microorganisms have to perform biochemical reactions within the homeostatic constraints of a living system. Enzymes enable organisms to operate within these parameters by lowering the activation energy and increasing the selectivity of chemical reactions. For instance, the spontaneous hydrolysis of phosphate monoesters would take one trillion years, which is 21 orders of magnitude slower than the phosphatase catalyzed reaction (Lad et al. 2003). Thus, enzymes serve a wide variety of metabolic and digestive functions for living organisms. As such, the biological system of an organism could be described as the sum of the total number of enzymatic reactions taking place per unit of time. Enzymes are classified based on the overall reaction that they catalyze by the Enzyme Commission (EC) number system. The top-level classification is:

- EC 1 Oxidoreductases: catalyze oxidation/reduction reactions.
- EC 2 Transferases: transfer a functional group.
- EC 3 Hydrolases: catalyze the hydrolysis of various bonds.
- EC 4 Lyases: cleave various bonds by means other than hydrolysis and oxidation.

- EC 5 Isomerases: catalyze isomerization changes within a single molecule.
- EC 6 Ligases: join two molecules with covalent bonds.

Besides their significant physiological roles, enzymes have already proven useful in numerous synthetic applications, particularly the preparation of high valuable and often chiral compounds demanded by the pharmaceutical, agricultural, and food industries (Hult and Berglund 2007). Oxidoreductases such as peroxidases and oxygenases comprise a large class of enzymes that catalyze biological oxidation-reduction reactions. Many of them are heme-containing proteins and are found with abundances of 2% - 4% in most proteomes (Sem et al. 2004).

## 1.1 Heme proteins

Heme proteins are metalloproteins containing a heme prosthetic group that is covalently or non-covalently bound to the protein. The heme moiety consists of an iron center and a substituted porphyrin (Greek, *πορφύρα*, porphyra, tyrian purple) ligand. Four pyrrole rings are bonded by methene bridges, giving a planar and highly conjugated porphyrin (Nagababu and

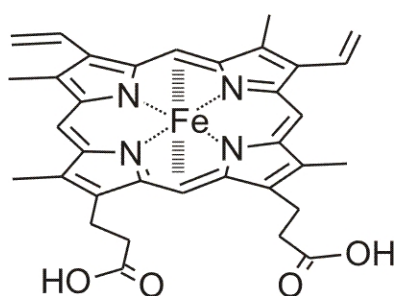


Figure 2 Iron-Protoporphyrin IX.

Rifkind 2004). Six heteroatoms coordinate the heme iron octahedrally. The four porphyrin nitrogens are the equatorial ligands (coordination sites 1-4); the remaining two axial ligands are located below (fifth coordination site, proximal) and above (sixth coordination site, distal) the plane of the heme. The most widespread heme prosthetic group is the iron protoporphyrin IX (or heme type b, Figure 2) (Cirino and Arnold 2003b).

Regarding the original evolutionary function of heme proteins it is suggested that they were involved in electron transfers in primitive sulfur-based photosynthesis pathways in ancestral cyanobacteria before the appearance of molecular oxygen (Hardison 1999). The formation of free O<sub>2</sub> around 2.5 billion years ago as a toxic waste product of photosynthesis was an “ecological disaster”. Organisms developed strategies for the successful degradation of oxygen and its toxic intermediates, such as hydrogen peroxide (H<sub>2</sub>O<sub>2</sub>), the superoxide anion (O<sub>2</sub><sup>•-</sup>) and the free hydroxyl radical (•OH). Moreover organisms integrated oxygen into the process of cellular respiration (Bernroitner et al. 2009). As a consequence of this evolutionary process, heme proteins are widespread from *Archaea* to higher organisms and carry out diverse biological functions, including the



transportation/storage of diatomic gases and their detection, catalysis of redox reactions and electron transfer (Kaim 2005). A few heme proteins are involved in the catalysis of partly reduced nitric- and sulfur oxides and in the generation of reactive nitrogen species (Monzani et al. 2008, Roncone et al. 2006). As such, heme proteins are important in numerous vital biological processes such as steroid biosynthesis and aerobic respiration. Figure 3 shows the diverse catalytic activities observed in heme proteins. The protein that surrounds the heme prosthetic group plays an essential role in defining the specificity of different reactions catalyzed.

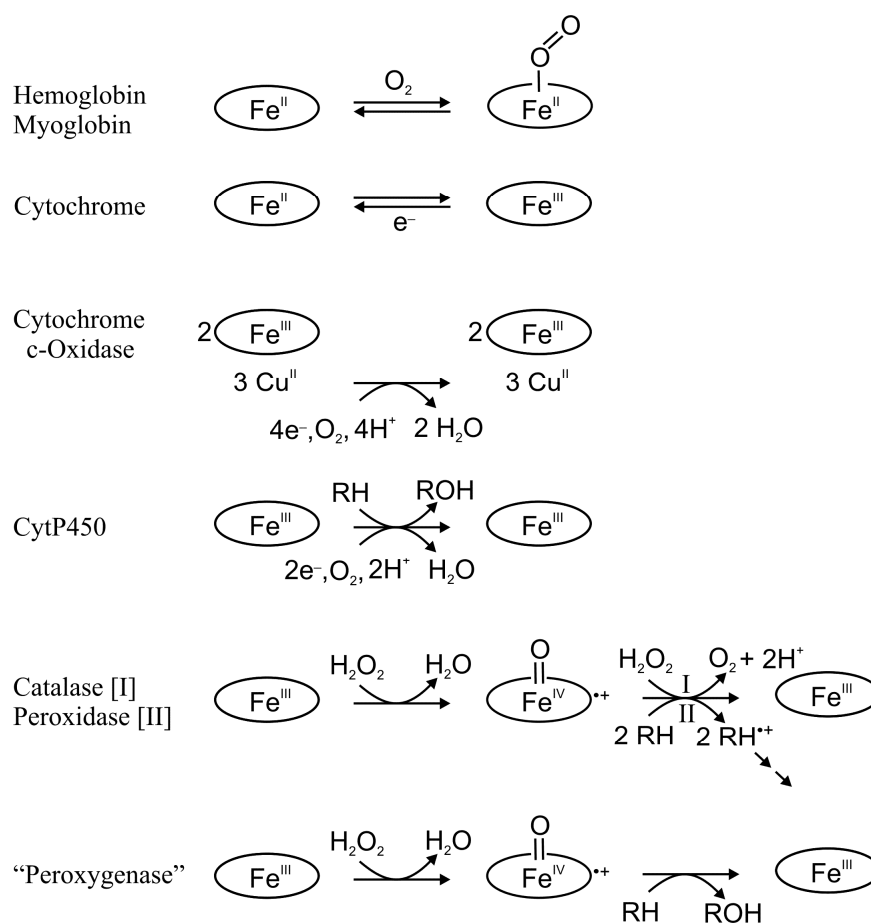


Figure 3 Catalytic activities found in heme proteins modified according to (Kaim 2005).

For example, in heme enzymes whose iron does not directly bind oxygen or peroxides, the proximal and distal coordination sites are occupied by heteroatoms from nucleophilic amino acid residues. These atoms are an imidazole nitrogen from histidine and a methionine sulfur in the case of cytochrome c. Heme enzymes that bind oxygen from either O<sub>2</sub>, H<sub>2</sub>O or H<sub>2</sub>O<sub>2</sub> at the distal coordination site have a basic amino acid heteroatom as the proximal ligand, which is highly conserved throughout each enzyme family. For instance, all heme peroxidases, except

for the chloroperoxidase from *Caldariomyces fumago* (*CfuCPO*), carry nitrogen from histidine as the proximal ligand. Sulfur from cysteinate is the proximal ligand in *CfuCPO* and in all P450s whereas it is oxygen from tyrosine in catalase. This distal side of the heme serves as the catalytic center, and its coordination varies during the catalytic cycle (Cirino and Arnold 2003b).

Most of the heme proteins of one family also exhibit catalytic behavior characteristic of a different family (Cirino and Arnold 2003b). It was demonstrated that peroxidases show activities typically associated with that of P450s, and vice versa (Rabe et al. 2008, Guengerich 2001). Enzymes from both families show catalase activity, and catalase has slight peroxidase activity (Zamocky et al. 2008, Bernroither et al. 2009). Moreover, myoglobin (Mb), whose physiological function is the transport of oxygen, can also oxidize diverse substrates (Hayashi et al. 2006). In addition to these cross reactivities of heme proteins, there is an enormous catalytic variety within one protein family with regard to the primary reaction catalyzed, substrate specificity, and catalytic rate. This variation is affected by the construction of the protein itself, which determines parameters such as the redox potential and stability of the oxidative iron species, the accessibility of substrates to the active site, and overall enzyme stability (Cirino and Arnold 2003b).

### 1.1.1 Cytochrome P450 monooxygenases

Cytochromes P450s belong to a large superfamily of monooxygenases that are of central physiological importance in the detoxification or activation of a tremendous number of foreign hydrophobic compounds, including various therapeutic drugs, chemical carcinogens, and environmental pollutants (Phillips 2006). These monooxygenases, with an average molecular mass of 50 kDa, were named “P450s” because they exhibit a characteristic UV-absorption maximum at 450 nm upon binding of carbon monoxide by the reduced protein. P450s are ubiquitous enzymes found in all five biological kingdoms (Nebert et al. 1989), although it is known that certain primitive species of bacteria do not contain any forms of the enzyme, possibly indicating that the ancestral P450 gene developed around 3.5 billion years ago (Nelson et al. 1996, Nelson et al. 1993). More than 6300 protein sequences and 31 X-ray structures of different P450s have been determined so far (Fischer et al. 2007). While their sequence identities are quite low (typically 20% on the amino acid level), the overall P450 fold is quite conserved (Figure 4). At the sequence level, there are only a few conserved residues: the heme-coordinating cysteine that is essential for the function of P450s, a phenylalanine located seven amino acids *N*-terminal to the conserved cysteine, a threonine in

the I-helix, which is involved in proton transfer to the heme center (Vidakovic et al. 1998), and a glutamic acid/arginine pair of the ExxR motif located in the K-helix (Ravichandran et al. 1993).

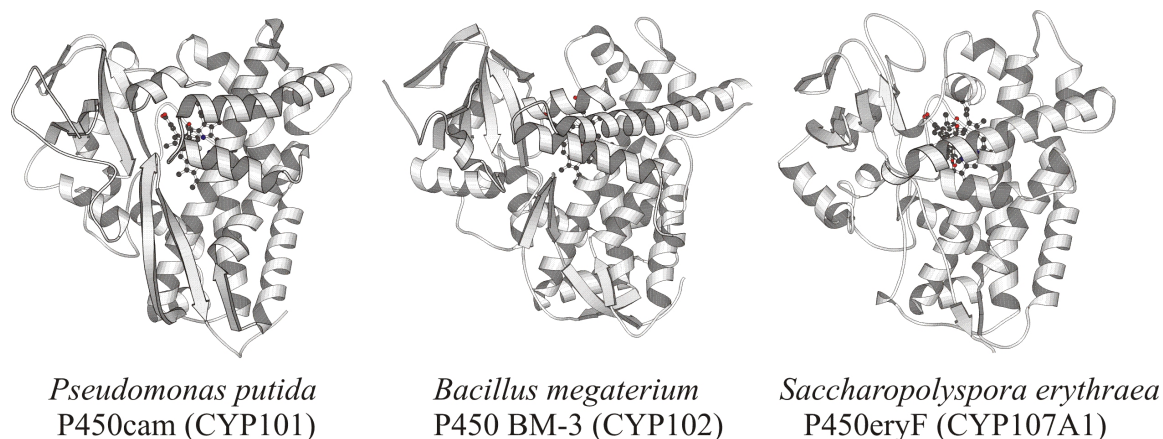
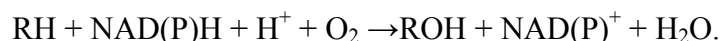


Figure 4 An example of some P450s structures from different organisms illustrating the common three-dimensional fold. (CYP101) complex with camphor (Poulos et al. 1987); (CYP102), heme domain (Ravichandran et al. 1993); (CYP107A1) complex with 6-deoxyerythronolide B, (Cupp-Vickery and Poulos 1995). Structures adapted from Kirill ([http://www.icgeb.org/~p450srv/P450\\_MOLSCRIPT.html](http://www.icgeb.org/~p450srv/P450_MOLSCRIPT.html), 2009).

Thus, the P450 fold appears to be uniquely adapted for the heme-thiolate chemistry required for oxygen activation, the binding of redox partners and the stereochemical requirements of substrate recognition (Poulos and Johnson 2005, Poulos 2005).

#### 1.1.1.1 Cytochrome P450-catalyzed reactions

P450s predominantly catalyze the incorporation of an O<sub>2</sub>-derived oxygen atom into a carbon-hydrogen (C-H) bond. NADH or NADPH serves as a reductant for the oxygen, and transfers its reducing equivalents by way of a protein electron transport system. Depending on the P450, this system consists of either two proteins (reductase and ferredoxin protein) or a P450 reductase flavoprotein (Phillips 2006). The P450 reaction mechanism can be formally described as:



As a result of substrate activation via oxygen incorporation, P450s are some of the most versatile redox proteins, catalyzing diverse reactions such as hydrocarbon hydroxylations, heteroatom releases, heteroatom oxygenations, dealkylations (ethers, thioethers and substituted amines) as well as epoxidations and group migrations (Isin and Guengerich 2007). Some unusual P450-dependent reactions are oxidations involving C-C and C=N bond

cleavage, or reductions such as dehydrase, reductase and isomerase reactions (Mansuy 1998).

Figure 5 illustrates several reactions catalyzed by P450s.

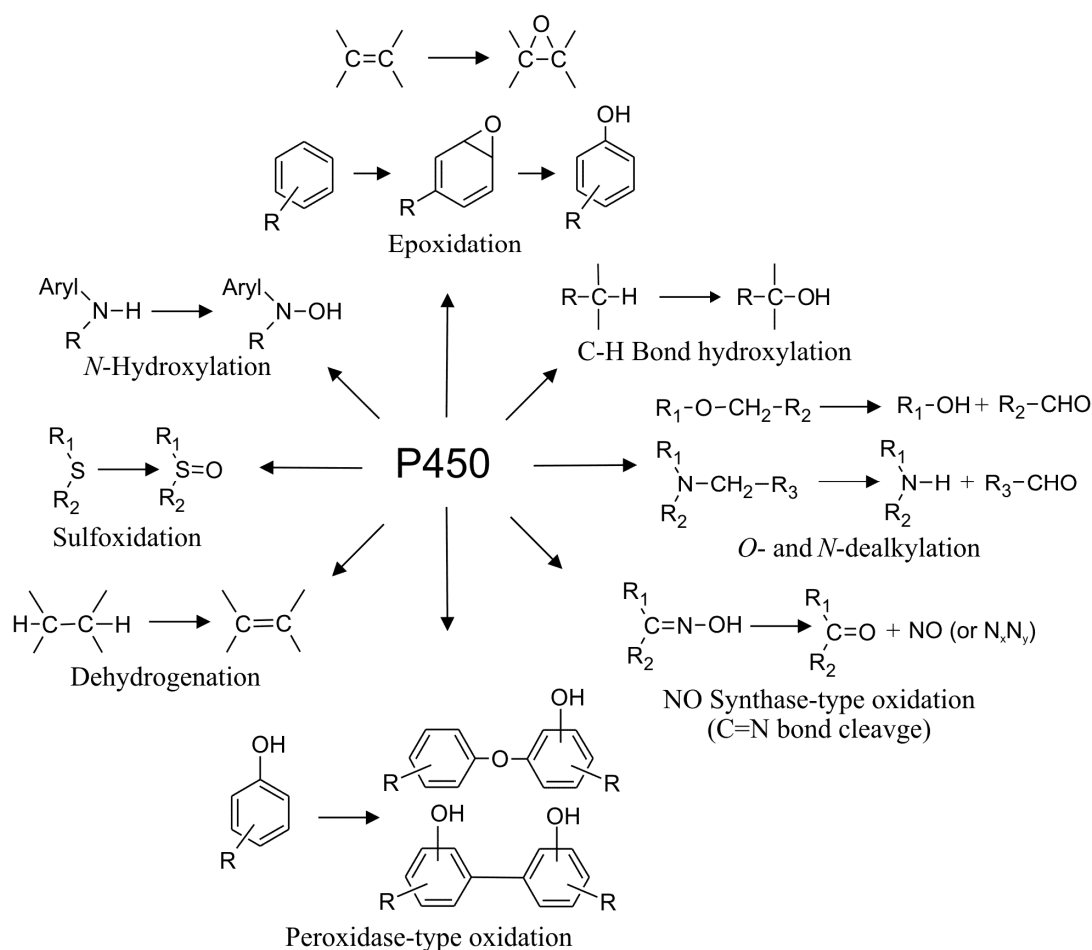


Figure 5 Selected P450s-catalyzed reactions according to (Mansuy 1998, Ortiz de Montellano 2009, Grobe et al. 2009)

### 1.1.1.2 Reaction mechanism

The catalytic cycle of cytochrome P450s involves at least one or more short-lived highly oxidizing intermediates at the heme iron close to the bound substrate (Cirino and Arnold 2003b). The reaction cycle of P450s is illustrated in Figure 6. It starts with a P450 low-spin six-coordinate iron (Sligar and Gunsalus 1976) in the ferric state [(1), H<sub>2</sub>O...heme(Fe<sup>III</sup>)] with water as the distal ligand. Binding of the substrate (R-H) near the distal region of the heme causes a dehydration of the active site resulting in a five-coordinated heme iron within the enzyme-substrate complex [(2), R-H...heme(Fe<sup>III</sup>)] (Ortiz de Montellano 2005). Water exclusion from the active site is believed to be important for the change in coordination and reduction potential as well as to improve the coupling efficiency of electron transfer. Depending on the enzyme, the iron turns predominantly to the high spin state in the substrate-free situation. This causes an increase of the reduction potential which primes the enzyme for

substrate turnover by allowing electron transfer to occur (Sligar 1976). The reaction step from (1) to (2) may or may not facilitate the next reaction step depending on the P450 (Guengerich 2001). It has been shown that this reaction step is faster, which is why it is shown first. Oxygen can now bind to the activated ferrous P450 [(3), (R-H)...heme ( $\text{Fe}^{\text{II}}$ )] after (2) has been reduced by a flavin/ferredoxin or diflavin reductase with an NAD(P)H-derived electron forming an unstable ferrous-oxy species [(4), (R-H)...heme ( $\text{Fe}^{\text{II}}\text{-O}_2$ )], which then accepts the second electron (Groves 2006). The electron transfer steps are believed to be rate determining under natural conditions as they depend on the protein electron transport system.

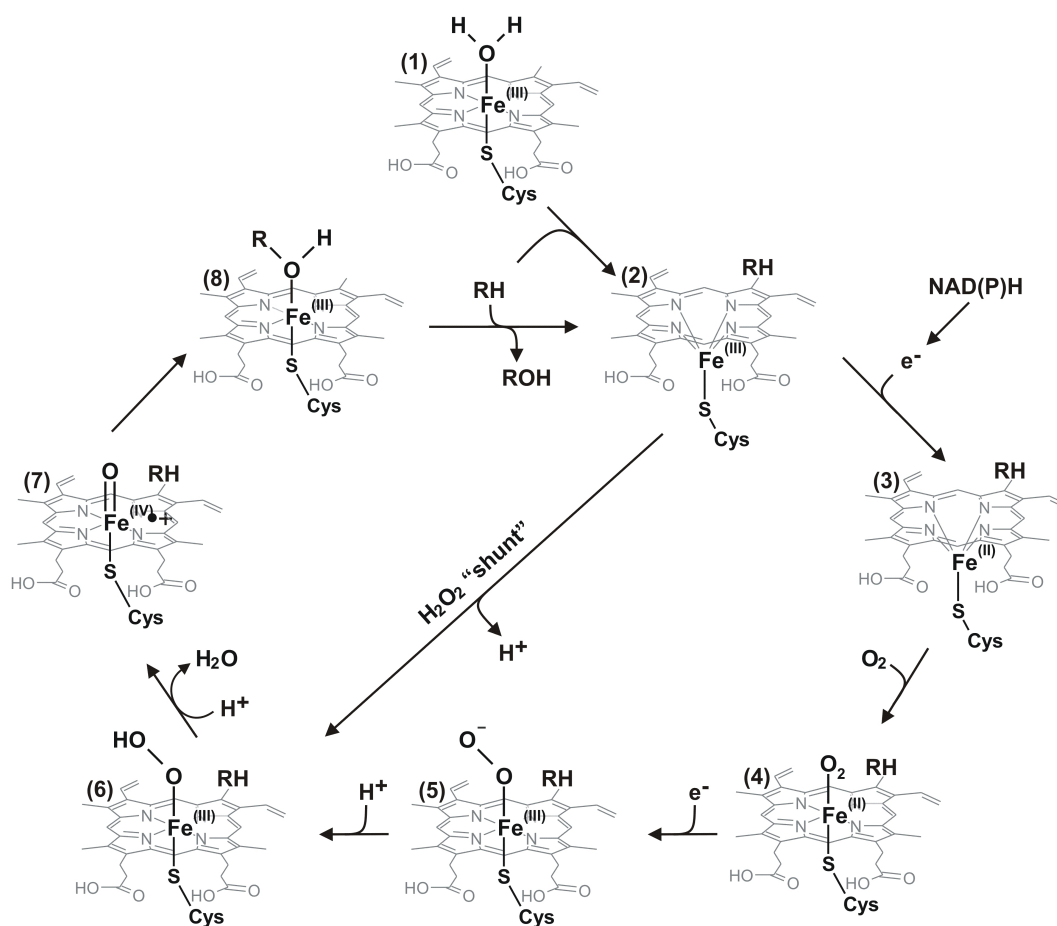


Figure 6 Catalytic cycle of P450s including the peroxide “shunt” pathway. RH is substrate, and ROH is product of the reaction. Overall charges: (3)<sup>-</sup>, (4)<sup>-</sup>, (5)<sup>2-</sup> and (6)<sup>-</sup>. Modified according to (Ullrich and Hofrichter 2007). (1) native (hydro)ferric enzyme (resting state), (2) ferric heme-substrate complex, (3) ferrous heme-substrate complex, (4) ferrous-dioxygen complex, (5) ferric peroxy anion complex, (6) ferric hydroperoxy complex (Compound 0), (7) putative oxy-ferryl radical complex (compound I), (8) product-ferric enzyme complex.

The resulting ferric peroxy anion [(5), (R-H)...heme ( $\text{Fe}^{\text{III}}\text{-O}_2^-$ )] is protonated to form the hydroperoxy complex (also referred to as Compound 0, [(6), (R-H)...heme ( $\text{Fe}^{\text{III}}\text{-O-OH}$ )], which then undergoes heterolytic/homolytic cleavage between the oxygen atoms with the

release of H<sub>2</sub>O giving rise to the putative oxy-ferryl state [(**7**), (R-H)...heme (Fe<sup>IV</sup>=O)<sup>•+</sup>]. The two electrons required for the two reaction steps from (**5**) to (**7**) originate from the heme, resulting in heme oxidation forming the suggested oxy-ferryl porphyrin  $\pi$ -cation radical. The highly reactive porphyrin species (**7**) can be written as [Fe<sup>V</sup>=O] but the precise electronic configuration is unknown. Relating to the precedent of heme peroxidase and catalase Compound I, which are stable and have been extensively studied, the most common perception is that the iron Fe<sup>4+</sup> and the porphyrin is one-electron deficient [Fe<sup>IV</sup> O<sub>2</sub>-porphy<sup>•+</sup>] (Guengerich 2001). This electron-deficient complex may abstract a hydrogen atom or one electron from the substrate to form a sigma complex (**8**) with the substrate. A consequent collapse of the complex generates the reaction product, which then dissociates and the cycle can restart (Guengerich 2001, Isin and Guengerich 2007). From studies of site-directed mutants it has been proposed that besides the putative oxy-ferryl species (**7**) the reactive intermediates peroxy-iron (**5**) and hydroperoxy-iron (**6**) are active oxygenating species with varying electrophilic or nucleophilic properties, contributing to the versatility of P450s (Vaz et al. 1998, Vaz et al. 1996, Kimata et al. 1995).

### 1.1.2 Fungal heme peroxidases

Peroxidases are secreted, microsomal or cytosolic enzymes found in all kingdoms of life and the majority of them are b-type heme proteins (Rogerio et al. 2008). The historical nomenclature of peroxidases within the EC-number system, which identifies the enzyme in terms of the particular reaction catalyzed, stands in contrast to the phylogenic observations that divided peroxidases into seven superfamilies (Passardi et al. 2007b). Thus peroxidases with very different molecular architecture and mechanistic behavior can be found under the same EC-number (Figure 7). Considering these complexities, it is reasonable to classify peroxidases according to their structural properties and sequence information (Passardi et al. 2007a). Concerning the heme peroxidases, this has led to the classification of different superfamilies, among which those of peroxidase-cyclooxygenases (former animal peroxidases) and non-animal peroxidases (former plant peroxidases) are the largest groups. The non-animal peroxidases comprise three classes based on structural similarities and suspected common evolutionary origin (Welinder 1992, Azevedo et al. 2003).

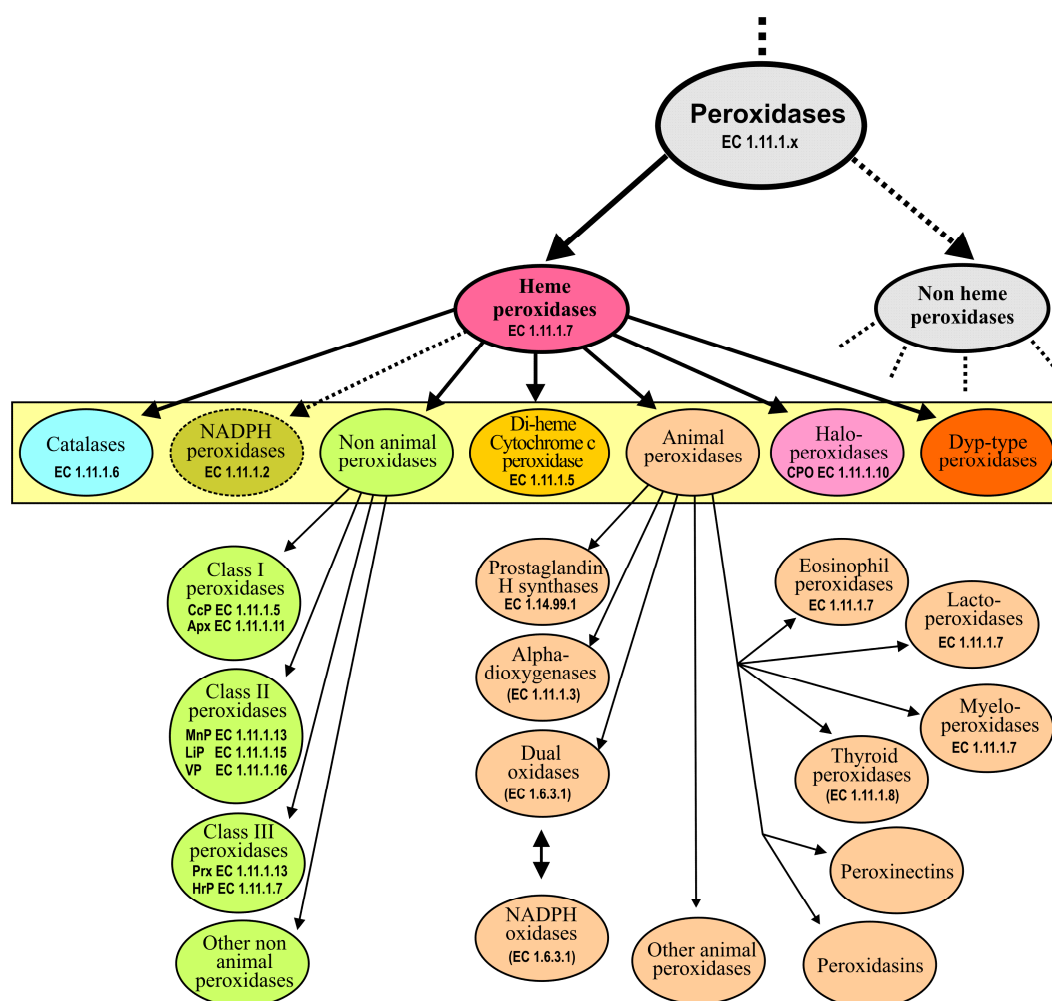


Figure 7 Schematic representation of the phylogenetic relations between the different families of peroxidases. Modified according to (Passardi et al. 2007b, Passardi et al. 2007a, Oliva et al. 2009).

Class I peroxidases are intracellular proteins predominantly found in organelles of prokaryotic origin (plastids and mitochondria) including cytochrome c peroxidases (CcPs), chloroplast and cytosolic ascorbate peroxidases (Apx), hybrid ascorbate-cytochrome c peroxidase (APx-CcP) and the gene duplicated catalase-peroxidases (CPs). A general feature of these proteins is their lack of bound carbohydrates, disulphide bridges, calcium ions or peptide sequences for secretion (Banci 1997).

Class II peroxidases are secreted by fungi and include lignin peroxidases (LiPs) and manganese peroxidases (MnPs) both from white rot fungi such as *Phanerochaete chrysosporium*, *Phlebia radiata* and *Lentinula edodes*, as well as versatile peroxidases (VPs) from various *Pleurotus* and *Bjerkandera* species and other peroxidases, for example from *Coprinus cinereus* (CiP) as well as from *Arthromyces ramosus* (ARP). Class III peroxidases are secreted by plants and comprise more than 3000 known enzymes. Well known examples

include horseradish peroxidase (HrP) from *Armoracia rusticana* and the soybean peroxidase (SbP) from *Glycine max.* (Cosio and Dunand 2009). Class II and III peroxidases share several structural features such as signal peptide sequences for secretion, protein glycosylation (Class II up to 5% and Class III up to 30%) as well as four conserved disulphide bridges and two calcium ions (Banci 1997). Heme peroxidases and catalases are closely related to P450s (Passardi et al. 2007a). Peroxidases are also found as manganese- and vanadium- containing or even metal-free proteins. In contrast to P450s, peroxidases are capable of using the peroxide form of O<sub>2</sub> to catalyze reactions via unstable highly reactive intermediates. H<sub>2</sub>O<sub>2</sub> as an early evolutionary intermediate of photosynthetic water oxidation and respiration processes may have favored the evolution of proteins that are able to use this toxic side product (Bernroitner et al. 2009). From this point of view peroxidases and predominantly catalases, which are capable of using H<sub>2</sub>O<sub>2</sub> as the second substrate, can be considered as detoxifying enzymes. In this connection, several biological active compounds such as fatty acids, amines, phenols, halogens and xenobiotics are substrates for various peroxidases. Physiological reactions include the *alpha*-oxidation of fatty acids during plant growth, iodination and coupling of tyrosine (thyroid hormone) by thyroid peroxidases, the oxidation of cytochrome c by cytochrome c peroxidases, the oxidation of chloride to antibacterial hypochlorite and the oxidative degradation of lignin structures by manganese and lignin peroxidases. A very interesting example is the usage of H<sub>2</sub>O<sub>2</sub> and hydroquinone in an explosive peroxidase-catalyzed reaction yielding oxygen and oxidizing benzoquinone used by the bombardier beetle (Kaim 2005). The structural conservation among heme peroxidases is quite high. The three-dimensional structure of these proteins mainly consists of an *alpha*-helix and a single short beta-thread. The general topology is conserved among family members including the ten *alpha*-helices and four disulfide bridges. In all heme peroxidases, the heme group is located between the two  $\alpha$ -helices. Class III peroxidases present three additional *alpha*-helices (Dunford 1999).

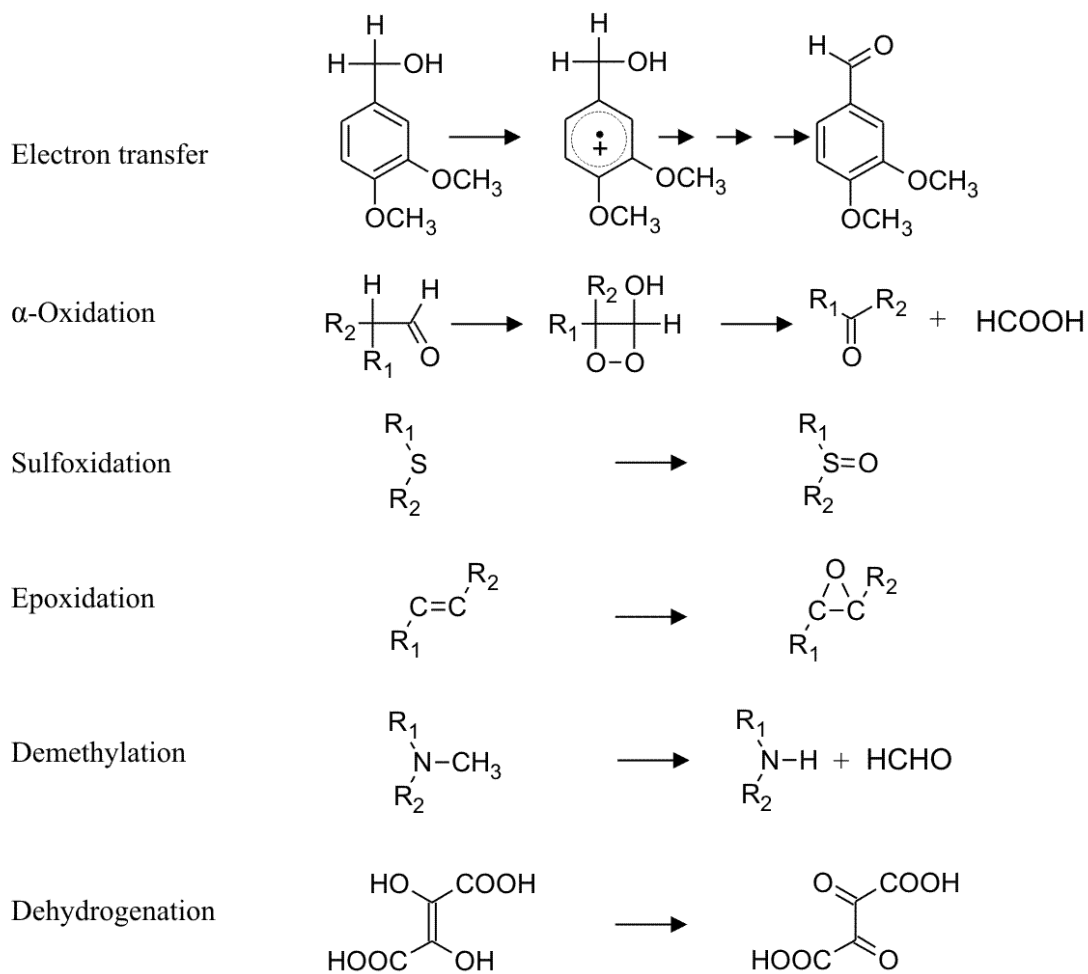
#### 1.1.2.1 Peroxidase-catalyzed reactions

The oxidative dehydrogenation is the major physiological reaction catalyzed by peroxidases (Cirino and Arnold 2003b). The peroxidase reaction mechanism can be formally described as a one-electron oxidation:

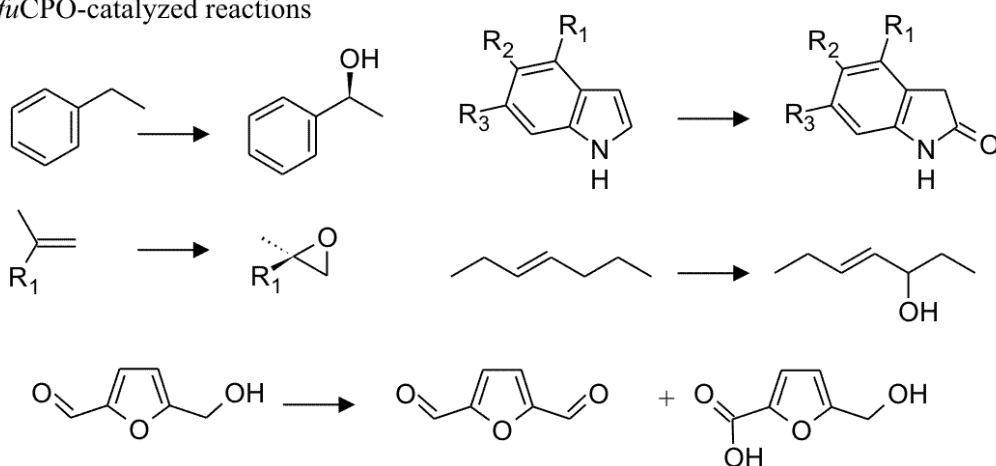




Table 1 Peroxidase-catalyzed reactions adapted from (Adam et al. 1999, van Deurzen et al. 1997, Cirino and Arnold 2003b)

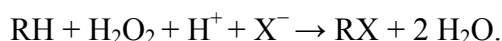


*Cfu*CPO-catalyzed reactions

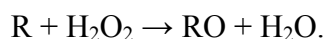


The enzymatic decomposition (disproportionation) of metastabilized H<sub>2</sub>O<sub>2</sub> by catalases is one of the most efficient enzymatic reactions with maximum turnover numbers up to 10<sup>7</sup> s<sup>-1</sup> (Deisseroth and Dounce 1970).

Heme haloperoxidases have been shown to catalyze the peroxide and halide ion-dependent halogenation of activated (benzylic or allylic) carbon (Littlechild 1999, Hofrichter and Ullrich 2006). The halide ion is initially oxidized to an active halogenating intermediate, which then halogenate the substrate (Cirino and Arnold 2003b, Hofrichter and Ullrich 2006). The overall reaction scheme is:



A few heme peroxidases such as *Cfu*CPO can perform two-electron oxidations along with oxygen transfer reactions and resemble in this respect P450s (Hofrichter and Ullrich 2006). They are being explored for synthetic applications, as the reactions often proceed stereospecifically. The overall reaction for this peroxygenase activity is:



Some of the reactions catalyzed by peroxidases are listed in Table 1 and include oxidation of aromatic and heteroatom compounds, epoxidation, enantioselective reduction of racemic hydroperoxides, oxidation of C-H bonds in allylic/benzylic compounds, alcohols, and indole, free radical oligomerizations and polymerizations of electron-rich aromatics, and the oxidative degradation of lignin structures (van Deurzen et al. 1997, Adam et al. 1999, Colonna et al. 1999).

#### 1.1.2.2 Reaction mechanism

P450s and peroxidases share key elements of their mechanisms. The proximal ligands and distal and proximal protein environments influence the mechanism of O-O bond cleavage, the stability of the intermediates and the accessibility of substrates to the heme. The peroxidase cycle shows similarities to the P450 cycle and passes through the following intermediates: the native (hydro)ferric peroxidase [(**1**), heme(Fe<sup>III</sup>-H<sub>2</sub>O)] binds H<sub>2</sub>O<sub>2</sub> to form an extremely short-lived iron(-III)-peroxide complex [(**2**), heme(Fe<sup>III</sup>-O-OH)] (“Compound 0” of P450s), which is heterolytically cleaved between the oxygen atoms by a two-electron transfer from the heme. As a result, a water molecule is expelled and Compound I, an oxy-ferryl heme radical cation complex [heme((**3**), Fe<sup>IV</sup>=O)<sup>+</sup>], emerges and can react with a first substrate to give a

phenoxy radical and Compound II. The latter is an oxy-ferryl heme [(4), heme( $\text{Fe}^{\text{IV}}=\text{O}$ )] and reacts with the second substrate molecule resulting in the formation of a second radical and the native ferric enzyme.

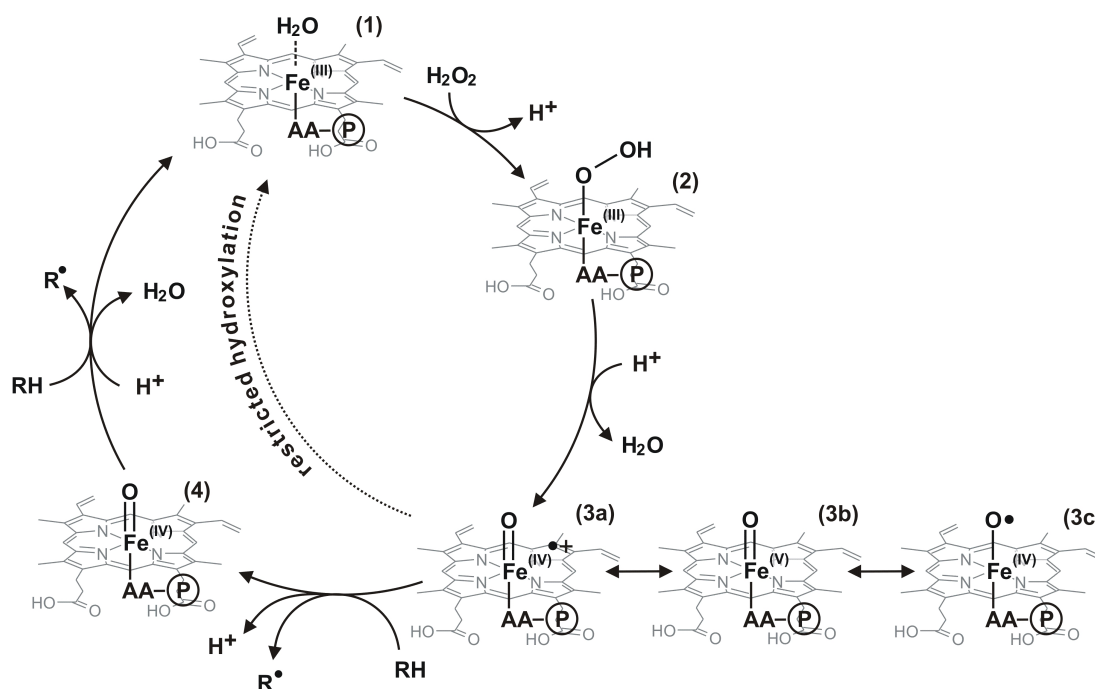


Figure 8 Catalytic cycle of peroxidases. RH is the substrate and  $\text{R}^\bullet$  is the product radical. Modified according to (Ullrich and Hofrichter 2007). (1) Native (hydro)ferric enzyme, (2) iron(III)-peroxide complex (analogous to Compound 0 of P450s), (3a) peroxidase Compound I (oxy-ferryl radical complex) that exists in different mesomeric forms: (3b) oxyiron (V) complex, (3c) oxy-radical ferryl complex, (4) Compound II (oxy-ferryl complex).

The oxy-ferryl radical complex is suggested to exist in different mesomeric forms: (3b) oxyiron (V) complex, (3c) oxy-radical ferryl complex, (4) Compound II (oxy-ferryl complex). In summary, within the typical heme-peroxidase cycle, two substrate molecules are oxidized by one-electron abstraction (but without oxygen transfer) while one molecule of  $\text{H}_2\text{O}_2$  is consumed and two water molecules are produced.

### 1.1.2.3 Lignin peroxidases (LiPs)

Lignin peroxidases (LiPs) were first discovered in the extracellular medium of *Phanerochaete chrysosporium* grown under nitrogen-limiting conditions by two independent groups (Kuwahara et al. 1984, Gold et al. 1984, Tien and Kirk 1983, Tien and Kirk 1984). They are monomeric glycosylated heme proteins with molecular masses around 40 kDa consisting of 343-344 amino acids. They resemble classical peroxidases, in that their  $\text{Fe}^{\text{III}}$  is pentacoordinated to the four heme tetrapyrrole nitrogens and to a histidine residue. LiPs

perform the reaction cycle illustrated above (Figure 8). The key functional difference between LiPs and classical peroxidases is that LiPs can oxidize aromatics that are only moderately activated by electron-donating substituents, whereas classical heme peroxidases act only on strongly activated aromatic substrates. For this reason LiPs have been suggested to play an essential role in the biodegradation of lignin (Hammel and Cullen 2008).

#### 1.1.2.4 Manganese Peroxidases (MnPs)

A longstanding problem with the idea of a central ligninolytic role for LiPs is that many white rot fungi apparently lack them. A different group of secreted oxidoreductases, the manganese peroxidases (MnPs) is more widespread and has been extensively researched as a possible alternative (Orth et al. 1993, Gold Michael et al. 2009). The first MnP was discovered in the fungus *Phanerochaete chrysosporium*, almost simultaneously with *PceLiP* (Kuwahara et al. 1984). The purified enzyme was found to be a monomeric glycoprotein with a molecular weight of 46 kDa that contains a ferriprotoporphyrin IX and four calcium ions per protein molecule. MnPs are also strongly oxidizing and undergo a classical peroxidase cycle but do not oxidize nonphenolic lignin-related structures directly because they lack the invariant tryptophan residue required for electron transfer to aromatic substrates. Instead, they have a manganese-binding site that consists of several acidic amino acid residues plus one of the heme propionate groups. Accordingly, one-electron transfer to Compound I of MnP occurs from bound  $Mn^{2+}$  (Wariishi et al. 1992). The product,  $Mn^{3+}$ , is released from the active site if various bidentate chelators are available to stabilize it against disproportionation to  $Mn^{2+}$  and insoluble  $Mn^{4+}$ . The physiological chelator is thought to be oxalate, an extracellular metabolite of many white rot fungi (Kuan and Tien 1993). The purpose of this reaction is evidently to transfer the oxidizing power of MnP to a small agent -  $Mn^{3+}$  - that can diffuse into the lignified cell wall and attack it from within (Hammel and Cullen 2008).

#### 1.1.2.5 Versatile Peroxidases (VPs)

When an  $Mn^{2+}$ -binding site was introduced into a *Phanerochaete chrysosporium* LiP (*PceLiP*) by site-directed mutagenesis, the resulting enzyme had MnP activity (Mester and Tien 2001). Conversely, when a tryptophan residue analogous to the essential one in LiPs was introduced into a *PcMnP*, this enzyme acquired LiP activity (Timofeevski et al. 1999). These results show that hybrid peroxidases with both activities could occur naturally. Recently, enzymes of this type, now termed versatile peroxidases (VPs), have been found in various *Pleurotus* and *Bjerkandera* species and extensively characterized (Camarero et al. 1999,

Mester and Field 1998). The *Pleurotus eryngii* VP (*PeVP*) termed VPL has the three acidic amino acid residues required for  $Mn^{2+}$  binding, and a catalytic efficiency ( $k_{cat}/K_m$ ) for  $Mn^{2+}$  oxidation in the general range exhibited by typical MnPs. In addition, *PeVP* has a tryptophan residue, trp164, analogous to the *PceLiP* trp171 that participates in electron transfer from aromatic donors and consequently enables the enzyme to oxidize nonphenolic lignin-related structures (Perez-Boada et al. 2005). However, the catalytic efficiency of *PeVP* on veratryl alcohol is relatively low at about  $1 \times 10^3 M^{-1} s^{-1}$ , as opposed to about  $3 \times 10^4 M^{-1} s^{-1}$  when the same reaction is catalyzed by *PceLiP* (Perez-Boada et al. 2005, Tien et al. 1986). Given the already low efficiency of *PceLiP* when it directly oxidizes large lignin model compounds, it will be important to determine how well VPs deal with these and with even larger synthetic lignins (Hammel and Cullen 2008).

#### 1.1.2.6 DyP-type Peroxidases (DyPs)

An exceptional group of peroxidases was recently identified in fungi and bacteria. These heme proteins are capable of catalyzing the oxidative decolorization of synthetic high redox-potential reactive dyes of the anthraquinone type, which are not converted by any of the peroxidases mentioned above (Kim and Shoda 1999). Based on this distinctive feature they were named as dye-decolorizing peroxidases or, in short, DyP-type peroxidases (DyPs) (Kim and Shoda 1999, Zubieta et al. 2007b, Zubieta et al. 2007a). Comparison based on structural informations and sequence alignments with representative members of all classes of the peroxidases demonstrated that DyPs cannot be integrated within either of these classes (Sugano et al. 2007). They show only slight sequence similarity (0.5–5%) to fungal peroxidases such as MnPs, LiPs or CiP and lack the typical heme-binding region, which is conserved within the plant peroxidase superfamily (Sugano et al. 1999, Sugano 2009). Even if several peptide sequences of DyP-type peroxidases are deposited in protein databases, just seven proteins from two bacterial species have been characterized so far (Kim and Shoda 1999, Sugano et al. 1999, Zubieta et al. 2007a, Scheibner et al. 2008). An involvement of DyPs in lignin degradation has been suggested as these enzymes were able to cleave dimeric non-phenolic lignin model compounds (Liers et al. 2009). However, the physiological function of this enzyme remains obscure.

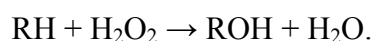
#### 1.1.2.7 Peroxidase from *Coprinopsis cinerea* (CiP)

*Coprinopsis cinerea* (formerly *Coprinus cinereus*) peroxidase (CiP), essentially identical to *Arthromyces ramosus* peroxidase (ARP), exhibits a specific activity such as the oxidation of

nonphenolic lignin model compounds but also maintains the broad substrate specificity of peroxidases such as HrP (Morita et al. 1988, Dunford 1999, Pezzotti et al. 2004, Kim et al. 2009). In addition, CiP comprises a single species of enzyme, whereas HrP consists of several isoenzymes with unique catalytic properties (Kim et al. 2009). CiP is commercially produced on a large scale by Novozymes Co. and has been a target for directed evolution (Cherry et al. 1999). Promising applications are dye transfer inhibition in laundry detergents, *in situ* stain bleaching and dye house wastewater treatment.

### 1.1.3 Heme proteins with peroxygenase activity

The term “peroxygenase” is attributed to a group of oxidoreductases that catalyzes the direct transfer of one liberated oxygen atom from a hydroperoxide that is reduced, to a substrate which will be oxidized (Hanano et al. 2006). The mechanism can be formally described as:



Although natural peroxygenase activities have been found in many organisms and also occur as a side reaction of other enzymes, the activity has no EC-number yet (Pecyna et al. 2009). Peroxygenases are of commercial interest as they perform the regio- and stereoselective incorporation of oxygen into organic molecules (Otey et al. 2006). Consequently, scientists are focused on the exploration of natural peroxygenase activities and in the assembling of synthetic peroxygenases because they are able to utilize  $\text{H}_2\text{O}_2$  as single oxygen donor and electron acceptor thus avoiding the need for cost-intensive cofactors such NAD(P)H.

#### 1.1.3.1 Plant seed peroxygenases

In general the term peroxygenase is used for special heme proteins from plants, which neither belong to the P450s nor to the peroxidases but show sequence similarity with calcium-binding proteins named caleosins (Hanano et al. 2006, Partridge and Murphy 2009). They are able to catalyze the  $\text{H}_2\text{O}_2$ -dependent hydroxylation of aromatics, the sulfoxidation of xenobiotics, and epoxidations of unsaturated fatty acids (Blee et al. 1993, Ishimaru and Yamazaki 1977, Blee and Durst 1987, Hamberg and Hamberg 1990). Caleosins with peroxygenase activity are generally found as lipid-body associated, seed-specific proteins in the plant storage tissues. Recently it has been shown also that separate membrane-bound isoforms of caleosins are expressed during stress by salt or drought or through pathogen infection of plants (Partridge and Murphy 2009). Caleosin-like genes are ubiquitous in multicellular plants, green algae and

true fungi, where their peroxygenase activity is suggested to have a role in the formation of epoxy hydroxyl alcohols from fatty acids hydroperoxides. These oxylipin metabolites are known to play a role in plant response to abiotic and biotic stresses. Similar oxylipins are also involved in various aspects of fungal spore development and probably serve as anti-fungal compounds in some fungi that can deter the growth of competing fungal species (Tsitsigiannis and Keller 2007).

#### 1.1.3.2 Peroxide “shunt” of P450s

Peroxygenase-like activities have also been reported as side reactions in P450s, which can utilize an oxygen atom from a peroxide to catalyze oxygen insertion without electron transport proteins or the NAD(P)H cofactor (Joo et al. 1999). This alternative pathway offers the opportunity to employ cell-free P450s catalysis without cofactor regeneration, additional proteins, or dioxygen and eliminates rate-limiting electron transfer steps (Cirino and Arnold 2003a). As illustrated in Figure 6 the peroxide “shunt” pathway bypasses a large portion of the enzyme’s natural catalytic cycle, including the rate-limiting first electron transfer step. Various peroxides and other oxidants (e.g., iodosobenzene, peracids and sodium periodate) will support the reaction, depending on the enzyme (Ortiz de Montellano 2005).

#### 1.1.3.3 Peroxygenase activity of Chloroperoxidase (*Cfu*CPO)

The filamentous fungus *Caldariomyces fumago* secretes a heme-thiolate hemoprotein that has versatile catalytic properties. While functionally categorized as a haloperoxidase, *Cfu*CPO possesses catalytic characteristics of peroxidases, P450s and catalases. Thus, *Cfu*CPO chlorinates, brominates, and iodinate organic compounds including aromatic substrates and catalyzes a series of non-halogenating oxidations, among others, epoxidation and hydroxylation of activated C-H bonds, as well as selective sulphoxidations (van Rantwijk and Sheldon 2000). The *Cfu*CPO proximal ligand is cysteinate sulfur as in P450s. In the distal pocket, the catalytic base used for O-O cleavage is glutamate rather than the typical peroxidase histidine and the distal region is more hydrophobic than in other peroxidases, which allows it to bind substrates and promote P450-type reactions (Table 1). However, the presence of polar residues and restricted access to the distal face make the active site more peroxidase-like than P450-like. Thus the peroxygenase activity of *Cfu*CPO is restricted to activated, non-aromatic substrates (Ullrich and Hofrichter 2007, Manoj and Hager 2008). The tertiary structure of *Cfu*CPO resembles neither the P450s nor peroxidases (Sundaramoorthy et al. 1995).

#### 1.1.3.4 Engineered peroxygenases

The idea of using laboratory-evolved bacterial P450s for selective oxygenation by optimizing the protein structure is a scientific approach to produce commercial available and selective redox biocatalysts. Suggested fields for synthetic applications of optimized P450s are the production of reference metabolites as well as reactive intermediates of drugs, fine chemicals and fragrances, the development of biosensors and for bioremediation (Urlacher and Eiben 2006). Site-directed mutagenesis has been widely used for optimizing the stability, activity, specificity and the electron transport and redox partner interactions of P450s (Otey et al. 2006, Gillam 2008, Damsten et al. 2008). However, significant scope remains for optimizing artificial fusion proteins by improving the coupling between P450s and reductase domains and exploiting alternative electron transport partners (Gillam 2008).

A myoglobin from *Physeter macrocephalus* (sperm whale) was engineered at the distal pocket to form a peroxygenase, which catalyzed the sulfoxxygenation of thioanisole and the epoxidation of styrene with incorporation of oxygen from H<sub>2</sub>O<sub>2</sub>. The results showed that this mutant is a much better peroxygenase than wild type Mb and even HrP (Ozaki et al. 1997).

The HrP is the best-characterized heme peroxidase because of its high catalytic activity and its broad specificity for electron donors. Commercial HrP was shown to hydroxylate benzene to phenol when benzene was used as the solvent with just 0.1– 5% phosphate buffer, whereas in aqueous buffered media benzene was inert to HrP attack (Akasaka et al. 1995). Oxygen, in this reaction, came from H<sub>2</sub>O<sub>2</sub>, as demonstrated in reactions using H<sub>2</sub><sup>18</sup>O<sub>2</sub>. HrP is currently the subject of genetic engineering to improve the oxygen transfer potential. Variants have been obtained that have at least some of the key functional properties of P450 (Savenkova et al. 1998, van Rantwijk and Sheldon 2000, Smith and Ngo 2007). It was recently shown that engineered HrP show stereoselectivity and activity similar to that of the P450s and *Cfu*CPO (Smith and Ngo 2007).

#### 1.1.3.5 Extracellular fungal aromatic peroxygenases (APOs)

Recently a new group of heme-thiolate oxidoreductases was identified in several litter-decay fungi such as *Coprinellus radians*, *Coprinopsis verticillata* and *Agrocybe aegerita* (Ullrich et al. 2004, Anh et al. 2007). These very stable and highly glycosylated proteins with an average molecular mass of 44 kDa have been shown to oxidize many organic chemicals. The absorption spectrum of the native enzymes and of their carbon monoxide adduct closely resemble those of P450s (Ullrich and Hofrichter 2005, Anh et al. 2007). They show some



functional similarities with heme peroxidases by catalyzing the H<sub>2</sub>O<sub>2</sub>-dependent oxidation of ABTS, halogens and phenols but also with P450 by mediating selective hydroxylation of numerous substrates.

The best-characterized fungal enzyme of this type, from *Agrocybe aegerita*, was first claimed to be a haloperoxidase due to its ability to catalyze the bromination of phenols in acidic solution that contain bromide ions. Moreover, its ability to oxidize aryl alcohols, such as veratryl- and benzyl alcohols into the corresponding aldehydes and further typical peroxidase substrates such as 2,6-dimethoxyphenol or 2,2'-azinobis-(3-ethylbenzothiazoline-6-sulfonate) (ABTS) indicated that the enzyme acts as a true peroxidase (Ullrich et al. 2004). However, later investigation showed that the enzyme can oxidize toluene and naphthalene to produce hydroxylated derivatives at neutral pH (Ullrich and Hofrichter 2005, Kluge et al. 2007). Consequently, it has been suggested that aside from its peroxidase activity, the reactions catalyzed by this novel enzyme proceed via a peroxide “shunt”-like pathway as observed in P450s (Ullrich and Hofrichter 2007).

A screening for this new enzyme activity was recently performed, and it was found to exist in *Coprinellus radians* and *Coprinopsis verticillata*, exhibiting the same catalytic properties such as hydroxylation of aromatic substrates (Anh et al. 2007). Thus, these enzymes are widely distributed and may belong to a new superfamily of fungal extracellular heme-thiolate enzymes that act as aromatic hydrocarbon monooxygenating catalysts. As a consequence of this catalytic activity, in particular the oxidation of aromatic substrates, the novel enzyme was named Aromatic Peroxygenase (APO), by analogy to the nomenclature used for aromatic hydroxylases (Suske et al. 1997). Another enzyme, classified as a peroxidase, has been isolated from crude extracts of *Coprinus spec.* and has been found to catalyze the oxidation of diverse benzylic compounds to give corresponding aldehydes (Russ et al. 2002, Hauer et al. 2004) but it was not purified or further investigated.

The affiliation of APOs to a new superfamily of oxidoreductases was confirmed recently as the APO from *Agrocybe aegerita* (*AaeAPO*) exhibits low sequence and structure identity (Figure 9, *ca.* 29%) with heme *CfuCPO* and no significant genomic sequence identity with the P450s (Pecyna et al. 2009).

The core helices of *AaeAPO* and *CfuCPO* are reasonably well conserved and structural conservation around the heme is high e.g. in the “*CfuCPO*-signature” region and at the cation binding site. The cation Mn<sup>2+</sup> in *CfuCPO* is an Mg<sup>2+</sup> in *AaeAPO*, which may mediate structural stability of the protein, similar to Ca<sup>2+</sup> ions in LiP and MnP. The X-ray results indicate that the active side of *AaeAPO* has a broad entrance for relatively large molecules.

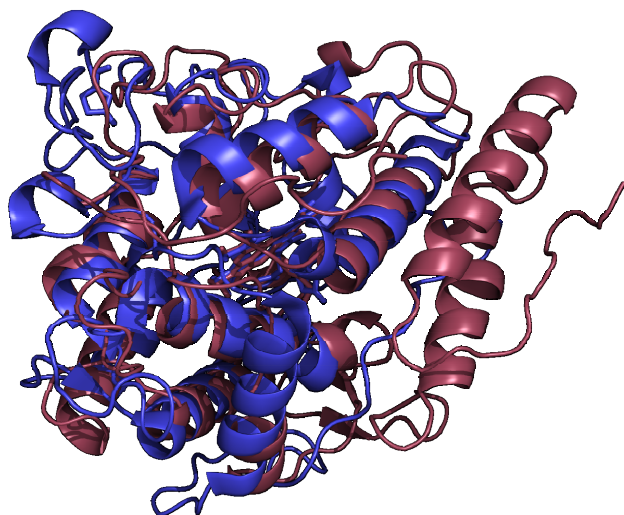


Figure 9 Superposition of *Aae*APO (red) and *Cfu*CPO (blue) (Piontek 2009).

This is supported by the observation that PAHs like pyrene and perylene are oxygenated at the active heme-thiolate side of *Aae*APO (Aranda et al. 2009). It has been shown that a phenylalanine (phe204) is in contact with the heme, and from there extends a relay of stacked phenylalanines to a phenylalanine (phe232) at the surface. Some of these phenylalanines (phe233) are sandwiched by arginine (arg208)

and nearby are two acidic residues, which is a situation similar to that found for tryptophan (trp171) in LiP. This result may indicate the presence of a long-range electron transfer (LRET) pathway for bulky substrates. Six *N*-glycosylation sites were identified (at Asn 11, 141, 161, 182, 286, 295) with high-mannose type *N*-glycosylation site at Asn 141 with eight carbohydrate molecules. No evidence for *O*-glycosylation sites has been found.

## 1.2 Aims and objectives

So far, little is known about the catalytic cycle of the *Aae*APO and other fungal peroxygenases. The physiological function of these enzymes is also unclear, but their extracellular location and widespread occurrence in the fungal kingdom (Pecyna et al. 2009) suggest a role in the biodegradation or detoxification of organic chemicals encountered by the fungi. Their hydroxylation activity towards aromatic substrates raises the assumption that APOs can also be applied in diverse fields of synthetic chemistry.

The overall aim of this study was to obtain catalytic and physiologic parameters of the novel peroxygenase from *Agrocybe aegerita* including following objectives:

- A screening for novel enzyme activities
- Mechanistic characterization of single reactivities
- Proposal for a general reaction cycle based on mechanistic studies
- Structural suggestions for the active site

Further objectives that address the physiological role of the enzyme were:

- Assessment of whether the enzyme is involved in the degradation of polymers such as lignin
- Screening for potential physiological substrates of the enzyme

Finally, this study aimed to develop perspectives for synthetic applications of fungal peroxygenases in the field of selective hydroxylation.

## 2. Materials and Methods

Some of the methods used in this work are standard procedures in the laboratory of the International Graduate School of Zittau and were not described in detail: cultivation of fungi on agar plates, in submerge cultures and fermentors, spectrophotometric enzyme assays, the determination of protein amounts (Bradford test), protein electrophoresis, micro- and ultrafiltration, vacuum distillation, accelerated solvent extraction, freeze drying, solid phase micro extraction and centrifugations. Sally Ralph (USDA Forest Product Laboratories, Madison, USA) performed the NMR analyses. Some of the used materials and methods were described and published before (Kinne et al. 2008, Kinne et al. 2009b, Kinne et al. 2009a, Aranda et al. 2008).

### 2.1 Reactants

Commercially available chemicals were purchased from Sigma-Aldrich, Fluka, Chemos GmbH, Merck and TCI Europe.  $\text{H}_2^{18}\text{O}_2$  (90 atom %, 2% wt/vol) was obtained from Icon Isotopes. Terminally brominated polyethylene glycol (PEG, approx. 2 kDa) was purchased from Iris Biotech GmbH. Pisatin was obtained from Apin Chemicals Ltd. All of the aliphatic ethers used as substrates were the highest grade available, contained no antioxidant, and were received from the manufacturer under nitrogen in small bottles. A new bottle of each aliphatic ether was opened for each experiment and analyzed beforehand by gas chromatography/ mass spectrometry (GC/MS). The results showed that none of these ethers contained detectable levels of the alcohols, aldehydes, or ketones that have been detected as reaction products in the experiments described below.

#### 2.1.1 Methyl 3,4-dimethoxybenzyl ether

Methyl 3,4-dimethoxybenzyl ether was prepared by reacting 3,4-dimethoxybenzyl alcohol in methanol containing *para*-toluenesulfonic acid as previously described (Schmidt et al. 1989), but with modified product purification. At the conclusion of the reaction, the mixture was extracted with several portions of cyclohexane, which were dried over  $\text{MgSO}_4$  and concentrated on a rotary evaporator to produce a thick syrup. This crude product was fractionated by vacuum column chromatography on silica gel with cyclohexane as the eluant (Pedersen and Rosenbohm 2001). Fractions were analyzed by thin layer chromatography and by  $^1\text{H}$  NMR analysis, and those showing no detectable impurities were pooled for solvent

removal. MS  $m/z$  (%) 182 ( $M^+$ , 44), 166 (3), 151 (100), 139 (7), 124 (4), 107 (14), 91 (9), 77 (12), 65 (5), 51 (4).  $^1\text{H}$  NMR ( $\text{CDCl}_3$ )  $\delta$  (ppm) 3.35 (s, 3H,  $-\text{CH}_2\text{OCH}_3$ ), 3.86 (s, 3H,  $-\text{OCH}_3$ ), 3.87 (s, 3H,  $-\text{OCH}_3$ ), 4.37 (s, 2H,  $-\text{CH}_2\text{O}-$ ), 6.81 (d,  $J = 8.1$  Hz, 1H,  $-\text{ArC}_5\text{H}$ ), 6.85 (dd,  $J = 8.1$  Hz, 2.0 Hz, 1H,  $-\text{ArC}_6\text{H}$ ), 6.87 (d,  $J = 2.0$  Hz,  $-\text{ArC}_2\text{H}$ ).

### 2.1.2 Methyl 4-nitrobenzyl ether

Methyl 4-nitrobenzyl ether was prepared from 4-nitrobenzyl alcohol and  $\text{CH}_3\text{I}$  as described previously (Lawson et al. 1995) and recrystallized twice at 4 °C, first from petroleum ether and then from water. MS  $m/z$  (%) 167 ( $M^+$ , 4), 166 (11), 136 (11), 121 (14), 120 (35), 108 (13), 107 (100), 106 (14), 105 (13), 91 (27), 90 (25), 89 (85), 78 (47), 77 (81), 65 (11), 63 (27), 51 (28), 50 (16).  $^1\text{H}$  NMR ( $\text{CDCl}_3$ )  $\delta$  (ppm) 3.48 (s, 3H,  $-\text{OCH}_3$ ), 4.59 (s, 2H,  $-\text{CH}_2\text{O}-$ ), 7.53 (d,  $J = 8.6$  Hz, 2H,  $-\text{ArC}_{2,6}\text{H}$ ), 8.24 (d,  $J = 8.6$  Hz, 2H,  $-\text{ArC}_{3,5}\text{H}$ ).

### 2.1.3 1-Methoxy-4-trideuteromethoxybenzene

1-Methoxy-4-trideuteromethoxybenzene was prepared from 4-methoxyphenol and  $\text{CD}_3\text{I}$  (99.5 atom % D) as described previously (Foster et al. 1974) and recrystallized twice from aqueous ethanol. MS  $m/z$  (%) 141 ( $M^+$ , 100), 126 (70,  $-\text{CH}_3$ ), 123 (62,  $-\text{CD}_3$ ), 98 (34,  $-\text{CH}_3$ ,  $-\text{CO}$ ), 95 (31,  $-\text{CD}_3$ ,  $-\text{CO}$ ).  $^1\text{H}$  NMR (360 MHz,  $\text{CDCl}_3$ )  $\delta$  6.84 (s, 4H), 3.77 (s, 3H).

### 2.1.4 PEG terminated 4-nitrophenyl ether

PEG terminated with 4-nitrophenyl ethers was prepared by stirring 1 g of dibromo-PEG (approx. 0.5 mmol) overnight in acetone that contained 10 mmol each of 4-nitrophenol and powdered  $\text{K}_2\text{CO}_3$ . The acetone was then removed by rotary evaporation and the product was redissolved in water, after which it was dialyzed twice against 100 mM  $\text{NaHCO}_3$  and twice against distilled water, using a 1 kDa cutoff bag, and finally lyophilized. Approximately 60% of the PEG end groups were 4-nitrophenyl-substituted by this method, as shown by integration of the  $^1\text{H}$ -NMR signals (in  $\text{CDCl}_3$ ) for the aromatic protons (6.99 and 8.20 ppm) and the internal polyoxyethylene protons (3.65 ppm).

### 2.1.5 4-Hydroxybutanal 2,4-dinitrophenylhydrazone

4-Hydroxybutanal 2,4-dinitrophenylhydrazone standards were prepared by adding aliquot portions of 2-ethoxytetrahydrofuran to excess 0.1% 2,4-dinitrophenylhydrazine solution in 0.6 N HCl.

### 2.1.6 Arylglycerol *beta*-aryl ethers

Arylglycerol *beta*-aryl ethers and a dehydrogenase polymer (DHP) of coniferyl alcohol were prepared by Paula Nousiainen (Laboratories of Organic Chemistry, University of Helsinki, Finland) according to methods described previously (Sipilä and Syrjänen 1995, Hofrichter et al. 1999). *Threo*-1-(4-ethoxy-3-methoxy-ring-[<sup>14</sup>C]phenyl)-2-(2-methoxyphenoxy)-1,3-dihydroxypropane (1.0 mCi mmol<sup>-1</sup>), a model of the major nonphenolic arylglycerol-*beta*-aryl ether structure in lignin, was prepared as described previously (Kawai et al. 1995, Landucci et al. 1981).

### 2.1.7 Milled pine and poplar wood

Milled pine and poplar wood was prepared from a mixture of air-dried sap- and heartwood of Scots pine (*Pinus silvestris*) and Poplar (*Populus spec.*). The obtained powder contained all wood components including the extractives. Part of the wood was further extracted in 5 mg portions with (a) 3 x 1 ml of 0.5% Tween 20 in 50 mM potassium phosphate and (b) 3 x 1 ml of H<sub>2</sub>O<sub>2</sub> with vigorous shaking for 10 min. After centrifugation, the supernatant containing the extractable wood constituents (mostly aromatic compounds) was separated from the insoluble wood pellet. The latter was washed with water prior to use.

## 2.2 Enzyme preparations

The extracellular peroxygenase of *A. aegerita* (isoform II, 44 kDa) was produced and purified as described previously (Ullrich et al. 2004, Ullrich et al. 2009). The enzyme preparation was homogeneous by SDS polyacrylamide gel electrophoresis and exhibited an A<sub>418</sub>/A<sub>280</sub> ratio of 1.75. The specific activity of the peroxygenase was around 120 U mg<sup>-1</sup>, where 1 U represents the oxidation of 1 μmol of 3,4-dimethoxybenzyl alcohol to 3,4-dimethoxybenzaldehyde in 1 min at 23 °C at pH 7 (Ullrich et al. 2004).

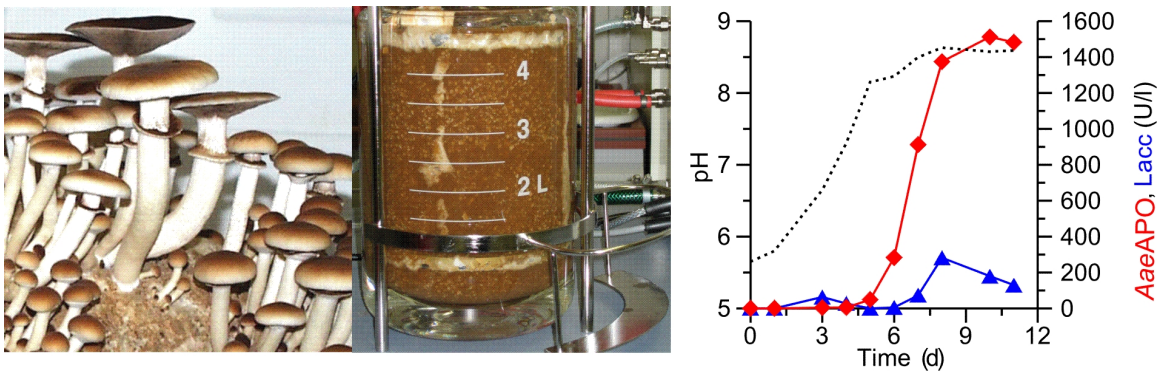


Figure 10 Fruiting bodies of *A. aegerita* formed during solid state fermentation (left). Submerge cultivation of the *A. aegerita* in a stirred bioreactor for the production of extracellular proteins. Soybean served as complex medium. The time course shows the volume activity of *AaeAPO* (red line), laccase blue line and the pH during fermentation process (Ullrich et al. 2009).

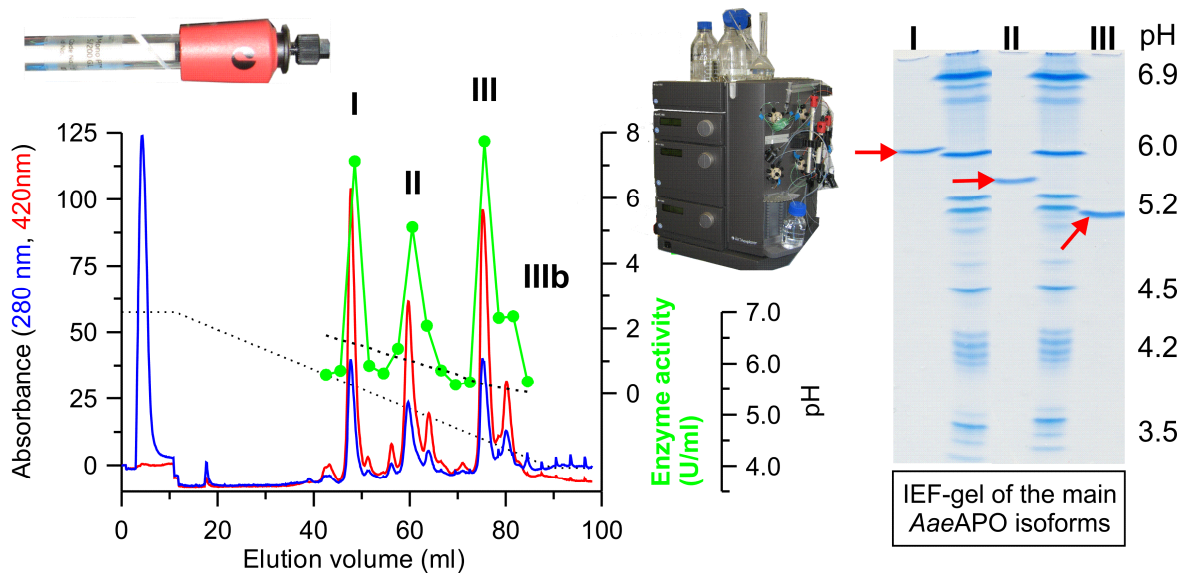


Figure 11 Separation of different *AaeAPO* forms by chromatofocusing. Left: Elution profile recorded after chromatofocusing on the mixed anion exchanger Mono P; separated *AaeAPO* forms are highlighted in gray. Red line, absorbance at 420 nm; green circles, *AaeAPO* activity assayed with veratryl alcohol (pH 7.0). (Right) Separated *AaeAPO* forms visualized in an IEF gel; *AaeAPO* I (pI 6.1), *AaeAPO* II (pI 5.6), *AaeAPO* III (pI 5.2). The FPLC-instrument and the ion exchange column are shown. Data and drawings according to (Ullrich et al. 2009).

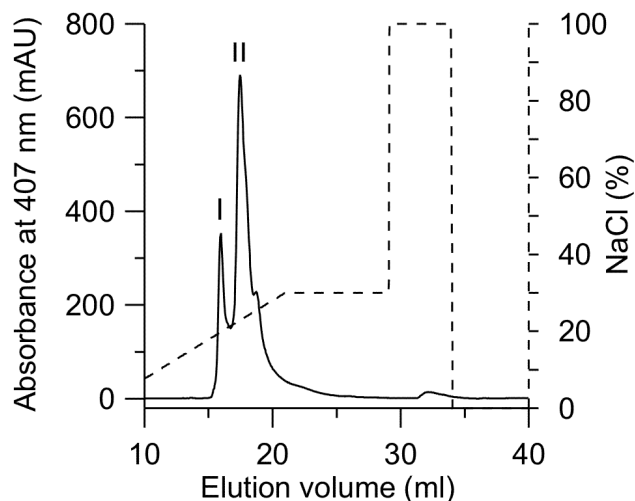


Figure 12 FPLC-elution profile of different isoforms (I and II) of *CfuCPO*.

*CfuCPO* was obtained from Sigma Aldrich and purified by Fast Protein Liquid Chromatography (FPLC). *CfuCPO* was separated and fractionated with an ÄKTA FPLC instrument (GE Healthcare Europe GmbH, Freiburg, Germany) equipped with a strong anion exchanger (Mono Q HR 5/5) using a linear gradient from 10 mM Na-acetate to 30% of 1 M NaCl over 22 column volumes and was held for 5 column volumes at pH 5.5 (Figure 12). The collected fractions with the highest

*CfuCPO*-activities were combined. The specific activity of the *CfuCPO* was around 310 U  $\text{mg}^{-1}$ , where 1 U represents the oxidation of 1  $\mu\text{mol}$  of monochloro dimedone (1,1-dimethyl-4-chloro-3,5-cyclohexaenedione) to dichloro dimedone (1,1-dimethyl-4,4-dichloro-3,5-cyclohexaenedione) in 1 min at 23 °C at pH 2.75 (Hager et al. 1966).

## 2.3 UV-Vis Spectroscopy

UV-Vis spectra of resting *AaeAPO* (6-8  $\mu\text{M}$ ) as well as of its ligand complexes were recorded in quartz cuvettes (diameter 10 mm) containing 50 mM potassium phosphate buffer (pH 7 or pH 3) in the scanning range from 200 to 800 nm at 23 °C using a Cary 50 spectrophotometer (Varian, Darmstadt, Germany). For the reduced enzyme complex, samples were reduced with a few grains of sodium dithionite until the UV-Vis spectra exhibit no changes anymore. The NO-enzyme complex was achieved by flushing the enzyme sample using NO until steady conditions were reached. Other ligand spectra's were recorded by adding an appropriate amount of the ligand until the steady spectral conditions. Difference spectra were recorded as described before but reaction mixtures were split prior to each experiment. One aliquot was transferred into the reference cuvette and the other in the sample cuvette. The instrument baseline was set to zero with the reference cuvette in the sample beam. Then the sample cuvette was placed into the spectrophotometer, the ligand was added and the spectrum was recorded.



## 2.4 Standard reaction conditions

Typical reaction mixtures (0.2-1.0 ml) contained purified peroxygenase (1-2 U ml<sup>-1</sup>), potassium phosphate buffer (50 mM, pH 7.0 and for halogenation reactions pH 3), and the substrate (0.1-10 mM). Some of the reactions contained ascorbic acid (4-12 mM) to inhibit further oxidation of the phenolic products that were released (Kinne et al. 2008, Kinne et al. 2009b). The reactions were started by the addition of H<sub>2</sub>O<sub>2</sub> (0.1-5 mM) and stirred at room temperature for 3 min, at which time chromatographic analyses showed that product formation was complete. In some of the reaction, H<sub>2</sub>O<sub>2</sub> was supplied continuously via a syringe pump (KDSscientific).

## 2.5 Product identification

### 2.5.1 HPLC-Method

Reaction products such as 4-methoxyphenol, 4-ethoxyphenol, 4-propoxyphenol 2-methoxyphenol, 3-methoxyphenol, 4-methylanisol, 2-chloro-4-methoxyphenol, *O*-desmethylnaproxen, 6-*alpha*-hydroxymaackiain, 2-(4-hydroxyphenoxy)propionic acid, 1-naphthol, *N*-desisopropylpropranolol, 5-hydroxypropranolol, 4-hydroxypropranolol, 5-hydroxydiclofenac, 4'-hydroxydiclofenac, halogenated methoxybenzenes and *para*-benzoquinone were analyzed HPLC using an Agilent Series 1050, 1100 or 1200 instrument (Waldbronn, Germany) equipped with a diode array detector, which was fitted with a reversed phase Synergi Fusion 4- $\mu$ m RP-80A column (4.6 mm diameter by 150 mm length, 5  $\mu$ m particle size, Phenomenex). The column was eluted at 40 °C and 1 ml min<sup>-1</sup> with aqueous phosphoric acid solution (15 mM, pH 3)/acetonitrile, 95:5, for 5 min, followed by a 20-min linear gradient to 100% acetonitrile.

### 2.5.2 HPLC-MS Method I

Reaction products such as 3,4-dimethoxybenzaldehyde, 1-(4-hydroxy-3-methoxyphenyl)-2-(2-methoxyphenoxy)propane-1,3-diol, 4-nitrophenol, 4-nitrocatechol, benzyl alcohol, 4-nitro benzyl alcohol, benzaldehyde, 4-nitrobenzaldehyde, benzoic acid, and 4-nitrobenzoic acid were analyzed by high performance liquid chromatography (HPLC) using the instrument described above and an Agilent LC/MSD VC (Waldbronn, Germany) electrospray ionization mass spectrometer (ESI-MS). Reverse phase chromatography was performed on a Luna C18 column (4.6 mm diameter by 150 mm length, 5  $\mu$ m particle size, Phenomenex), which was

eluted at 0.35 ml min<sup>-1</sup> and 40 °C with aqueous 0.1% vol/vol ammonium formate (pH 3.5)/acetonitrile, 95:5 for 5 min, followed by a 25-min linear gradient to 100% acetonitrile. Products were identified relative to authentic standards, based on their retention times, UV absorption spectra, and [M + H]<sup>+</sup> or [M-H]<sup>-</sup> ions.

### 2.5.3 HPLC-MS Method II

Phenolic reaction products such as 2-methoxyphenol, 3-methoxyphenol, 4-methoxyphenol, 4-ethoxyphenol, 4-propoxyphenol etc. were analyzed by liquid chromatography/ mass spectroscopy using a reversed phase Synergi Gemini C6-Phenyl 110A column (4.6 mm diameter by 150 mm length, 5 µm particle size, Phenomenex). The isocratic mobile phase consisted of 5% vol/vol acetonitrile and 95% aqueous 0.1% vol/vol ammonium formate that had been adjusted to pH 10 beforehand with NaOH. The column was operated at 40 °C and 1 ml min<sup>-1</sup> for 5 min. Electrospray ionization was performed in the negative ionization mode. For each *m/z* value, the average total ion count within the 4-nitrobenzaldehyde peak was used after background correction to generate the ion count used for mass abundance calculations.

### 2.5.4 Aliphatic aldehydes or ketones

Aliphatic aldehydes or ketones were analyzed as their 2,4-dinitrophenylhydrazones after addition of 0.2 volume of 0.1% 2,4-dinitrophenylhydrazine solution in 0.6 N HCl to each reaction mixture. The derivatized products were analyzed using the same HPLC apparatus as above, but the Luna C18 column was eluted with aqueous 0.1% vol/vol ammonium formate (pH 3.5)/acetonitrile, 70:30 for 5 min, followed by a 25-min linear gradient to 100% acetonitrile. With two exceptions, the dinitrophenylhydrazones were identified relative to authentic standards, based on their retention times, UV absorption spectra, and [M-H]<sup>-</sup> ions. As no standards of the 5-hydroxypentanal or 2-(2-hydroxyethoxy)acetaldehyde derivatives were available, they were tentatively identified based on their [M-H]<sup>-</sup> ions.

### 2.5.5 4-Nitrobenzaldehyde

The reaction product 4-nitrobenzaldehyde was analyzed by GC of a benzene extract, using a Hewlett Packard 6890 chromatograph equipped with a Hewlett Packard 5973 mass spectrometer. GC was performed isothermally at 150 °C, using helium as the carrier gas at a column flow rate of 1 ml min<sup>-1</sup> on a 5% polysiloxane column (Zebron ZB-5, 250 µm diameter by 30 m length, 0.25 µm film thickness, Phenomenex). The product was identified relative to an authentic standard by its retention time and by electron impact MS at 70 eV.

### 2.5.6 Ethanol, 2-propanol and *tert*-butanol

The products ethanol, 2-propanol and *tert*-butanol were detected by subjecting dichloromethane extracts of the aqueous reaction mixtures to GC/MS analysis using the equipment just described. GC was performed using a linear temperature program from 40 °C to 150 °C (10 °C min<sup>-1</sup>), using helium as the carrier gas at a column flow rate of 1 ml min<sup>-1</sup>, on a 5% phenyl-methylpolysiloxane column (DB-5MS, 250 µm diameter by 30 m length, 0.25 µm film thickness, J&W Scientific). The products were identified relative to authentic standards by their retention times and by electron impact MS at 70 eV.

### 2.5.7 Methanol

The reaction product methanol was analyzed by GC/MS as described previously (Li et al. 2007) using the equipment just described plus a Hewlett Packard 7694 headspace sampler. The aqueous sample solutions (2 ml) were equilibrated at 90 °C in the headspace oven, after which GC was performed isothermally at 45 °C, using helium as the carrier gas at a column flow rate of 1 ml min<sup>-1</sup>, on the DB-5MS column described above. The methanol was identified relative to an authentic standard by its retention time and by electron impact MS at 70 eV.

### 2.5.8 4-nitrophenyl-terminated PEG

To look for evidence that the peroxygenase cleaved ether bonds in 4-nitrophenyl-terminated PEG, we analyzed reaction mixtures by gel permeation chromatography on a column of Sephadex G-25 superfine (15 mm diameter, 300 mm length, GE Healthcare) in aqueous Na<sub>2</sub>SO<sub>4</sub> (0.35 M, adjusted to pH 3.5) at room temperature (Kerem et al. 1999). The UV absorbance of the eluant was monitored with a diode array detector to determine whether a shift in the polymer's molecular weight distribution had occurred (Hernandez and Ruiz 1998).

### 2.5.9 (*R*) and (*S*)-2-(4-hydroxyphenoxy)propionic acid

The (*R*) and (*S*)-enantiomers of 2-(4-hydroxyphenoxy)propionic acid (HPOPA) were analyzed using the instrument described above but equipped with an reversed phase Zorbax SB-C18 Rapid Resolution Cartridge column (2.1 mm diameter by 30 mm length, 3.5 µm particle size, Agilent) connected in series with an ORpak CDBS-453 column (4.6 mm diameter by 150 mm length, 3 µm particle size, Shodex). The isocratic mobile phase consisted of 10% acetonitrile

and 90% aqueous 0.2 mM sodium chloride that contained 1% vol/vol acetic acid. The columns were operated at 10 °C and 0.5 ml min<sup>-1</sup> for 35 min.

### 2.5.10 Milled wood and DHP

The reaction mixtures were analyzed by high performance size exclusion chromatography (HPSEC) for the determination of the molecular mass distribution of lignocellulose fragments suggested to be formed by *Aae*APO. The HPLC instrument equipped with a diode array detector was fitted with a HEMA-Bio linear column (8 by 300 mm, 100 μm, Polymer Standard Service Mainz). The mobile phase consisted of 20% acetonitrile and 80% of an aqueous solution of 0.5% NaCl and 0.2% K<sub>2</sub>HPO<sub>4</sub>; the pH was adjusted to 10.0 by the addition of NaOH.

### 2.5.11 Amines

Aniline, 4-(methylamino)phenol, 2-aminophenol and 4-aminophenol were analyzed using the HPLC-MS Method I but with an ammonium formate buffer at pH 7.

## 2.6 Stoichiometrical analyses

Stoichiometrical analyses of tetrahydrofuran cleavage were performed by HPLC as described above, using an external standard curve of 4-hydroxybutanal-2,4-dinitrophenylhydrazone for quantification of UV absorbance at 360 nm. Stoichiometrical analyses of methyl 3,4-dimethoxybenzyl ether cleavage were also performed by HPLC as described above, using an external standard curve of 3,4-dimethoxybenzaldehyde for quantification. Both standard curves had linear regression values with  $R^2 > 0.99$ . Concentrations of H<sub>2</sub>O<sub>2</sub>-solution were spectrophotometrically determined using the extinction coefficient of 39.4 M<sup>-1</sup> cm<sup>-1</sup> at 240 nm prior to each experiment.

## 2.7 Enzyme kinetics

### 2.7.1 1,4-dimethoxybenzene

The kinetic of 1,4-dimethoxybenzene cleavage was analyzed in stirred reactions (0.20 ml, 23 °C) that contained 0.52 μM of the peroxygenase, potassium phosphate buffer (50 mM, pH 7.0), and 0.010-1.500 mM of the ether. The reactions were initiated with 2.00 mM H<sub>2</sub>O<sub>2</sub> and stopped with 0.020 ml of 50% trichloric acid solution after 5 s, at which time less than 6% of

the tetrahydrofuran had been consumed. The resulting 4-methoxyphenol was quantified by HPLC as described above, and an apparent value of the  $K_m$  for 1,4-dimethoxybenzene was obtained by nonlinear regression using the Michaelis-Menten model in the ANEMONA program (Hernandez and Ruiz 1998).

### 2.7.2 Tetrahydrofuran

The kinetic of tetrahydrofuran cleavage was analyzed in stirred reactions (0.20 ml, 23 °C) that contained 0.193  $\mu\text{M}$  of the peroxygenase, potassium phosphate buffer (50 mM, pH 7.0), and 0.060-2.500 mM of the ether. The reactions were initiated with 2.00 mM  $\text{H}_2\text{O}_2$  and stopped with 0.400 ml of 0.1% 2,4-dinitrophenylhydrazine solution in 0.60 N HCl after 10 s, at which time less than 6% of the tetrahydrofuran had been consumed. The resulting 4-hydroxybutanal-2,4-dinitrophenylhydrazone was quantified by HPLC as described above, and an apparent value of the  $K_m$  for tetrahydrofuran was obtained by nonlinear regression using the Michaelis-Menten model in the ANEMONA program (Hernandez and Ruiz 1998).

### 2.7.3 Methyl 3,4-dimethoxybenzyl ether

The kinetics of methyl 3,4-dimethoxybenzyl ether cleavage were analyzed in stirred reactions (2.00 ml, 23 °C) that contained 0.098  $\mu\text{M}$  of the peroxygenase, potassium phosphate buffer (25 mM, pH 7.0), and 0.500-2.000 mM of the ether. The reactions were initiated with 0.067-0.200 mM  $\text{H}_2\text{O}_2$ , and the initial velocity of 3,4-dimethoxybenzaldehyde formation was measured by the increase in absorbance at 310 nm ( $\epsilon = 9300 \text{ M}^{-1} \text{ cm}^{-1}$ ) (Tien et al. 1986) using a Cary 50 UV/visible spectrophotometer. Three kinetic traces were obtained for each pair of substrate concentrations. Kinetic parameters were determined by nonlinear regression using the ping-pong model in the ANEMONA program (Hernandez and Ruiz 1998).

## 2.8 Experiments with $^{18}\text{O}$ -isotopes

### 2.8.1 Methyl 4-nitrobenzyl ether

The reaction mixtures (0.50 ml, stirred at room temperature) contained 2 U  $\text{ml}^{-1}$  of the peroxygenase, potassium phosphate buffer (50 mM, pH 7.0), and 0.5 mM methyl 4-nitrobenzyl ether. The reaction was initiated with 2.0 mM  $\text{H}_2^{18}\text{O}_2$  and stopped after 5 s by rapid mixing with 0.50 ml of benzene. A portion of the upper organic phase was immediately removed with a pipette and analyzed by GC/MS as described above. For each  $m/z$  value, the

average total ion count within the 4-nitrobenzaldehyde peak was used after background correction to generate the ion count used for mass abundance calculations.

### 2.8.2 Aromatic substrates

The reaction mixtures (0.20 ml, stirred at room temperature) contained 0.4 U ml<sup>-1</sup> of the peroxygenase, potassium phosphate buffer (25 mM, pH 7.0), and 0.5 mM of the substrate (1,4-dimethoxybenzene, 1,4-diethoxybenzene, 4-nitroanisole, propranolol, diclofenac and acetanilide). The reactions were initiated with 2.0 mM H<sub>2</sub><sup>18</sup>O<sub>2</sub>. The reaction products were analyzed as described before. The products were identified relative to an authentic standard, based on its retention time and [M-H]<sup>-</sup> ion. For each *m/z* value, the average total ion count within the product peak was used after background correction to generate the ion count used for mass abundance calculations.

### 2.8.3 Arylglycerol *beta*-aryl ethers

The reaction mixtures (0.20 ml) contained 0.4 U of the purified peroxygenase, potassium phosphate buffer (50 mM, pH 7.0), acetonitrile (5 %) and the arylglycerol *beta*-aryl ether (0.5 mM). When indicated the reactions also contained ascorbic acid (12 mM) to inhibit further oxidation of the phenolic products that were released (Kinne et al. 2008). The reactions were started by the addition of H<sub>2</sub><sup>18</sup>O<sub>2</sub> (5 mM) via syringe pump and continuously stirred for 1 hour at room temperature, at which time chromatographic analyses (HPLC-MS Method I) showed that product formation was complete. Aliquots of the reactions were derivatized using the 2,4-dinitrophenylhydrazine-solution (0.1%) to analyze the aldehydes released during reaction. In some of the reaction H<sub>2</sub><sup>18</sup>O (99 % atom) was added.

### 2.8.4 2-Phenoxypropionic acid

The reaction mixtures (0.2 ml) contained 2 U ml<sup>-1</sup> (0.9 μM) of purified *AaeAPO*, 50 mM potassium phosphate buffer (pH 7), and 0.5 mM of the substrate. The reaction was started by the addition of H<sub>2</sub>O<sub>2</sub> (2 mM) and stirred at room temperature. Ascorbic acid was added to a final concentration of 4 mM. The reactions mixtures were analyzed by HPLC-MS Method II.

## 2.9 Deuterium isotope effect experiment

The reaction mixtures (0.20 ml, stirred at room temperature) contained 0.4 U of the peroxygenase, potassium phosphate buffer (50 mM, pH 7.0), 4 mM ascorbate, and 0.5 mM 1-

methoxy-4-trideuteromethoxybenzene. The reaction was initiated with 2.0 mM H<sub>2</sub>O<sub>2</sub>, and 10 s later a portion was analyzed by LC/MS as described above. For each *m/z* value, the average total ion count within the 4-methoxyphenol peak was used after background correction to generate the ion count used for mass abundance calculations.

## 2.10 Experiments with <sup>14</sup>C-labeled compounds

To detect and quantify radio labeled products, fractions (0.5 ml) of HPLC-separated reaction mixtures were collected and assayed for <sup>14</sup>C by liquid scintillation counting (Tri-Carb 2900TR, Perkin-Elmer, USA) after mixing of the fraction with an scintillation cocktail (Emulsifier-Safe, Perkin-Elmer, USA) to a total volume of 5 ml.

## 2.11 Experiments with milled wood

The reaction mixture contained in a total of 1 ml of 50 mM potassium phosphate buffer (pH 7.0), 0.5% Tween 20, 10 mM glucose, 0.16 U ml<sup>-1</sup> of glucose oxidase (from *Aspergillus niger*; Sigma-Aldrich) and 2 U ml<sup>-1</sup> of *Aae*APO. The extracted wood (Tween 20 and water extracts) and the wood extract supernatant were incubated in reaction tubes (2 ml) closed with parafilm with vigorous stirring at 25°C for 24 h and 48 h after which time samples were analyzed by HPSEC as described above.

## 2.12 *In vivo*-incubation experiments

Liquid cultures (25 ml) of *Agrocybe aegerita* containing a soybean medium were prepared as described before (Ullrich et al. 2004). After five days of incubation a solution that contains Adlerol (1-(4-methoxy-3-methoxyphenyl)-2-(2-methoxyphenoxy)propane-1,3-diol) solved in ethanol was added to give a final concentration of approximately 100 μM. The *Aae*APO activity was monitored for 30 days of incubation using the veratryl alcohol assay described previously (Ullrich et al. 2004). To extract the Adlerol a whole culture flask was solved in ethanol (42 ml) mixed, centrifuged and analyzed by an HPLC-calibrated method as described above.

### 3. Results

#### 3.1 UV-Vis spectrophotometric features of *Aae*APO

*Aae*APO exhibits spectrophotometric and kinetic features of heme-thiolate proteins. Data from UV-Vis spectroscopy and difference spectroscopy are reported.

##### 3.1.1 Ligands of *Aae*APO

UV-Visible spectrophotometry has been used extensively in the detection and characterization of heme proteins, where the influence of substrate binding has marked effect on the appearance of the overall spectrum, especially with respect to the positions and intensities of the major absorption bands (Dawson et al. 1983). To describe the electronic structure and ligand binding properties a search for *Aae*APO-ligands was performed.

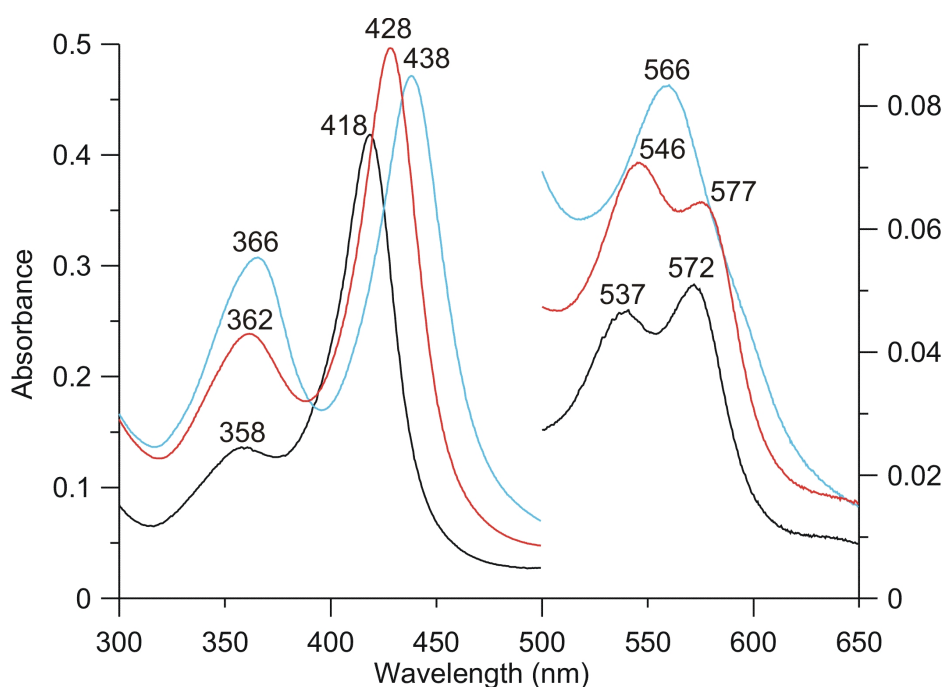


Figure 13 Absorption spectra of resting state *Aae*APO (black), the  $N_3^-$ -complex (red) and its  $CN^-$ -complex (blue).

The UV-Visible spectrum of the purified resting *Aae*APO exhibits a characteristic absorption peak at 418 nm (Soret band) and two charge transfer maxima at 537 and 572 nm (Figure 13, (Ullrich 2004)). Electronegative ligands, such as azide and cyanide were found to cause characteristic shifts of the Soret and charge transfer bands in the UV-Visible absorption spectra. Band positions of different *Aae*APO ligand complexes are shown in Table 2.



Table 2 *delta*-, Soret-, *beta*- and *alpha*-bands of *Aae*APO ligand complexes.

<b>Ligand</b>	<b><math>\delta</math></b>	<b>Soret band</b>	<b><math>\beta</math></b>	<b><math>\alpha</math></b>
<b>nm</b>				
Resting	357	418	537	572
Reduced (dithionite)	-	407	553	(565)
CO (Fe <sup>2+</sup> )	363	445	553	567
NO	359	430	544	579
CN <sup>-</sup> / CN <sup>-</sup> (Fe <sup>2+</sup> )	366	438/443	566	-
N <sub>3</sub> <sup>-</sup>	362	428	546	577
1-Phenylimidazole	360	424	542	(570)
Hydroxylamine	359	420	542	(572)

### 3.1.2 Difference spectrophotometry

The addition of a wide variety of substrates and inhibitors to P450s causes characteristic changes in the optical absorption spectrum, which reflect changes in the environment and electron density of the heme. According to Lewis two major specific types of difference binding spectra have been identified (Lewis and Sheridan 2001):

- Type I, which is characterized by a decrease in intensity of the Soret absorption peak around 418 nm, coupled with a concomitant increase in the band intensity of the 390 nm absorption. This type of UV-Visible absorption is indicative of the substrate's influence on the P450 heme iron spin-state equilibrium (Figure 14, A).
- Type II changes correspond to a shift of the Soret to longer wavelengths, with a consequent decrease in absorption at around 390- 420 nm and the formation of a peak at 420 to 435 nm in the difference spectrum (Figure 14, B).

The results in Figure 14 indicate that phenol, a substrate of *Aae*APO (Ullrich et al. 2004), caused a type I spectral change with the formation of a maximum around 390 nm and a minimum around 419 nm. A binding type II-like spectral change with a consequent formation of a minimum at 417 nm and a maximum around 440 nm was found when the heme protein inhibitor cyanide was added to the enzyme solution.

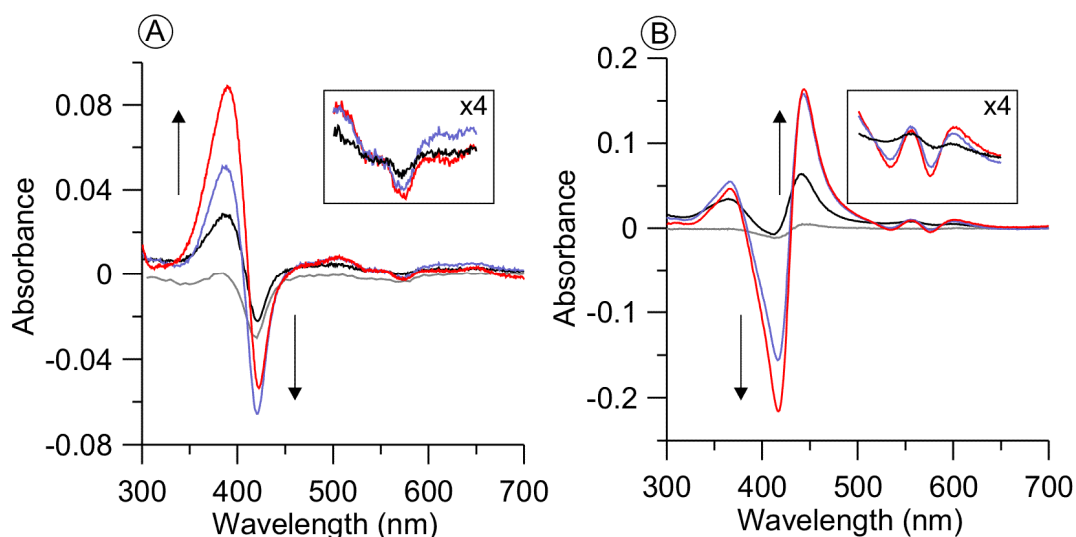


Figure 14 Difference absorption spectra of *Aae*APO obtained by the addition of A: phenol, (gray: 250  $\mu$ M, black: 1 mM; blue: 5 mM; red: 10 mM) and B: cyanide (gray: 1  $\mu$ M; black: 10  $\mu$ M; blue: 100  $\mu$ M; red: 250  $\mu$ M).

The difference spectra obtained for several compounds that were added to the peroxygenase solution are given in Table 3. The results show that substrates of *Aae*APO such as 3,4-dimethoxybenzyl alcohol, cause a type I binding spectrum whereas known heme protein inhibitors like azide cause a type II binding spectrum.

Table 3 Difference absorption spectra of *Aae*APO obtained by the addition different compounds

Ligand	$\lambda_{\text{max}}$ (nm)	$\lambda_{\text{min}}$ (nm)	Spectral type
3,4-dimethoxybenzyl alcohol	390	418	I
Phenol	389	419	I
H <sub>2</sub> O <sub>2</sub>	---	418	n.d.
Kaempferol	379	422	I
DMF	380	418	I
<sup>1</sup> Br <sup>-</sup>	392	421	I
<sup>1</sup> Cl <sup>-</sup>	405	390/416	I
<sup>1</sup> J <sup>-</sup>	385	425	I
SH <sup>-</sup>	378	419	I
HCOO <sup>-</sup>	430	408	II
CH <sub>3</sub> COO <sup>-</sup>	428	408	II
CN <sup>-</sup>	440	417	II
N <sub>3</sub> <sup>-</sup>	428	417	II
<sup>1</sup> F <sup>-</sup>	425	390	II

<sup>1</sup>pH was 3

The halogen ions caused no changes in the absorption spectra at pH 7 but show spectral changes at lower pH. For example, chloride induced a split of the Soret band with two maxima at 390 and 416 nm.

## 3.2 Oxidation of ethers

*AaeAPO* cleaves many types of ether, including some significant environmental pollutants, pharmaceuticals, phytoalexins and lignin model compounds. Data from stoichiometrical analyses, steady-state kinetics experiments, H<sub>2</sub><sup>18</sup>O<sub>2</sub>-labeling studies, determinations of intramolecular deuterium isotope effects and <sup>14</sup>C-radiolabeling tests are reported. In addition, limitations on the etherolytic reactions that the enzyme can accomplish are shown. Information about reaction products, which were identified by their mass spectra rather than by an authentic standard and which have not been published before is found in the appendix section.

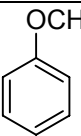
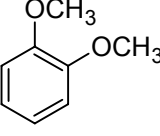
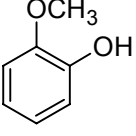
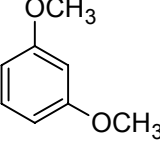
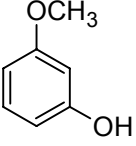
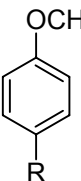
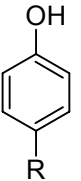
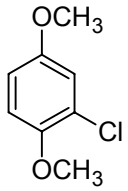
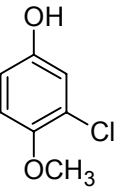
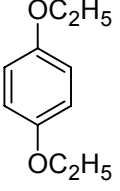
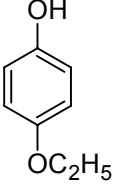
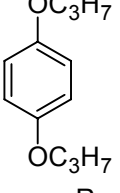
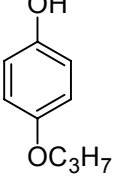
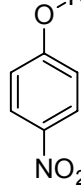
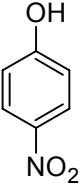
### 3.2.1 Aromatic ethers

Table 4 provides an overview of some alkyl aryl ethers that were cleaved by *AaeAPO* in the presence of H<sub>2</sub>O<sub>2</sub>. The methoxybenzenes I-V (Table 4) were cleaved by *AaeAPO* with a consequent formation of formaldehyde and the corresponding phenolic products. For some of the substrates it could be shown that aromatic ring hydroxylation was the preferred reaction catalyzed via the general peroxygenase activity of *AaeAPO*. Additionally a number of the phenols tended to undergo further oxidation to quinones and polymeric products because *AaeAPO* exhibits a peroxidase activity. To prevent product polymerization for some of the reactions ascorbic acid was used, scavenging the phenoxy radicals produced via the peroxidase activity of *AaeAPO*.

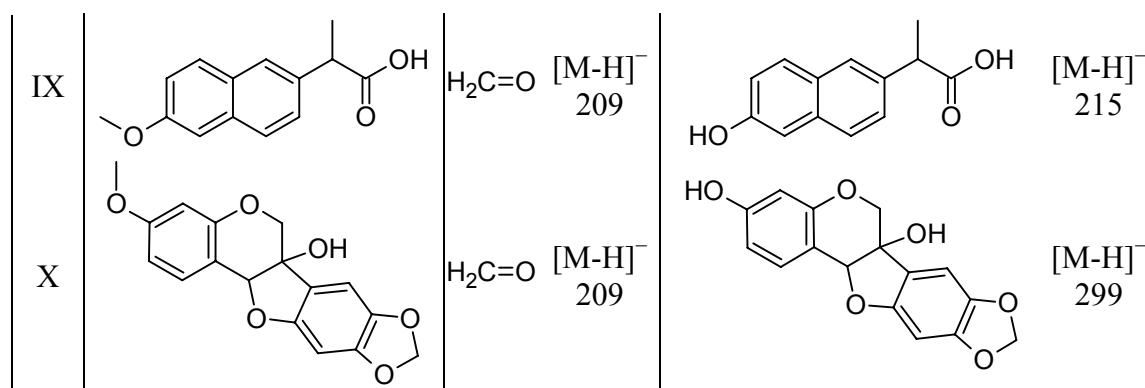
For example anisole (I) was completely converted by *AaeAPO*. The major reaction product in the presence of ascorbic acid was 4-methoxyphenol. Without ascorbate, *para*-benzoquinone was detected and the formation of a brown colored reaction liquid could be observed. Formaldehyde was released with and without ascorbate but phenol was not detectable. The formation of several hydrophilic reaction products could be observed but they were not identified. To study the regioselectivity of *AaeAPO*-catalyzed demethylation the dimethoxybenzenes II-IV were investigated and found to show different behavior as shown by product spectra. *AaeAPO* converted all the tested dimethoxybenzenes (*ortho*, *meta* and *para*). In a comparative analysis without ascorbate, the maximum conversion was: 5% for 1,2-dimethoxybenzene (II), 96% for 1,3-dimethoxybenzene (III) and 75% for 1,4-dimethoxybenzene (IV).

## RESULTS

Table 4 Products identified by mass spectroscopy after cleavage of alkyl aryl ethers by *Aae*APO in the presence of limiting  $\text{H}_2\text{O}_2$ . The  $m/z$  value for the major observed diagnostic ion is shown in each case.

	Substrate	Carbonyl product	Phenol product
I		$\text{H}_2\text{C}=\text{O}$ $[\text{M}-\text{H}]^-$ 209	n.d.
II		$\text{H}_2\text{C}=\text{O}$ $[\text{M}-\text{H}]^-$ 209	 $[\text{M}-\text{H}]^-$ 123
III		$\text{H}_2\text{C}=\text{O}$ $[\text{M}-\text{H}]^-$ 209	 $[\text{M}-\text{H}]^-$ 123
IV	 R: $\text{CH}_3$ , $\text{NO}_2$ , $\text{OCH}_3$ , F, Br	$\text{H}_2\text{C}=\text{O}$ $[\text{M}-\text{H}]^-$ 209	 <ul style="list-style-type: none"> <li><math>\text{CH}_3</math> <math>[\text{M}-\text{H}]^-</math> 107</li> <li><math>\text{NO}_2</math> <math>[\text{M}-\text{H}]^-</math> 138</li> <li><math>\text{OCH}_3</math> <math>[\text{M}-\text{H}]^-</math> 123</li> <li>F <math>[\text{M}]^+</math> 112</li> <li>Br <math>[\text{M}]^+</math> 172</li> </ul>
V		$\text{H}_2\text{C}=\text{O}$ $[\text{M}-\text{H}]^-$ 209	 $[\text{M}]^+$ 158
VI		$\text{H}_5\text{C}_2=\text{O}$ $[\text{M}-\text{H}]^-$ 223	 $[\text{M}-\text{H}]^-$ 137
VII		$\text{H}_7\text{C}_3=\text{O}$ $[\text{M}-\text{H}]^-$ 237	 $[\text{M}-\text{H}]^-$ 151
VIII	 R: $\text{C}_2\text{H}_4\text{OH}$ , $\text{CH}_2\text{CO}_2\text{H}$	n.d.	 $[\text{M}-\text{H}]^-$ 138

## RESULTS



However, 1,2-dimethoxybenzene and 1,3-dimethoxybenzene gave only traces of the corresponding phenols and formaldehyde, whereas 1,4-dimethoxybenzene gave 4-methoxyphenol as the major products of the reaction with *Aae*APO and  $\text{H}_2\text{O}_2$  in the presence of ascorbate (Figure 15A II and B).

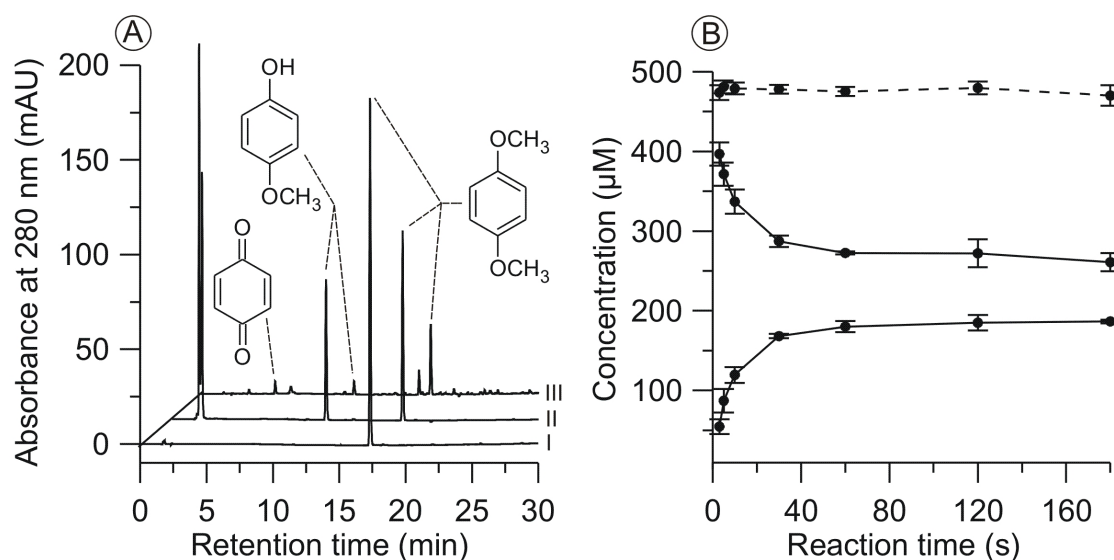


Figure 15 A: HPLC elution profiles showing the *O*-demethylation of 1,4-dimethoxybenzene to the corresponding 4-methoxyphenol after incubation with *Aae*APO. Control without enzyme (I). Completed reaction with ascorbic acid added (II). Completed reaction without ascorbic acid (III). B: Time course showing the formation of 4-methoxyphenol and the decomposition of 1,4-dimethoxybenzene in the presence of ascorbic acid. The dashed line represents the sum of the concentration of substrate and product.

Additionally, *para*-benzoquinone and some side products were formed when the reaction was conducted without a radical scavenger (Figure 15A III). The apparent  $K_m$  of the peroxygenase for 1,4-dimethoxybenzene was 0.36 mM, and the  $k_{\text{cat}}$  was  $106 \text{ s}^{-1}$ . When the reactions were conducted with the related phenols 2-, 3- and 4- methoxyphenol conversion during the *Aae*APO-catalyzed reaction was 100% with production of formaldehyde and colored byproducts. When 4-nitroanisole (IV) was used as the substrate, 4-nitrophenol and

formaldehyde were the major reaction products with and without a radical scavenger. No polymerization was observed. When the reaction was conducted with 2-chloro-1,4-dimethoxybenzene (V), a secondary metabolite of white rot fungi, two major reaction products appeared and were suggested as 3-chloro-4-methoxyphenol (see Appx. 1) and formaldehyde. *Aae*APO converted the alkoxybenzenes VI-VII (Table 4) with formation of the corresponding aldehydes and phenolic products. For example 1,4-diethoxybenzene (VI) and 1,4-dipropoxybenzene (VII) were converted to the corresponding phenols (4-ethoxy- and 4-propoxyphenol) and aldehydes (acetaldehyde and propionaldehyde) in the *Aae*APO-catalyzed reaction with H<sub>2</sub>O<sub>2</sub>. Several reaction products could be detected in the presence of a radical scavenger. The amount of byproducts increased with the size of the alkyl side chain. Without ascorbate, *para*-benzoquinone was detected and the formation of a brown colored reaction liquid could be observed.

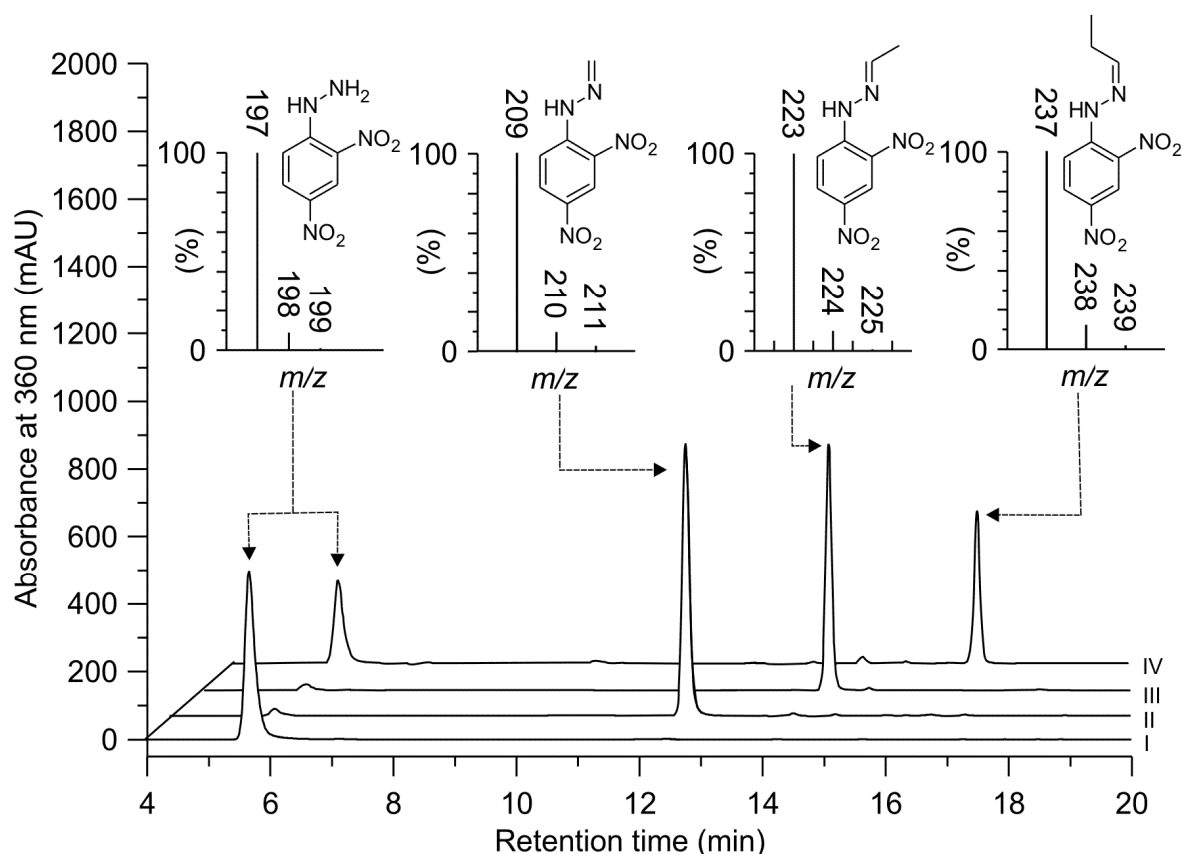


Figure 16 HPLC elution profiles showing different 2,4-dinitrophenylhydrazones from the reaction of *Aae*APO with 1,4-dimethoxybenzene (II), 1,4-diethoxybenzene (III), 1,4-dipropoxybenzene (IV) and H<sub>2</sub>O<sub>2</sub>. Control without enzyme (I, 2,4-dinitrophenylhydrazine).

Corresponding aldehydes were produced with and without ascorbate and could be detected as their 2,4-dinitrophenylhydrazones (Figure 16). The mass spectra in Figure 16 give conclusive

evidence that the aldehydes have the same carbon content as the alkyl side chain of the dimethoxybenzenes where they were released.

When reactions were conducted with 2-(4-nitrophenoxy)ethanol and 2-(4-nitrophenoxy)acetic acid (VIII), the major reaction products was 4-nitrophenol. Naproxen ((*S*)-2-(6-methoxynaphthalen-2-yl)propanoic acid, IX) a non-steroidal anti-inflammatory drug, was selectively demethylated to give formaldehyde and (+)-(*S*)-2-(6-hydroxynaphthalen-2-yl)propanoic acid, which is a human drug metabolite via liver metabolism. The phytoalexin pisatin (X) from *pisum sativum* was selectively oxidized to give formaldehyde and although in this case no authentic standards were available, the *m/z* value for one of the reaction products was the same as that expected for the demethylated product 3,6-*alpha*-dihydroxy-8,9-methylene-dioxypterocarpan (also called 6-*alpha*-hydroxymaackiain, 6-*alpha*-hydroxyinermin, see Appx. 2). Other phytoalexins such as 3,5-dimethoxystilbene were rapidly oxidized and polymerized (see Appx. 3).

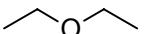
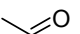
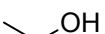
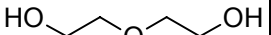
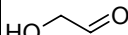
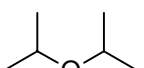
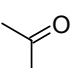
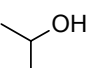
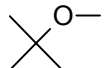
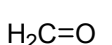
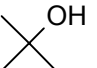
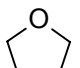
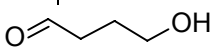
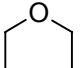
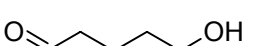
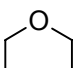
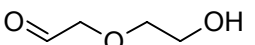
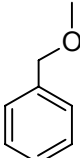
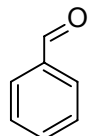
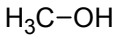
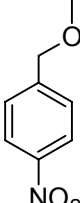
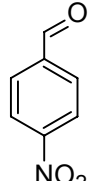
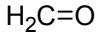
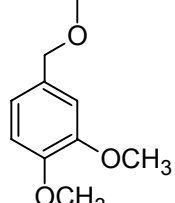
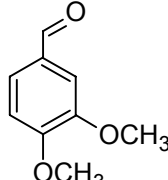
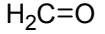
### 3.2.2 Aliphatic ethers

Table 5 provides an overview of the alkyl ethers that were cleaved via *Aae*APO-catalyzed reactions in the presence of H<sub>2</sub>O<sub>2</sub>. In qualitative experiments done with limiting H<sub>2</sub>O<sub>2</sub>, *Aae*APO cleaved diverse aliphatic ethers (I-VII, Table 5). The products were carbonyls (aldehydes and ketones), which were identified by HPLC/MS as their 2,4-dinitrophenylhydrazones, and alcohols, which were identified directly by GC/MS.

For example diethyl ether (I) was selectively cleaved by *Aae*APO to give formaldehyde and ethanol. The GC-MS elution profile clearly shows that both metabolites are formed (Figure 17). Some of the metabolites were further oxidized by *Aae*APO to give aliphatic acids. Diethylene glycol (II) a building block compound in organic synthesis was cleaved to give hydroxyacetaldehyde and other reaction products (see Appx. 4). The widely used solvent diisopropyl ether (III) gave the cleavage products acetone and isopropyl alcohol. Notably, the gasoline additive methyl *t*-butyl ether (IV) yielded formaldehyde and *tert*-butanol, and diethylene glycol was cleaved to give 2-hydroxyacetaldehyde. The cyclic ether tetrahydrofuran (V) was ring-opened to give 4-hydroxybutanal as the initial reaction product during the *Aae*APO-catalyzed reaction.

## RESULTS

Table 5 Products identified by mass spectroscopy after cleavage of alkyl ethers by *Aae*APO in the presence of limiting H<sub>2</sub>O<sub>2</sub>. The *m/z* value for the major observed diagnostic ion is shown in each case.

	Substrate	Carbonyl product	Alcohol product
I		 [M-H] <sup>-</sup> 223	 [M] <sup>+</sup> 46
II		 [M-H] <sup>-</sup> 239	n.d.
III		 [M-H] <sup>-</sup> 237	 [M-CH <sub>3</sub> ] <sup>+</sup> 45
IV		 [M-H] <sup>-</sup> 209	 [M-CH <sub>3</sub> ] <sup>+</sup> 59
V		 [M-H] <sup>-</sup> 267	
VI		 [M-H] <sup>-</sup> 281	
VII		 [M-H] <sup>-</sup> 283	
VIII		 [M] <sup>+</sup> 106	 [M+H] <sup>+</sup> 31
IX		 [M] <sup>+</sup> 151	 [M+H] <sup>+</sup> 31
X		 [M+H] <sup>-</sup> 167	 [M+H] <sup>+</sup> 31

The solvents tetrahydropyran (VI) and 1,4-dioxane (VII) were oxidized, and although in this case no authentic standards were available, the *m/z* values for the derivatized products were the same as those expected for the 2,4-dinitrophenylhydrazones of the ring-opened product 5-



hydroxypentanal in the case of tetrahydropyran and 2-(2-hydroxyethoxy)acetaldehyde in the case of 1,4-dioxane.

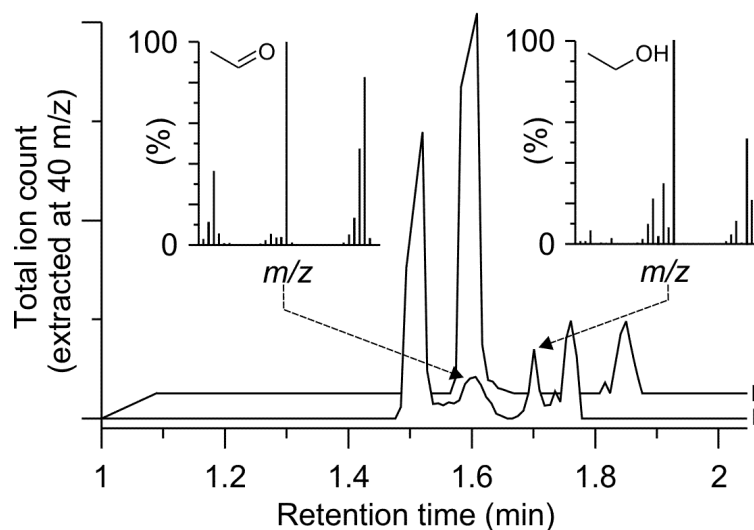


Figure 17 GC-MS profile showing products formed by *AaeAPO* after conversion of diethylether. Completed reaction (I). Control without enzyme (II). Insets show the mass spectra of the reaction products.

When these reactions were conducted with nonlimiting  $\text{H}_2\text{O}_2$ , oxidation of the resulting alcohol moieties also occurred, thus generating additional carbonyl groups. For example, 1,4-dioxane was cleaved at both ether linkages and then further oxidized to glyoxal under these conditions.

### 3.2.3 Stoichiometry of ether cleavage

A quantitative analysis of tetrahydrofuran cleavage in the presence of limiting oxidant showed that one equivalent of 4-hydroxybutanal was formed per equivalent of  $\text{H}_2\text{O}_2$  supplied (Table 6).

Table 6 Stoichiometry of tetrahydrofuran oxidation by *AaeAPO*.<sup>a</sup>

$\text{H}_2\text{O}_2$ added	4-Hydroxybutanal produced	4-Hydroxybutanal/ $\text{H}_2\text{O}_2$
	$\mu\text{M}$	
100	101	1.01
200	194	0.97
300	292	0.97
400	375	0.94
500	489	0.98

<sup>a</sup>The initial tetrahydrofuran concentration was 10 mM.

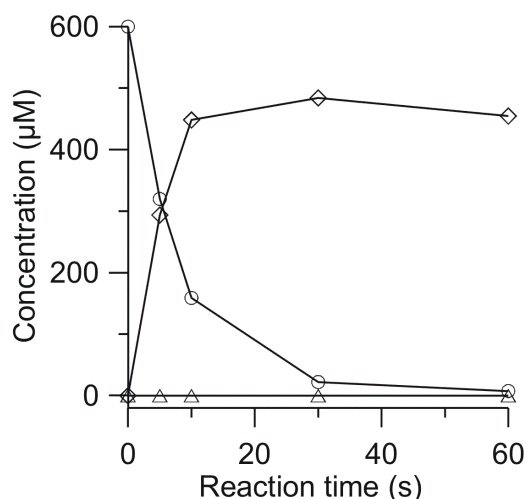


Figure 18 Time course showing the formation of 4-nitrobenzaldehyde (◊) and the decomposition of methyl 4-nitrobenzyl ether (o) during *AaeAPO* catalyzed reaction. 4-nitrobenzyl alcohol (Δ) was not detected.

methyl 4-nitrobenzyl ether (IX) showed that the initial reaction product of the *AaeAPO* catalyzed reaction was 4-nitrobenzaldehyde (Figure 18). The presence of 4-nitrobenzyl alcohol was not observed but 4-nitrobenzaldehyde was further oxidized by *AaeAPO* to give 4-nitrobenzoic acid.

The apparent  $K_m$  of the peroxygenase for tetrahydrofuran was 2.1 mM, and the initial turnover rate of the enzyme with 2.5 mM of this ether and 2.0 mM  $H_2O_2$  was  $33\ s^{-1}$ . The peroxygenase cleaved methyl benzyl ethers such as VIII, IX and X (Table 5), yielding benzaldehydes and methanol, which were identified by HPLC and GC/MS without derivatization.

The benzyl alcohols were not detectable as products, even when  $H_2O_2$  was limiting, and formaldehyde was found only in extended reactions with excess  $H_2O_2$ . For example, the HPLC results obtained with

Table 7 Stoichiometry of methyl 3,4-dimethoxybenzyl ether oxidation by *AaeAPO*<sup>a</sup>

$H_2O_2$ added	3,4-Dimethoxybenzaldehyde produced	3,4-Dimethoxybenzaldehyde/ $H_2O_2$
	µM	
11	12	1.09
22	23	1.05
33	33	1.00
44	43	0.98
55	54	0.98
110	105	0.95

<sup>a</sup>The initial methyl 3,4-dimethoxybenzyl ether concentration was 1.0 mM.

HPLC/MS results obtained with methyl benzyl ether (VIII) and methyl 3,4-dimethoxybenzyl ether (X) showed no formation of the corresponding alcohols but rather give clear evidence that the aldehyde was the initial reaction product.

A quantitative analyses of methyl 3,4-dimethoxybenzyl ether cleavage in the presence of limiting  $H_2O_2$  was consistent with this picture, showing that one equivalent of 3,4-dimethoxybenzaldehyde was produced per equivalent of oxidant supplied (Table 7).

### 3.2.4 pH-Optimum of ether cleavage

The pH optimum the *Aae*APO-catalyzed reaction of 3,4-dimethoxybenzyl ether was 7.0, with 50% activity occurring at pH 5.4 and pH 8.4 (Figure 19).

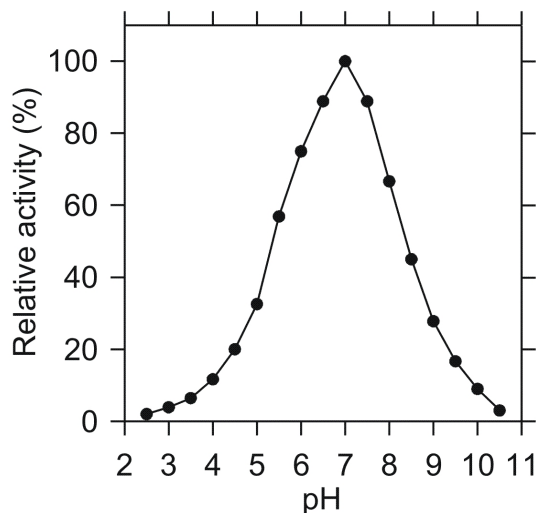
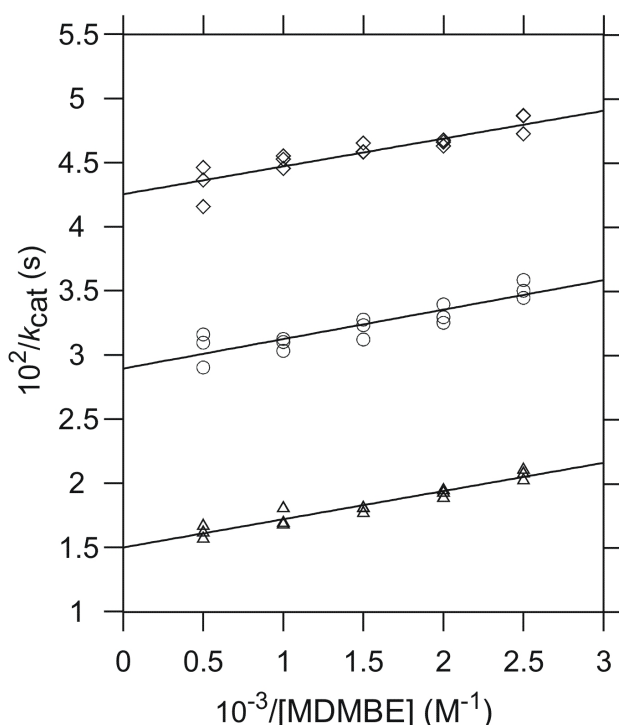


Figure 19 Relative rates of methyl 3,4-dimethoxybenzyl ether cleavage by the *Aae*APO at various pH values.

### 3.2.5 Bisubstrate kinetics



Since a direct spectrophotometric assay is available to monitor the production of 3,4-dimethoxybenzaldehyde (Tien et al. 1986), methyl 3,4-dimethoxybenzyl ether was selected for initial rate kinetics experiments at pH 7.0, assuming steady-state conditions and using a nonlinear regression method to calculate the kinetic parameters (Hernandez and Ruiz 1998). The results gave a  $k_{\text{cat}}$  of  $720 \pm 87 \text{ s}^{-1}$ , a  $K_{\text{m}}$  for  $\text{H}_2\text{O}_2$  of  $1.99 \pm 0.25 \text{ mM}$  ( $k_{\text{cat}}/K_{\text{m}} = 3.6 \times 10^5 \text{ M}^{-1} \text{ s}^{-1}$ ), and a  $K_{\text{m}}$  for methyl 3,4-dimethoxybenzyl ether of  $1.43 \pm 0.23$

Figure 20 Double reciprocal plots of the kinetics data for methyl 3,4-dimethoxybenzyl ether (MDMBE) cleavage by *Aae*APO. The  $\text{H}_2\text{O}_2$  concentrations used were 0.067 mM ( $\diamond$ ), 0.100 mM ( $\circ$ ), and 0.200 mM ( $\triangle$ ). The kinetic parameters reported in the text were calculated by a nonlinear regression method (Hernandez and Ruiz 1998).

mM ( $k_{\text{cat}}/K_m = 5.0 \times 10^5 \text{ M}^{-1} \text{ s}^{-1}$ ). Double reciprocal plots of the same data gave parallel lines (Figure 20).

### 3.2.6 Source of the oxygen introduced during ether cleavage

It was shown by  $^{18}\text{O}$ -labeling that  $\text{H}_2\text{O}_2$  supplies the oxygen atom that the *Aae*APO introduces when it hydroxylates aromatic rings. The analogous experiment is difficult with alkyl ethers, because the oxygen on the resulting aliphatic aldehyde exchanges rapidly in water. However,

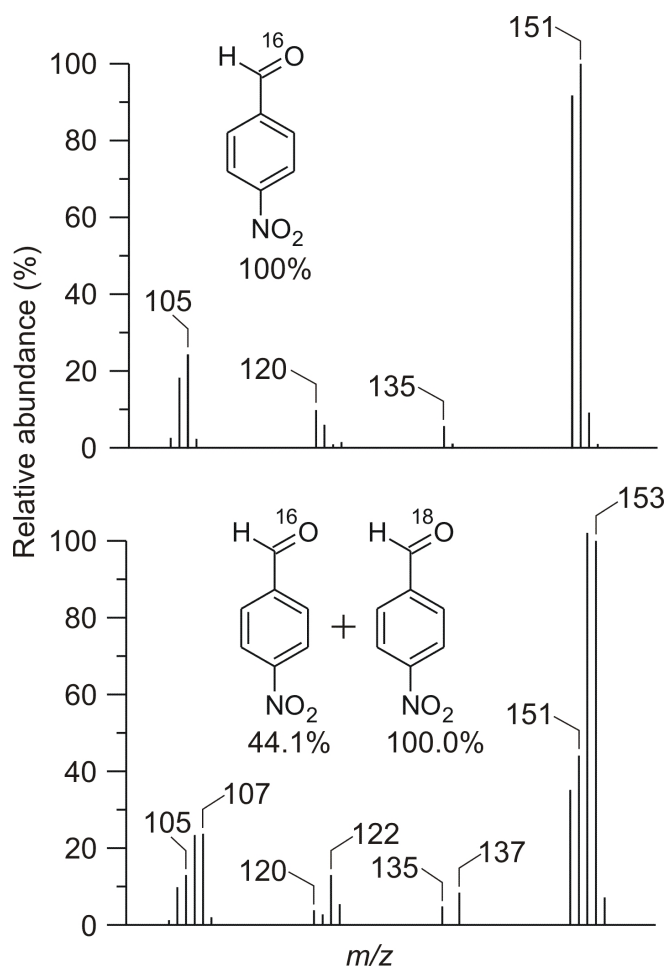


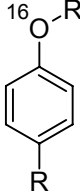
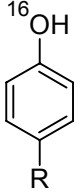
Figure 21 Incorporation of  $^{18}\text{O}$  from  $\text{H}_2^{18}\text{O}_2$  into the carbonyl group of 4-nitrobenzaldehyde after cleavage of methyl 4-nitrobenzyl ether by *Aae*APO. *Upper*: MS of the product obtained with natural abundance  $\text{H}_2\text{O}_2$ . Structural assignments for  $m/z$  values are as follows:  $[\text{M}]^+$ , 151;  $[\text{M} - \text{O}]^+$ , 135;  $[\text{M} - \text{NO} - \text{H}]^+$ , 120;  $[\text{M} - \text{NO}_2]^+$ , 105. *Lower*: MS of the product obtained with 90 atom %  $\text{H}_2^{18}\text{O}_2$ .

(Figure 21). The results indicate that the introduced  $^{18}\text{O}$ -species from  $\text{H}_2\text{O}_2$  is released with the carbonyl product instead of with the alcoholic product during the ether cleavage by *Aae*APO. Experiments done with 4-nitroanisole, 1,4-dimethoxybenzene and 1,4-diethoxybenzene and *Aae*APO in the presence of  $^{18}\text{O}$ -labeled  $\text{H}_2\text{O}_2$  and/ or  $\text{H}_2\text{O}$  were consistent with this picture. The results showed no changes in the mass of the molecular ion

benzaldehyde oxygens exchange less rapidly, making the assay feasible with benzyl ethers if a short reaction time is employed (Tien and Kirk 1984). Methyl 4-nitrobenzyl ether (IX, Table 5) was selected as the substrate because the nitro substituent in the resulting benzaldehyde has been reported to slow the exchange additionally (Samuel 1965). GC/MS analysis showed that the peroxygenase-catalyzed cleavage of this ether in the presence of 90 atom %  $\text{H}_2^{18}\text{O}_2$  resulted in 69%  $^{18}\text{O}$  incorporation into the carbonyl group of the resulting 4-nitrobenzaldehyde, as evidenced by the shift of the principal molecular ion from  $m/z$  151 to  $m/z$  153

of the corresponding phenolic (alcoholic) mass (Table 8). The release of  $^{18}\text{O}$ -labeled formaldehyde or acetaldehyde was not observed because of the rapid exchange rates of oxygen in aliphatic aldehydes with water.

Table 8 Conversion of alkyl aryl ethers with the *AaeAPO* in the presence  $^{18}\text{O}$ -isotope enriched  $\text{H}_2^{18}\text{O}$  und  $\text{H}_2^{18}\text{O}_2$

Substrate	Reaction with...	Product
	$\text{H}_2^{16}\text{O}_2$ in $\text{H}_2^{16}\text{O}$	
	$\text{H}_2^{18}\text{O}_2$ in $\text{H}_2^{16}\text{O}$	
	$\text{H}_2^{16}\text{O}_2$ in $\text{H}_2^{18}\text{O}$	

### 3.2.7 Deuterium isotope effect experiments

As previously shown, *AaeAPO* cleaved alkyl aryl ethers, yielding aliphatic aldehydes and phenols. The phenols tended to undergo further oxidation to polymeric products and 1,4-benzoquinone because this enzyme exhibits general peroxidase activity (Ullrich and Hofrichter 2007). However, the phenolic products were readily detectable when ascorbate was included in the assay to suppress their further oxidation (Kinne et al. 2009b, Kinne et al. 2008). By this method it was found, for example, that 1,4-dimethoxybenzene (IV, Table 4) was oxidized to 4-methoxyphenol. Since 1,4-dimethoxybenzene is symmetrical and its methoxyl carbons are not prochiral, it is a suitable substrate to determine whether a catalyzed etherolytic reaction exhibits an intramolecular deuterium isotope effect, which gives an approximate value for the intrinsic deuterium isotope effect on cleavage of the ether bond (Foster et al. 1974, Yun et al. 2005, Nelson and Trager 2003). HPLC/MS analysis showed that the peroxygenase-catalyzed cleavage of 1-methoxy-4-trideuteriomethoxybenzene resulted in a marked preponderance of 4-methoxyphenol- $d_3$  ( $m/z$  126,  $[\text{M}-\text{H}]^-$ ) over 4-methoxyphenol- $h_3$  ( $m/z$  123,  $[\text{M}-\text{H}]^-$ ) and a preponderance of formaldehyde-2,4-dinitrophenylhydrazone- $h_2$  ( $m/z$  209,  $[\text{M}-\text{H}]^-$ ) over formaldehyde-2,4-dinitrophenylhydrazone- $d_2$  ( $m/z$  211,  $[\text{M}-\text{H}]^-$ ) (Figure 22). The observed mean intramolecular isotope effect  $[(k_{\text{H}}/k_{\text{D}})_{\text{obs}}]$  from three experiments was  $11.9 \pm 0.4$ .

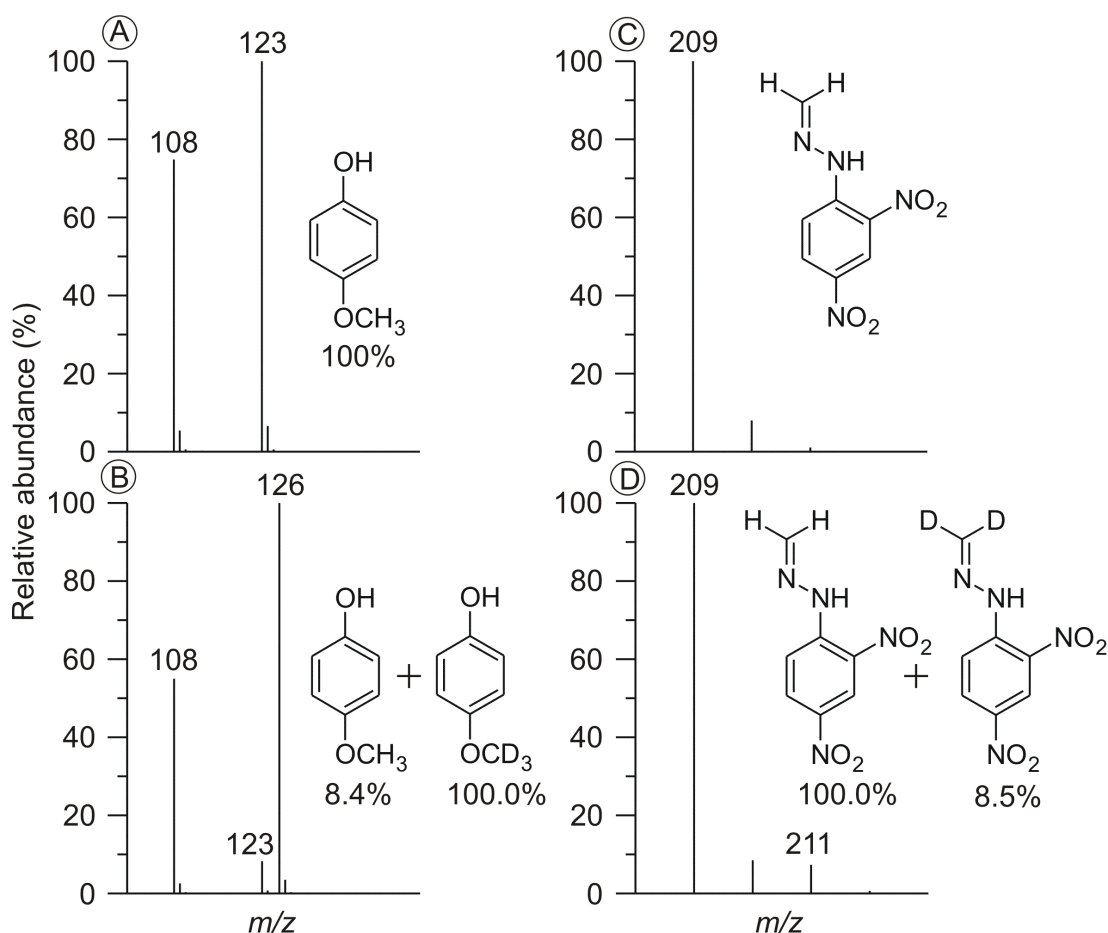
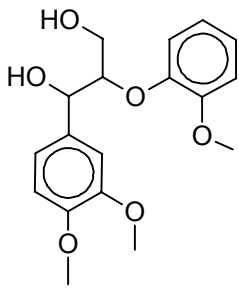
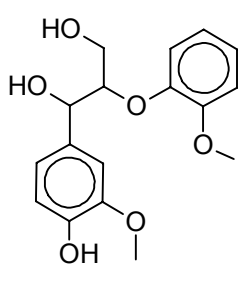
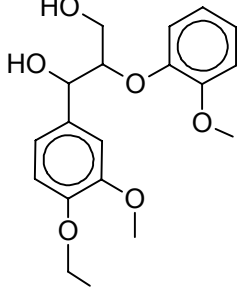


Figure 22 Preferential cleavage by *Aae*APO of the non-deuterated methoxyl group in 1-methoxy-4-trideutero-methoxy-benzene. **A:** MS of 4-methoxyphenol-*h*3 obtained from the oxidation of natural abundance 1,4-dimethoxybenzene. **B:** MS of the 4-methoxyphenol-*h*3/4-methoxyphenol-*d*3 mixture obtained from the oxidation of 1-methoxy-4-trideuteromethoxybenzene. **C:** MS of formaldehyde-2,4-dinitrophenylhydrazone obtained from the oxidation of natural abundance 1,4-dimethoxybenzene. **D:** MS of the formaldehyde-2,4-dinitrophenylhydrazone-*h*2/formaldehyde-2,4-dinitrophenylhydrazone-*d*2 mixture obtained from the oxidation of 1-methoxy-4-trideuteromethoxybenzene. **B:** MS shown is one of three used to calculate the observed mean intramolecular isotope effect.

### 3.2.8 Arylglycerol *beta*-aryl ether

*Aae*APO cleaves nonphenolic lignin model compounds of the arylglycerol *beta*-aryl ether (*beta*-O-4) type by selective demethylation of the *para*-methoxyl group to give the corresponding aldehydes and phenols followed by oxidative cleavage of the phenolic dimer and polymerization of the monomeric reaction products. Hydroxylation of aromatic rings was observed. Table 9 provides an overview of the arylglycerol *beta*-aryl ethers that were cleaved by the *Aae*APO in the presence of H<sub>2</sub>O<sub>2</sub>. Typical HPLC elution profiles for completed *Aae*APO-catalyzed reactions of a lignin model compounds are shown in Figure 23.

Table 9 Products identified by mass spectroscopy after cleavage of non-phenolic arylglycerol *beta*-aryl ethers by the *Aae*APO in the presence  $H_2O_2$  and ascorbic acid. The  $m/z$  value for the major observed diagnostic ion is shown.

	Substrate	Carbonyl product	Phenol product
I		$H_2C=O$ $[M-H]^-$ 209	 $[M-H]^-$ 319
II		$H_5C_2=O$ $[M-H]^-$ 223	

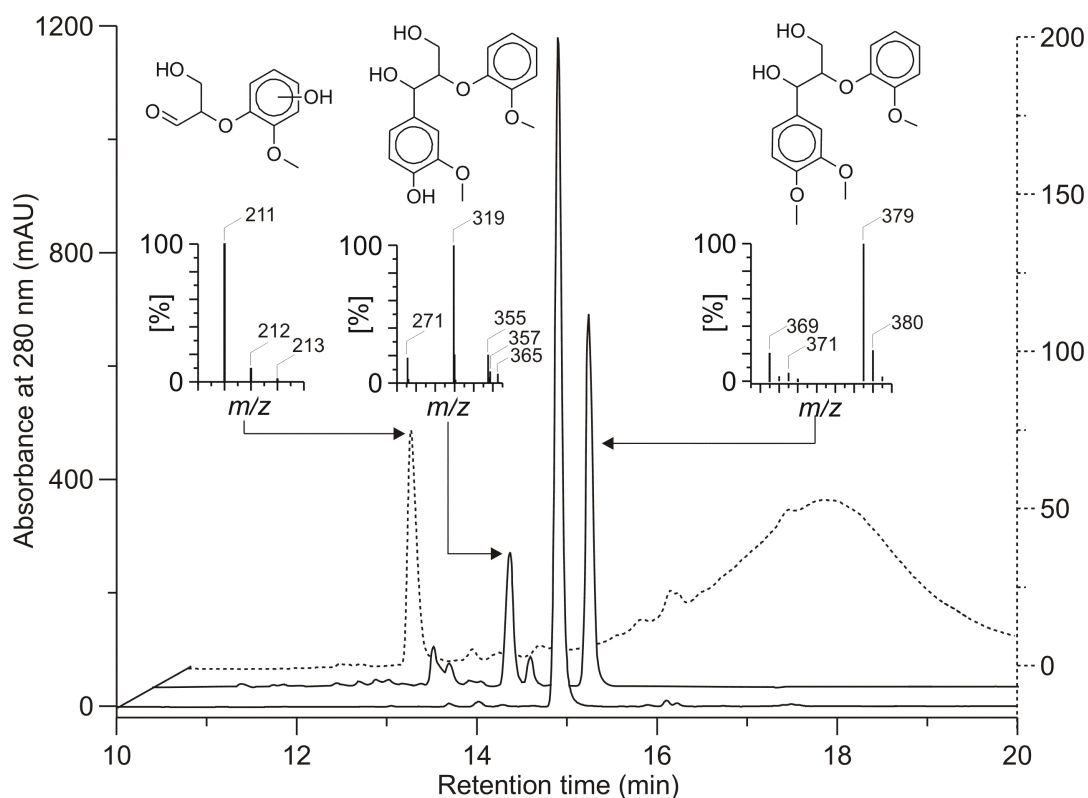


Figure 23 HPLC elution profile of *Aae*APO-catalyzed conversion of compound I. *Front line*: reaction without enzyme, *second line*: reaction in the presence of ascorbic acid (12 mM) and *dotted line*: reaction in the absence of ascorbic acid. Insets of respective mass spectra are shown. The substrate mass is  $[M+HCOOH-H]^-$  379.

*Aae*APO-catalyzed the H<sub>2</sub>O<sub>2</sub>-dependent cleavage of 1-(4-methoxy-3-methoxyphenyl)-2-(2-methoxyphenoxy)propane-1,3-diol (I, adlerol) a dimeric model compound that represents the major nonphenolic structure in lignin. The results show that *Aae*APO generated numerous products from the lignin model I in the presence of H<sub>2</sub>O<sub>2</sub>.

In the presence of ascorbic acid, solely dimeric products of model I could be detected. The total conversion of compound I (500 μM) was 175 μM (35%) with a consequent formation of 110 μM of the major reaction product III (Table 10, 1-(4-hydroxy-3-methoxyphenyl)-2-(2-methoxyphenoxy)propane-1,3-diol; 63% of total conversion) and 20 μM of formaldehyde-2,4-dinitrophenylhydrazone. When the reaction was conducted with compound II, 1-(4-ethoxy-3-methoxyphenyl)-2-(2-methoxyphenoxy)propane-1,3-diol, (etherol; 400 μM) instead of compound I, total conversion was 170 μM (43%) with a consequent formation of 150 μM compound III (88% of total conversion) and 30 μM acetaldehyde-2,4-dinitrophenylhydrazone.

The formation of ring-hydroxylated products can be suggested, as some of the minor peaks in Figure 23 show mass spectra with appropriate ion shifts of the principal [M-H]<sup>-</sup> ions of I, II and III to *m/z* [M-H+16]<sup>-</sup> and *m/z* [M-H+32]<sup>-</sup>. When H<sub>2</sub><sup>18</sup>O<sub>2</sub> was added as oxidant instead of natural abundance H<sub>2</sub>O<sub>2</sub>, the *m/z* of the demethylated product III stayed constant as described before.

Table 10 Products identified by mass spectroscopy after cleavage of phenolic arylglycerol *beta*-aryl ethers by the *Aae*APO in the presence H<sub>2</sub>O<sub>2</sub> and ascorbic acid. The *m/z* value for the major observed diagnostic ion is shown.

		Further Reaction Products	
III			
IV		[M-H] <sup>-</sup> 211	 [M+H] <sup>+</sup> 349



## RESULTS

The principal  $[M-H]^-$  ion masses of some side product ions shifted from natural abundance  $m/z$  ( $[m/z + 16]$  and  $[m/z + 32]$  of I, II and III) to  $[m/z + 16 + 2]$  and  $[m/z + 16 + 4]$  suggesting ring hydroxylation with oxygen introduction into the substrate from  $H_2O_2$ . The identification of ring-hydroxylated products by means of authentic standards was not performed, as the yields were very low. A formation of *alpha*-carbon ketones from substrate I and II was not observed. In the absence of ascorbic acid, predominantly monomeric and polymerization products of compound I and II could be detected (Figure 23). Models I and II were cleaved to give the hydroxylated species of 3-hydroxy-2-(2-methoxyphenoxy)propanal and traces of 2-methoxybenzoquinone.

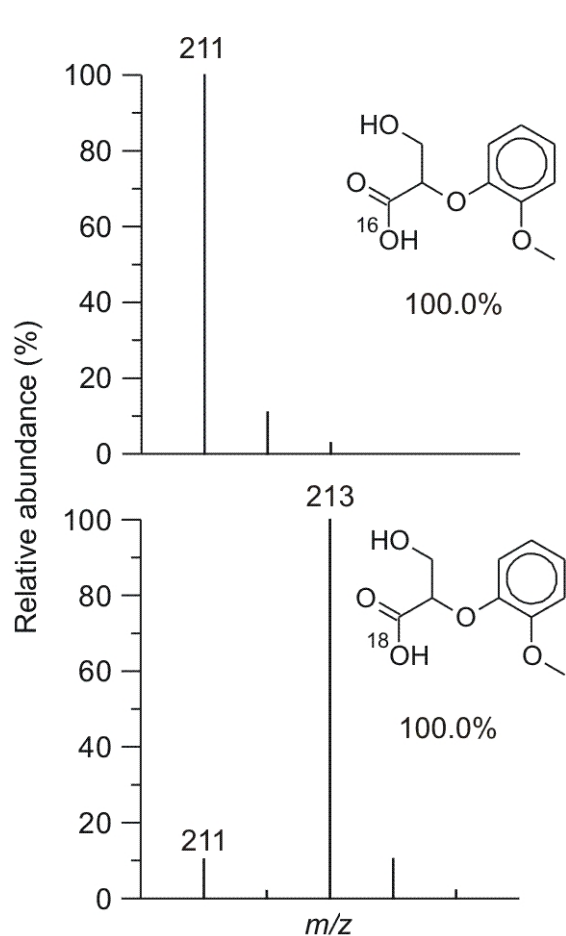


Figure 24 Incorporation of  $^{18}O$  from  $H_2^{18}O_2$  into the suggested hydroxylated species of 3-hydroxy-2-(2-methoxyphenoxy)propanal after hydroxylation of the arylglycerol aryl ether by *AaeAPO*. *Upper*: MS of the product obtained with natural abundance  $H_2O_2$ . *Lower*: MS of the product obtained with 90 atom %  $H_2^{18}O_2$ .

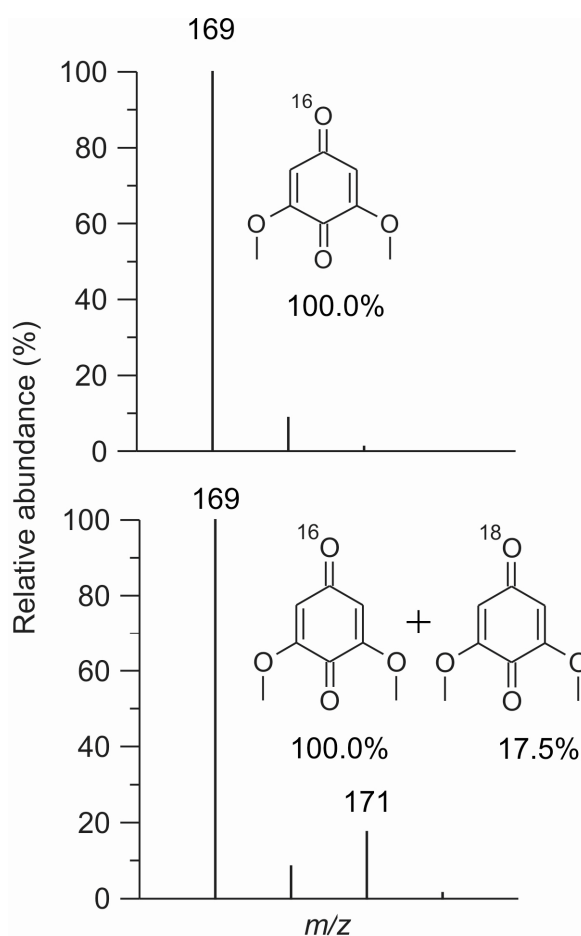


Figure 25 Incorporation of  $^{18}O$  from  $H_2^{18}O$  into the quinone group of 3,5-dimethoxybenzoquinone after cleavage of compound I by *AaeAPO*. *Upper*: MS of the product obtained with natural abundance  $H_2O_2$ . *Lower*: MS of the product obtained with 20% of 90 atom %  $H_2^{18}O$ .

When the *Aae*APO-catalyzed oxidations of I and II were conducted with  $\text{H}_2^{18}\text{O}_2$  in place of  $\text{H}_2\text{O}_2$ , mass spectral analysis of the resulting hydroxylated species of 3-hydroxy-2-(2-methoxyphenoxy)propanal showed that the principal  $[\text{M}-\text{H}]^-$  ion had shifted from the natural abundance  $m/z$  of 211 to  $m/z$  213 (Figure 24). 2-Methoxybenzoquinone could not be detected by mass spectrometry as it was rapidly polymerized by *Aae*APO.

To analyze quinone formation compound III, 1-(4-hydroxy-3,5-dimethoxyphenyl)-2-(2-methoxyphenoxy)propane-1,3-diol, the substrate was incubated with *Aae*APO, which gave the products 3,5-dimethoxybenzoquinone and hydroxylated species of 3-hydroxy-2-(2-methoxyphenoxy)propanal during the *Aae*APO-catalyzed reaction. HPLC/MS analysis showed that the peroxygenase-catalyzed cleavage of IV in the presence of 20%  $\text{H}_2^{18}\text{O}$  resulted in 20%  $^{18}\text{O}$  incorporation into 3,5-dimethoxybenzoquinone, as evidenced by the shift of the principal molecular ion from  $m/z$  169 to  $m/z$  171 (Figure 25). The presence of 3-hydroxy-1-(4-hydroxy-3,5-dimethoxyphenyl)-2-(2-methoxyphenoxy)propan-1-one (Table 10) was confirmed from its mass spectrum.

Polymerization of the reaction products from the reaction of arylglycerol *beta*-aryl ethers with

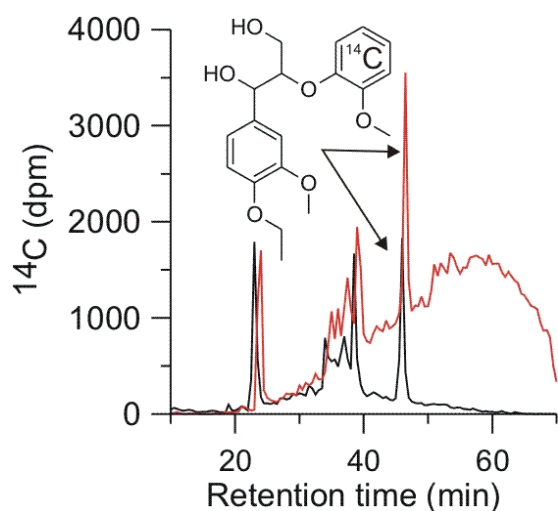


Figure 26 HPLC radiochromatogram of products obtained from the treatment of radiolabeled model II with *Aae*APO. Red: completed reaction. Black: 10 kDa permeate of the completed reaction.

*Aae*APO and  $\text{H}_2\text{O}_2$  was observed in the absence of a radical scavenger. To quantify the polymerization products *threo*-1-(4-ethoxy-3-methoxy-*ring*- $^{14}\text{C}$ )phenyl)-2-(2-methoxyphenoxy)propane-1,3-diol was incubated with *Aae*APO and  $\text{H}_2\text{O}_2$  and then filtered through a filter membrane with a 10-kDa cut-off (Figure 26). In a reaction were a total activity of 97599 dpm of the radiolabeled substrate was used 25996 dpm (27%) was found to pass the membrane and 71633 dpm (73%) was retained. In the presence of ascorbic acid no polymerization was detected.

### 3.2.9 Scope of ether cleavage

It was found that the *Aae*APO failed to cleave some ethers. For example, although it produced 4-nitrophenol from 4-nitroanisole (Table 4), no release of 4-nitrophenol was detectable when 4-(4-nitrophenoxy)benzoic acid was employed instead as a substrate. Hexaethylene glycol was not converted by *Aae*APO. It was also found that the ether linkages in a 4-nitrophenyl-

terminated PEG (Figure 27) and in a dehydrogenative polymer (DHP) of coniferyl alcohol (*i.e.*, synthetic lignin) were not detectably cleaved.

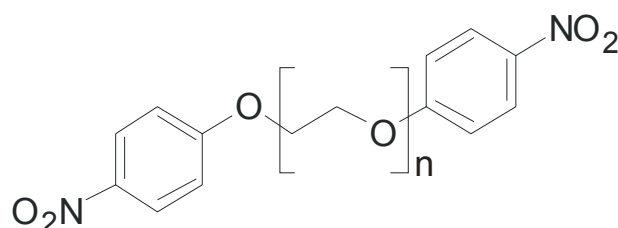


Figure 27 4-Nitrophenyl-terminated polyethylene glycol ( $n \approx 45$ ).

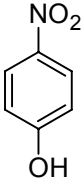
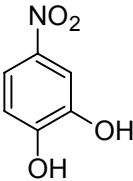
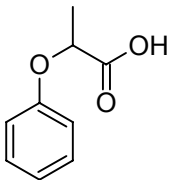
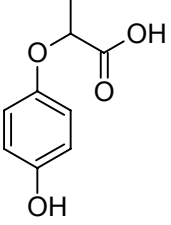
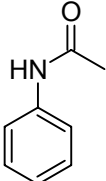
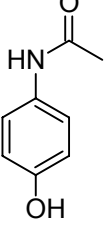
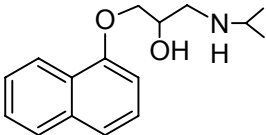
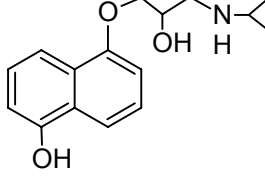
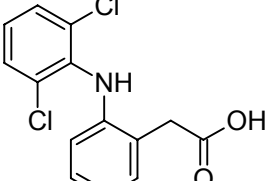
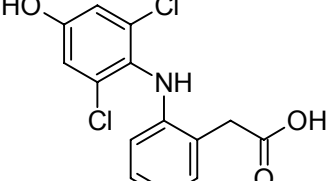
As described previously, it was found that the peroxygenase released *n*-propanal efficiently from 1,4-di-*n*-propoxybenzene, but released only traces of *n*-butanal from 1,4-di-*n*-butoxybenzene. The enzyme failed to cleave phenoxypropionic acid and propranolol (Table 11). *In vivo* experiments conducted with arylglycerol *beta*-aryl ethers and *Agrocybe aegerita* showed no conversion of the lignin model compounds even when the enzyme was secreted. Moreover, SEC-results from reactions mixtures of *Aae*APO incubated with milled pine and poplar wood in the presence of glucose oxidase and glucose as an  $H_2O_2$ -generating system showed no release of soluble aromatic compounds. The wood extracts (supernatant fractions) were polymerized by *Aae*APO.

### 3.3 Ring hydroxylation of aromatic compounds

*Aae*APO hydroxylated aromatic rings of many compounds, including some significant pharmaceuticals and industrially relevant substances. Data from  $^{18}O$ -labeling studies and an enantio- and regioselective analysis are reported. Table 11 provides an overview of some aromatics that were hydroxylated by *Aae*APO in the presence of  $H_2O_2$ .

Table 11 Products identified by mass spectroscopy after ring hydroxylation of aromatics by *Aae*APO in the presence of  $H_2O_2$ . The  $m/z$  value for the major observed diagnostic ion is shown in each case.

	Substrate	Phenolic product
1		 $[M-H]^-$ 138

II			[M-H] <sup>-</sup> 154
III			[M-H] <sup>-</sup> 181
IV			[M-H] <sup>-</sup> 152
V			[M-H] <sup>-</sup> 274
VI			[M-H] <sup>-</sup> 311

### 3.3.1 Nitroaromatics

Nitrobenzene was hydroxylated by *Aae*APO to give 4-nitrophenol in experiments conducted with continuous addition of H<sub>2</sub>O<sub>2</sub> via a syringe pump. For example, in reactions where one equivalent of H<sub>2</sub>O<sub>2</sub> was added over 40 min using 5 U ml<sup>-1</sup> of the peroxygenase, approximately 2% of nitrobenzene was hydroxylated to 4-nitrophenol.

Figure 28 illustrates the HPLC elution profiles of reaction mixtures after *Aae*APO-catalyzed oxidation of nitrophenol. After treatment with *Aae*APO, one major metabolite appeared and was identified as 4-nitrocatechol in the presence of a radical scavenger. In the absence of ascorbic acid, 4-nitrocatechol was further oxidized to give several unidentified hydrophilic products. Polymerization was not observed.

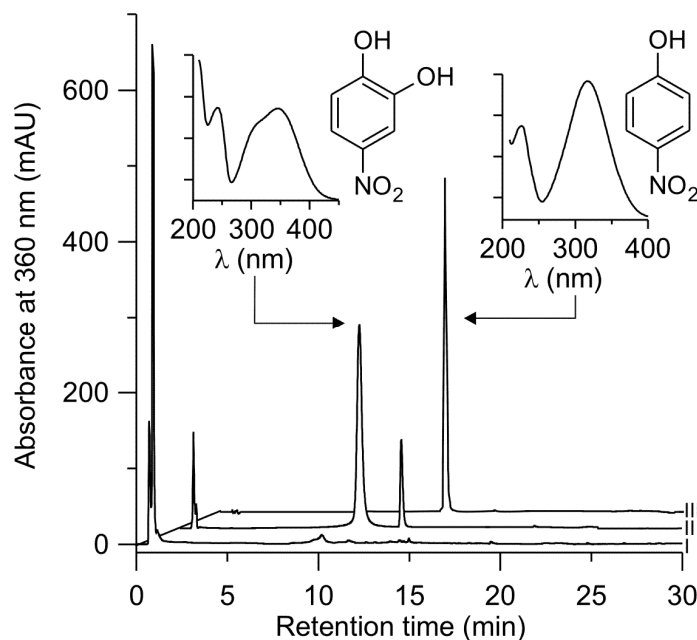


Figure 28 HPLC elution profile of *Aae*APO-catalyzed conversion of 4-nitrophenol **I**: reaction in the absence of ascorbic acid, **II**: reaction in the presence of ascorbic acid and **III**: reaction without enzyme, Insets of respective UV-Vis spectra are shown.

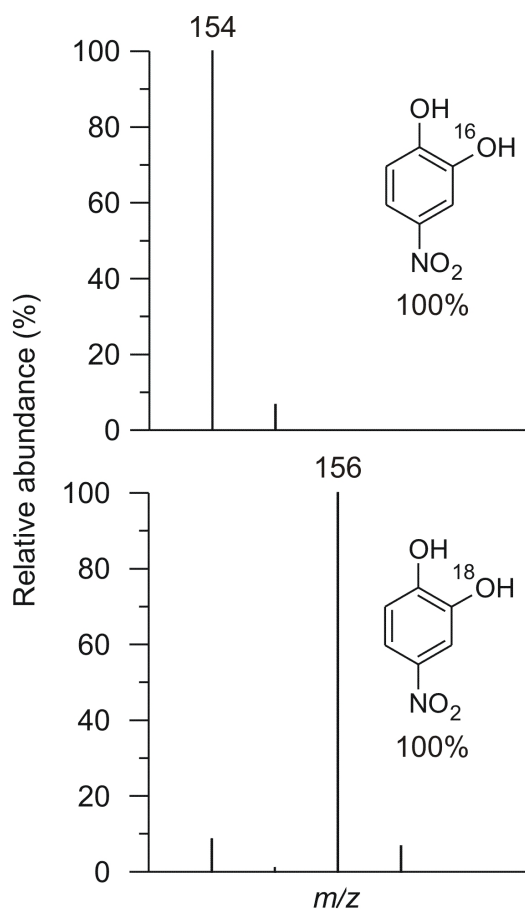


Figure 29 Incorporation of  $^{18}\text{O}$  from  $\text{H}_2^{18}\text{O}_2$  into the phenolic group of 4-nitrocatechol after hydroxylation of 4-nitrophenol by *Aae*APO. *Upper*: MS of the product obtained with natural abundance  $\text{H}_2\text{O}_2$ . *Lower*: MS of the product obtained with 90 atom %  $\text{H}_2^{18}\text{O}_2$ .

When reactions were conducted with  $^{18}\text{O}$ -enriched  $\text{H}_2\text{O}_2$  the ion mass  $m/z$  of 4-nitrocatechol shifted from 154 to 156 (Figure 29). The presence of  $^{18}\text{O}$ -enriched  $\text{H}_2\text{O}$  had no influence on the ion mass of 4-nitrocatechol. Reaction mixtures that have been flushed with nitrogen showed no changes in the rate of product formation. The results obtained from  $^{18}\text{O}$  isotope labeling experiments shows that in the presence of ascorbate a product can be observed, in which the  $m/z$  had shifted from natural abundance 170 to 172 and 174 when  $\text{H}_2^{18}\text{O}_2$  was used as oxidant. In the absence of ascorbic acid, two further reaction products with different retention times were identified.

The  $m/z$  of these metabolites shifted from natural

abundance 170 to 172 and from 186 to 188 in the presence of  $\text{H}_2^{18}\text{O}$ . The detected reactions products show typical UV-Vis spectra of nitro-aromatics with bands in the near visible region around 360 nm. *para*-Benzoquinone was not detected.

### 3.3.2 Regio- and stereoselective hydroxylations

Some of the *Aae*APO-catalyzed aromatic hydroxylations were shown to proceed regio- and stereoselectively. With respect to the broad substrate spectrum of *Aae*APO, selected results from biocatalytic conversion of compounds of pharmacological and industrial interest are reported.

#### 3.3.2.1 2-Phenoxypropionic acid

*Aae*APO catalyzed the  $\text{H}_2\text{O}_2$ -dependent hydroxylation of 2-phenoxypropionic acid (POPA) to give the herbicide precursor 2-(4-hydroxyphenoxy)propionic acid (HPOPA). To assess POPA hydroxylation, a racemic mixture of POPA was treated with purified *Aae*APO and two equivalents of  $\text{H}_2\text{O}_2$  in the presence of ascorbic acid. This last ingredient was included to prevent HPOPA polymerization, an undesirable side reaction attributable to the general peroxidase activity of *Aae*APO (Koizumi and Titani 1938).

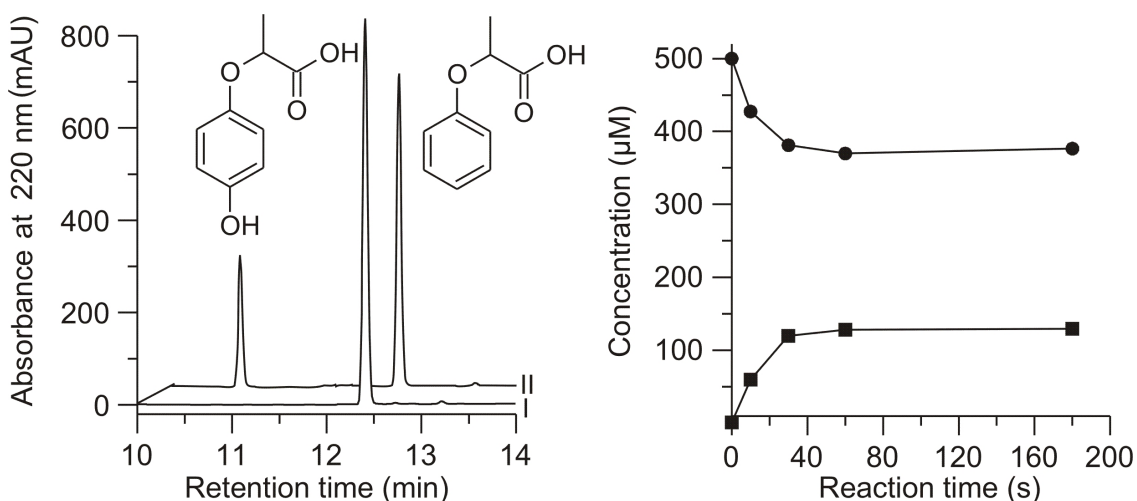


Figure 30 HPLC elution profile (left) of products formed by *Aae*APO during the conversion of POPA to HPOPA in the presence of ascorbic acid. Control without enzyme (I); Complete reaction (II); The reaction was started by addition of  $\text{H}_2\text{O}_2$  at pH 7.0. Time course of *Aae*APO-catalyzed hydroxylation of POPA to HPOPA (right).

The results showed that the reaction proceeded rapidly and regioselectively, giving HPOPA as the sole detectable product (Figure 30, left; calculated isomeric purity was 98%), and that 27% conversion of the POPA occurred under these conditions (Figure 30, right). Chiral

HPLC analyses after *Aae*APO catalyzed oxidations of racemic POPA showed that both enantiomers were hydroxylated, but that (*R*)-POPA was clearly the preferred substrate. The resulting HPOPA contained a 60% enantiomeric excess (*ee*) of the *R*-enantiomer (Figure 31). When the oxidations were performed on either of the pure POPA enantiomers, the corresponding HPOPA enantiomer was obtained as the sole detectable product in each case.

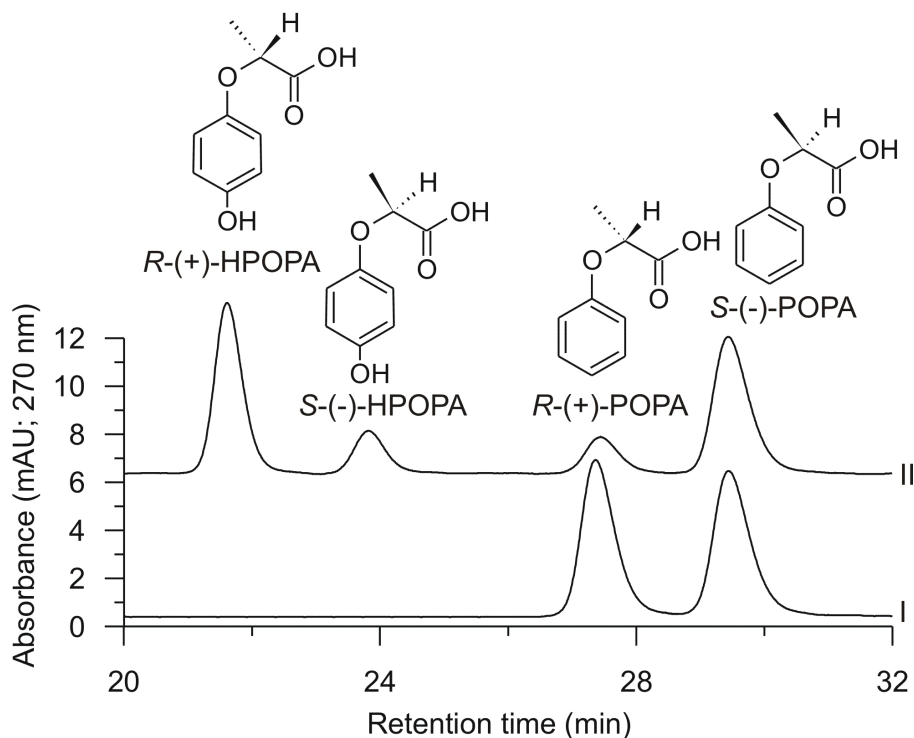


Figure 31 HPLC elution profile of products formed by *Aae*APO during the conversion of racemic POPA to HPOPA in the presence of ascorbic acid. Control without enzyme (I); Completed reaction (II). The reaction was started by the addition of  $\text{H}_2\text{O}_2$  at pH 7.0.

Natural abundance  $\text{H}_2\text{O}_2$  with  $\text{H}_2^{18}\text{O}_2$  as the oxidant in *Aae*APO-catalyzed hydroxylations of POPA to HPOPA was compared. The mass spectra of the products (Figure 32) show that the principal  $[\text{M}-\text{H}]^-$  ion had an  $m/z$  of 181, as expected for the reaction with natural abundance  $\text{H}_2\text{O}_2$ , but shifted to  $m/z$  183 with almost complete disappearance of the  $m/z$  181 ion when  $\text{H}_2^{18}\text{O}_2$  was used. A similar experiment using  $\text{H}_2^{18}\text{O}$  gave no detectable  $^{18}\text{O}$  incorporation, as expected because phenolic oxygens are not readily exchangeable with water under our reaction conditions (Koizumi and Titani 1938). An additional experiment with natural abundance  $\text{H}_2\text{O}_2$  in an  $\text{N}_2$ -purged reaction mixture showed that HPOPA production was not inhibited by depletion of  $\text{O}_2$  and therefore molecular oxygen did not

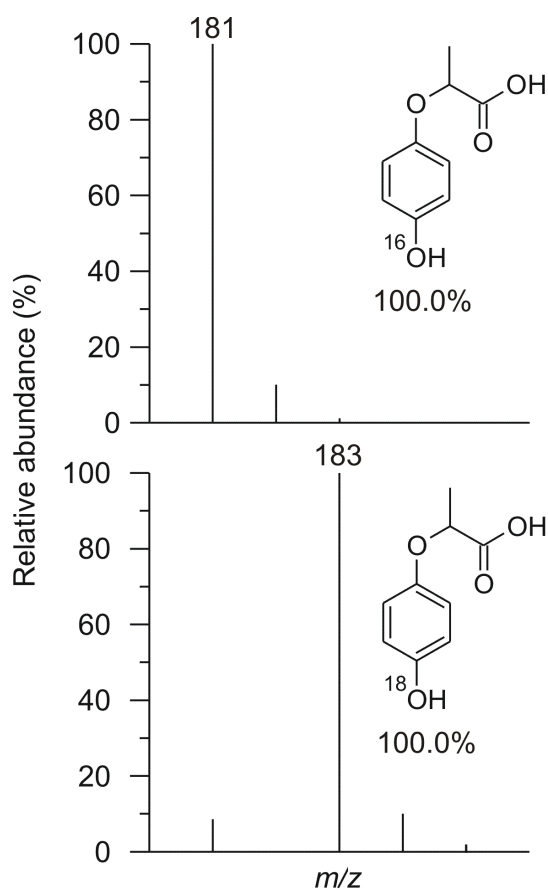


Figure 32 Incorporation of  $^{18}\text{O}$  from  $\text{H}_2^{18}\text{O}$  into the phenolic group of HPOPA after hydroxylation of POPA by *Aae*APO. *Upper*: MS of the product obtained with natural abundance  $\text{H}_2\text{O}_2$ . *Lower*: MS of the product obtained with 90 atom %  $\text{H}_2^{18}\text{O}_2$ .

### 3.3.2.2 Propranolol

*Aae*APO catalyzed the  $\text{H}_2\text{O}_2$ -dependent hydroxylation of the multi-function *beta*-adrenergic blocker propranolol [2-hydroxy-3-(naphthalen-1-yloxy)propyl](propan-2-yl)amine to give the human drug metabolite 5-hydroxypropranolol. A racemic mixture of the compound was treated with purified *Aae*APO and  $\text{H}_2\text{O}_2$  in the presence of ascorbic acid. The reaction proceeded rapidly and regioselectively, converting about 20% of the propranolol to 5-OHP. The formation of byproducts was insignificant: 4-hydroxypropranolol and 1-naphthol occurred only in trace quantities, and *N*-desisopropylpropranolol was not found. The enantiomeric excess of *S*-5-OHP during *Aae*APO-catalyzed hydroxylation of propranolol was less than 2% (*i.e.*, the reaction was not enantioselective. Control reactions without *Aae*APO or with heat-inactivated enzyme gave no conversion of propranolol.

contribute significantly as an electron acceptor.

These results show that the new phenolic oxygen in HPOPA originated from  $\text{H}_2\text{O}_2$ . A similar experiment using  $\text{H}_2^{18}\text{O}$  gave no detectable  $^{18}\text{O}$  incorporation, as expected because phenolic oxygens are not readily exchangeable with water under our reaction conditions (Ullrich and Hofrichter 2005). An additional experiment with natural abundance  $\text{H}_2\text{O}_2$  in an  $\text{N}_2$ -purged reaction mixture showed that HPOPA production was not inhibited by depletion of  $\text{O}_2$ .



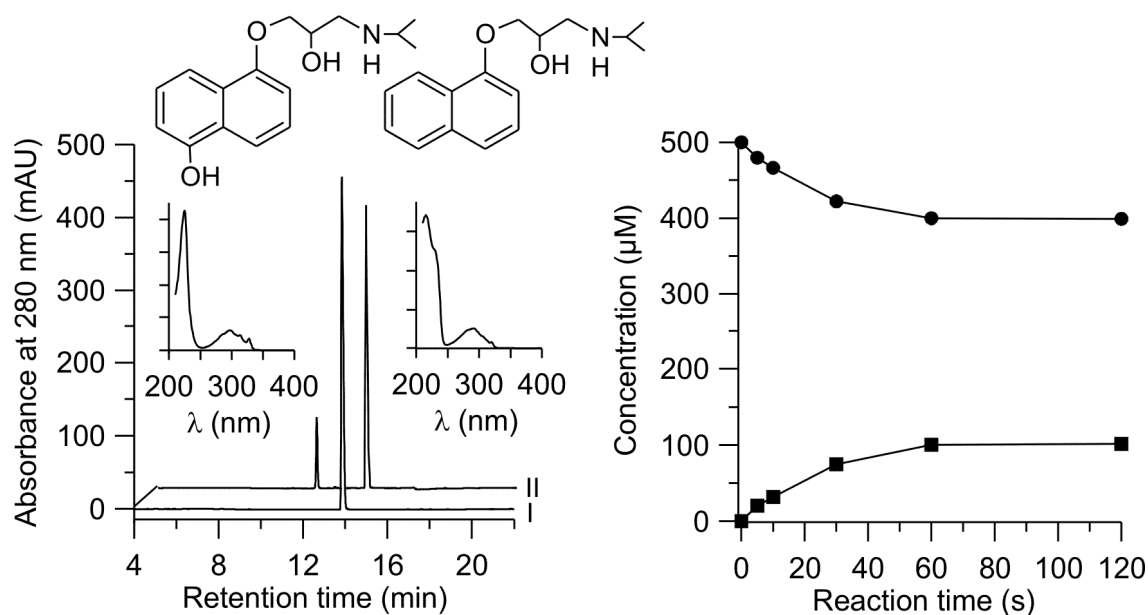
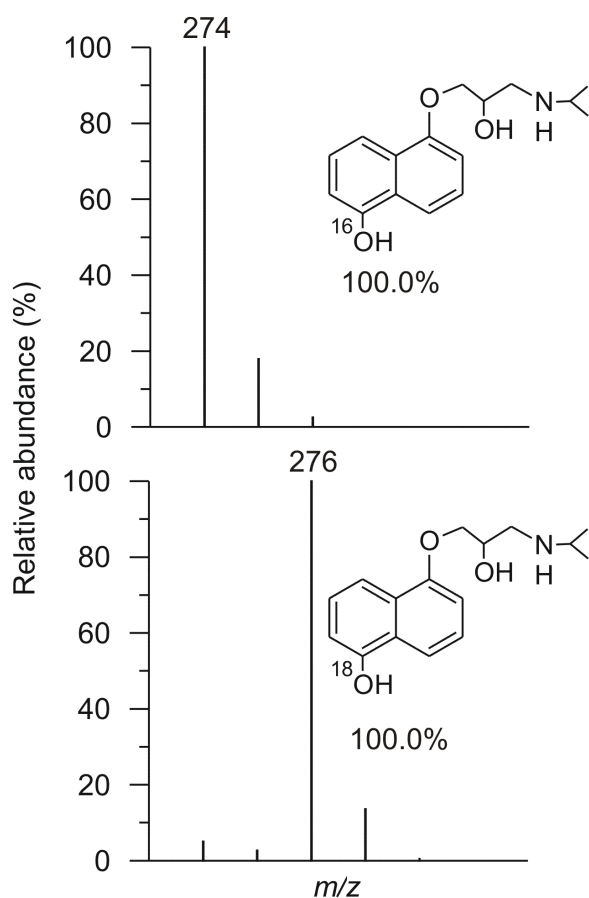


Figure 33 HPLC elution profile (left) of products formed by *AaeAPO* during the conversion of propranolol to 5-OHP. Control without enzyme (I). Complete reaction (II). Insets show UV/visible absorption spectra of the reactants. Time course of *AaeAPO*-catalyzed hydroxylation of propranolol to 5-OHP (right).



When the *AaeAPO*-catalyzed oxidation of propranolol was conducted with  $\text{H}_2^{18}\text{O}_2$  in place of  $\text{H}_2\text{O}_2$ , mass spectral analysis of the resulting 5-OHP (Figure 34) showed that the principal  $[\text{M}-\text{H}]^-$  ion had shifted from the natural abundance  $m/z$  of 274 to  $m/z$  276. A similar experiment using  $\text{H}_2^{18}\text{O}$  gave no detectable  $^{18}\text{O}$  incorporation. An additional experiment with natural abundance  $\text{H}_2\text{O}_2$  in an  $\text{N}_2$ -purged reaction mixture showed that propranolol production was not inhibited by depletion of  $\text{O}_2$ , and therefore  $\text{O}_2$  did not contribute significantly as an electron acceptor. These results show that the new phenolic oxygen in 5-OHP originated from  $\text{H}_2\text{O}_2$ .

Figure 34 Mass spectra showing molecular ions of 5-OHP obtained from the oxidation of propranolol with *AaeAPO* in the presence of natural abundance  $\text{H}_2\text{O}_2$  (top) or  $\text{H}_2^{18}\text{O}_2$  (bottom)

## 3.3.2.3 Diclofenac

*Aae*APO catalyzed the H<sub>2</sub>O<sub>2</sub>-dependent hydroxylation of the non-steroidal anti-inflammatory drug diclofenac (2-[2-[(2,6-dichlorophenyl)amino]phenyl]acetic acid) to give the human drug metabolite 4'-hydroxydiclofenac (4'-OHD). The reaction proceeded rapidly and regioselectively, converting about 65% of diclofenac to 4'-OHD (Figure 35, left). During diclofenac oxidation, the second human drug metabolite 5-hydroxydiclofenac (5-OHD) was not formed, but traces of several other unidentified byproducts were detected. Control reactions without *Aae*APO or with heat-inactivated enzyme gave no conversion of diclofenac.

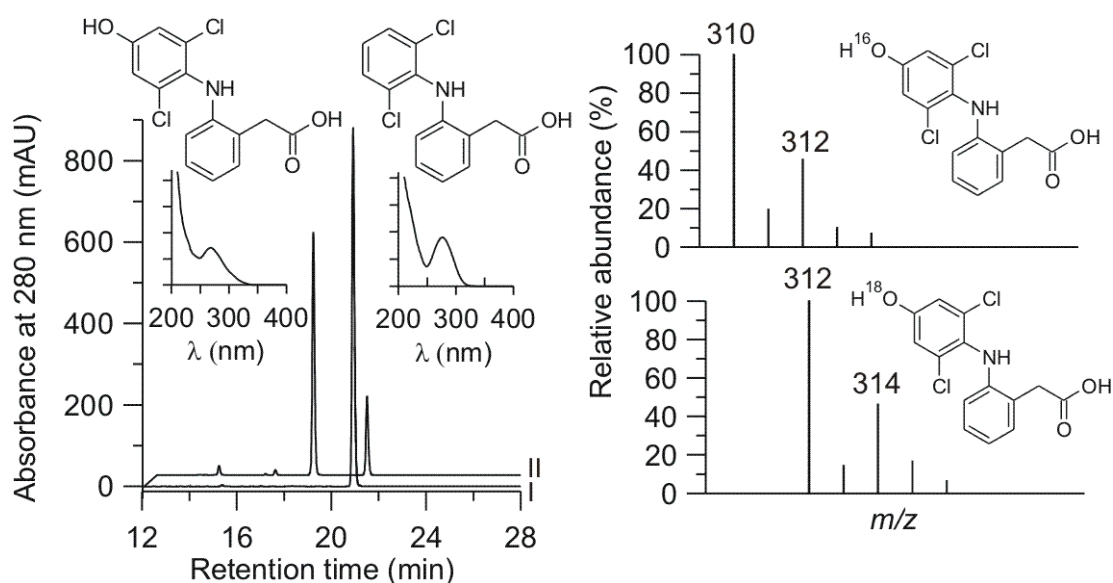


Figure 35 HPLC elution profile (left) of products formed by *Aae*APO during the conversion of diclofenac to 4'-hydroxydiclofenac. Control without enzyme (I). Complete reaction (II). Insets show UV/visible absorption spectra the reactants. Mass spectra (right) showing molecular ions of 4'-hydroxydiclofenac obtained from the oxidation of diclofenac with *Aae*APO in the presence of natural abundance H<sub>2</sub>O<sub>2</sub> (top) or H<sub>2</sub><sup>18</sup>O<sub>2</sub> (bottom)

When the *Aae*APO-catalyzed oxidation of diclofenac was conducted with H<sub>2</sub><sup>18</sup>O<sub>2</sub> in place of H<sub>2</sub>O<sub>2</sub>, the principal [M-H]<sup>-</sup> ion of the resulting 4'-OHD shifted from an *m/z* of 310 to an *m/z* of 312 (Figure 35, right). Experiments using H<sub>2</sub><sup>18</sup>O gave no detectable <sup>18</sup>O incorporation, as expected because phenolic oxygens are not readily exchangeable with water under our reaction conditions. An additional experiment with natural abundance H<sub>2</sub>O<sub>2</sub> in an N<sub>2</sub>-purged reaction mixture showed that 4'-hydroxydiclofenac production was not inhibited by depletion of O<sub>2</sub>, and therefore O<sub>2</sub> did not contribute significantly as an electron acceptor. These results show that the new phenolic oxygens in 4'-OHD originated from H<sub>2</sub>O<sub>2</sub>.

## 3.3.2.3 Acetanilide

Acetanilide, a precursor of paracetamol was selectively *para*-hydroxylated to give the major reaction product paracetamol (acetaminophen, *N*-(4-hydroxyphenyl)acetamide) and 3-hydroxyacetaminophen (Figure 36, left). The reaction proceeded rapidly and regioselectively, converting about 80% of the acetanilide to paracetamol (Figure 36, right). The formation of byproducts was insignificant: 3-hydroxyacetaminophen occurred only in trace quantities.

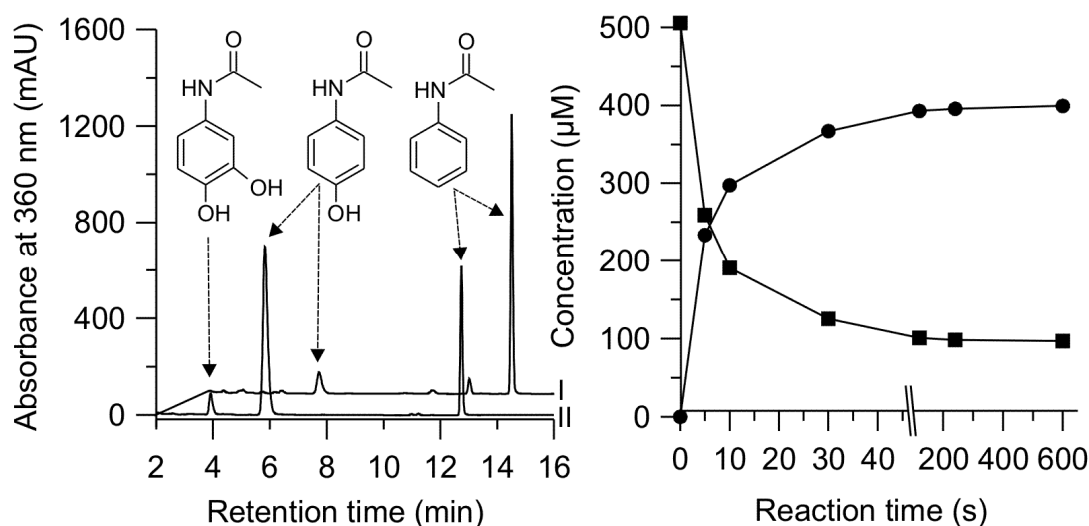


Figure 36 HPLC elution profile (left) of products formed by *Aae*APO during the conversion of acetanilide to paracetamol and 3-hydroxyacetaminophen. Control without enzyme (I). Complete reaction (II). Time course of *Aae*APO-catalyzed hydroxylation of acetanilide to paracetamol (right).

When *Aae*APO-catalyzed oxidation of acetanilide was conducted with  $\text{H}_2^{18}\text{O}_2$  in place of  $\text{H}_2\text{O}_2$ , mass spectral analysis of the resulting paracetamol showed that the principal  $[\text{M}-\text{H}]^-$  ion had shifted from the natural abundance  $m/z$  of 150 to  $m/z$  152 and for 3-hydroxyacetaminophen from  $m/z$  of 166 to  $m/z$  170.

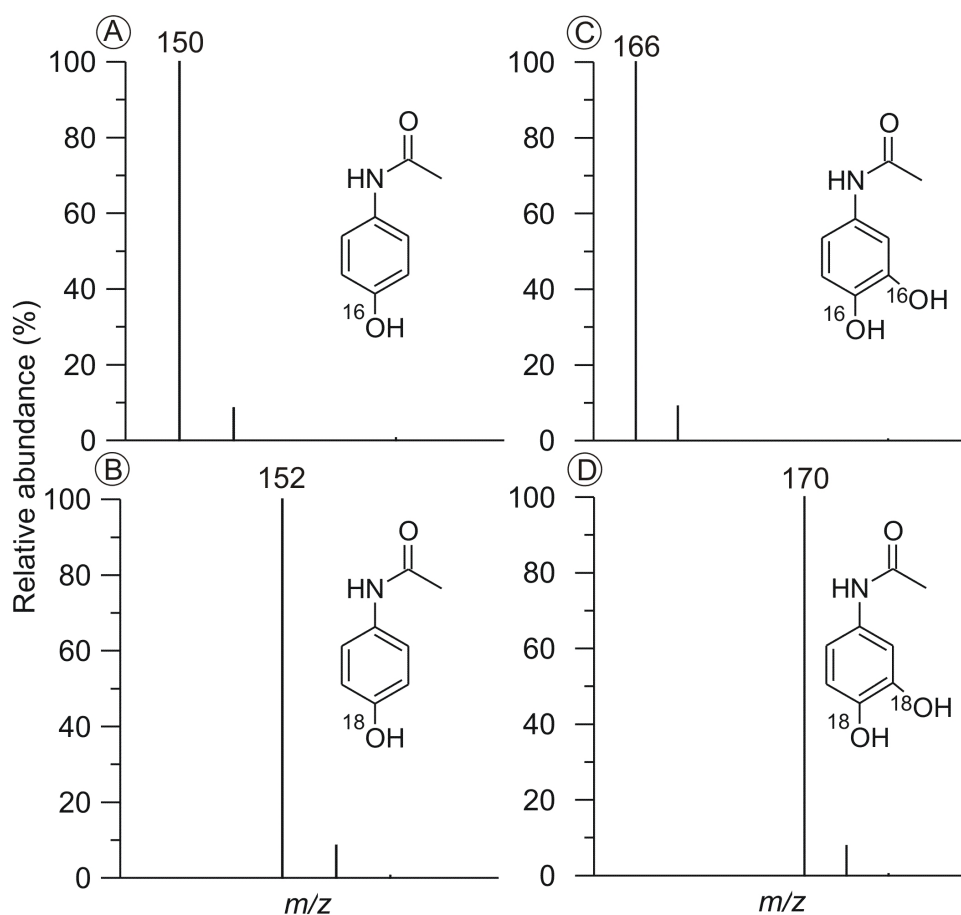


Figure 37 Mass spectra showing molecular ions of paracetamol (A and B) and 3-hydroxyacetaminophen (C and D) obtained from the oxidation of acetanilide with *Aae*APO in the presence of natural abundance  $\text{H}_2\text{O}_2$  (top) or  $\text{H}_2^{18}\text{O}_2$  (bottom).

### 3.4 Benzylic oxygenation

*Aae*APO hydroxylated toluene and 4-nitrotoluene to give the corresponding benzyl alcohols, benzaldehydes and benzoic acids. The reactions proceeded rapidly with total conversions of 93% for toluene and 12% for 4-nitrotoluene (Figure 38). The low extent of 4-nitrotoluene oxidation is attributable to inhibition of the enzyme by the substrate, which has also been observed during P450-catalyzed oxidations of nitroaromatics (Sternson and Gammans 1975, Kuropteva and Kudriavstev 1997). The initial product of toluene oxidation was benzyl alcohol, which then declined with concomitant production of benzaldehyde, which in turn declined with concomitant production of benzoic acid. When benzyl alcohol was used instead of toluene as the starting substrate, the products were benzaldehyde and benzoic acid, whereas with benzaldehyde as the starting material, only benzoic acid was formed.

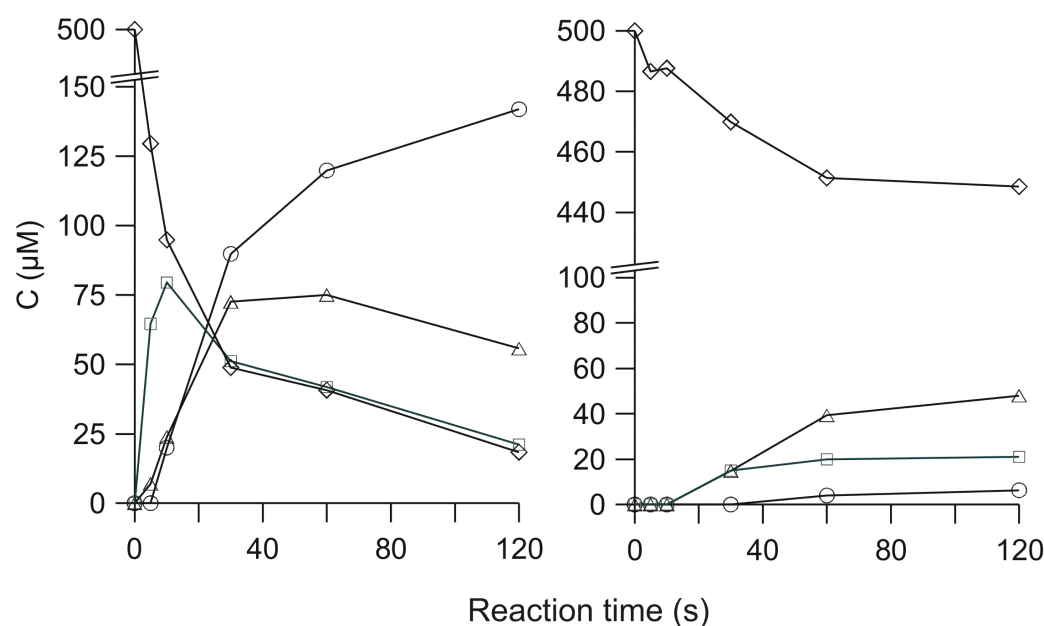


Figure 38 Time course of *Aae*APO-catalyzed hydroxylation of toluene ( $\diamond$ , left) and 4-nitrotoluene ( $\diamond$ , right) to the corresponding benzyl alcohols ( $\square$ ), benzaldehydes ( $\Delta$ ) and benzoic acids (O).

In reactions with 4-nitrotoluene as the starting substrate, the reaction sequence was not as apparent (Figure 38), but other experiments with 4-nitrobenzyl alcohol or 4-nitrobenzaldehyde as starting substrates showed the same precursor-product relationships as in the experiments with toluene.

An  $^{18}\text{O}$ -labeling study established that  $\text{H}_2\text{O}_2$  supplied the oxygen incorporated during *Aae*APO-catalyzed oxidation of the two toluenes (Figure 39). When the reaction was conducted with toluene and  $\text{H}_2^{18}\text{O}_2$ , mass spectral analysis of the resulting benzyl alcohol showed that its principal ion had shifted from the natural abundance  $m/z$  of 108 to  $m/z$  110. Similarly, the reaction with 4-nitrotoluene and  $\text{H}_2^{18}\text{O}_2$  yielded 4-nitrobenzyl alcohol in which the principal ion had shifted from  $m/z$  153 to  $m/z$  155. It was also observed that incorporation of  $^{18}\text{O}$  from  $\text{H}_2^{18}\text{O}_2$  occurred in the benzaldehyde and benzoic acid formed from toluene in these experiments. To clarify this finding, we performed labeling experiments using each of the intermediate products as *Aae*APO substrates, and thus showed that  $^{18}\text{O}$  was incorporated from  $\text{H}_2^{18}\text{O}_2$  at each oxidation step. With benzyl alcohol as the substrate, some of the resulting benzaldehyde shifted from its natural abundance  $m/z$  of 106 (100%) to  $m/z$  108 (22%), which indicates 18% incorporation of  $^{18}\text{O}$  from  $\text{H}_2^{18}\text{O}_2$ . The  $m/z$  values for the benzoic acid formed in this experiment also shifted, in this case from  $m/z$  121 to  $m/z$  123 (100%) and  $m/z$  125 (9.5%).

## RESULTS

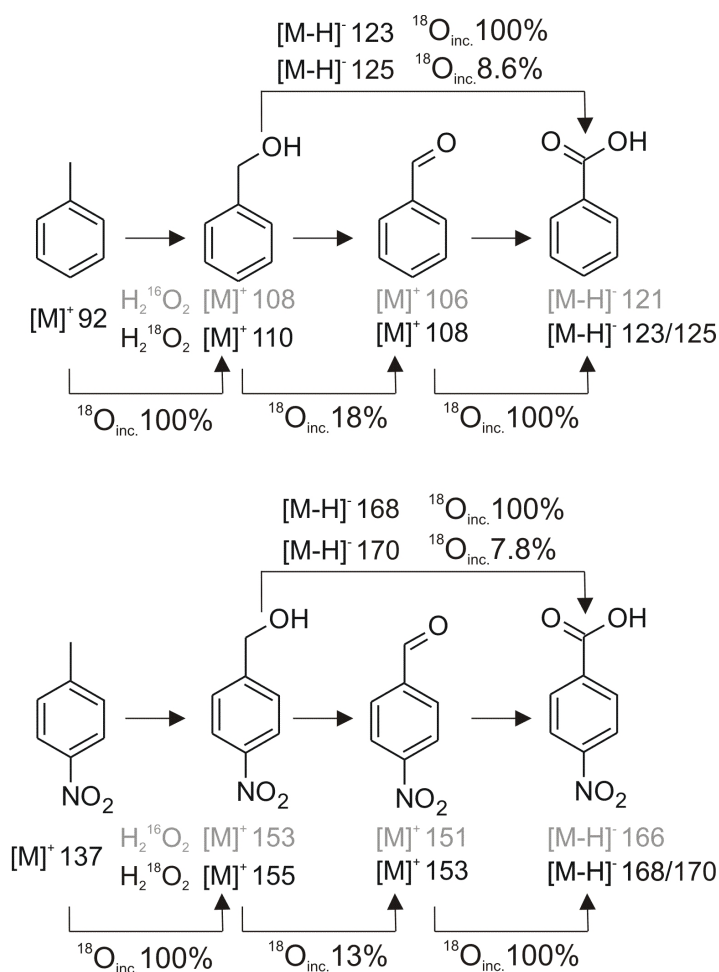


Figure 39 Reaction scheme showing the yields of  $^{18}\text{O}$ -incorporation into reaction products during *Aae*APO-catalyzed oxidation of toluene and 4-nitrotoluene in the presence of  $\text{H}_2^{18}\text{O}_2$ .

When benzaldehyde was used as the substrate instead, the resulting benzoic acid shifted quantitatively from its natural abundance  $m/z$  of 121 to  $m/z$  123 (Figure 40).

The same trend was apparent with 4-nitro-substituted substrates. In reactions started from 4-nitrobenzyl alcohol, some of the resulting 4-nitrobenzaldehyde shifted from the natural abundance  $m/z$  of 151 (100%) to  $m/z$  153 (15.5%), thus indicating 13% incorporation of  $^{18}\text{O}$  from  $\text{H}_2^{18}\text{O}_2$ . The  $m/z$  values for the 4-nitrobenzoic acid formed in this experiment also shifted, in this case from  $m/z$  166 to  $m/z$  168 (100%) and  $m/z$  170 (9.5%). The shift from the natural abundance  $m/z$  of 166 to  $m/z$  168 was quantitative for 4-nitrobenzoic acid when 4-nitrobenzaldehyde was used instead as the starting substrate (Figure 40).

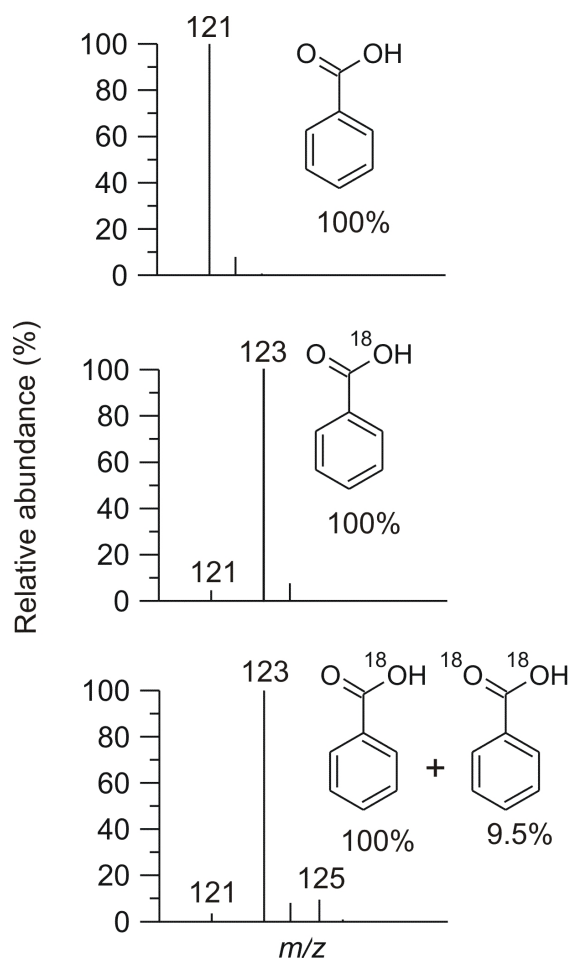


Figure 40 Incorporation of <sup>18</sup>O from H<sub>2</sub><sup>18</sup>O<sub>2</sub> into the carboxyl group of benzoic acid after oxidation of benzaldehyde (middle) and benzyl alcohol (bottom) by *Aae*APO. MS of the product obtained with natural abundance H<sub>2</sub>O<sub>2</sub> (top).

### 3.5 Further oxidation reactions

A substrate screening of *Aae*APO-catalyzed oxygenating activity was performed. The results showed that *Aae*APO is able to oxidize diverse substrates, yielding intermediates that subsequently undergo specific autocatalytic reactions.

#### 3.5.1 Phenol oxidation

Figure 41 illustrates the HPLC elution profiles of the *Aae*APO-catalyzed oxidation of phenol. After treatment with *Aae*APO in the presence of ascorbic acid, two major metabolites appeared and one of them was identified as 1,4-hydroquinone. In the absence of ascorbic acid, phenol was completely oxidized to give 1,4-benzoquinone, biphenyl-4,4'-diol and polymerization products. The products 1,2-benzoquinone and catechol were detected as side products.

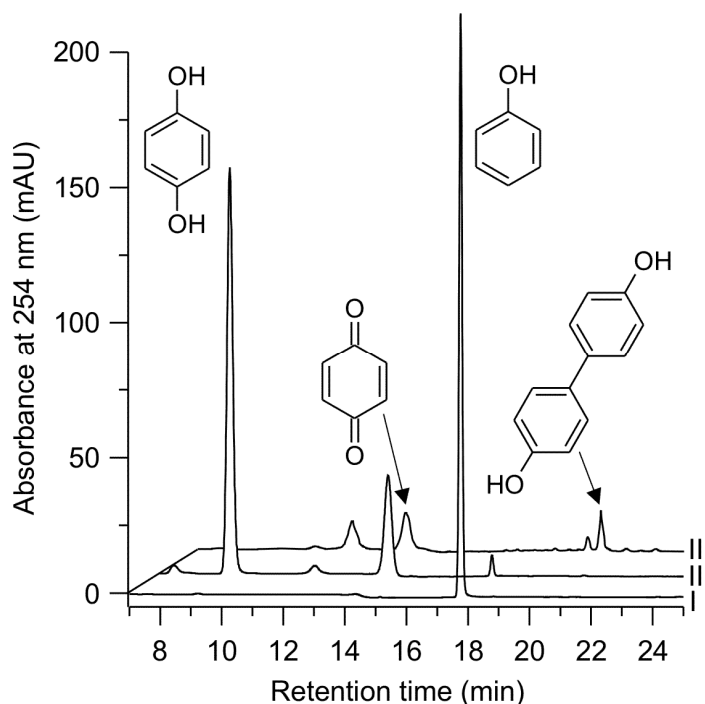


Figure 41 HPLC elution profiles of products formed by *AaeAPO* during the conversion of phenol. Control without enzyme (I). Complete reaction with ascorbic acid (II). Completed reaction (III).

### 3.5.2 Dehalogenation

Figure 42 illustrates the HPLC elution profile of the *AaeAPO*-catalyzed oxidation of benzyl chloride. After treatment with *AaeAPO*, one major metabolite appeared and was identified as benzaldehyde.

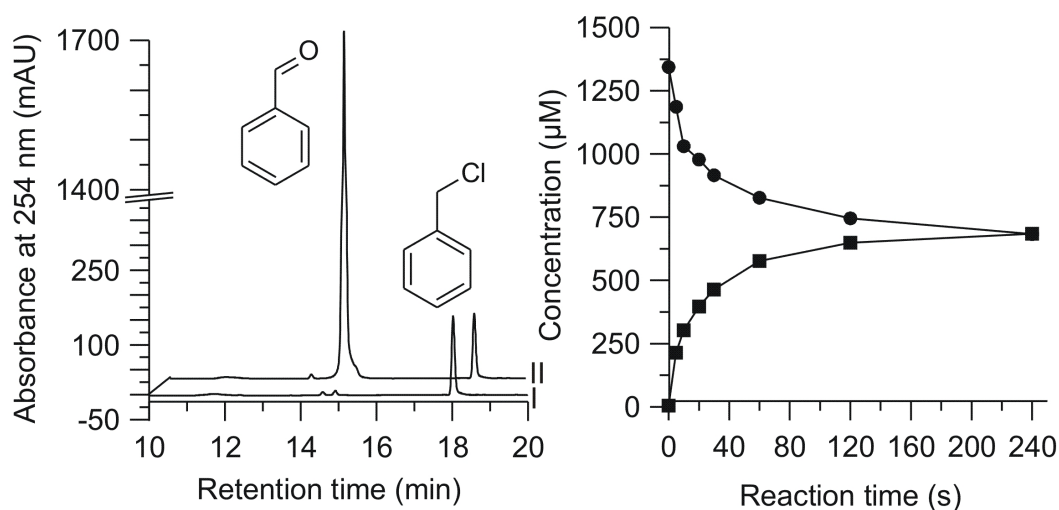


Figure 42 HPLC elution profile (left) of products formed by *AaeAPO* during the conversion of benzyl chloride. Control without enzyme (I). Complete reaction (II). A fresh solution of benzyl chloride was prepared prior to each experiment since benzyl chloride hydrolyzes to form benzyl alcohol and hydrochloric acid. (Beste and Hammett 1940)



The formation of benzaldehyde shows the ability of *Aae*APO to catalyze dehalogenations. The results showed that the reaction proceeded rapidly and regioselectively, giving benzaldehyde as the initial reaction product (Figure 42, left), and that 52% conversion of benzyl chloride occurred under these conditions (Figure 30, right). When 4-nitrobenzyl chloride was incubated with *Aae*APO two major reaction products appeared and were identified as their 4-nitrobenzaldehyde (initial reaction product) and 4-nitrobenzoic acid. Aldehydes released from qualitative reactions of *Aae*APO, 2,2-dichlorodiethylether and H<sub>2</sub>O<sub>2</sub> could be detected as their 2,4-dinitrophenylhydrazones (Figure 43). Several metabolites appeared and were proposed as 2-hydroxyacetaldehyde, glyoxal, (2-chloroethoxy)acetaldehyde and chloroacetaldehyde. While the formation of chloroacetaldehyde and glyoxal shows again the ether-cleaving activity of *Aae*APO, the formation of (2-chloroethoxy)acetaldehyde and glyoxal shows the ability of *Aae*APO to catalyze dechlorination reactions.

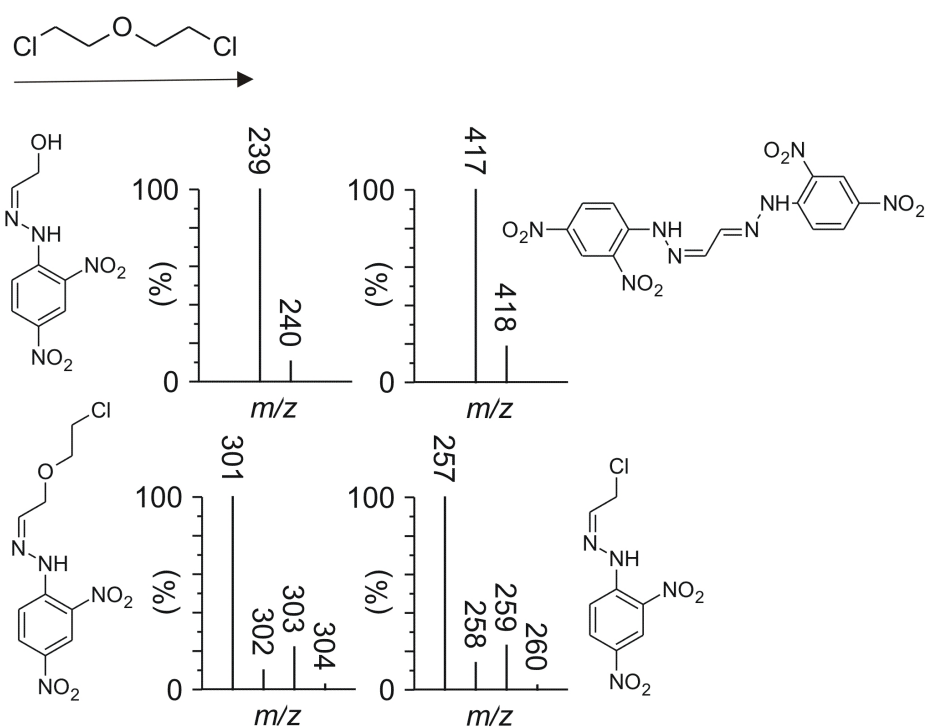


Figure 43 Mass spectra showing molecular ions of products obtained from the oxidation of 2,2-dichlorodiethylether with *Aae*APO in the presence DNPH.

### 3.5.3 *N*-dealkylation

Figure 44 illustrates the HPLC elution profiles for the *Aae*APO-catalyzed oxidation of *N*-methylaniline. After treatment with *Aae*APO, several metabolites appeared and were identified as aniline (yield  $\approx$  50%), 4-(methylamino)phenol (yield  $<$  23%), 2-aminophenol (yield  $\approx$  1%) and 4-aminophenol (yield  $\approx$  10%).

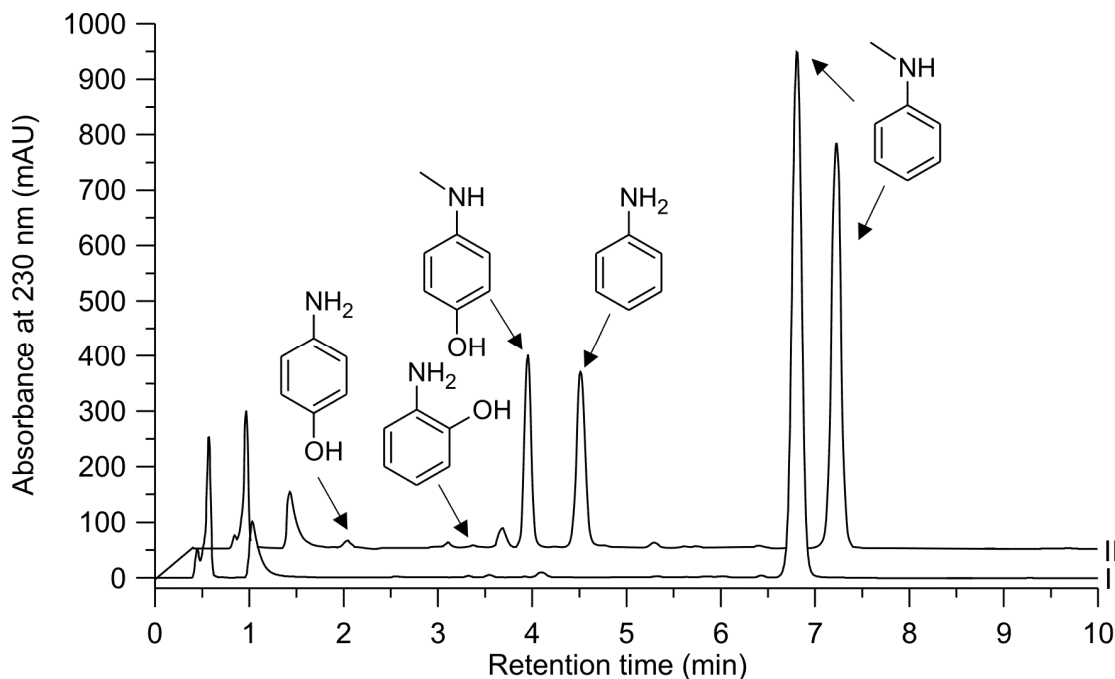


Figure 44 HPLC elution profile of *Aae*APO-catalyzed conversion of *N*-methylaniline. I: Control without *Aae*APO, II: completed reaction in the presence of ascorbic acid.

While the formation of 4-aminophenols shows again the hydroxylation activity of *Aae*APO, the formation of aniline shows the ability of *Aae*APO to catalyze *N*-dealkylation. When the reaction was conducted without ascorbic acid, reaction mixtures became dark-colored with formation of insoluble reaction products. Some of the mass spectra indicated that the amino group becomes hydroxylated.

### 3.5.4 Halogenation

*Aae*APO catalyzed the hydrogen peroxide-dependent halogenation of anisole in the presence of chloride or bromide in a pH range from 2 to 5. The major reaction products were identified as 2- and 4-bromoanisole in the presence of bromide and 2- and 4-chloroanisole when chloride was added to the reaction mixtures.

## RESULTS

Table 12 The halogenation activity of *Aae*APO compared to *Cfu*CPO

Enzyme	Halogen	Anisole left	2-Br-anisole	4-Br-anisole	2-Cl-anisole	4-Cl-anisole
		$\mu\text{M}$				
<i>Aae</i> APO	-	498	-	-	-	-
	Br <sup>-</sup>	0	19	520	-	-
	Cl <sup>-</sup>	327	-	-	24	37
<i>Cfu</i> CPO	-	497	-	-	-	-
	Br <sup>-</sup>	57	24	558	-	-
	Cl <sup>-</sup>	366	-	-	90	144

The results are summarized in Table 12 and are compared with those obtained with *Cfu*CPO. It is evident that *Aae*APO exhibits a strong brominating and a weak chlorinating activity towards anisole. *Cfu*CPO, by contrast, was able to catalyze both reactions to give relatively high yields of the halogenated anisoles.

## 4. Discussion

### 4.1 Reaction mechanisms of *Aae*APO-catalyzed reactions

#### 4.1.1 General mechanistic aspects

The results provide an experimental base for formulating a general mechanism of *Aae*APO-catalysis. Activities of *Aae*APO, which results from this general mechanism, will be discussed separately.

##### 4.1.1.1 *Aae*APO shares spectrophotometric features with heme-thiolate proteins

The nature of the axial ligand of a heme protein has an essential effect on the balance between *low spin* and *high spin*-configuration of the heme iron. For example a strong axial heme ligand causes a relatively large split of the d-orbitals of the heme iron leading to *low spin* configuration (Segall 1997). This behavior is apparent, when reduced carbon monoxide complexes of proteins with a histidine ligand (hemoglobin, horseradish peroxidase) and proteins with a cysteine ligand (P450s, *Cfu*CPO) are compared. The axial ligand field strength of cysteine is lower compared to that of histidine and as a result the

Table 13 Ligand complexes of different heme proteins. Soret-bands of *Aae*APO are almost identical to the respective bands of *Cfu*CPO and P450s. <sup>1</sup>(Dunford 1999) <sup>2</sup>(Lewis 2001)

Ligand	<i>Aae</i> APO	<i>Cfu</i> CPO	P450cam <sup>1</sup>	HrP <sup>2</sup>
	(nm)			
Resting	418	399	417	402
Reduced (dithionite)	407	408	408	439
CO (Fe <sup>2+</sup> )	445	445	446	423
NO	430	437	430	419
CN <sup>-</sup> / CN <sup>-</sup> (Fe <sup>2+</sup> )	438/443	439/454	439/n.d.	423/432
N <sub>3</sub> <sup>-</sup>	428	432	427	416
1-Phenylimidazole	424	424	424	402
Hydroxylamine	420	421	n.d.	402
F <sup>-</sup>	(418)	420	(417)	404

carbon monoxide complex of P450 shows a shift in the Soret absorption band to higher wavelength (450 nm) as compared to hemoglobin (420 nm) (Segall 1997). When the positions of the stationary Soret bands of different *ferric* (Fe<sup>III</sup>) and *ferrous* (Fe<sup>II</sup>) ligand complexes are

compared with those of common heme proteins (*CfuCPO*, P450cam from *Pseudomonas putida* and HrP), it is evident that the Soret positions of *AaeAPO*, *CfuCPO* and P450cam display a high correspondence of complexes for all ligands tested but differ considerably from that of HrP. For example, P450s, *CfuCPO*, and *AaeAPO* exhibits an absorption maximum at 445 nm for its CO-coordinated state, indicating cysteine as the proximal ligand of the heme iron (Table 13). However, some differences of the Soret wavelength for *CfuCPO* and *AaeAPO* are found in the resting state. *AaeAPO* also shows difference binding type spectra typical of P450s. For example, camphor gives a binding type I spectrum, whereas cyanide gives a binding type II spectrum for both *AaeAPO* and P450s (Lewis 2001). In general, these results suggest that the electron environment of *AaeAPO* resemble that of heme thiolate proteins such as P450s.

#### 4.1.1.2 The substrate range of *AaeAPO* resembles that of heme-thiolate proteins

$H_2O_2$ -dependent *AaeAPO*-catalyzed reactions exhibit two major activities: (a) a strong monooxygenation activity, which yields oxygenated reaction products and (b) a peroxidase activity, which may yield radicals that form halogenated or polymerized products (Figure 45).

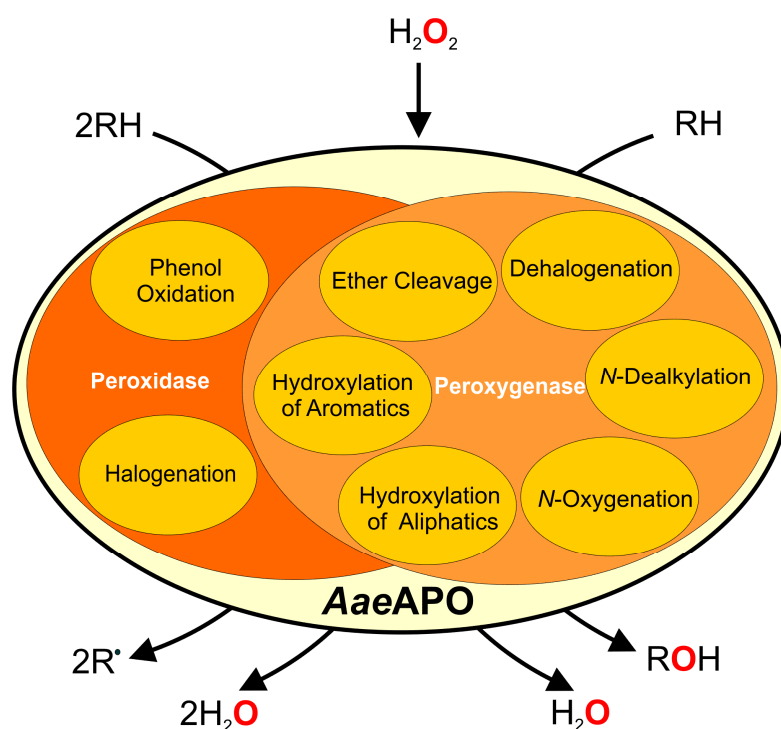


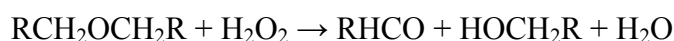
Figure 45 Suggested reactions catalyzed by *AaeAPO*.

The peroxygenase activity of *AaeAPO* is related to the P450 peroxide “shunt” pathway, as both enzymes are able to catalyze the incorporation of an  $H_2O_2$ -derived oxygen into an

aromatic or aliphatic C-H bond or into a heteroatom (Isin and Guengerich 2007). *Cfu*CPO has also been shown to catalyze the monooxygenation of many substrates but aromatic rings are not susceptible to oxygen transfer by *Cfu*CPO (Ullrich and Hofrichter 2007). The peroxidase activity of *Aae*APO is related to that found for heme peroxidases such as *Cfu*CPO, LiPs and MnPs, as these enzymes are able to catalyze the oxidation of halogens, phenols and ABTS (Ullrich et al. 2004). However, one key functional difference between *Aae*APO and peroxidases is that *Aae*APO has not been observed to directly abstract electrons from aromatic rings to form aryl cation radicals as observed for peroxidases such as LiPs (Ullrich and Hofrichter 2007).

#### 4.1.1.3 Reactions exhibit an equimolar stoichiometry

The results presented here demonstrate that there exists a 1:1 stoichiometry in the oxidation of the aliphatic ether moiety in tetrahydrofuran (and in methyl 3,4-dimethoxybenzyl ether) by H<sub>2</sub>O<sub>2</sub>. This stoichiometry of the reaction is consistent with the following overall process:



in which RCHO corresponds to the aldehyde and HOCH<sub>2</sub>R to the alcohol. For instance, analyses of tetrahydrofuran cleavage in the presence of limiting oxidant showed that one equivalent of 4-hydroxybutanal was formed per equivalent of H<sub>2</sub>O<sub>2</sub> supplied, thus identifying the catalyzed reaction as a two-electron oxidation that splits this ether into one aldehyde and one alcohol. This reaction is independent of the presence of dioxygen, as shown by the results presented above.

#### 4.1.1.4 Bisubstrate kinetics suggest a ping-pong mechanism

Kinetic investigations of the *Aae*APO-catalyzed reactions presented some experimental problems. First, oxidation kinetics done at a saturating H<sub>2</sub>O<sub>2</sub> concentration will underestimate the intrinsic kinetic values of the reaction, because under these conditions *Aae*APO exhibits an interfering catalase activity (Ullrich 2008). To address this problem, bisubstrate reactions require an experimental design that varies the concentrations of both substrates (Segel 1994). Furthermore, the cumbersome nature of an HPLC assay for the calculation of enzyme kinetics makes initial rate determinations difficult. A spectrophotometric assay will generally give results for the kinetic constants with superior accuracy. Both of the above approaches were adopted for the kinetics study reported here. Data from bisubstrate kinetics under steady state

conditions, which were spectrophotometrically recorded for the *Aae*APO-catalyzed reactions at varying concentrations of 3,4-dimethoxybenzyl ether and  $\text{H}_2\text{O}_2$ , give parallel lines for double reciprocal plots of the data. This result is consistent with a ping-pong enzymatic mechanism (Segel 1994). In such a mechanism, the substrate [A] binds to the resting enzyme [E] to form the enzyme substrate complex [EA]. Substrate [A] converts the enzyme to the enzyme substrate complex [E\*A]. Only after the substrate [A] is released in the form of [P] can the second substrate [B] bind to the transformed enzyme [E\*], yielding the enzyme substrate complex [E\*B], and then react with the modified enzyme, finally regenerating the unmodified enzyme to [E] with release of the product [Q] (Bisswanger 2000).

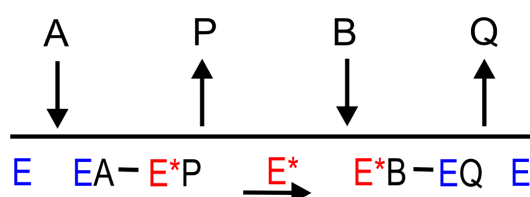


Figure 46 Reaction sequence of a ping-pong mechanism. The enzyme constantly bounces back and forth between the two states of the enzyme E and E\* (like a ping-pong ball).

It is interesting to compare the kinetic values obtained in this work with those obtained for functionally similar enzymes. Some P450s that cleave aromatic ethers such as alkoxycompounds bind them more strongly with  $K_m$  values around 1-10  $\mu\text{M}$ , but have much lower  $k_{\text{cat}}$  values in the vicinity of 0.1  $\text{s}^{-1}$  or less. Similarly, fungal LiPs have relatively low  $K_m$  values around 10-100  $\mu\text{M}$  for  $\text{H}_2\text{O}_2$  and for simple aromatic substrates such as 3,4-dimethoxybenzyl alcohol, but also exhibit low  $k_{\text{cat}}$  values on the order of 1-10  $\text{s}^{-1}$  (Tien et al. 1986). As a result, the  $k_{\text{cat}}/K_m$  ratios for methyl 3,4-dimethoxybenzyl ether cleavage by the *Aae*APO are somewhat higher than those *Pce*LiP-catalyzed benzyl alcohol oxidations and are much higher than those for P450-catalyzed ether oxidations. Data obtained in this work for tetrahydrofuran and 1,4-dimethoxybenzene at a saturating  $\text{H}_2\text{O}_2$  concentration and using an HPLC assay gave slightly different results, but are still in the same range as the results found for methyl 3,4-dimethoxybenzyl ether (Table 14).

#### 4.1.1.5 Oxygen introduced into reaction product derives from the peroxide

The results presented here and elsewhere show that reactions catalyzed by *Aae*APO proceeded with incorporation of one oxygen atom from  $\text{H}_2\text{O}_2$  into the oxidized product. The oxygens found in the phenolic moiety or in the epoxy group after the hydroxylation of aromatics (Kinne et al. 2008, Aranda et al. 2008, Kinne et al. 2009b, Kluge et al. 2009), in the

sulfoxide after sulfoxxygenation of dibenzothiophene (Aranda et al. 2008), in the *N*-oxides after *N*-oxygenation of pyridine derivatives (Ullrich et al. 2008) and in the carbonyls after the cleavage of ethers (Kinne et al. 2009a) by *Aae*APO all derive from H<sub>2</sub>O<sub>2</sub>.

The incorporation of an H<sub>2</sub>O<sub>2</sub>-derived oxygen into the substrate to yield an oxygenated product, was earlier shown to occur in reactions catalyzed by P450 via the peroxide “shunt” pathway (Otey et al. 2006), by *Cfu*CPO (Manoj and Hager 2008), by plant seed peroxygenases (Partridge and Murphy 2009) and in side reactions of other enzymes such as tyrosinase (Valero et al. 2003) and engineered myoglobin (Pfister et al. 2005). In summary, H<sub>2</sub>O<sub>2</sub> serves as both oxygen donor and electron acceptor for *Aae*APO. One substrate molecule is monooxygenated while one H<sub>2</sub>O<sub>2</sub> molecule is reduced to water.

#### 4.1.1.6 High deuterium isotope effect points to a hydrogen abstraction

The determination of an deuterium isotope effect has proven to be a powerful tool to help understand the intricacies of carbon hydrogen bond cleavage and characterize the mechanism of specific chemical reactions (Nelson and Trager 2003). An isotopic substitution will significantly modify the reaction rate if the isotopic replacement is in a chemical bond that is broken or formed in the rate limiting step of a chemical or enzymatic reaction (Miller et al. 2009). This change is termed a primary isotope effect (Kohen and Limbach 2006). In general, the accuracy of a deuterium isotope effect determination for an enzymatic reaction depends on how different the intrinsic isotope effect ( $k_H/k_D$ ) is from the observed isotope effect [ $(k_H/k_D)_{obs}$ ]. The experimental design for estimating the deuterium isotope effect has a large influence on this difference. Whereas experiments of an intermolecular design depend on complex determinations of rate constants, an experimental setup of the symmetrical intramolecular design is comparatively simpler, because it is kinetically independent of all steps besides the one that breaks the C-H bond. In practice, a substrate is chosen that is susceptible to enzymatic attack at either of two symmetrically equivalent sites. One site contains a more strongly carbon-bound deuterium and the other retains its natural complement of hydrogen, which is less strongly bound. The [ $(k_H/k_D)_{obs}$ ] can be determined from the ratio of product resulting from attack at the *protio* site versus product resulting from attack at the *deuterio* site, for example in mass spectrometric experiments. The determination of intramolecular [ $(k_H/k_D)_{obs}$ ] will produce values that are closer to the intrinsic values than those obtained from an intermolecular experiment (Nelson and Trager 2003). The most extensive use of intramolecular isotope effects has been in the study of the P450s, and much



of the formal description of the theory has been developed with regard to these enzymes (Kohen and Limbach 2006).

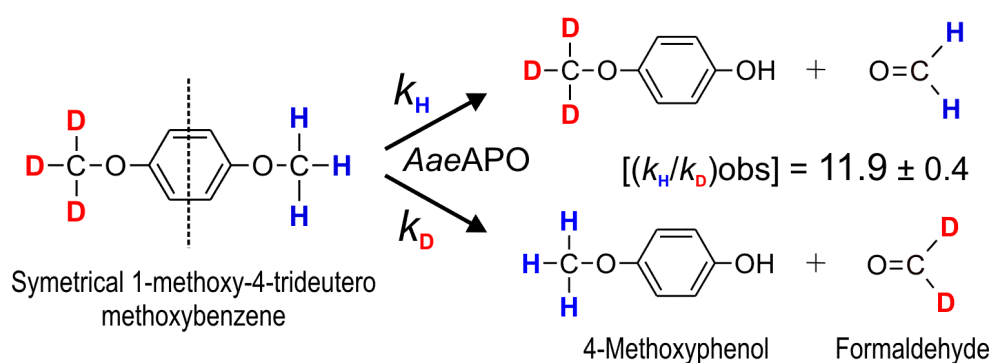


Figure 47 The  $(k_H/k_D)_{\text{obs}}$  value for the *AaeAPO*-catalyzed O-demethylation of 1,4-dimethoxybenzene determined from an experiment of intramolecular design. The ratio of the rate constants  $k_H$  and  $k_D$  can be directly calculated from the signal intensities of the corresponding ions in the mass spectra.

The results of this work showed that *AaeAPO* exhibited a high intramolecular  $(k_H/k_D)_{\text{obs}}$  near 12. In general, oxidations that occur via hydrogen abstraction exhibit intrinsic deuterium isotope values of this magnitude, whereas those that occur via insertion of an oxygen atom show much lower isotope effects with  $(k_H/k_D)_{\text{obs}} \approx 2$  (Yun et al. 2003, Nelson and Trager 2003). For example, an intramolecular  $(k_H/k_D)_{\text{obs}}$  of 11 for benzylic hydroxylation was measured from the relative amounts of hydrogen and deuterium in 1-HO-1,3-diphenylpropane formed from 1,1-D<sub>2</sub>-1,3-diphenylpropane by rat microsomes (Hjelmeland et al. 1976, Ortiz de Montellano 2009). Accordingly, the results reported here for ether cleavage by *AaeAPO* suggest a mechanism involving abstraction of an ether *beta*-hydrogen followed by oxygen rebound (Figure 47)

#### 4.1.1.7 *AaeAPO* active site fails to accommodate polymers

Some apparent size limitations were noted on ether substrates for *AaeAPO*. For example, although the enzyme cleave 4-nitroanisole to 4-nitrophenol, it failed to cleave a 4-nitrophenyl-terminated PEG. The gel permeation chromatography method that was used to assess cleavage provides a sensitive assay for random *endo*-scissions of the polyoxyethylene ethers in PEG (Kerem et al. 1999), yet no shift was observed in the molecular weight distribution of the polymer after enzymatic treatment. Moreover, no evidence was found for *exo*-cleavage of the model compound, which would have released 4-nitrophenol if it had occurred. Although *AaeAPO* was able to cleave diethylene glycol, it was unable to oxidize hexaethylene glycol (n=6) or larger PEG polymers (n=45). The first X-ray structures of *AaeAPO* confirm this

picture, showing that the distance between *Aae*APO-bound octaethylene glycol ( $n=8$ ) and the heme iron is around 12 Å (1.2 nm), whereas that for the *Aae*APO substrate 4-(hydroxymethyl)imidazole is only 2.25 Å (0.23 nm) (Figure 48). The hypothetical critical distance of the substrate from the heme iron for the suggested *Aae*APO-catalyzed hydrogen abstraction can be estimated by considering the length of the Fe-O-H species assumed to results after the initial hydrogen abstraction. This length is roughly the sum of the naturally occurring H-O bond length (1.0 Å in liquid water at 25° C and for *intermolecular* bonds up to 1.8 Å) and that of the Fe-O bond (around 1.7 Å) (Harris and Loew 1998). This sum gives a critical distance from the substrate to the iron of approx 2.5-3.5 Å, which suggests hat no bond in octaethylene glycol can approach closely enough to interact directly with the oxygen of the oxy-ferryl iron species of *Aae*APO.

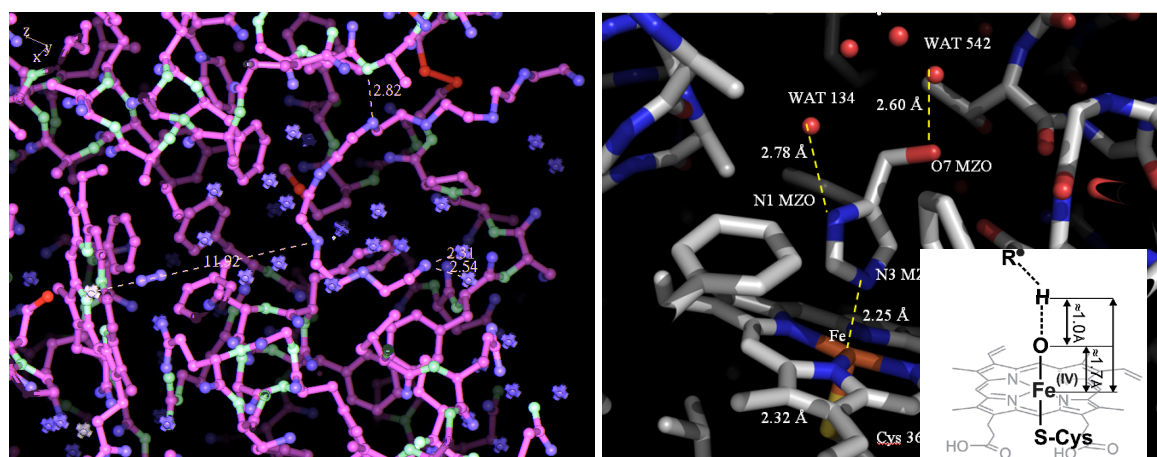


Figure 48 Octaethylene glycol molecule (left) and 4-(hydroxymethyl)imidazole (right) bound to the resting *Aae*APO at pH 7.0 (Piontek 2009).

In addition, the work reported here shows that, the peroxygenase released *n*-propanal efficiently from 1,4-di-*n*-propoxybenzene, but released only traces of *n*-butanal from 1,4-di-*n*-butoxybenzene. Moreover, *Aae*APO apparently did not cleave lignin ether structures in a synthetic dehydrogenative polymer of coniferyl alcohol nor in milled wood, as shown by negative results of analyses for aldehydes or other soluble fragments. These results, like those obtained with polyethylene glycols, suggest that the active site of *Aae*APO is unlikely to accommodate macromolecular ethers such as lignin or polyoxyethylene surfactants.

#### 4.1.2 The hypothetical reaction cycle

In summary the data show that *Aae*APO exhibits: (a) spectrophotometric features of classic heme-thiolate enzymes, (b) a wide catalytic spectrum encompassing that of P450s and

peroxidases, (c) a stoichiometry identifying the catalyzed monooxygenations as two-electron oxidations, (e) reaction kinetics that are consistent with a ping-pong reaction mechanism, (f) incorporation of  $\text{H}_2\text{O}_2$ -derived oxygen into the oxidized product, and (g) a high intramolecular deuterium isotope effect suggesting abstraction of a substrate hydrogen by the enzyme. These results support a mechanism similar to that envisaged for the peroxygenase activity of P450 (Ortiz de Montellano and de Voss 2005, Guengerich 2001).

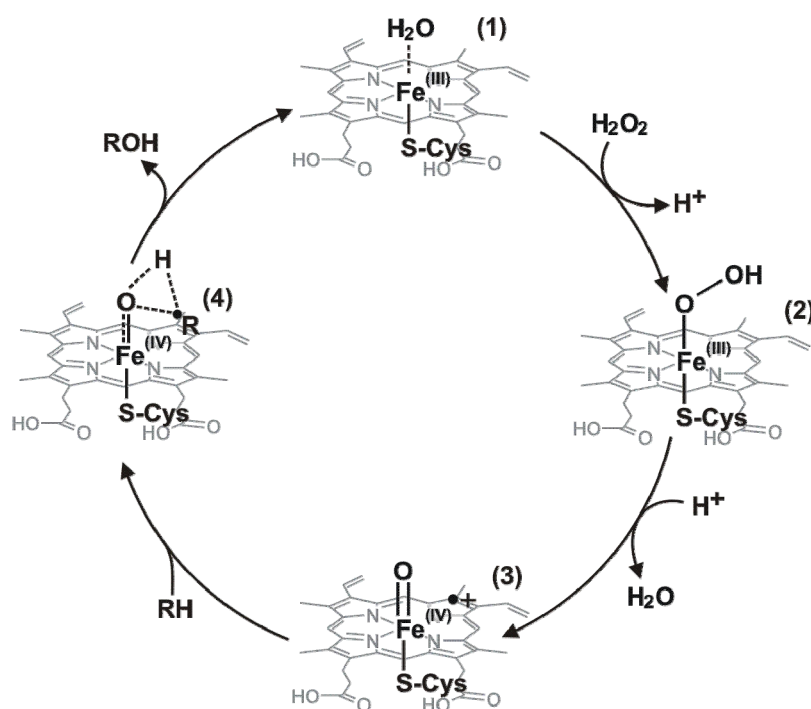


Figure 49 The hypothetical catalytic cycle of *AaeAPO*. (1) native (hydro)ferric enzyme, (2) iron(III)-peroxide complex (Compound 0), (3) Compound I and (4) putative transition state of a protonated Compound I/II-substrate complex.

Figure 49 illustrates the hypothetical reaction cycle of *AaeAPO*-catalyzed monooxygenation, based on results obtained from the mechanistic studies. The cycle is suggested to start with an *AaeAPO* low-spin six-coordinate iron in the ferric state [(1),  $\text{heme}(\text{Fe}^{\text{III}}-\text{H}_2\text{O})$ ] with water as the sixth ligand. According to the suggested ping pong mechanism, the co-substrate  $\text{H}_2\text{O}_2$  binds to the resting enzyme to form an extremely short-lived iron-(III)-peroxide complex [(2),  $\text{heme}(\text{Fe}^{\text{III}}-\text{O}-\text{OH})$ ] (“Compound 0” of P450), that is heterolytically cleaved between the oxygen atoms by a two-electron transfer from the heme. As a result, a water molecule is expelled and an oxy-ferryl radical cation complex of the heme [(3),  $\text{heme}(\text{Fe}^{\text{IV}}=\text{O})^+$ ] (“Compound I” of peroxidases) emerges and can react with the substrate. The oxygen transfer proceeds within this short-lived enzyme-substrate complex [(4),  $\text{R}-\text{H}\dots\text{heme}(\text{Fe}^{\text{IV}}=\text{O})^+$ ], which then dissociates with release of the oxygenated reaction product and the native enzyme.

As described for P450s, a large observed deuterium isotope effect for *Aae*APO-catalyzed ether cleavage suggests that a ferryl-oxygen abstracts a hydrogen from the substrate, producing a carbon-centered substrate radical, which in turn recombines with the equivalent of a hydroxyl radical (oxygen rebound) coordinated to the iron atom (Ortiz de Montellano 2009). The existence of an oxygen rebound is supported by the result that the oxygen that is incorporated into R-H originated from the peroxide. The rates of oxygen rebound for the  $[\text{Fe}^{\text{IV}}\text{-OH} + \cdot\text{RC}]$  radical pair have been found to occur in the range of  $10^{10}\text{-}10^{11} \text{ s}^{-1}$  for bacterial P450s with average radical lifetimes of in the range 0.3-250 picoseconds (Rachel et al. 2006). These radicals are trapped at the active site of P450, undergoing rapid oxygen rebound from the oxy-ferryl moiety in a typical “cage reaction”. In contrast to P450s, heme peroxidases have been shown to form highly reactive oxy-ferryl intermediates (compound I). However, the initial reaction products of peroxidases are predominantly radicals, which do not undergo oxygen rebound but rather exit the active site (“escape” reaction). The reason for the different reactivity of P450s and peroxidases is the different protein environment of their heme centers. Unlike P450s, the majority of heme peroxidases bear a neutral histidine residue as the fifth ligand. Histidine is thus a weak electron donating ligand in contrast to the anionic thiolate-ligand of P450s. This property of peroxidases may cause a shift of radical character from the iron bound oxygen to the ligand- $\pi$ -system during electrophilic attack by the enzyme, resulting in electron abstraction followed by oxygen release as water rather than oxygen rebound (Kaim 2005). This proposal is supported by the fact that peroxidases like *Cfu*CPO, bearing a cysteine as the fifth ligand, are able to catalyze the “cage” type of reaction yielding oxygenated products (Manoj and Hager 2008). From this point of view, the results observed indicate that the *Aae*APO mechanism resembles the peroxide “shunt” mechanism of P450.

However, *Aae*APO also exhibits peroxidase activity, which yields coupling and polymerization products from phenolic substrates. These results suggest that *Aae*APO is able to perform peroxidases like oxidations. In such a reaction mechanism, it is likely that a hydrogen atom is abstracted as described above but the oxygen is not rebounded to the substrate. Instead one radical is released from (4) with formation of an oxy-ferryl heme [heme( $\text{Fe}^{\text{IV}}\text{=O}$ )] (intermediate (4), Figure 8), which then reacts with the second substrate molecule, resulting in the formation of a second radical and the native ferric enzyme. The  $\text{H}_2\text{O}_2$ -derived oxygen at the active site is then released as water (*i.e.*, two one-electron oxidation steps occur).

The question arises as to whether *Aae*APO is able to catalyze single one-electron oxidations that occur remotely from the oxy-ferryl iron, as suggested to occur on binding sites at the

surface of peroxidases such as LiPs (Camarero et al. 1999), VPs (Tinoco et al. 2007) and *CfuCPO* (Kuhnel et al. 2006, Manoj and Hager 2008). One indication that supports such a long-range one-electron transfer reaction is the observation that *AaeAPO* oxidizes ABTS to the ABTS<sup>•+</sup> radical with an unusually low  $K_m$  (37  $\mu$ M) under acidic conditions (Ullrich et al. 2004). Moreover, *AaeAPO*-catalyzed halogenation reactions may proceed via a long-range mediated oxidation as suggested for *CfuCPO*, which has a binding site on its surface for halides (Manoj and Hager 2008). On the other hand, *AaeAPO* failed to oxidize polymers such as DHP, which has been suggested to bind to the surface of LiP and become oxidized via one-electron transfer (Johjima et al. 1999).

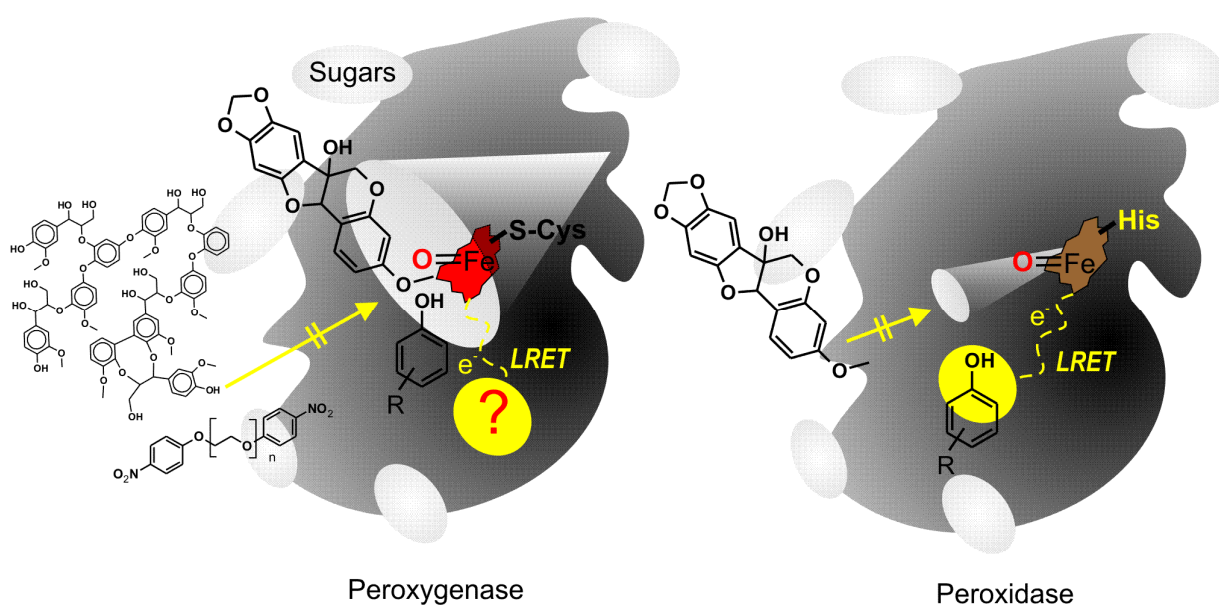


Figure 50 A simplified model of the active site (heme) of a peroxygenase compared to a classic peroxidase.

It is thus likely that *AaeAPO* substrates have to enter the binding pocket to become oxidized at the heme site (Figure 50). Recent results have shown that the *AaeAPO* pocket is able to accommodate relatively large non-polymeric molecules such as pyrene and perylene (Aranda et al. 2009) as well as pisatin. Furthermore, *AaeAPO* catalyzes oxidation of compounds with high redox potentials such as anisole, toluene and nitrobenzene, which are not oxidized by heme peroxidases. These results suggest a direct interaction of the substrate with the active site of *AaeAPO*. From this point of view, it is likely that the channel to the heme pocket is open to solvent. Preliminary results show that hydrophobic phenylalanine residues are located in this channel, which may explain the high affinity of *AaeAPO* for inactivated aromatic and aliphatic structures.

The proposed working models for *Aae*APO obviously need refinement, especially regarding the structure of the oxidized heme. Attempts to observe oxidized intermediates after titration of the enzyme with H<sub>2</sub>O<sub>2</sub> have been unsuccessful because they result in bleaching of the heme, and further progress will probably require a rapid transient-state kinetics approach. The sequence of substrate binding to the peroxygenase also remains to be established, and additional experiments with molecular clock and deuterated substrates would be advisable to check whether they yield data consistent with the radical rebound mechanism that has been proposed (Ortiz de Montellano and de Voss 2005).

#### 4.1.3 *Aae*APO an enzyme of a new sub-sub class?

The recent discovery and purification of diverse peroxygenases from fungi such as *Coprinellus radians*, *Coprinopsis verticillata*, other *Agrocybe* sp. and recently *Marasmius* sp. suggests that a novel superfamily of fungal oxidoreductases (EC 1.x.x.x) has been found (Pecyna et al. 2009, Anh et al. 2007). As discussed previously, peroxygenases in general have no EC-number yet, but could form a separate sub-subclass (EC 1.11.2.x in addition to peroxidases 1.11.1.x, see Figure 7) within the group of enzymes that use peroxides as electron acceptors (EC 1.11.x.x). However, the highest sequence and structural similarities found so far for *Aae*APO are with *Cfu*CPO (Figure 7).

#### 4.1.4 Ether cleavage

The data presented here show that *Aae*APO cleaved diverse aromatic and aliphatic ethers. According to the reaction mechanism described above, the enzyme heme is oxidized by H<sub>2</sub>O<sub>2</sub> to give an iron species that carries one of the peroxide oxygens and can be depicted as heme(Fe<sup>IV</sup>=O)<sup>+</sup> (Figure 49). This intermediate then abstracts a hydrogen located *beta* to the ether oxygen of **I**, which is followed by rebound of an <sup>•</sup>OH equivalent to produce a hemiacetal (or hemiketal when R<sub>2</sub> and R<sub>3</sub> is not hydrogen) **I'** that subsequently hydrolyzes into the corresponding alcohols **II** and carbonyls **III** (Figure 51).

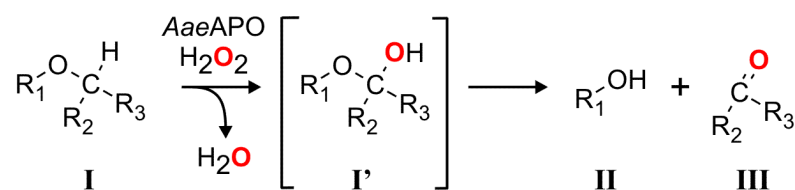


Figure 51 Reaction mechanism of *Aae*APO-catalyzed cleavage of ethers.

In reactions with an alkyl aryl ether ( $R_1$ =aromatic ring), a phenol is released instead of an alcohol ( $R_1$ =aliphatic carbon). For instance, 4-nitrophenol and formaldehyde were formed during the *Aae*APO-catalyzed ether cleavage of 4-nitroanisole whereas diethylether yielded ethanol and acetaldehyde. When  $R_2$  and  $R_3$  are alkyl or aryl residues, a ketone is released from a hemiketal intermediate instead of an aldehyde ( $R_2$  or  $R_3$ = H). For example, diisopropyl ether yielded acetone. In the case of a methyl benzyl ether ( $R_1$ =CH<sub>3</sub>,  $R_2$ =H,  $R_3$ =aromatic ring), methanol and benzyl aldehyde were released. Cyclic ethers split into hydroxy aldehydes *e.g.*, tetrahydrofuran yields 4-hydroxybutanal. At least one C-H bond located *beta* to the ether oxygen appears necessary for the reaction to proceed. For example in this work diphenyl ethers, were not cleaved by *Aae*APO. Thus *Aae*APO-catalyzed ether cleavage may be considered a consequence of carbon hydroxylation.

Table 14 Kinetic constants of ether cleavage by *Aae*APO in comparison to data obtained for other *Aae*APO substrates (Ullrich et al. 2004, Kluge et al. 2007, Ullrich et al. 2008).

Substrate	pH	$K_m$ ( $\mu$ M)	$k_{cat}$ ( $s^{-1}$ )	$k_{cat} / K_m$ ( $s^{-1} M^{-1}$ )
Thioanisole	6.8	25	444	$1.8 \times 10^7$
ABTS	4.5	37	283	$7.7 \times 10^6$
<b>3,4-Dimethoxybenzyl methyl ether</b>		<b>467</b>	<b>351</b>	<b><math>7.5 \times 10^5</math></b>
Naphthalene		320	166	$5.2 \times 10^5$
2,6-Dimethoxyphenol		298	108	$3.6 \times 10^5$
H <sub>2</sub> O <sub>2</sub>	7	1313	367	$2.8 \times 10^5$
Benzyl alcohol		1001	269	$2.7 \times 10^5$
<b>3,4-Dimethoxybenzene</b>		<b>987</b>	<b>214</b>	<b><math>2.2 \times 10^5</math></b>
Veratryl alcohol		2637	85	$3.6 \times 10^4$
<b>Tetrahydrofuran</b>		<b>3226</b>	<b>96</b>	<b><math>2.9 \times 10^4</math></b>
Pyridine		69	0.21	$3.0 \times 10^3$

The comparison of kinetic constants in Table 14 illustrates that the values for ether cleavage are in the same range as those for other *Aae*APO-catalyzed oxidations. This is an indication that ethers may be among the physiological substrates of *Aae*APO.

The biochemical cleavage of an ether bond is a remarkable feature. The high dissociation energies of ether bonds ( $360 \text{ kJ mol}^{-1}$ ) and the relatively low yields of assimilable carbon energy generated may underlie the scarcity of ether cleaving enzymes found in organisms (Kim and Engesser 2004, White et al. 1996). The majority of ether cleavage systems apparently convert the substrate to a hemiacetal structure, which then fragments to break the erstwhile ether linkage, probably via a nonenzymatic step. However, no enzyme has been

specifically observed to catalyze hemiacetal production, presumably because these structures are so unstable (White et al. 1996).

Intracellular heme containing monooxygenases such as P450s have been reported to *O*-dealkylate alkyl-aryl ethers by various mechanisms (Urano 1996). For anisole one possibility is a hydrogen abstraction to give a phenoxyethyl radical followed by rapid oxygen rebound that results in hydroxylation of the *alpha*-carbon followed by breakdown to a phenol and the corresponding aldehyde (Brodie et al. 1958, Foster et al. 1974, Miwa et al. 1984, Harada et al. 1984). Alternatively, *ipso*-substitution on the aromatic ring could yield a hydroxycyclohexadienyl radical, which is then converted into a phenol via a phenoxy radical with release of methanol (Urano 1996).

The results presented here clearly show that ring carbons of alkyl aryl ethers are not attacked by *Aae*APO, as this reaction would release the alkyl group as an alcohol rather than aldehyde, and would also result in incorporation of labeled oxygen from the peroxide into the phenolic product. The results presented here agree with those found for many P450s, which oxidized only those ethers that contain a vicinal C-H bond (Ortiz de Montellano and de Voss 2005).

Additional enzymes have been shown to cleave ethers. Recently it was suggested that a flavin-containing monooxygenase from *Rhodococcus* is involved in the cleavage of bis(1-chloro-2-propyl) ether (Moreno Horn et al. 2003). Moreover, dioxygenases, which are able to introduce both oxygens from O<sub>2</sub> into an ether substrate, have been shown to be involved in the cleavage of diaryl ethers (Schmidt et al. 1992). Peroxidases such as LiP and SbP have also been shown to catalyze the cleavage of alkyl aryl ethers nonselectively by abstracting electrons from aromatic rings, which then undergo spontaneous scission reactions (Mester et al. 2001, Tien 1987, Joshi and Gold 1996, McEldoon et al. 1995, Kirk et al. 1986). However, these reactions are restricted by the redox potential of the peroxidases. For instance, HrP has been shown to be unable to oxidize 1,4-dimethoxybenzene (Kersten et al. 1990). Even the synthetic heme-based minicatalyst microperoxidase 8 (MP8), which catalyzes peroxidase-type one-electron oxidations (Wang et al. 1991, Boersma et al. 2000) as well as P450-type of oxygen transfer reactions, is unable to oxidize alkyl aryl ethers with ionization potentials higher than 8.4 eV (Veeger 2002, Osman et al. 1996).

There are additional oxidative and reductive pathways described for ether cleavage. Besides oxygenation, the list includes dehydrogenation, hydroxyl group transfers, hydrolysis, reduction, nucleophilic substitution and dismutation. For some of these reactions, there is compelling evidence to support proposed pathways (e.g., monooxygenations in aerobic degradation of methyl aryl ethers, hydroxyl shifts mechanisms in the anaerobic degradation of



PEGs, and methyl transfers to tetrahydrofolate in anaerobic degradation of methyl aryl ethers), whereas for other pathways the evidence is more fragmentary (White et al. 1996). However, only three ether cleavage enzymes are accredited with a formal listing, namely isochorismate pyruvate lyase (EC 3.3.2.1), carboxymethyloxysuccinate lyase (EC 4.2.99.12) and 4-methoxybenzoate monooxygenase (EC 1.14.99.15).

#### 4.1.4.1 Cleavage of arylglycerol *beta*-aryl ethers

*Aae*APO cleaved non-phenolic arylglycerol *beta*-aryl ethers (*beta*-O-4-linked ethers) via selective demethylation of the *para*-methoxyl group to give the corresponding aldehydes and phenolic dimers, which then underwent further oxidations by *Aae*APO, yielding monomers and polymerization products. Figure 52 illustrates the hypothetical reaction mechanism. *Aae*APO dealkylates the non-phenolic arylglycerol *beta*-aryl ether **I**, which yields the phenolic lignin model compound **II** after release of the corresponding aldehyde by the reaction mechanism described above. In the absence of a radical scavenger, compound **II** underwent further oxidation to yield a monomeric hydroxylated species **VIII** and polymeric reaction products. This reaction is inhibited in the presence of a radical scavenger such as ascorbic acid, which suggests that *Aae*APO oxidizes the phenolic moiety to form a phenoxyl radical that can be reduced by ascorbic acid.

As described above, compound **III**, bearing an additional methoxyl moiety, served as a suitable substrate to establish the reaction mechanism for *Aae*APO-catalyzed oxidation of the phenolic arylglycerol *beta*-aryl ethers. Once a phenolic moiety is formed in the arylglycerol *beta*-aryl ether, *Aae*APO abstracts an electron from the phenolic lignin model **III**, yielding the cyclohexadienyl radical **III'**, which is subsequently oxidized by *Aae*APO to give the corresponding cation **III''**.

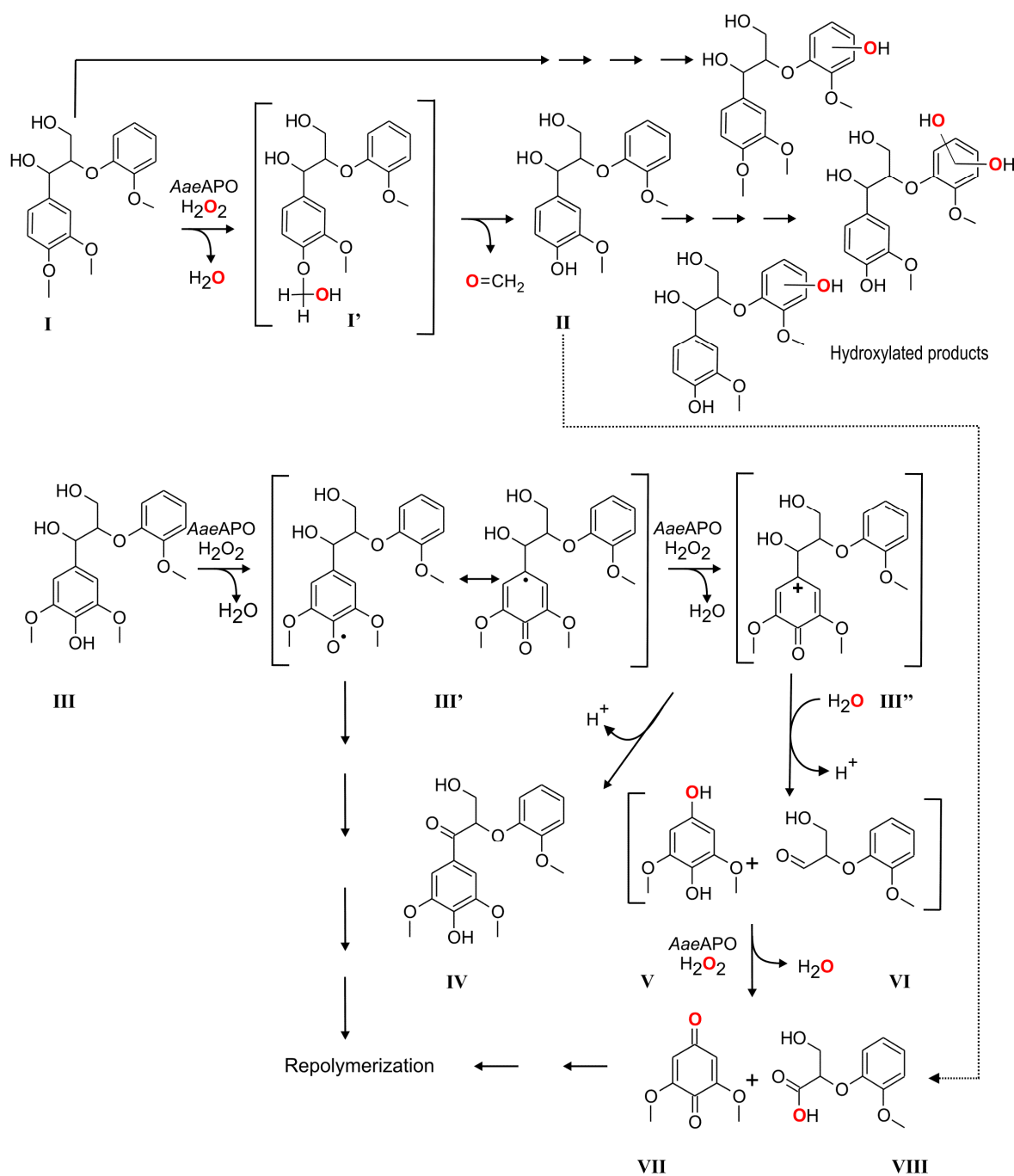


Figure 52 Hypothetical reaction mechanism of *AaeAPO*-catalyzed cleavage of arylglycerol  $\beta$ -aryl ethers adapted and modified according to (Tuor et al. 1992).

Loss of an  $\alpha$ -proton then results in the formation of an uncharged quinone methide intermediate that rearranges to yield the phenolic ketone **IV**. In support of this mechanism, no labelled oxygen from molecular oxygen or  $\text{H}_2^{18}\text{O}$  was incorporated into **IV**. Moreover, ketone formation from the non-phenolic substrate **I** was not observed, which indicates that *AaeAPO* needs a phenolic moiety to cleave the arylglycerol  $\beta$ -aryl ether. Alternatively, the cation intermediate **III''** may be attacked by water, yielding a hydroxy-substituted cyclohexadienone

intermediate, which undergoes alkyl-phenyl bond cleavage to yield the hydroquinone **V** and the phenoxy-substituted propanal **VI**. Under these reaction conditions, *Aae*APO oxidizes the hydroquinone **V** to the benzoquinone **VII** and the phenoxy-substituted propanal **VI** to a phenoxy-substituted propionic acid **VIII**. As predicted by this pathway, one atom of  $^{18}\text{O}$  from  $\text{H}_2^{18}\text{O}$  was incorporated into the benzoquinone **VII**. No incorporation of  $^{18}\text{O}$  from  $\text{H}_2^{18}\text{O}$  was observed during the formation of the phenoxy-substituted propionic acid **VIII**, but incorporation from  $\text{H}_2^{18}\text{O}_2$  occurred. The released radical intermediates **III'** and benzoquinone finally undergo further oxidation to form polymeric reaction products. The oxidation mechanism of **II** is identical to that proposed previously for the *C-alpha* oxidation of phenolic arylglycerol *beta*-aryl ethers by MnP (Tuor et al. 1992). The structure of reaction product **VIII** is proposed on the basis of the data, which show that, *a*) oxygen incorporation was detected when the oxygen originated from  $\text{H}_2^{18}\text{O}_2$ , *b*) this compound accumulated and was not polymerized, *c*) this reaction product was released when either compound **I** and **III** were incubated, which indicates a common reaction mechanism.

#### 4.1.5 Aromatic hydroxylation

The results show that *Aae*APO catalyzes the selective hydroxylation of aromatic rings to give phenolic reaction products. This is consistent with previous results, showing that *Aae*APO catalyze the hydroxylation of aromatic rings via formation of epoxide intermediates (Kluge et al. 2009).

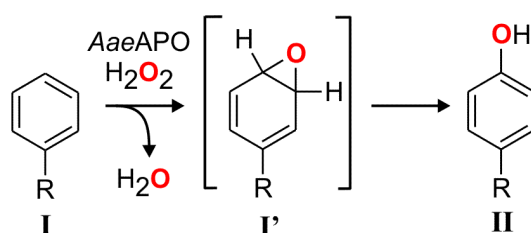


Figure 53 Hypothetical reaction mechanism of *Aae*APO-catalyzed hydroxylation of aromatics.

Therefore, it is likely that the hydroxylation of aromatics **I** involves the oxidation of one of the  $\pi$ -bonds, rather than the direct insertion of the oxygen into one of the aromatic C-H bonds. However, this has not been investigated, as the unstable epoxide intermediates **I'** expected from the oxidation readily undergo heterolytic cleavage of one of the epoxide C-O bonds. This cleavage is followed by a migration of a hydride from the carbon retaining the oxygen in the adjacent carbocation to give a ketone intermediate [“NIH-shift” shown for P450 (Ortiz de

Montellano and de Voss 2005)]. Tautomerisation of this ketone yields a phenolic product **II**. The results of *Aae*APO-catalyzed hydroxylation are consistent with this mechanism and the one described above, showing that one oxygen found in the hydroxylated aromatic product originates from  $\text{H}_2^{18}\text{O}_2$  and therefore from the suggested oxy-ferryl species [Figure 49,  $\text{heme}(\text{Fe}^{\text{IV}}=\text{O})^{*\text{+}}$ ].

A remarkable feature of *Aae*APO is the hydroxylation of inactivated nitrobenzene, which yielded 4-nitrophenol. The *in vivo para*-hydroxylation of nitrobenzene via P450s has been found in animal liver microsomes (Wisniewska-Knypl et al. 1975) and in a plant subcellular microsomal fraction (Varazashvili et al. 2001). Nitrobenzene is a poor substrate for *Aae*APO, yielding reaction products only after hours of incubation with syringe pump-mediated  $\text{H}_2\text{O}_2$  supply. The slow reaction is perhaps a consequence of the high activation energy of this substrate. The energy needed for the oxidation of the *para*-position of nitrobenzene with a porphyrin model was calculated on the basis of density functional theory, yielding values of  $81 \text{ kJ mol}^{-1}$  in the doublet and of  $78 \text{ kJ mol}^{-1}$  in the quartet spin state (Rydberg et al. 2008). This assumption is consistent with the results obtained for *Aae*APO-catalyzed hydroxylation of diclofenac, which is a better substrate for *Aae*APO as its activation energy for the 4-position has been calculated to be lower (around  $70 \text{ kJ mol}^{-1}$ ). Once 4-nitrophenol is formed, *Aae*APO can hydroxylate it further to give 4-nitrocatechol. This reaction has been used as an *in vitro* marker of human P450s (Tassaneeyakul et al. 1993).

#### 4.1.6 Benzylic oxygenation

The results reported here show that *Aae*APO converted toluenes to benzoic acids via sequential two-electron oxidations, and that the intermediate benzyl alcohols and benzaldehydes were released from the enzyme active site. In addition to side chain oxidation, *Aae*APO also catalyzes the oxygenation of the aromatic ring of toluene (but not of 4-nitrotoluene) leading to mixtures of *para*- and *ortho*-cresol and their oxidation products (Ullrich and Hofrichter 2005). As reported earlier, these reactions may compete with side chain oxidation. In the present study, where the focus has been on side chain oxidations, ring oxygenation of toluene was ignored.

The  $^{18}\text{O}$ -labeling experiments establish that the oxygens introduced during oxidations originate from  $\text{H}_2\text{O}_2$ . The results support a mechanism similar to that envisaged for the peroxygenase activity of P450s (Ortiz de Montellano and de Voss 2005, Guengerich 2001) and for ether cleavage catalyzed by *Aae*APO (Kinne et al. 2009a). In such a mechanism the enzyme heme is oxidized by  $\text{H}_2\text{O}_2$  to give a ferryl oxygen intermediate (Hanzlik and Ling

1990) that carries one of the peroxide oxygens and can be depicted formally as  $(\text{FeO})^{3+}$ . The latter (very probably a Compound I-type intermediate) abstracts a hydrogen from the benzylic carbon of to give an enzyme-bound benzylic radical, after which rebound of an  $\bullet\text{OH}$  equivalent occurs to introduce a new hydroxyl group on the same carbon (Figure 54).

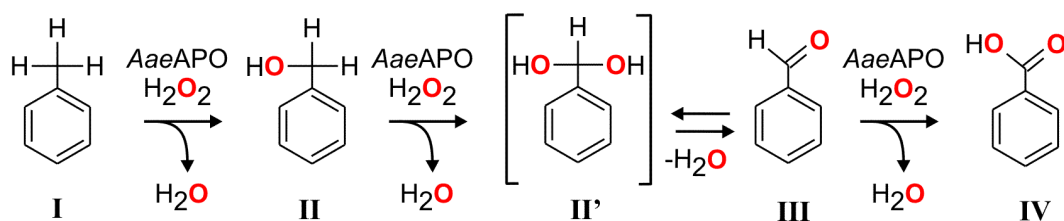


Figure 54 Reaction sequence of the benzylic oxidation catalyzed by *AaeAPO*.

According to this model, oxygen incorporation from  $\text{H}_2\text{O}_2$  should be quantitative when a toluene (**I**) is oxidized to a benzyl alcohol (**II**), and the data agree with this picture. When the substrate is a benzyl alcohol instead, the enzyme-bound intermediate will be an  $\alpha$ -hydroxybenzylic radical and the resulting initial product will be a *gem*-diol (**II'**) in equilibrium with the benzaldehyde (**III**). Consequently, some of the oxygens introduced from  $\text{H}_2\text{O}_2$  will be lost via non-stereospecific exchange with water, again in accord with the results. Finally, when the substrate is a benzaldehyde, the enzyme-bound intermediate will be an  $\alpha$ -oxobenzylic radical, oxygen incorporation from  $\text{H}_2\text{O}_2$  will be quantitative, and the resulting product will be the benzoic acid (**IV**), once more in agreement with the data. In theory, this last oxidation could proceed via the *gem*-triol, but this intermediate can be ruled out because it was found that no exchange of incorporated oxygen occurred during the oxidation of either benzaldehyde (Figure 40).

The sequential *AaeAPO*-catalyzed oxidations that have been described here are also typical of P450s (Scheller et al. 1998, Teramoto et al. 2004), but the latter enzymes are intracellular, whereas *AaeAPO* is secreted into the surrounding environment by the fungal hyphae. Some other oxidative fungal enzymes such as LiPs and *CfuCPO* also have an extracellular location, but are more limited than *AaeAPO* in the variety of compounds they can utilize as electron donors. For example, *PceLiP* does not oxidize benzyl alcohol, and neither of these peroxidases is able to oxidize 4-nitrotoluene (Scheller et al. 1998, Miller et al. 1995, Russ et al. 2002).

#### 4.1.7 Further oxidation reaction catalyzed by *Aae*APO

The discussion in this chapter is based on preliminary results obtained from observations of side reactions that occurred during mechanistic investigations. Mechanistic studies were not performed and therefore reaction mechanisms proposed are tentative.

##### 4.1.7.1 Oxidation of the phenolic moiety

The results illustrate that *Aae*APO forms quinones, coupling- and polymerization products during the oxidation of the phenolic moieties. *Para*-benzoquinone, biphenyl-4,4'-diol and polymers are the major reaction products of the *Aae*APO-catalyzed oxidation of phenol. When a radical scavenger is added to the reaction mixture, hydroquinone is the dominant reaction product.

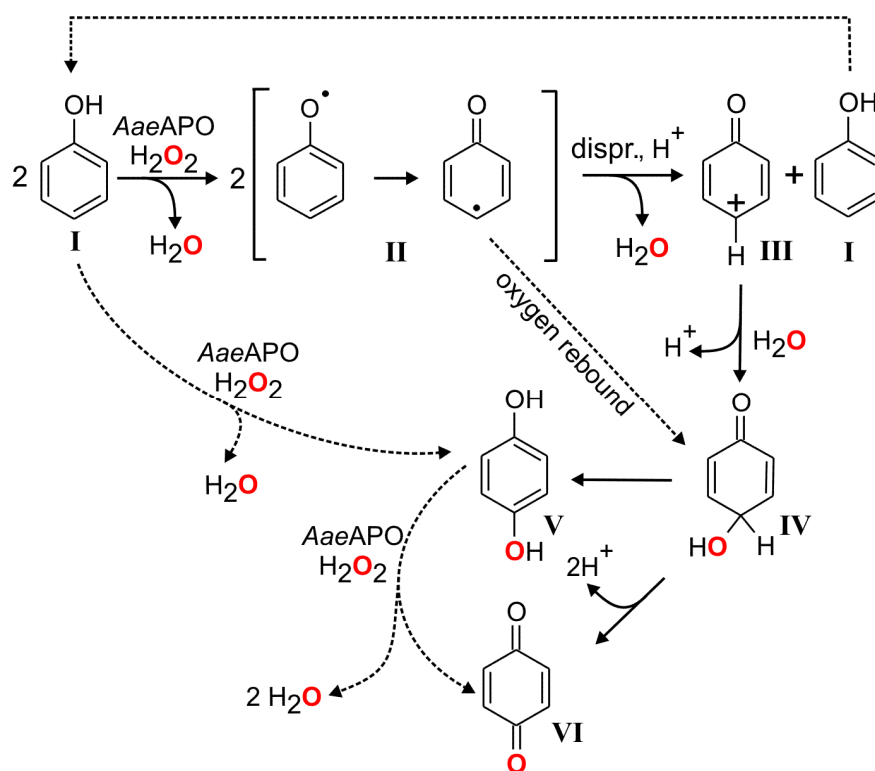


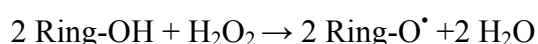
Figure 55 Hypothetical reaction mechanisms for the phenol oxidation catalyzed by *Aae*APO. The released radicals may migrate from the active site (or from the surface LRET-amino acid) and undergo autocatalytic reactions such as polymerization.

The quinones add oxygen from  $\text{H}_2\text{O}$  as shown above (compound VII see Figure 52). Moreover, *para*-benzoquinone is released during the *Aae*APO-catalyzed reaction of *para*-aryloxy phenols such as 4-methoxyphenol or 4-ethoxyphenol in the absence of ascorbic acid. The *Aae*APO-catalyzed oxidation of 4-nitrophenol yields 4-nitrocatechol as the initial

reaction product, which indicates that the nitro-moiety is not eliminated by *Aae*APO. By contrast, liver microsome-located P450s have been shown to catalyze the elimination of the nitro group of 4-nitrophenol (Ortiz de Montellano and de Voss 2005).

In summary the results indicate that *Aae*APO is involved in the formation of phenoxyl radicals **II** and quinones **VI** from phenols **I** (Figure 55), which can be reduced by ascorbic acid (Valero et al. 2003), but otherwise undergo coupling and polymerization reactions. These reaction products are also present in reactions catalyzed by peroxidases (Kaim 2005, Dunford 1999). According to this mechanism the oxy-ferryl species of *Aae*APO, formally depicted as  $[\text{Fe}=\text{O}]^{3+}$ , abstracts an hydrogen from the phenol to give  $[\text{Fe}---\text{OH}]^{3+}$  and a free phenoxyl radical with formation of water. This reaction mechanism (double one-electron oxidation) is similar to that envisaged for heme peroxidases (Figure 8) with the difference that the oxygen rebound is not restricted for *Aae*APO. Results from difference binding spectra of *Aae*APO (Figure 14) indicate a direct binding of phenol at the active site of *Aae*APO, indicating an oxy-ferryl mediated hydrogen abstraction of the phenolic group.

An electron may also be abstracted via LRET by an amino acid (for example the sandwiched phe233) located on the surface of *Aae*APO (single one-electron oxidation). The two mesomeric forms of the phenoxyl radical can disproportionate to a cyclodienone cation **III** and a phenol molecule **I**. A hydroxyl from water then adds to **III** to form the unstable hydroxycyclodienone **IV**, which then rearrange to hydroquinone **V** or *para*-benzoquinone **VI**. *Aae*APO may then oxidize hydroquinone **V** by the same mechanism to give *para*-benzoquinone **VI**. The stoichiometry of such an *Aae*APO-catalyzed radical generation is:



On the other hand, the formation of dihydroxy aromatics and *para*-benzoquinone rather than the formation of coupling products has been proposed for P450-catalyzed reactions of phenols (Ortiz de Montellano and de Voss 2005). In this mechanism, direct aromatic hydroxylation of the carbon *para*-located to the phenolic group would yield hydroquinone **V**. The question arises if this hydroxylation proceeds via epoxide formation as discussed before, or if the phenoxy radical undergo oxygen rebound (Figure 55). This last mechanism, named *ipso*-recombination, has been proposed for P450s, which form *para*-benzoquinone **VI** from *para*-substituted phenols with release of the *para* substituent (Ortiz de Montellano and de Voss 2005). Previous results suggest that *Aae*APO does not oxygenate the ring carbon via an *ipso*-substitution mechanism. Moreover, it has been recently shown that P450s are involved in

oxidative coupling of phenols (Grobe et al. 2009) and this reaction was suggested to occur via single electron transfer to give phenoxyl radicals or via formation of an arene-oxide intermediate (Woithe et al. 2007). However, the detailed reaction mechanism remains obscure.

The major question that comes up is if the phenoxy radical is completely released from the active site of *Aae*APO (“escape” reaction also suggested to proceed via long range electron transfer) or if oxygen rebound can occur (“cage” reaction). Recent preliminary results indicate that *Aae*APO may act with both activities on phenols. A hybrid behavior of enzymes bearing activities of both peroxidases and P450s is a common phenomenon. For example, synthetic catalysts like MP8, have been shown to catalyze the oxidation of phenols with formation of both coupling products and hydroquinone (Osman et al. 1996). More research is needed to understand how *Aae*APO acts on the phenols.

#### 4.1.7.2 Dehalogenation

*Aae*APO catalyze the H<sub>2</sub>O<sub>2</sub>-dependent dechlorination of aliphatic and benzylic substrates with formation of aldehydes. This catalytic property of *Aae*APO is similar to the oxidative heteroatom elimination catalyzed by P450s (Ortiz de Montellano 2005). For example, it has been suggested that the *in vitro* cleavage and dehalogenation of 2,2-dichlorodiethyl ether and 2,2'-dichlorodiisopropyl ether is catalyzed by monooxygenases from *Xanthobacter* sp. and *Rhodococcus* sp. (McClay et al. 2007, Moreno Horn et al. 2003). The dehalogenation of aliphatic compounds by P450s might proceed by one or two electron reductive pathways or as proposed for the conversion of dihalomethanes by oxidative hydroxylation followed by the loss of a halogen as a result of nonenzymatic collapse of an unstable intermediate (Rietjens et al. 1997, Ulrik et al. 2003, Sono 1996). The results indicate that the *alpha*-carbon next to the chloro moiety is oxygenated by *Aae*APO to give a *gem* chloro alcohol, which then rapidly hydrolyzes to give HCl and the corresponding aldehyde (two-electron oxidation).

#### 4.1.7.3 *N*-Dealkylation

*Aae*APO catalyzes the *N*-dealkylation of *N*-methylaniline to aniline. This catalytic property of *Aae*APO is similar to reactions of P450s and peroxidases (Dunford 1999, Ortiz de Montellano and de Voss 2005). The demethylation of *N,N*-dimethylaniline was described for *Cfu*CPO (Kedderis 1980), for HrP which demethylated various *N*-substituted aromatic amines (Van der Zee et al. 1989) and for MP8 (Boersma et al. 2000). In general, two reaction mechanisms are proposed for P450 catalyzed *N*-dealkylations (Li et al. 2009): one is a formal hydroxylation of



a C-H bond on the carbon adjacent to the heteroatom (Shaik et al. 2005), the other is a one-electron oxidation of the heteroatom itself (Ortiz de Montellano and De Voss 2002). *Aae*APO was shown to catalyze heteroatom oxygenations such as *N*-oxygenation reactions (Ullrich et al. 2008) and heteroatom dealkylations such as *O*-demethylation reactions (Kinne et al. 2009a). The precise mechanism behind *Aae*APO-catalyzed *N*-dealkylations remains unclear, but future investigation should focus on the detection of aldehydes. The results further indicate that *Aae*APO is able to hydroxylate the amino group of anisole to give *N*-hydroxyanisole. The *N*-hydroxylation reaction has been shown for P450 (Sono 1996).

#### 4.1.7.4 Halogenation

*Aae*APO brominates and chlorinates anisole. *Aae*APO as well as *Cra*APO and *Cve*APO have been shown previously to brominate phenol at acidic pH, but could not efficiently chlorinate it (only traces of 2-chlorophenol were found) (Ullrich et al. 2004, Anh et al. 2007). To date, more than 3800 natural halogenated metabolites have been isolated from plants, fungi, lichens, bacteria, insects, some higher animals and even humans (Gribble 2003). Besides the production of organohalogens by marine organisms (algae, worms, bacteria), terrestrial fungi (mushrooms) in particular have been identified as potent producers of halogenated compounds (van Pée and Zehner 2003). Halogenation reactions can also be catalyzed by other peroxidases such as *Cfu*CPO, LiP and MnP (Farhangrazi et al. 1992, Hager et al. 1966, Sheng and Gold 1997), and thus the halogenating activities of these enzymes including *Aae*APO may be connected with the presence of various organohalogens ubiquitously found among basidiomycetous fungi (Verhagen et al. 1996). The haloperoxidase activity of *Aae*APO resembles that of *Cra*APO and *Cve*APO, which also preferred bromide to chloride during phenol halogenation (Anh et al. 2007). This finding differs from the behavior of classical *Cfu*CPO and vanadium haloperoxidases. However, as for all haloperoxidases, *Aae*APO-catalyzed halogenations lack substrate specificity and regioselectivity, presumably because free hypohalous acids are the proximal halogenating species (Littlechild 1999, Manoj and Hager 2008).

## 4.2 Physiological role of *Aae*APO

*Aae*APO-catalyzed reactions have the following impacts on the reactants: (a) increase in the hydrophilicity and reactivity via oxygen introduction or hydrogen abstraction with consequent formation of unstable intermediates, (b) fragmentation caused by dealkylation and heteroatom release, (c) polymerization initiated by phenol oxidation and (d) reduction of hydroperoxides

to alcohols and, in the case of hydrogen peroxide, to water. *Aae*APO- catalyzed hydroxylations/ dealkylations or heteroatom oxygenations (peroxygenase activity) are followed by the oxidation of the generated phenolic moieties (peroxidase activity) to give free radicals, and thence coupling products (Figure 56).

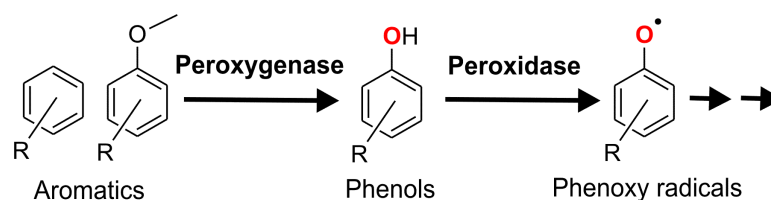


Figure 56 Suggested physiological reaction sequence of *Aae*APO during bioactivation of aromatics

As such, *Aae*APO not only combines diverse enzyme activities (etherase, peroxidase, peroxygenase, haloperoxidase) but also acts as a substrate donator for phenol-oxidizing enzymes such as laccases and peroxidases.

These observations indicate a likely role for *Aae*APO and other fungal peroxygenases in the extracellular breakdown of natural and anthropogenic low molecular weight compounds (Figure 57). Some of these reactions are probably fortuitous, as are many of the extracellular xenobiotic oxidations carried out by lignocellulolytic fungi (Tortella et al. 2005). In other cases, the catalyzed reactions may have a physiological function, for example in the biodegradation of low molecular lignin fragments, or in the detoxification of fungicidal compounds derived from plants or microorganisms via hydroxylation or demethylation and subsequent polymerization (Delserone et al. 1999). Moreover, the results indicate that *Aae*APO may be involved in humification due to its H<sub>2</sub>O<sub>2</sub>-dependent polymerization activity. It is pertinent that many lignocellulolytic fungi produce the necessary extracellular H<sub>2</sub>O<sub>2</sub> (Leonowicz et al. 1999), and that this oxidant is also deposited in soils from rainwater (Kok 1980).

*A. aegerita*, the black poplar mushroom colonize the surface and subsurface root tissue of dead or enfeebled hardwoods (*e.g.*, poplar, willow, and aspen stumps) as well as the surrounding litter and soil, and grows on mulch-like materials (Stamets and Chilton 1983). This environment includes dead trunks, stumps, leaves, needles, twigs, branches, roots, and the remains of insects, bacteria, fungi, and animals. From a chemical point of view, this habitat consists primarily of lignocellulose and older humic fractions derived from it, but also contains a wide variety of other chemical components.

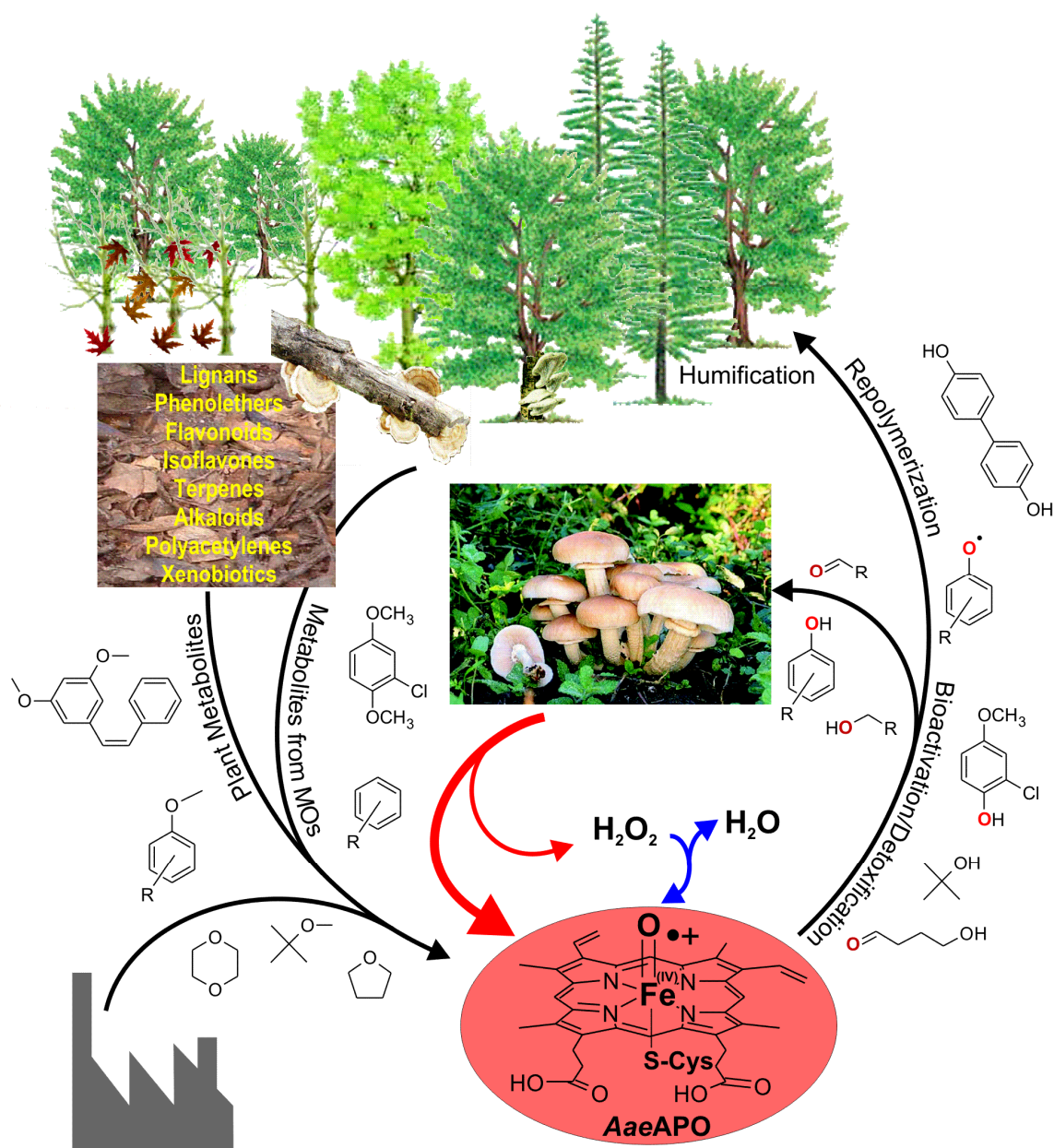


Figure 57 The physiological role of *AaeAPO* in the cleavage of ethers.

These components include: (1) cellulose, (2) hemicellulose, (3) lignin, (4) water-soluble sugars, amino acids, and aliphatic acids, (5) ether- and alcohol-soluble constituents, including fats, oils, waxes, resins, and many pigments, and (6) proteins (Satchell 1976). Moreover, additional natural products are included within this heterogenic matrix, *e.g.*, lignans, phenolic ethers, flavonoids, isoflavones, terpenes, alkaloids, tannins, polyacetylenes and oxylipins.

Hence, *AaeAPO*-catalyzed reactions may be bio-physiochemically related to these special habitats, which are characterized by high amounts of aromatic compounds and lignocellulose fragments that can be utilized as carbon source. These specific features of the habitats, in particular the high pH that does not enable “classic ligninolytic peroxidases” (LiPs, MnPs,

VPs) to be active (they work only between pH 2 and 5), support the assumption that the production of extracellular peroxygenases is characteristic for agaric and alkaliphilic fungi. In this context, it is interesting to note that *A. aegerita* does not produce these “classic ligninolytic peroxidases”. It may be that in more alkaline environments, fungi have developed alternative strategies to transform aromatic and heterocyclic substances, for example by using extracellular peroxygenases.

Provision of nutrients or compounds protective against microbial attack is a major function of fungal extracellular enzymes. Aromatic compounds are widely distributed in the habitats of the litter decaying fungi that secrete *AaeAPO* and other peroxygenases (Ullrich and Hofrichter 2007). In particular, polymeric lignin is the major repository of aromatic structures derived from higher plants. However, the results presented here show that *AaeAPO* is not able to attack polymeric structures, which indicates that the enzyme may not have an essential role in lignin depolymerization. This observation is consistent with *in vivo* experiments that indicate *Agrocybe aegerita* is only a moderate delignifier of wood (Isikhuemhen et al. 2009).

The depolymerization of lignin, an oxidative process predominantly achieved by aerobic fungi (Hammel and Cullen 2008), leads to the production of numerous oligomeric and monomeric aromatics including alkyl aryl ethers that are potential substrates for fungal ether cleavage systems (White et al. 1996). Moreover the lot of secondary plant metabolites carrying the methoxyl moiety. As described in the preceding sections, dealkylation of alkyl aryl ethers may occur via peroxygenases in agaric fungi. It is likely that the evolution of these catalytic activities for scission of alkyl aryl ethers was a response to exposure to these natural compounds throughout evolutionary time.

Another important physiological function, which corresponds to the P450-like substrate spectrum of *AaeAPO*, is detoxification. The oxidation of fungicidal compounds outside the cell is an efficient mechanism fungi use to modify their environment. Natural fungicidal substances derive from plants (phytoalexins or phytoanticipins) or microorganisms (mycotoxins and antibiotics). An initial pathway of oxidative toxin biotransformation is the introduction of a hydroxyl group via hydroxylation or demethylation, which are typical phase I reactions (Sonia et al. 2009). The biochemical goal of this reaction is to increase the polarity of the organic toxicant, thereby enabling its further metabolism (Varazashvili et al. 2001). The methoxyl moiety is widely distributed in biochemicals synthesized by plants and microorganisms (Hamill et al. 1957), where it protects a phenolic or alcoholic moiety and thus modulates metabolic activity.

For example, pisatin from pea plants is an extensively investigated methoxylated phytoalexin that interacts with parasitic fungi (Bednarek and Osbourn 2009). It is now known that selective demethylation of the methoxyl moiety catalyzed by a fungal P450 system decreases the toxicity of pisatin and thus enables the fungi to grow on the plant leaves (George and VanEtten 2001). As shown here, *AaeAPO* very rapidly demethylates pisatin via its “etherase” activity. Although *A. aegerita* is not a phytoparasitic fungus, it has been shown that *AaeAPO*-like genes are found in plant pathogenic fungi such as corn smut (*Ustilago maydis*) and heterokonts such as potato blight (*Phytophthora infestans*) (Pecyna et al. 2009), which may indicate an early evolutionary origin for APOs. Another important fact is that *A. aegerita* exhibits its highest *AaeAPO* activity, when grown on soybean medium (Ullrich et al. 2004). It is known that soybean, a leguminous plant, produces phytoalexins such as glyceollin, which are structurally related to pisatin (Zimmermann et al. 2009) and may act as enzyme inducers.

The natural environment of *A. aegerita* consists of a heterogeneous matrix containing different species of toxic phytoalexins and antibiotic phytoanticipins (preinfectious compounds), which come into contact with the mycelium. For this reason, plant litter shows fungicidal activity (Harrison 1971, Vane et al. 2006). Diverse fungicidal compounds have been isolated from sapwood, bark and leaves of woody plants and identified over the past decades (Gottstein and Gross 1992). For instance, the pinosylvin 3,5-dimethoxystilbene, which is found in leaves of spruce and pines (Celimene et al. 1999), is rapidly oxidized by *AaeAPO*. Methoxylated phytoalexins such as derivatives of the antifungal lignan syringaresinol and its dimethyl ether, as well as the sapwood alkaloid glaucine, are found in yellow poplar (*Liriodendron tulipifera*) (Kemp and Burden 1986). Poplar (*Populus spec*) wood contains diverse secondary plant metabolites, predominantly phenols, phenolic glycosides, flavonoids and tannins, which also show fungicidal activities.

Microorganisms also produce diverse fungicidal compounds to survive competition with other organisms. For example, it has been shown that soradins, a natural class of antifungal agents that inhibit fungal protein biosynthesis, are produced by *Podospora pleiospora* in its natural substrate (dung) at sufficiently high doses to produce antibiosis against yeasts but not against filamentous fungi (Weber et al. 2005, Vicente et al. 2009). *AaeAPO* may have a role in the detoxification of such fungicidal compounds.

*AaeAPO* is also able to cleave 2-chloro-1,4-dimethoxybenzene, which is produced *de novo* by several white rot fungi, where it is utilized as a catalytic cofactor for oxidation reactions catalyzed by LiPs (Teunissen and Field 1998). Therefore, *AaeAPO* may additionally be

involved in the degradation of redox mediators used by other fungal extracellular enzymes or redox systems.

### 4.3 Potential applications of *Aae*APO-catalyzed reactions

*Aae*APO exhibits several potentially useful properties: (a) it exhibits high specific activity, catalytic efficiency and (in some cases) selectivity; (b) it catalyzes reactions using inexpensive peroxides and does not require expensive cofactors; (c) it acts independently of other enzymes and proteins such as flavin reductases or ferredoxins; (d) it is extracellular and thus may be cost-effective to produce in bulk; and (e) it is stable and water-soluble due to its high degree of glycosylation. Thus, possibilities for synthetic applications of *Aae*APO are found in the following scientific areas: (a) regio- and enantioselective oxidations of bulk and fine chemicals, (b) production of reference metabolites and reactive intermediates of drugs, (c) development of *Aae*APO-functionalized biosensors, (d) bioremediation and (e) biomimetics.

Selective hydroxylations of aromatic compounds are among the most challenging reactions in synthetic chemistry and have gained steadily increasing attention during recent years because hydroxylated aromatic precursors are used extensively in the chemical and pharmaceutical industries (Ullrich and Hofrichter 2007). For example, (*R*)-2-(4-hydroxyphenoxy)propionic acid [(*R*)-HPOPA] is an intermediate in the synthesis of enantiomerically pure aryloxyphenoxypropionic acid-type herbicides, in which the crop protection activity normally derives from one enantiomer (Siegel et al. 1998). Although chemical syntheses of (*R*)-HPOPA from hydroquinone and an (*S*)-2-halopropionic acid are available, problems with the removal of byproducts prevent the cost-effective use of this approach (Cleugh 2007, Cooper et al. 1992). Instead, (*R*)-HPOPA is currently prepared from (*R*)-2-phenoxypropionic [(*R*)-POPA] with whole cells of the ascomycete *Beauveria bassiana*, which produces regioselective oxidases that catalyze this hydroxylation (Dingler et al. 1996, Ladner et al. 1999). The company BASF currently produces about 1000 tons per year of (*R*)-HPOPA in this way (Schmid et al. 2002, Liese et al. 2006, van Beilen et al. 2003). The required feedstock, (*R*)-POPA, is synthesized from (*S*)-2-chloropropionic acid isobutylester and phenol (Liese et al. 2006).

A similar but simpler approach is to use purified microbial enzymes to hydroxylate POPA in one step. One possibility would be to use intracellular monooxygenases such as P450s (Urlacher and Eiben 2006, van Beilen et al. 2003), but current applications of these enzymes

are restricted to whole-cell biotransformations because P450s are not highly stable and their intracellular location makes them hard to produce in quantity (Urlacher et al. 2004, Eiben et al. 2006). Alternatively, modified hemoproteins such as MPs (MP8) might be used to catalyze aromatic hydroxylations by a P450-like oxygen transfer mechanism, but more research is needed to improve the performance of these catalysts (Veeger 2002, Caputi et al. 2005, Prieto et al. 2006, Dorovska-Taran et al. 1998, Dallacosta et al. 2003, Osman et al. 1996).

The results reported here show that *Aae*APO, besides its high regioselectivity of hydroxylation (98%), exhibits significant enantioselectivity towards phenoxypropionic acid, with the industrially more important *R*-enantiomer reacting more rapidly. This property of *Aae*APO could be exploited to improve the yield of *R*-HPOPA from the POPA feedstock currently used, which although enriched in *R*-POPA is not enantiopure (Liese et al. 2006, Schmid and Urlacher 2007). Further work is needed to ascertain how *Aae*APO recognizes the asymmetric center in POPA, but it is surmised that a structural interaction between the enzyme's active site and the carboxylic acid moiety of the substrate may be important.

Another example of a promising application for *Aae*APO is its activity towards drugs with consequent formation of naturally occurring drug metabolites. For example, 5-hydroxypropranolol, a human metabolite of the *beta*-blocker propranolol (1-naphthalen-1-yloxy-3-(propan-2-ylamino)propan-2-ol), is of pharmacological interest as it is frequently used in metabolic studies and has been demonstrated to be equipotent to propranolol as a *beta*-receptor antagonist (Greenslade and Newquist 1978). Another important human drug metabolite is 4'-hydroxydiclofenac (4'-OHD), a major metabolite of the anti-inflammatory drug diclofenac (2-[2-[(2,6-dichlorophenyl)amino]phenyl]acetic acid) in humans (Webster et al. 1998).

Table 15 illustrates the *Aae*APO-catalyzed reaction on propranolol relative to that of an engineered P450, which was optimized for the selective hydroxylation of propranolol (Kinne et al. 2009b).

Table 15 Conversion of propranolol (5 mM) to 5-OHP by *Aae*APO and P450.<sup>3</sup>

Enzyme in reaction ( $\mu$ M)	Conversion of propranolol to 5-OHP (%)	Reaction time (min)	Products formed
<i>Aae</i> APO <sup>1</sup> (0.6)	13.6	2	1
CytP450 <sup>2</sup> (5.0)	0.5	180	4

<sup>1</sup>H<sub>2</sub>O<sub>2</sub> concentration was 5 mM.

<sup>2</sup>H<sub>2</sub>O<sub>2</sub> concentration was 1 mM. Data are for mutant D6H10 (Otey et al. 2006).

<sup>3</sup>Conversion of diclofenac to 4'-OHD under these reaction conditions was 30%.

The desired human drug metabolite 5-OHP is a highly valuable reaction product because its four-step chemical synthesis from 1,5-naphthalenediol shows low overall yields of less than 5% and formation of byproducts (Oatis et al. 1981). *AaeAPO* appears to be the better choice as a biocatalyst because it is easier to produce, is more efficient, is more stable to  $H_2O_2$ , and in the case of propranolol exhibits higher regioselectivity. The failure of the reactions to proceed to completion was probably not a consequence of enzyme inactivation, because reactions conducted with more *AaeAPO* did not give significantly higher yields. It appears more likely that the phenolic products prevented further oxidation of the parent compounds because they also are *AaeAPO* substrates. Under the reaction conditions tested, these phenols probably consumed some of the  $H_2O_2$  by undergoing continuous, competitive *AaeAPO*-catalyzed oxidation to product phenoxy radicals, which in turn were continuously re-reduced to phenols by the excess ascorbate that was included. This conclusion is supported by the observation that propranolol and phenoxypropionic acid were rapidly polymerized when the reactions were conducted in the absence of ascorbate. However, although *AaeAPO* regioselectively hydroxylate other precursors as well it has some limitations. For example, it was observed that, although *AaeAPO* efficiently hydroxylates acetanilide to paracetamol (yields up to 80%) it very poorly adds the second 3'-hydroxyl needed to produce the human drug metabolite 3'-hydroxyacetaminophen.

Another potential application is that *AaeAPO* catalyze the selective cleavage of diverse ethers with formation of phenols, alcohols, and aldehydes. The protection of a reactive hydroxyl moiety via alkylation is a frequently used method in synthetic chemistry and selective removal of the alkyl protecting groups is not always chemically straightforward. In these cases, *AaeAPO* might be utilized for the removal of an alkyl group, thus liberating the desired hydroxyl group.

#### 4.4 Key findings

- (1) The *AaeAPO* exhibited a UV-Vis-spectral behavior similar to that found for heme-thiolate enzymes such as *CfuCPO* and P450s, but was clearly distinguishable from histidine-containing peroxidases such as heme HrP.
- (2) *AaeAPO* cleaved diverse aliphatic and aromatic ethers, including, environmentally significant compounds such as tetrahydrofuran and 1,4-dioxane, as well as, the phytoalexin pisatin and the pharmaceutical naproxen.



- (3) The stoichiometry of *Aae*APO-catalyzed tetrahydrofuran cleavage showed that the reaction was a two-electron oxidation that generated one aldehyde group and one alcohol group, yielding the ring-opened product 4-hydroxybutanal.
- (4) Steady-state bisubstrate kinetics of *Aae*APO-catalyzed methyl 3,4-dimethoxybenzyl ether cleavage, which yielded 3,4-dimethoxybenzaldehyde, gave parallel double reciprocal plots suggestive of a ping-pong mechanism ( $K_{m(\text{peroxide})}$ ,  $1.99 \pm 0.25$  mM;  $K_{m(\text{ether})}$ ,  $1.43 \pm 0.23$  mM;  $k_{\text{cat}}$ ,  $720 \pm 87$  s<sup>-1</sup>).
- (5) The *Aae*APO-catalyzed cleavage of methyl 4-nitrobenzyl ether, hydroxylation of aromatics such as diclofenac and nitrophenol and the oxygenation of benzylic compounds resulted in incorporation of an H<sub>2</sub><sup>18</sup>O<sub>2</sub>-derived <sup>18</sup>O into the reaction products, which identifies these reactions as oxygenation.
- (6) The demethylation of 1-methoxy-4-trideuteromethoxybenzene by *Aae*APO showed an observed intramolecular deuterium isotope effect [ $(k_{\text{H}}/k_{\text{D}})_{\text{obs}}$ ] of  $11.9 \pm 0.4$ , which points to an H-abstraction oxygen rebound mechanism.
- (7) *Aae*APO catalyzed the selective demethylation of dimeric lignin model compounds and initiated their autocatalytic cleavage but also oxidized phenolic dimers with consequent polymerization.
- (8) *Aae*APO catalyzed the regio- and enantioselective monohydroxylation of diverse aromatic compounds such as pharmaceuticals and herbicide precursors. Some of these reactions may be useful in the field of synthetic chemistry.
- (9) *Aae*APO catalyzed an oxygenation cascade that converted toluene and 4-nitrotoluene into benzoic acid derivatives via its peroxygenase activity.
- (10) *Aae*APO oxidized phenols with formation of free phenoxy radicals, which underwent coupling and polymerization reactions.
- (11) *Aae*APO catalyzed *N*-dealkylation of secondary amines such as *N*-methylaniline, as well as the dechlorination of some benzylic and aliphatic substrates.

- (12) *Aae*APO-catalyzed reactions may have a physiological function, for example in the biodegradation of low molecular lignin fragments, or in the detoxification of fungicidal compounds derived from plants or microorganisms via hydroxylation or demethylation and subsequent polymerization.

**The most important finding of this work is that *Aae*APO is able to catalyze the cleavage of diverse ethers via a hydrogen abstraction and oxygen rebound mechanism.**

## 4.5 Outlook

Future mechanistic investigations should focus on the oxidized intermediate states of *Aae*APO. Further progress will probably require a rapid transient-state kinetics approach. The sequence of substrate binding to the peroxygenase also remains to be established, and additional experiments with molecular clock substrates would be advisable to check whether they yield data consistent with the radical rebound mechanism that has been proposed in this work. The peroxidase activity of *Aae*APO should be investigated and the question answered as to whether there is a LRET or whether intermediates such as phenoxy radicals can be released from the active site.

As shown by this work, the oxygenation activity of *Aae*APO may be useful for diverse applications. The most interesting question, however, remains unanswered: **What is the true physiological function of *Aae*APO?**

## 5 References

- Adam W, Lazarus M, Saha-Moller CR, Weichold O, Hoch U, Haring D, Schreier P. 1999. Biotransformations with peroxidases. *Adv Biochem Eng Biotechnol*, 63:73-108.
- Akasaka R, Mashino T, Hirobe M. 1995. Hydroxylation of benzene by horseradish peroxidase and immobilized horseradish peroxidase in an organic solvent. *Bioorg Med Chem Lett*, 5:1861-1864.
- Anh DH, Ullrich R, Benndorf D, Svatos A, Muck A, Hofrichter M. 2007. The coprophilous mushroom *Coprinus radians* secretes a haloperoxidase that catalyzes aromatic peroxygenation. *Appl Environ Microbiol*, 73 (17):5477-5485.
- Aranda E, Ullrich R, Hofrichter M. 2009. Conversion of polycyclic aromatic hydrocarbons, methyl naphthalenes and dibenzofuran by two fungal peroxygenases. *Biodegradation*, 21 (2):267-281.
- Aranda E, Kinne M, Kluge M, Ullrich R, Hofrichter M. 2008. Conversion of dibenzothiophene by the mushrooms *Agrocybe aegerita* and *Coprinellus radians* and their extracellular peroxygenases. *Appl Microbiol Biotechnol*, 82 (6):1057-1066.
- Azevedo AM, Martins VC, Prazeres DM, Vojinovic V, Cabral JM, Fonseca LP. 2003. Horseradish peroxidase: a valuable tool in biotechnology. *Biotechnol Annu Rev*, 9:199-247.
- Banci L. 1997. Structural properties of peroxidases. *J Biotechnol* 53 (2-3):253-263.
- Bednarek P, Osbourn A. 2009. Plant-microbe interactions: chemical diversity in plant defense. *Science*, 324 (5928):746-748.
- Bernroitner M, Zamocky M, Furtmuller PG, Peschek GA, Obinger C. 2009. Occurrence, phylogeny, structure, and function of catalases and peroxidases in cyanobacteria. *J Exp Bot*, 60 (2):423-440.
- Beste GW, Hammett LP. 1940. Rate and mechanism in the reactions of benzyl chloride with water, hydroxyl ion and acetate ion. *J Am Chem Soc*, 62 (9):2481-2487.
- Bisswanger H. 2000. *Enzymkinetik Theorie und Methoden*. 3 Aufl. Weinheim: Wiley-VCH Verlag.
- Blee E, Durst F. 1987. Hydroperoxide-dependent sulfoxidation catalyzed by soybean microsomes. *Arch Biochem Biophys*, 254 (1):43-52.
- Blee E, Wilcox AL, Marnett LJ, Schuber F. 1993. Mechanism of reaction of fatty acid hydroperoxides with soybean peroxygenase. *J Biol Chem*, 268 (3):1708-1715.
- Boersma MG, Primus JL, Koerts J, Veeger C, Rietjens IM. 2000. Heme-(hydro)peroxide mediated *O*- and *N*-dealkylation. A study with microperoxidase. *Eur J Biochem*, 267 (22):6673-6678.
- Brodie BB, Gillette JR, La Du BN. 1958. Enzymatic metabolism of drugs and other foreign compounds. *Annu Rev Biochem*, 27 (3):427-454.
- Camarero S, Sarkar S, Ruiz-Duenas FJ, Martinez MJ, Martinez AT. 1999. Description of a versatile peroxidase involved in the natural degradation of lignin that has both manganese peroxidase and lignin peroxidase substrate interaction sites. *J Biol Chem*, 274 (15):10324-10330.
- Caputi L, Di Tullio A, Di Leandro L, De Angelis F, Malatesta F. 2005. A new microperoxidase from *Marinobacter hydrocarbonoclasticus*. *Biochim Biophys Acta*, 1725 (1):71-80.
- Celimene CC, Micales JA, Ferge L, Young RA. 1999. Efficacy of Pinosylvins against White-Rot and Brown-Rot Fungi. *Holzforchung*, 53 (5):491-497.
- Cherry JR, Lamsa MH, Schneider P, Vind J, Svendsen A, Jones A, Pedersen AH. 1999. Directed evolution of a fungal peroxidase. *Nat Biotechnol*, 17 (4):379-384.

- Cirino PC, Arnold FH. 2003a. A self-sufficient peroxide-driven hydroxylation biocatalyst. *Angew Chem Int Ed Engl*, 42 (28):3299-3301.
- Cirino PC, Arnold FH. 2003b. Exploring the diversity of heme enzymes through directed evolution. In: Dr. Susanne Brakmann PDKJ, Hrsg. Directed molecular evolution of proteins. 215-243.
- Cleugh ES. 2007. Production process of optically pure 2-(4-hydroxyphenoxy)-propionic acid compounds. United States Patent 7268249.
- Colonna S, Gaggero N, Richelmi C, Pasta P. 1999. Recent biotechnological developments in the use of peroxidases. *Trends Biotechnol*, 17 (4):163-168.
- Cooper B, Ladner W, Hauer B, Siegel H. 1992. Process for fermentative production of 2-(4-hydroxyphenoxy)-propionic acid. European Patent EP0465494.
- Cosio C, Dunand C. 2009. Specific functions of individual class III peroxidase genes. *J Exp Bot*, 60 (2):391-408.
- Cupp-Vickery JR, Poulos TL. 1995. Structure of cytochrome P450eryF involved in erythromycin biosynthesis. *Nat Struct Biol*, 2 (2):144-153.
- Dallacosta C, Monzani E, Casella L. 2003. Reactivity study on microperoxidase-8. *J Biol Inorg Chem*, 8 (7):770-776.
- Damsten MC, van Vugt-Lussenburg BMA, Zeldenthuis T, de Vlieger JSB, Commandeur JNM, Vermeulen NPE. 2008. Application of drug metabolising mutants of cytochrome P450 BM3 (CYP102A1) as biocatalysts for the generation of reactive metabolites. *Chem-Biol Interact* 171 (1):96-107.
- Dawson JH, Sono M, Hager LP. 1983. The active sites of chloroperoxidase and cytochrome P-450-CAM: Comparative spectroscopic and ligand binding properties. *Inorg Chim Acta* 79:184-186.
- Deisseroth A, Dounce AL. 1970. Catalase: Physical and chemical properties, mechanism of catalysis, and physiological role. *Physiol Rev*, 50 (3):319-375.
- Delserone LM, McCluskey K, Matthews DE, Vanetten HD. 1999. Pisatin demethylation by fungal pathogens and nonpathogens of pea: association with pisatin tolerance and virulence. *Phys Mol Plant Pathol*, 55 (6):317-326.
- Dingler C, Ladner W, Krei GA, Cooper BS, Hauer B. 1996. Preparation of (R)-2-(4-hydroxyphenoxy)propionic acid by biotransformation. *Pestic Sci*, 46:33-53.
- Dorovska-Taran V, Posthumus MA, Boeren S, Boersma MG, Teunis CJ, Rietjens IM, Veeger C. 1998. Oxygen exchange with water in heme-oxo intermediates during H<sub>2</sub>O<sub>2</sub>-driven oxygen incorporation in aromatic hydrocarbons catalyzed by microperoxidase-8. *Eur J Biochem*, 253 (3):659-568.
- Dunford HB. 1999. Heme Peroxidases. New York: Wiley-VCH.
- Eiben S, Kaysser L, Maurer S, Kuhnel K, Urlacher VB, Schmid RD. 2006. Preparative use of isolated CYP102 monooxygenases-A critical appraisal. *J Biotechnol*, 124 (4):662-669.
- Farhangrazi ZS, Sinclair R, Yamazaki I, Powers LS. 1992. Haloperoxidase activity of *Phanerochaete chrysosporium* lignin peroxidases H2 and H8. *Biochemistry*, 31 (44):10763-10768.
- Field CB, Behrenfeld MJ, Randerson JT, Falkowski P. 1998. Primary production of the biosphere: integrating terrestrial and oceanic components. *Science*, 281 (5374):237-240.
- Fischer M, Knoll M, Sirim D, Wagner F, Funke S, Pleiss J. 2007. The cytochrome P450 engineering database: a navigation and prediction tool for the cytochrome P450 protein family. *Bioinformatics*, 23 (15):2015-2017.
- Foster AB, Jarman M, Stevens JD, Thomas P, Westwood JH. 1974. Isotope effects in O- and N-demethylations mediated by rat liver microsomes: an application of direct insertion electron impact mass spectrometry. *Chem Biol Interact*, 9 (5):327-340.

- George HL, VanEtten HD. 2001. Characterization of pisatin-inducible cytochrome p450s in fungal pathogens of pea that detoxify the pea phytoalexin pisatin. *Fungal Genet Biol*, 33 (1):37-48.
- Gillam EM. 2008. Engineering cytochrome p450 enzymes. *Chem Res Toxicol*, 21 (1):220-231.
- Gold MH, Kuwahara M, Chiu AA, Glenn JK. 1984. Purification and characterization of an extracellular H<sub>2</sub>O<sub>2</sub>-requiring diarylpropane oxygenase from the white rot basidiomycete, *Phanerochaete chrysosporium*. *Arch Biochem Biophys*, 234 (2):353-362.
- Gold Michael H, Wariishi H, Valli K. 2009. Extracellular peroxidases involved in lignin degradation by the white rot basidiomycete *phanerochaete chrysosporium*. *Biocatalysis in Agricultural Biotechnology*. Washington, DC: American Chemical Society, 127-140.
- Gottstein D, Gross D. 1992. Phytoalexins of woody plants. *Trees*, (6):55-68.
- Greenslade FC, Newquist KL. 1978. In vitro measurement of the beta-adrenergic blocking properties of ORF 12592, the 5-hydroxy analog of propranolol. *Arch Int Pharmacodyn Ther*, 233 (2):270-280.
- Gribble. 2003. The diversity of naturally produced organohalogenes. *Chemosphere*, (52):289-297.
- Grobe N, Zhang B, Fisinger U, Kutchan TM, Zenk MH, Guengerich FP. 2009. Mammalian cytochrome P450 enzymes catalyze the phenol-coupling step in endogenous morphine biosynthesis. *J Biol Chem*, 284 (36):24425-24431.
- Groves JT. 2006. High-valent iron in chemical and biological oxidations. *J Inorg Biochem*, 100 (4):434-447.
- Guengerich FP. 2001. Common and uncommon cytochrome P450 reactions related to metabolism and chemical toxicity. *Chem Res Toxicol*, 14 (6):611-650.
- Hager LP, Morris DR, Brown FS, Eberwein H. 1966. Chloroperoxidase. II. Utilization of halogen anions. *J Biol Chem*, 241 (8):1769-1777.
- Hamberg M, Hamberg G. 1990. Hydroperoxide-dependent epoxidation of unsaturated fatty acids in the broad bean (*Vicia faba* L.). *Arch Biochem Biophys*, 283 (2):409-416.
- Hamill RL, Byerrum RU, Ball CD. 1957. A study of the biosynthesis of the methoxyl groups of lignin in tobacco plants. *J Biol Chem*, 224 (2):713-716.
- Hammel KE, Cullen D. 2008. Role of fungal peroxidases in biological ligninolysis. *Curr Opin Plant Biol*, 11 (3):349-355.
- Hanano A, Burcklen M, Flenet M, Ivancich A, Louwagie M, Garin J, Blee E. 2006. Plant seed peroxygenase is an original heme-oxygenase with an EF-hand calcium binding motif. *J Biol Chem*, 281 (44):33140-33151.
- Hanzlik RP, Ling KHJ. 1990. Active site dynamics of toluene hydroxylation by cytochrome P-450. *J Org Chem* 55 (13):3992-3997.
- Harada N, Miwa GT, Walsh JS, Lu AY. 1984. Kinetic isotope effects on cytochrome P-450-catalyzed oxidation reactions. Evidence for the irreversible formation of an activated oxygen intermediate of cytochrome P-448. *J Biol Chem*, 259 (5):3005-3010.
- Hardison R. 1999. The evolution of hemoglobin. *American Scientist*, 82 (2):126 (121).
- Harris DL, Loew GH. 1998. Theoretical Investigation of the Proton Assisted Pathway to Formation of Cytochrome P450 Compound I. *J Am Chem Soc*, 120 (35):8941-8948.
- Harrison AF. 1971. The inhibitory effect of oak leaf litter tannins on the growth of fungi, in relation to litter decomposition. *Soil Biol Biochem*, 3 (3):167-172.
- Hauer B, Zelinski T, Habicher T, Breuer M, Anke T, Russ R. 2004. Method for selective oxidation of substituted toluenes by microbial coprinus peroxidases [A1]. Germany: BASF AG (DE)

- Hayashi T, Murata D, Makino M, Sugimoto H, Matsuo T, Sato H, Shiro Y, Hisaeda Y. 2006. Crystal structure and peroxidase activity of myoglobin reconstituted with iron porphycene. *Inorg Chem*, 45 (26):10530-10536.
- Hernandez A, Ruiz MT. 1998. An EXCEL template for calculation of enzyme kinetic parameters by non-linear regression. *Bioinformatics*, 14 (2):227-228.
- Hjelmeland LM, Aronow L, Trudell JR. 1976. Intramolecular determination of primary kinetic isotope effects in hydroxylations catalyzed by cytochrome P-450. *Biochem Biophys Res Commun*, 76 (2):541-549.
- Hofrichter M, Ullrich R. 2006. Heme-thiolate haloperoxidases: versatile biocatalysts with biotechnological and environmental significance. *Appl Microbiol Biotechnol*, 71 (3):276 - 288.
- Hofrichter M, Vares K, Scheibner K, Galkin S, Sipilä J, Hatakka A. 1999. Mineralization and solubilization of synthetic lignin by manganese peroxidases from *Nematoloma frowardii* and *Phlebia radiata*. *J Biotechnol*, 67 (2-3):217-228.
- Hult K, Berglund P. 2007. Enzyme promiscuity: mechanism and applications. *Trends in Biotechnology*, 25 (5):231-238.
- Ishimaru A, Yamazaki I. 1977. Hydroperoxide-dependent hydroxylation involving "H<sub>2</sub>O<sub>2</sub>-reducible hemoprotein" in microsomes of pea seeds. A new type enzyme acting on hydroperoxide and a physiological role of seed lipoxygenase. *J Biol Chem*, 252 (17):6118-6124.
- Isikhuemhen OS, Mikiashvili NA, Kelkar V. 2009. Application of solid waste from anaerobic digestion of poultry litter in *Agrocybe aegerita* cultivation: mushroom production, lignocellulolytic enzymes activity and substrate utilization. *Biodegradation*, 20 (3):351-361.
- Isin EM, Guengerich FP. 2007. Complex reactions catalyzed by cytochrome P450 enzymes. *Biochimica et Biophysica Acta (BBA) - General Subjects*, 1770 (3):314-329.
- Johjima T, Itoh N, Kabuto M, Tokimura F, Nakagawa T, Wariishi H, Tanaka H. 1999. Direct interaction of lignin and lignin peroxidase from *Phanerochaete chrysosporium*. *Proc Natl Acad Sci U S A*, 96 (5):1989-1994.
- Joo H, Lin Z, Arnold FH. 1999. Laboratory evolution of peroxid-mediated cytochrome P450 hydroxylation. *Nature*, 399:670-673.
- Joshi DK, Gold MH. 1996. Oxidation of dimethoxylated aromatic compounds by lignin peroxidase from *Phanerochaete chrysosporium*. *Eur J Biochem*, 237 (1):45-57.
- Jürgen A, Edivaldo Ximenes Ferreira F, Elba Pinto da Silva B. 2008. Biotechnology of holocellulose-degrading enzymes. In: Ching T. Hou J-FS, Hrsg. *Biocatalysis and Bioenergy*. 195-229.
- Kaim W, Schwederski, B. 2005. *Bioanorganische Chemie*. Wiesbaden: Teubner Verlag.
- Kawai S, Jensen KA, Jr., Bao W, Hammel KE. 1995. New polymeric model substrates for the study of microbial ligninolysis. *Appl Environ Microbiol*, 61 (9):3407-3414.
- Kedderis GLK, D.R. and Hollenberg, P.F. 1980. N-Demethylation reactions catalyzed by chloroperoxidase. *J Biol Chem*, 255 (21):10174-10182.
- Kemp MS, Burden RS. 1986. Phytoalexins and stress metabolites in the sapwood of trees. *Phytochemistry*, 25 (6):1261-1269.
- Kerem Z, Jensen KA, Hammel KE. 1999. Biodegradative mechanism of the brown rot basidiomycete *Gloeophyllum trabeum*: evidence for an extracellular hydroquinone-driven fenton reaction. *Febs Lett*, 446 (1):49-54.
- Kersten PJ, Kalyanaraman B, Hammel KE, Reinhammar B, Kirk TK. 1990. Comparison of lignin peroxidase, horseradish peroxidase and laccase in the oxidation of methoxybenzenes. *Biochem J*, 268 (2):475-480.

- Kim SJ, Shoda M. 1999. Purification and characterization of a novel peroxidase from *Geotrichum candidum* dec 1 involved in decolorization of dyes. *Appl Environ Microbiol*, 65 (3):1029-1035.
- Kim SJ, Lee JA, Won K, Kim YH, Song BK. 2009. Functional expression of *Coprinus cinereus* peroxidase in *Pichia pastoris*. *Process Biochem*, 44 (7):731-735.
- Kim YH, Engesser KH. 2004. Degradation of alkyl ethers, aralkyl ethers, and dibenzyl ether by *Rhodococcus* sp. strain DEE5151, isolated from diethyl ether-containing enrichment cultures. *Appl Environ Microbiol*, 70 (7):4398-4401.
- Kimata Y, Shimada H, Hirose T, Ishimura Y. 1995. Role of Thr-252 in cytochrome P450cam: a study with unnatural amino acid mutagenesis. *Biochem Biophys Res Commun*, 208 (1):96-102.
- Kinne M, Ullrich R, Hammel KE, Scheibner K, Hofrichter M. 2008. Regioselective preparation of (*R*)-2-(4-hydroxyphenoxy)propionic acid with a fungal peroxygenase. *Tetrahedron Lett*, 49 (41):5950-5953.
- Kinne M, Poraj-Kobielska M, Ralph SA, Ullrich R, Hofrichter M, Hammel KE. 2009a. Oxidative cleavage of diverse ethers by an extracellular fungal peroxygenase. *J Biol Chem*, 284 (43):29343-29349.
- Kinne M, Poraj-Kobielska M, Aranda E, Ullrich R, Hammel KE, Scheibner K, Hofrichter M. 2009b. Regioselective preparation of 5-hydroxypropranolol and 4'-hydroxydiclofenac with a fungal peroxygenase. *Bioorg Med Chem Lett*, 19 (11):3085-3087.
- Kirk TK, Farrell RL. 1987. Enzymatic "combustion": the microbial degradation of lignin. *Annu Rev Microbiol*, 41:465-505.
- Kirk TK, Tien M, Kersten PJ, Mozuch MD, Kalyanaraman B. 1986. Ligninase of *Phanerochaete chrysosporium*. Mechanism of its degradation of the non-phenolic arylglycerol beta-aryl ether substructure of lignin. *Biochem J*, 236 (1):279-287.
- Kluge M, Ullrich R, Dolge C, Scheibner K, Hofrichter M. 2009. Hydroxylation of naphthalene by aromatic peroxygenase from *Agrocybe aegerita* proceeds via oxygen transfer from H<sub>2</sub>O<sub>2</sub> and intermediary epoxidation. *Appl Microbiol Biotechnol*, 81 (6):1071-1076.
- Kluge MG, Ullrich R, Scheibner K, Hofrichter M. 2007. Spectrophotometric assay for detection of aromatic hydroxylation catalyzed by fungal haloperoxidase-peroxygenase. *Appl Microbiol Biotechnol*, 75 (6):1473-1478.
- Kohen A, Limbach H. 2006. *Isotope Effects in Chemistry and Biology*. Boca Raton: CRC Press Taylor & Francis Group, LLC.
- Koizumi M, Titani T. 1938. Austauschreaktionen der Sauerstoffatome zwischen Wasser und einigen organischen Verbindungen. *Bull Chem Soc*, 13:607.
- Kok GL. 1980. Measurements of hydrogen peroxide in rainwater. *Atmospheric Environment* (1967), 14 (6):653-656.
- Kuan IC, Tien M. 1993. Stimulation of Mn peroxidase activity: a possible role for oxalate in lignin biodegradation. *Proc Natl Acad Sci U S A*, 90 (4):1242-1246.
- Kuhnel K, Blankenfeldt W, Terner J, Schlichting I. 2006. Crystal structures of chloroperoxidase with its bound substrates and complexed with formate, acetate and nitrate. *J Biol Chem*.
- Kumar P, Barrett DM, Delwiche MJ, Stroeve P. 2009. Methods for pretreatment of lignocellulosic biomass for efficient hydrolysis and biofuel production. *Ind Eng Chem Res* 48 (8):3713-3729.
- Kuropteva ZV, Kudriavstev ME. 1997. Inhibition of cytochrome P-450 when exposed to nitro-compounds. *Biofizika*, 42 (2):484-489.

- Kuwahara M, Glenn JK, Morgan MA, Gold MH. 1984. Separation and characterization of two extracellular H<sub>2</sub>O<sub>2</sub>-dependent oxidases from ligninolytic cultures of *Phanerochaete chrysosporium*. FEBS Lett, 169:247-250.
- Lad C, Williams NH, Wolfenden R. 2003. The rate of hydrolysis of phosphomonoester dianions and the exceptional catalytic proficiencies of protein and inositol phosphatases. Proc Natl Acad Sci U S A, 100 (10):5607-5610.
- Ladner W, Staudenmaier HR, Hauer B, Müller U, Pressler U, Meyer J, Siegel H. 1999. Process for the hydroxylation of aromatic acids using strains of the fungus *Beauveria*. United States Patent 5928912.
- Landucci LL, Geddes SA, Kirk TK. 1981. Synthesis of <sup>14</sup>C labeled 3-methoxy-4-hydroxy- $\alpha$ -(2-methoxy-phenoxy)- $\beta$ -hydroxypropiofenone, a lignin model compound. Holzforschung, 35 (2):67-70.
- Lawson T, Gannett PM, Yau WM, Dalal NS, Toth B. 1995. Different patterns of mutagenicity of arenediazonium ions in V79 cells and *Salmonella typhimurium* TA102: evidence for different mechanisms of action. J Agric Food Chem, 43 (10):2627-2635.
- Leonowicz A, Matuszewska A, Luterek J, Ziegenhagen D, Wojtas-Wasilewska M, Cho NS, Hofrichter M, Rogalski J. 1999. Biodegradation of lignin by white rot fungi. Fungal Genet Biol, 27 (2-3):175-185.
- Lewis DF, Sheridan G. 2001. Cytochromes P450, oxygen, and evolution. ScientificWorldJournal, 1:151-167.
- Lewis DFV. 2001. Guide to Cytochromes P450: Structure & Function. Taylor & Francis.
- Li D, Wang Y, Yang C, Han K. 2009. Theoretical study of N-dealkylation of N-cyclopropyl-N-methylaniline catalyzed by cytochrome P450: insight into the origin of the regioselectivity. Dalton Trans, (2):291-297.
- Li H, Zhan H, Fu S, Liu M, Chai XS. 2007. Rapid determination of methanol in black liquors by full evaporation headspace gas chromatography. J Chromatogr, A, 1175 (1):133-136.
- Liers C, Bobeth C, Pecyna M, Ullrich R, Hofrichter M. 2009. DyP-like peroxidases of the jelly fungus *Auricularia auricula-judae* oxidize nonphenolic lignin model compounds and high-redox potential dyes. Appl Microbiol Biotechnol, 85 (6):1869-1879.
- Liese A, Seelbach K, Wandrey C. 2006. Industrial Biotransformation. Weinheim: Wiley-VCH Verlag GmbH & Co KGaA.
- Littlechild J. 1999. Haloperoxidases and their role in biotransformation reactions. Curr Opin Chem Biol, 3 (1):28-34.
- Liu C-F, Ren J-L, Xu F, Liu J-J, Sun J-X, Sun R-C. 2006. Isolation and characterization of cellulose obtained from ultrasonic irradiated sugarcane bagasse. J Agric Food Chem, 54 (16):5742-5748.
- Manoj KM, Hager LP. 2008. Chloroperoxidase, a janus enzyme. Biochemistry, 47 (9):2997-3003.
- Mansuy D. 1998. The great diversity of reactions catalyzed by cytochromes P450. Comparative Biochemistry and Physiology Part C: Pharmacology, Toxicology and Endocrinology, 121 (1-3):5-14.
- McClay K, Schaefer CE, Vainberg S, Steffan RJ. 2007. Biodegradation of bis(2-chloroethyl) ether by *Xanthobacter* sp. strain ENV481. Appl Environ Microbiol, 73 (21):6870-6875.
- McEldoon JP, Pokora AR, Dordick JS. 1995. Lignin peroxidase-type activity of soybean peroxidase. Enzyme Microb Technol 17:359-365.
- Mester T, Field JA. 1998. Characterization of a novel manganese peroxidase-lignin peroxidase hybrid isozyme produced by *Bjerkandera* species strain BOS55 in the absence of manganese. J Biol Chem, 273 (25):15412-15417.



- Mester T, Tien M. 2001. Engineering of a manganese-binding site in lignin peroxidase isozyme H8 from *Phanerochaete chrysosporium*. *Biochem Biophys Res Commun*, 284 (3):723-728.
- Mester T, Ambert-Balay K, Ciofi-Baffoni S, Banci L, Jones AD, Tien M. 2001. Oxidation of a tetrameric nonphenolic lignin model compound by lignin peroxidase. *J Biol Chem*, 276 (25):22985-22990.
- Miller FP, Vandome AF, McBrewster J. 2009. Kinetic isotope effect: reaction rate, chemical reaction, isotope, hydrogen, deuterium, reaction rate constant, chemical bond, rate-determining step, reaction mechanism, mass. Beau Bassin: Alphascript Publishing.
- Miller VP, Tschirret-Guth RA, Ortiz de Montellano PR. 1995. Chloroperoxidase-catalyzed benzylic hydroxylation. *Arch Biochem Biophys*, 319 (2):333-340.
- Miwa GT, Walsh JS, Lu AY. 1984. Kinetic isotope effects on cytochrome P-450-catalyzed oxidation reactions. The oxidative O-dealkylation of 7-ethoxycoumarin. *J Biol Chem*, 259 (5):3000-3004.
- Monzani E, Nicolis S, Roncone R, Barbieri M, Granata A, Casella L. 2008. Protein self-modification by heme-generated reactive species. *IUBMB Life*, 60 (1):41-56.
- Moreno Horn M, Garbe LA, Tressl R, Adrian L, Gorisch H. 2003. Biodegradation of bis(1-chloro-2-propyl) ether via initial ether scission and subsequent dehalogenation by *Rhodococcus* sp. strain DTB. *Arch Microbiol*, 179 (4):234-241.
- Morita Y, Yamashita H, Mikami B, Iwamoto H, Albara S, Terada M, Minami J. 1988. Purification, crystallization and characterization of peroxidase from *Coprinus cinereus*. *J Biochem* 103 (693-699).
- Nagababu E, Rifkind JM. 2004. Heme degradation by reactive oxygen species. *Antioxid Redox Signal*, 6 (6):967-978.
- Nebert DW, Nelson DR, Adesnik M, Coon MJ, Estabrook RW, Gonzalez FJ, Guengerich FP, Gunsalus IC, Johnson EF, Kemper B, et al. 1989. The P450 superfamily: updated listing of all genes and recommended nomenclature for the chromosomal loci. *DNA*, 8 (1):1-13.
- Nelson DR, Kamataki T, Waxman DJ, Guengerich FP, Estabrook RW, Feyereisen R, Gonzalez FJ, Coon MJ, Gunsalus IC, Gotoh O, et al. 1993. The P450 superfamily: update on new sequences, gene mapping, accession numbers, early trivial names of enzymes, and nomenclature. *DNA Cell Biol*, 12 (1):1-51.
- Nelson DR, Koymans L, Kamataki T, Stegeman JJ, Feyereisen R, Waxman DJ, Waterman MR, Gotoh O, Coon MJ, Estabrook RW, Gunsalus IC, Nebert DW. 1996. P450 superfamily: update on new sequences, gene mapping, accession numbers and nomenclature. *Pharmacogenetics*, 6 (1):1-42.
- Nelson SD, Trager WF. 2003. The use of deuterium isotope effects to probe the active site properties, mechanism of cytochrome P450-catalyzed reactions, and mechanisms of metabolically dependent toxicity. *Drug Metab Dispos*, 31 (12):1481-1498.
- Oatis JE, Jr., Russell MP, Knapp DR, Walle T. 1981. Ring-hydroxylated propranolol: synthesis and beta-receptor antagonist and vasodilating activities of the seven isomers. *J Med Chem*, 24 (3):309-314.
- Oliva M, Theiler G, Zamocky M, Koua D, Margis-Pinheiro M, Passardi F, Dunand C. 2009. PeroxiBase: a powerful tool to collect and analyse peroxidase sequences from Viridiplantae. *J Exp Bot*, 60 (2):453-459.
- Orth AB, Royse DJ, Tien M. 1993. Ubiquity of lignin-degrading peroxidases among various wood-degrading fungi. *Appl Environ Microbiol*, 59 (12):4017-4023.
- Ortiz de Montellano P. 2005. *Cytochrome P450 - Structure, Mechanism and Biochemistry*. New York: Kluwer Academic/Plenum Publishers.

- Ortiz de Montellano PR. 2009. Hydrocarbon hydroxylation by cytochrome P450 enzymes. *Chem Rev*.
- Ortiz de Montellano PR, De Voss JJ. 2002. Oxidizing species in the mechanism of cytochrome P450. *Nat Prod Rep*, 19 (4):477-493.
- Ortiz de Montellano PR, de Voss JJ. 2005. *Substrate Oxidation by Cytochrome P450 Enzymes*. third Aufl. New York: Kluwer Academic/Plenum Publishers.
- Osman AM, Koerts J, Boersma MG, Boeren S, Veeger C, Rietjens IM. 1996. Microperoxidase/H<sub>2</sub>O<sub>2</sub>-catalyzed aromatic hydroxylation proceeds by a cytochrome-P-450-type oxygen-transfer reaction mechanism. *Eur J Biochem*, 240 (1):232-238.
- Otey CR, Bandara G, Lalonde J, Takahashi K, Arnold FH. 2006. Preparation of human metabolites of propranolol using laboratory-evolved bacterial cytochromes P450. *Biotechnol Bioeng*, 93 (3):494-499.
- Ozaki S-i, Matsui T, Watanabe Y. 1997. Conversion of myoglobin into a peroxygenase: A catalytic intermediate of sulfoxidation and epoxidation by the F43H/H64L mutant. *J Am Chem Soc*, 119 (28):6666-6667.
- Partridge M, Murphy DJ. 2009. Roles of a membrane-bound caleosin and putative peroxygenase in biotic and abiotic stress responses in *Arabidopsis*. *Plant Physiol Biochem*, 47 (9):796-806.
- Passardi F, Zamocky M, Favet J, Jakopitsch C, Penel C, Obinger C, Dunand C. 2007a. Phylogenetic distribution of catalase-peroxidases: Are there patches of order in chaos? *Gene*, 397 (1-2):101-113.
- Passardi F, Theiler G, Zamocky M, Cosio C, Rouhier N, Teixera F, Margis-Pinheiro M, Ioannidis V, Penel C, Falquet L, Dunand C. 2007b. PeroxiBase: the peroxidase database. *Phytochemistry*, 68 (12):1605-1611.
- Pecyna MJ, Ullrich R, Bittner B, Clemens A, Scheibner K, Schubert R, Hofrichter M. 2009. Molecular characterization of aromatic peroxygenase from *Agrocybe aegerita*. *Appl Microbiol Biotechnol*, 84 (5):885-897.
- Pedersen DS, Rosenbohm C. 2001. *Dry column vacuum chromatography*. Synthesis-Stuttgart, (16):2431-2434.
- Perez-Boada M, Ruiz-Duenas FJ, Pogni R, Basosi R, Choinowski T, Martinez MJ, Piontek K, Martinez AT. 2005. Versatile peroxidase oxidation of high redox potential aromatic compounds: site-directed mutagenesis, spectroscopic and crystallographic investigation of three long-range electron transfer pathways. *J Mol Biol*, 354 (2):385-402.
- Pezzotti F, Okrasa K, Therisod M. 2004. Oxidation of chlorophenols catalyzed by *Coprinus cinereus* peroxidase with in situ production of hydrogen peroxide. *Biotechnol Prog*, 20 (6):1868-1871.
- Pfister TD, Ohki T, Ueno T, Hara I, Adachi S, Makino Y, Ueyama N, Lu Y, Watanabe Y. 2005. Monooxygenation of an aromatic ring by F43W/H64D/V68I myoglobin mutant and hydrogen peroxide. Myoglobin mutants as a model for P450 hydroxylation chemistry. *J Biol Chem*, 280 (13):12858-12866.
- Phillips IRaS, E. A. 2006. *Cytochrome P450 Protocols (Methods in Molecular Biology)*. 2 Aufl. New Jersey: Humana Press Inc.
- Piontek K. 2009. Partner 17 ALU-FR Period Oct. 2008 - April 2009. EU Biorenew Projekt Meeting. Leiden: <http://www.biorenew.org/>.
- Poulos TL. 2005. Structural biology of heme monooxygenases. *Biochem Biophys Res Commun*, 338 (1):337-345.
- Poulos TL, Johnson EF. 2005. *Structures of Cytochrome P450 Enzymes*. 3 Aufl. New York: Kluwer Academic/Plenum Publishers.

- Poulos TL, Finzel BC, Howard AJ. 1987. High-resolution crystal structure of cytochrome P450cam. *J Mol Biol*, 195 (3):687-700.
- Prieto T, Marcon RO, Prado FM, Caires AC, Di Mascio P, Brochsztain S, Nascimento OR, Nantes IL. 2006. Reaction route control by microperoxidase-9/CTAB micelle ratios. *Phys Chem Chem Phys*, 8 (16):1963-1973.
- Rabe KS, Kiko K, Niemeyer CM. 2008. Characterization of the peroxidase activity of CYP119, a thermostable P450 from *Sulfolobus acidocaldarius*. *Chembiochem*, 9 (3):420-425.
- Rachel NA, Dayi D, Yongying J, Kate L, Jan BvB, Paul ROdM, John TG. 2006. The diagnostic substrate bicyclohexane reveals a radical mechanism for bacterial cytochrome P450 in whole cells. *Angew Chem, Int Ed*, 45 (48):8192-8194.
- Ravichandran KG, Boddupalli SS, Hasermann CA, Peterson JA, Deisenhofer J. 1993. Crystal structure of hemoprotein domain of P450BM-3, a prototype for microsomal P450's. *Science*, 261 (5122):731-736.
- Rietjens IMCM, den Besten C, Hanzlik RP, van Bladeren PJ. 1997. Cytochrome P450-catalyzed oxidation of halobenzene derivatives. *Chem Res Toxicol*, 10 (6):629-635.
- Rogerio M, Christophe D, Felipe KT, Marcia M-P. 2008. Glutathione peroxidase family an evolutionary overview. *FEBS J*, 275 (15):3959-3970.
- Roncone R, Barbieri M, Monzani E, Casella L. 2006. Reactive nitrogen species generated by heme proteins: Mechanism of formation and targets. *Coord Chem Rev* 250 (11-12):1286-1293.
- Rubin EM. 2008. Genomics of cellulosic biofuels. *Nature*, 454 (7206):841-845.
- Russ R, Zelinski T, Anke T. 2002. Benzylic biooxidation of various toluenes to aldehydes by peroxidase. *Tetrahedron Lett*, 43 (5):791-793.
- Rydberg P, Ryde U, Olsen L. 2008. Prediction of activation energies for aromatic oxidation by cytochrome P450. *J Phys Chem A*, 112 (50):13058-13065.
- Samuel D, Silver, B.L.. 1965. *Adv Phys Org Chem*, 3:121-186.
- Sanchez C. 2009. Lignocellulosic residues: biodegradation and bioconversion by fungi. *Biotechnol Adv*, 27 (2):185-194.
- Sarkar P, Bosneaga E, Auer M. 2009. Plant cell walls throughout evolution: towards a molecular understanding of their design principles. *J Exp Bot*, 60 (13):3615-3635.
- Satchell JE. 1976. *Litter-interface of animate/inanimate matter*. London: Academic Press.
- Savenkova MI, Kuo JM, Ortiz de Montellano PR. 1998. Improvement of Peroxygenase Activity by Relocation of a Catalytic Histidine within the Active Site of Horseradish Peroxidase. *Biochemistry*, 37 (30):10828-10836.
- Scheibner M, Hulsdau B, Zelena K, Nimtz M, de Boer L, Berger RG, Zorn H. 2008. Novel peroxidases of *Marasmius scorodoni* degrade beta-carotene. *Appl Microbiol Biotechnol*, 77 (6):1241-1250.
- Scheller U, Zimmer T, Becher D, Schauer F, Schunck WH. 1998. Oxygenation cascade in conversion of n-alkanes to alpha,omega-dioic acids catalyzed by cytochrome P450 52A3. *J Biol Chem*, 273 (49):32528-32534.
- Schmid A, Hollmann F, Park JB, Buhler B. 2002. The use of enzymes in the chemical industry in Europe. *Curr Opin Biotechnol*, 13 (4):359-366.
- Schmid RD, Urlacher VB. 2007. *Modern Biooxidation Enzymes, Reactions and Applications*. Weinheim: Wiley-VCH Verlag GmbH & Co KGaA.
- Schmidt HWH, Haemmerli SD, Schoemaker HE, Leisola MSA. 1989. Oxidative degradation of 3,4-dimethylbenzyl alcohol and its methyl ether by the lignin peroxidase of *Phanerochaete chrysosporium*. *Biochem*, 28:1776-1783.

- Schmidt S, Wittich RM, Fortnagel P, Erdmann D, Francke W. 1992. Metabolism of 3-methyldiphenyl ether by *Sphingomonas* sp. SS31. *FEMS Microbiol Lett*, 75 (2-3):253-258.
- Segall M. 1997. *Understanding Cytochrome P450 - Ligand Interactions*: University of Cambridge.
- Segel HI. 1994. *Enzyme Kinetics: Behavior and Analysis of Rapid Equilibrium and Steady-State Enzyme Systems*. New York John Wiley Sons, Inc.
- Sem DS, Bertolaet B, Baker B, Chang E, Costache AD, Coutts S, Dong Q, Hansen M, Hong V, Huang X, Jack RM, Kho R, Lang H, Ma CT, Meininger D, Pellecchia M, Pierre F, Villar H, Yu L. 2004. Systems-based design of bi-ligand inhibitors of oxidoreductases: filling the chemical proteomic toolbox. *Chem Biol*, 11 (2):185-194.
- Shaik S, Kumar D, de Visser SP, Altun A, Thiel W. 2005. Theoretical perspective on the structure and mechanism of cytochrome P450 enzymes. *Chemical Reviews*, 105 (6):2279-2328.
- Sheng D, Gold MH. 1997. Haloperoxidase activity of manganese peroxidase from *Phanerochaete chrysosporium*. *Arch Biochem Biophys*, 345 (1):126-134.
- Siegel W, Sauter H, Schaefer G. 1998. Preparation of mixtures of (R)- and (S)-2-(4-alkanoylphenoxy)- or (R)- and (S)-2-(4-aryloxyphenoxy)propionic esters. United States Patent 5801272.
- Sipilä J, Syrjänen K. 1995. Synthesis and  $^{13}\text{C}$  NMR spectroscopic characterization of six dimeric arylglycerol- $\beta$ -aryl ether model compounds representative of syringyl and *p*-hydroxy-phenyl structures, in lignins: On the aldol reaction in  $\beta$ -ether preparation. *Holzforschung*, 49 (4):325-331.
- Sligar SG. 1976. Coupling of spin, substrate, and redox equilibria in cytochrome P450. *Biochemistry*, 15 (24):5399-5406.
- Sligar SG, Gunsalus IC. 1976. A thermodynamic model of regulation: modulation of redox equilibria in camphor monooxygenase. *Proc Natl Acad Sci U S A*, 73 (4):1078-1082.
- Smith AT, Ngo E. 2007. Novel Peroxidase and uses. WIPO, World Patent: WO 2007020428 20070222
- Sonia C, María Luisa Á-R, Eliseo R, Angel R, Juan-José RC. 2009. Biodegradation of 2,4,6-TCA by the white-rot fungus *Phlebia radiata* is initiated by a phase I (O-demethylation)-phase II (O-conjugation) reactions system: implications for the chlorine cycle. *Environ Microbiol*, 11 (1):99-110.
- Sono MR, M.P. Coulter, E.D. and Dawson, J.H. 1996. Heme-Containing Oxygenases. *Chem Rev*, 96:2841-2887.
- Stamets P, Chilton JS. 1983. *The mushroom cultivator*. Olympia: Agarikon Press.
- Sternson LA, Gammans RE. 1975. Interaction of aromatic nitro compounds with reduced hepatic microsomal cytochrome P-450. *Drug Metab Dispos*, 3 (4):266-274.
- Sugano Y. 2009. DyP-type peroxidases comprise a novel heme peroxidase family. *Cell Mol Life Sci*, 66 (8):1387-1403.
- Sugano Y, Sasaki K, Shoda M. 1999. cDNA cloning and genetic analysis of a novel decolorizing enzyme, peroxidase gene *dyp* from *Geotrichum candidum* Dec 1. *J Biosci Bioeng*, 87 (4):411-417.
- Sugano Y, Muramatsu R, Ichiyangi A, Sato T, Shoda M. 2007. DyP, a unique dye-decolorizing peroxidase, represents a novel heme peroxidase family: ASP171 replaces the distal histidine of classical peroxidases. *J Biol Chem*, 282 (50):36652-36658.
- Sun RC, Sun XF. 2002. Fractional and structural characterization of hemicelluloses isolated by alkali and alkaline peroxide from barley straw. *Carbohydr Polym* 49 (4):415-423.
- Sundaramoorthy M, Turner J, Poulos TL. 1995. The crystal structure of chloroperoxidase: a heme peroxidase--cytochrome P450 functional hybrid. *Structure*, 3 (12):1367-1377.

- Suske WA, Held M, Schmid A, Fleischmann T, Wubbolts MG, Kohler H-PE. 1997. Purification and characterization of 2-hydroxybiphenyl 3-monooxygenase, a novel NADH-dependent, FAD-containing aromatic hydroxylase from *Pseudomonas azelaica* HBP1. *J Biol Chem*, 272 (39):24257-24265.
- Tassaneeyakul W, Veronese ME, Birkett DJ, Gonzalez FJ, Miners JO. 1993. Validation of 4-nitrophenol as an in vitro substrate probe for human liver CYP2E1 using cDNA expression and microsomal kinetic techniques. *Biochem Pharmacol*, 46 (11):1975-1981.
- Teramoto H, Tanaka H, Wariishi H. 2004. Fungal cytochrome P450s catalyzing hydroxylation of substituted toluenes to form their hydroxymethyl derivatives. *FEMS Microbiol Lett*, 234 (2):255-260.
- Teunissen PJ, Field JA. 1998. 2-Chloro-1,4-dimethoxybenzene as a mediator of lignin peroxidase catalyzed oxidations. *FEBS Lett*, 439 (3):219-223.
- Tien M. 1987. Properties of ligninase from *Phanerochaete chrysosporium* and their possible applications. *Crit Rev Microbiol*, 15 (2):141-168.
- Tien M, Kirk TK. 1983. Lignin-degrading enzyme from the hymenomycete *Phanerochaete chrysosporium* burds. *Science*, 221:661-663.
- Tien M, Kirk TK. 1984. Lignin-degrading enzyme from *Phanerochaete chrysosporium*: Purification, characterization, and catalytic properties of a unique H<sub>2</sub>O<sub>2</sub>-requiring oxygenase. *Proc Natl Acad Sci U S A*, 81:2280-2284.
- Tien M, Kirk TK, Bull C, Fee JA. 1986. Steady-state and transient-state kinetic studies on the oxidation of 3,4-dimethoxybenzyl alcohol catalyzed by the ligninase of *Phanerochaete chrysosporium* Burds. *J Biol Chem*, 261 (4):1687-1693.
- Timofeevski SL, Nie G, Reading NS, Aust SD. 1999. Addition of veratryl alcohol oxidase activity to manganese peroxidase by site-directed mutagenesis. *Biochem Biophys Res Commun*, 256 (3):500-504.
- Tinoco R, Verdin J, Vazquez-Duhalt R. 2007. Role of oxidizing mediators and tryptophan 172 in the decoloration of industrial dyes by the versatile peroxidase from *Bjerkandera adusta*. *J Mol Catal B: Enzym*, 46 (1-4):1-7.
- Tortella GR, Diez MC, Duran N. 2005. Fungal diversity and use in decomposition of environmental pollutants. *Crit Rev Microbiol*, 31 (4):197-212.
- Tsitsigiannis DI, Keller NP. 2007. Oxylipins as developmental and host-fungal communication signals. *Trends Microbiol* 15 (3):109-118.
- Tuor U, Wariishi H, Schoemaker HE, Gold MH. 1992. Oxidation of phenolic arylglycerol beta-aryl ether lignin model compounds by manganese peroxidase from *Phanerochaete chrysosporium*: oxidative cleavage of an alpha-carbonyl model compound. *Biochemistry*, 31 (21):4986-4995.
- Ullrich R. 2004. Die Haloperoxidase des Pilzes *Agrocybe aegerita*: Ein extrazelluläres P450-Enzym Zittau: Internationales Hochschulinstitut.
- Ullrich R, Hofrichter M. 2005. The haloperoxidase of the agaric fungus *Agrocybe aegerita* hydroxylates toluene and naphthalene. *FEBS Lett*, 579 (27):6247-6250.
- Ullrich R, Hofrichter M. 2007. Enzymatic hydroxylation of aromatic compounds. *Cell Mol Life Sci*, 64 (3):271-293.
- Ullrich R, Dolge C, Kluge M, Hofrichter M. 2008. Pyridine as novel substrate for regioselective oxygenation with aromatic peroxygenase from *Agrocybe aegerita*. *FEBS Lett*, 582 (29):4100-4106.
- Ullrich R, Liers C, Schimpke S, Hofrichter M. 2009. Purification of homogeneous forms of fungal peroxygenase. *Biotechnol J*, 4 (11):1619-1626.

- Ullrich R, Nüske J, Scheibner K, Spantzel J, Hofrichter M. 2004. Novel haloperoxidase from the agaric basidiomycete *Agrocybe aegerita* oxidizes aryl alcohols and aldehydes. *Appl Environ Microbiol*, 70 (8):4575-4581.
- Ullrich R, Pecyna M, Kluge M, Kinne M, Liers C, Hofrichter M. 2008. Some special reactions of *Agrocybe aegerita* peroxygenase (AaP). 8th International Peroxidase Symposium. Tampere, Finland.
- Ulrik J, Håkan VW, Lars W, Andries PB. 2003. Comparison between electrochemistry/mass spectrometry and cytochrome P450 catalyzed oxidation reactions. *Rapid Commun Mass Spectrom* 17 (8):800-810.
- Urano Y, Higuchi T, Hirobe M. 1996. Substrate-dependent changes of the oxidative O-dealkylation mechanism of several chemical and biological oxidizing systems. *J Chem Soc, Perkin Trans 2*:1169-1173.
- Urlacher VB, Eiben S. 2006. Cytochrome P450 monooxygenases: perspectives for synthetic application. *Trends Biotechnol*, 24 (7):324-330.
- Urlacher VB, Lutz-Wahl S, Schmid RD. 2004. Microbial P450 enzymes in biotechnology. *Appl Microb Biotechnol*, 64:317-325.
- Valero E, Lozano MI, Varon R, Garcia-Carmona F. 2003. Enzymatic synthesis of 3'-hydroxyacetaminophen catalyzed by tyrosinase. *Biotechnol Prog*, 19 (6):1632-1638.
- van Beilen JB, Duetz WA, Schmid A, Witholt B. 2003. Practical issues in the application of oxygenases. *Trends Biotechnol*, 21 (4):170-177.
- Van der Zee J, Duling DR, Mason RP, Eling TE. 1989. The oxidation of N-substituted aromatic amines by horseradish peroxidase. *J Biol Chem*, 264 (33):19828-19836.
- van Deurzen MPJ, van Rantwijk F, Sheldon RA. 1997. Selective oxidations catalyzed by peroxidases. *Tetrahedron*, 53 (39):13183-13220.
- van Pée KH, Zehner S. 2003. Natural production of organohalogen compounds: Enzymology and molecular genetics of biological halogenation. In: Gribble GW, Hrsg. *The Handbook of Environmental Chemistry*. Berlin: Springer Verlag, 171-199.
- van Rantwijk F, Sheldon RA. 2000. Selective oxygen transfer catalysed by heme peroxidases: synthetic and mechanistic aspects. *Curr Opin Biotechnol*, 11 (6):554-564.
- Vane CH, Drage TC, Snape CE. 2006. Bark decay by the white-rot fungus *Lentinula edodes*: Polysaccharide loss, lignin resistance and the unmasking of suberin. *Int Biodet Biodeg*, 57 (1):14-23.
- Varazashvili T, Khatisashvili G, Kurashvili M, Pruidze M, Ananiashvili T, Ananiashvili G, Gordeziani M. 2001. Nitrobenzene oxidizing enzymes in plant cells. *J Biol Phys Chem*, 1:85-88.
- Vaz AD, McGinnity DF, Coon MJ. 1998. Epoxidation of olefins by cytochrome P450: evidence from site-specific mutagenesis for hydroperoxo-iron as an electrophilic oxidant. *Proc Natl Acad Sci U S A*, 95 (7):3555-3560.
- Vaz AD, Pernecky SJ, Raner GM, Coon MJ. 1996. Peroxo-iron and oxenoid-iron species as alternative oxygenating agents in cytochrome P450-catalyzed reactions: switching by threonine-302 to alanine mutagenesis of cytochrome P450 2B4. *Proc Natl Acad Sci U S A*, 93 (10):4644-4648.
- Veeger C. 2002. Does P450-type catalysis proceed through a peroxo-iron intermediate? A review of studies with microperoxidase. *J Inorg Biochem*, 91 (1):35-45.
- Verhagen FJM, Swarts HJ, Kuyper TW, Wijnberg JBPA, Field JA. 1996. The ubiquity of natural adsorbable organic halogen production among basidiomycetes. *Appl Microbiol Biotechnol* 45 (5):710-718.
- Vicente F, Basilio A, Platas G, Collado J, Bills GF, González Del Val A, Martín J, Tormo JR, Harris GH, Zink DL, Justice M, Nielsen Kahn J, Peláez F. 2009. Distribution of the antifungal agents sordarins across filamentous fungi. *Mycol Res*, 113 (6-7):754-770.

- Vidakovic M, Sligar SG, Li H, Poulos TL. 1998. Understanding the role of the essential Asp251 in cytochrome p450cam using site-directed mutagenesis, crystallography, and kinetic solvent isotope effect. *Biochemistry*, 37 (26):9211-9219.
- Wang JS, Baek HK, Van Wart HE. 1991. High-valent intermediates in the reaction of N alpha-acetyl microperoxidase-8 with hydrogen peroxide: models for compounds 0, I and II of horseradish peroxidase. *Biochem Biophys Res Commun*, 179 (3):1320-1324.
- Wariishi H, Valli K, Gold MH. 1992. Manganese(II) oxidation by manganese peroxidase from the basidiomycete *Phanerochaete chrysosporium*. Kinetic mechanism and role of chelators. *J Biol Chem*, 267 (33):23688-23695.
- Weber RW, Meffert A, Anke H, Sterner O. 2005. Production of sordarin and related metabolites by the coprophilous fungus *Podospora pleiospora* in submerged culture and in its natural substrate. *Mycol Res*, 109 (Pt 5):619-626.
- Webster R, Pacey M, Winchester T, Johnson P, Jezequel S. 1998. Microbial oxidative metabolism of diclofenac: production of 4'-hydroxydiclofenac using *Epicoccum nigrum* IMI354292. *Appl Microbiol Biotechnol*, 49 (4):371-376.
- Welinder KG. 1992. Superfamily of plant, fungal and bacterial peroxidases. *Curr Opin Struct Biol*, 2:388-393.
- White GF, Russell NJ, Tidswell EC. 1996. Bacterial scission of ether bonds. *Microbiol Rev*, 60 (1):216-232.
- Wisniewska-Knypl JM, Jablonska JK, Piotrowski JK. 1975. Effect of repeated exposure to aniline, nitrobenzene, and benzene on liver microsomal metabolism in the rat. *Br J Ind Med*, 32 (1):42-48.
- Woithe K, Geib N, Zerbe K, Li DB, Heck M, Fournier-Rousset S, Meyer O, Vitali F, Matoba N, Abou-Hadeed K, Robinson JA. 2007. Oxidative phenol coupling reactions catalyzed by OxyB: a cytochrome P450 from the vancomycin producing organism. implications for vancomycin biosynthesis. *J Am Chem Soc*, 129 (21):6887-6895.
- Yun CH, Kim KH, Calcutt MW, Guengerich FP. 2005. Kinetic analysis of oxidation of coumarins by human cytochrome P450 2A6. *J Biol Chem*, 280 (13):12279-12291.
- Yun CH, Lee HS, Lee HY, Yim SK, Kim KH, Kim E, Yea SS, Guengerich FP. 2003. Roles of human liver cytochrome P450 3A4 and 1A2 enzymes in the oxidation of myristicin. *Toxicol Lett*, 137 (3):143-150.
- Zamocky M, Furtmuller PG, Obinger C. 2008. Evolution of catalases from bacteria to humans. *Antioxid Redox Signal*, 10 (9):1527-1548.
- Zimmermann MC, Tilghman SL, Boue SM, Salvo VA, Elliott S, Williams KY, Skripnikova EV, Ashe H, Payton-Stewart F, Vanhoy-Rhodes L, Fonseca JP, Corbitt C, Collins-Burow BM, Howell MH, Lacey M, Shih BY, Carter-Wientjes C, Cleveland TE, McLachlan JA, Wiese TE, Beckman BS, Burow ME. 2009. Glyceollin I, a novel antiestrogenic phytoalexin isolated from activated soy. *J Pharmacol Exp Ther*, 332 (1):35-45.
- Zubieta C, Krishna SS, Kapoor M, Kozbial P, McMullan D, Axelrod HL, Miller MD, Abdubek P, Ambing E, Astakhova T, Carlton D, Chiu HJ, Clayton T, Deller MC, Duan L, Elsliger MA, Feuerhelm J, Grzechnik SK, Hale J, Hampton E, Han GW, Jaroszewski L, Jin KK, Klock HE, Knuth MW, Kumar A, Marciano D, Morse AT, Nigoghossian E, Okach L, Oommachen S, Reyes R, Rife CL, Schimmel P, van den Bedem H, Weekes D, White A, Xu Q, Hodgson KO, Wooley J, Deacon AM, Godzik A, Lesley SA, Wilson IA. 2007a. Crystal structures of two novel dye-decolorizing peroxidases reveal a beta-barrel fold with a conserved heme-binding motif. *Proteins*, 69 (2):223-233.
- Zubieta C, Joseph R, Krishna SS, McMullan D, Kapoor M, Axelrod HL, Miller MD, Abdubek P, Acosta C, Astakhova T, Carlton D, Chiu HJ, Clayton T, Deller MC, Duan

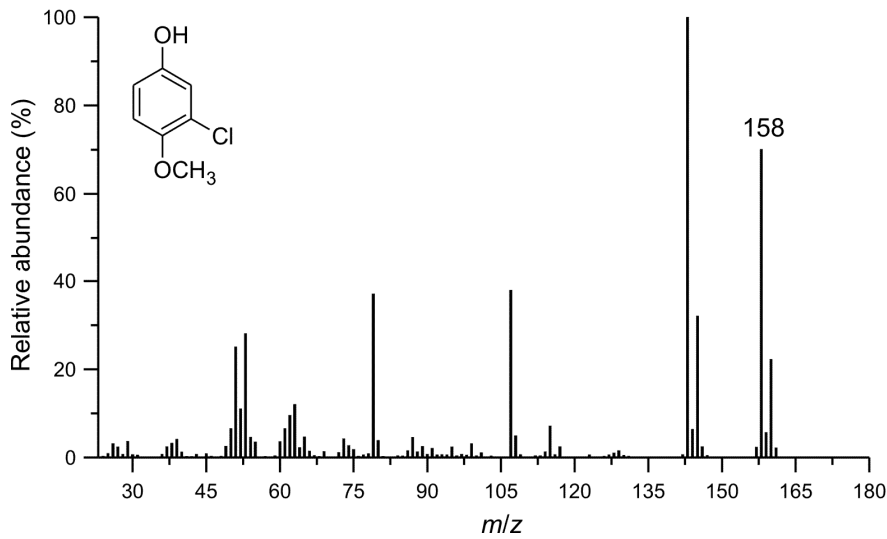
## REFERENCES

---

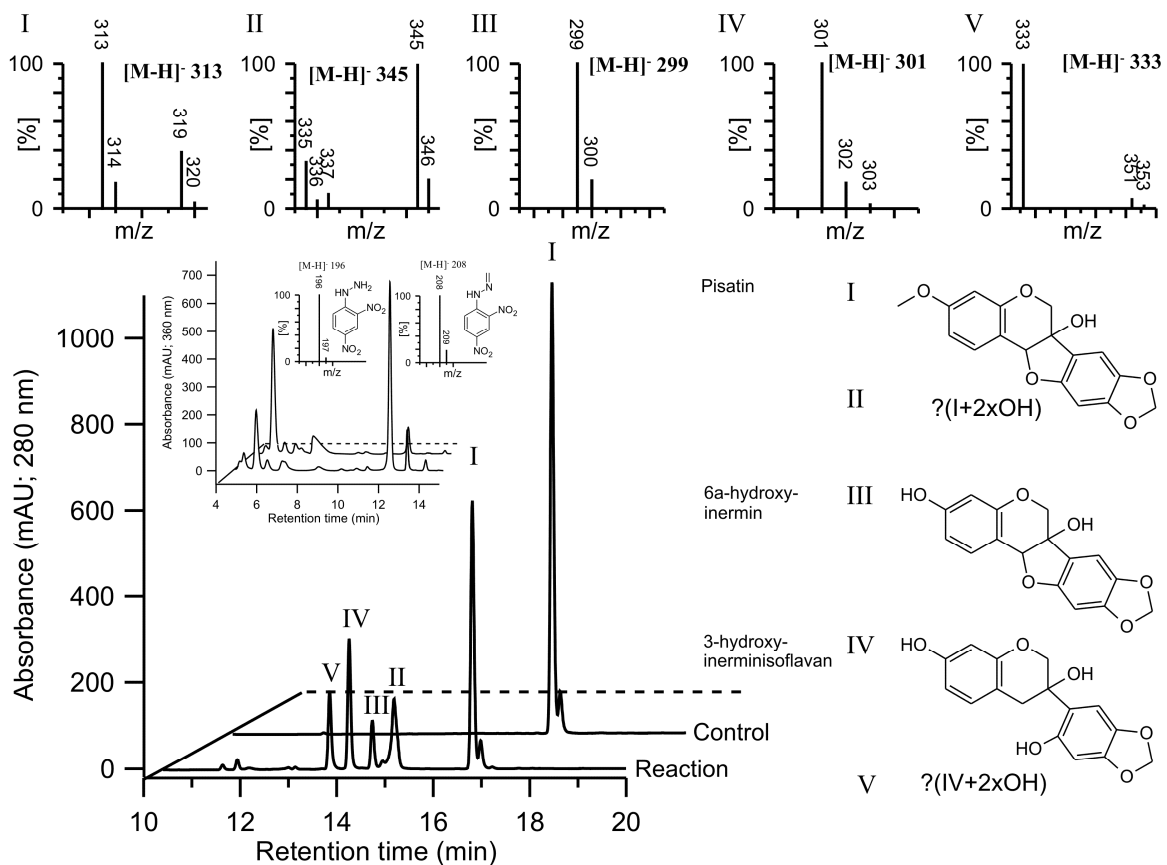
L, Elias Y, Elsliger MA, Feuerhelm J, Grzechnik SK, Hale J, Han GW, Jaroszewski L, Jin KK, Klock HE, Knuth MW, Kozbial P, Kumar A, Marciano D, Morse AT, Murphy KD, Nigoghossian E, Okach L, Oommachen S, Reyes R, Rife CL, Schimmel P, Trout CV, van den Bedem H, Weekes D, White A, Xu Q, Hodgson KO, Wooley J, Deacon AM, Godzik A, Lesley SA, Wilson IA. 2007b. Identification and structural characterization of heme binding in a novel dye-decolorizing peroxidase, TyrA. *Proteins*, 69 (2):234-243.



## 6 Appendix

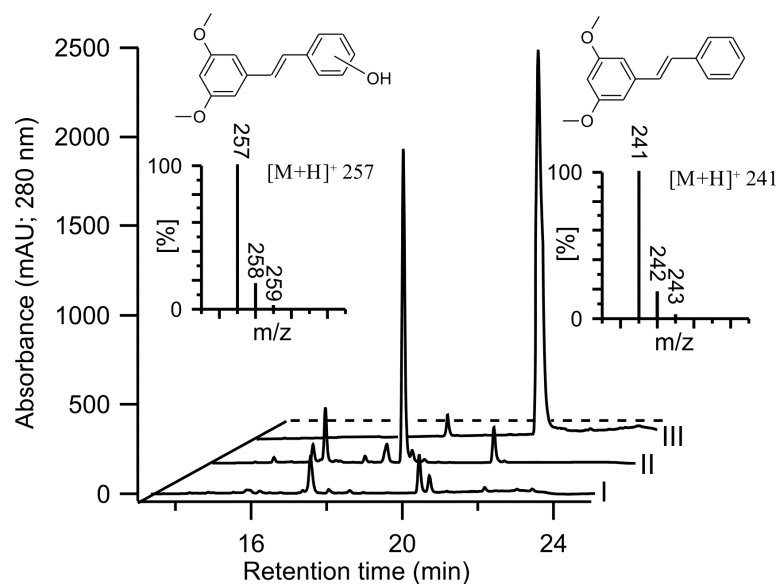


Appx. 1 GC-MS spectra of the suggested reaction product 3-chloro-4-methoxyphenol obtained from cleavage of 2-chloro-1,4-dimethoxybenzene by *Aae*APO.

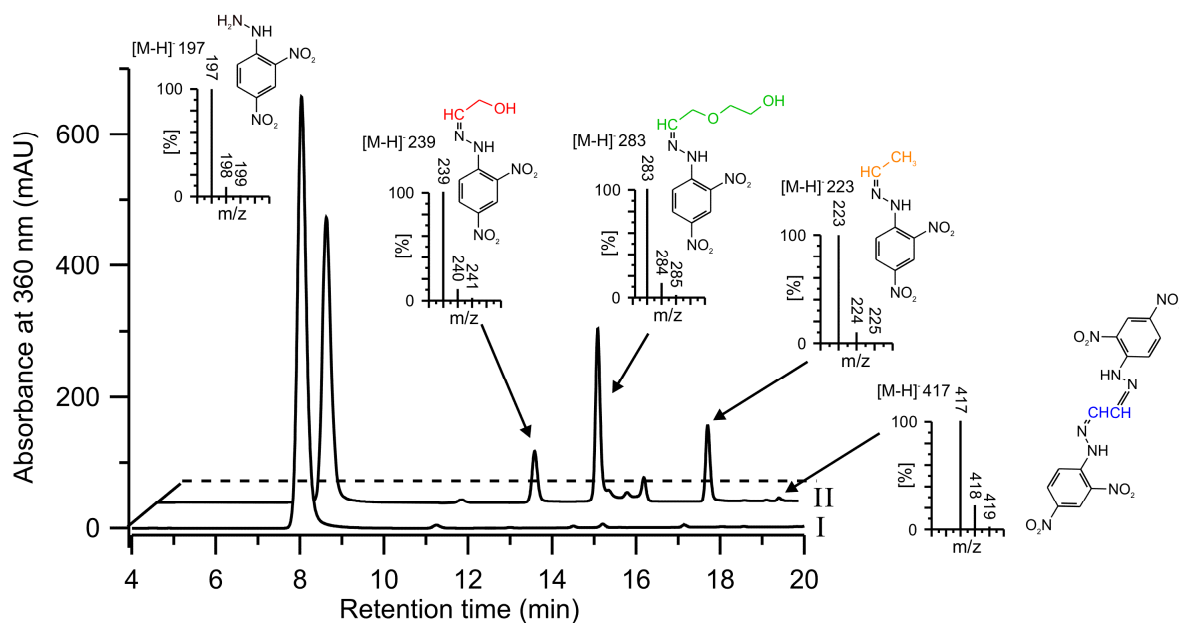


Appx. 2 HPLC elution profiles showing suggested products obtained from the reaction of *Aae*APO with pisatin. Insets of respective product mass spectra and a HPLC elution profile of formaldehyde-2,4-dinitrophenylhydrazone are shown.

APPENDIX



Appx. 3 HPLC elution profiles showing different reaction products obtained from the reaction of *Aae*APO with 3,5-dimethoxystilbene.



Appx. 4 HPLC elution profiles showing different 2,4-dinitrophenylhydrazones from the reaction of *Aae*APO with diethylene glycol.

## List of patents and publications

**I** Kinne M., Ullrich R., Scheibner K., Hofrichter, M. (2007) Verfahren zur *O*-Dealkylierung von Alkylarylethern. German Patent DE102007058741A1.

**II** Kinne M., Ullrich R., Scheibner K., Hofrichter, M. (2008) Verfahren zur Herstellung von 2-(4-Hydroxyphenoxy)propionsäure. German Patent DE102008034829A1.

**III** Kinne M., Ullrich R., Hammel K. E., Scheibner K., Hofrichter, M. (2008) Regioselective preparation of (*R*)-2-(4-hydroxyphenoxy)propionic acid with a fungal peroxygenase. *Tetrahedron Letters*, 49: 5950-5953.

**IV** Kinne M., Poraj-Kobielska M., Aranda E., Ullrich R., Hammel K. E., Scheibner K., Hofrichter M. (2009) Regioselective preparation of 5-hydroxypropranolol and 4'-hydroxydiclofenac with a fungal peroxygenase. *Bioorganic & Medicinal Chemistry Letters*, 19: 3085-3087.

**V** Kinne M., Poraj-Kobielska M., Ralph S. A., Ullrich R., Hofrichter M., Hammel K. E., (2009) Oxidative cleavage of diverse ethers by an extracellular fungal peroxygenase. *Journal of Biological Chemistry*, 284: 29343-29349.

**VI** Kinne M., Zeisig C., Ullrich R., Kayser G. Hammel K. E., Hofrichter M. (2010) Stepwise oxygenations of toluene and 4-nitrotoluene by a fungal peroxygenase. *Biochemical and Biophysical Research Communications*, 397 (1): 18-21.



(19)  
Bundesrepublik Deutschland  
Deutsches Patent- und Markenamt

(10) DE 10 2007 058 741 A1 2009.06.04

(12)

## Offenlegungsschrift

(21) Aktenzeichen: 10 2007 058 741.6

(22) Anmeldetag: 03.12.2007

(43) Offenlegungstag: 04.06.2009

(51) Int Cl.<sup>8</sup>: C12P 7/22 (2006.01)  
C07C 39/08 (2006.01)

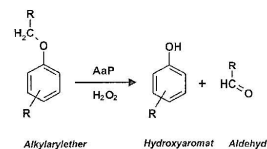
(71) Anmelder:  
JenaBios GmbH, 07749 Jena, DE

(74) Vertreter:  
Sonnefeld, Teichmann, Rechtsanwälte, 07743  
Jena

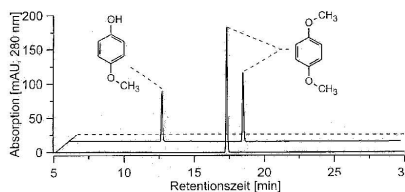
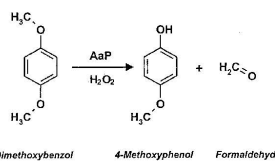
(72) Erfinder:  
Ullrich, Rene, Dr.rer.nat., 02763 Zittau, DE;  
Scheibner, Katrin, Prof. Dr.rer.nat., 07745 Jena,  
DE; Hofrichter, Martin, Prof.Dr.rer.nat.habil, 02763  
Zittau, DE; Kinne, Matthias, 02827 Görlitz, DE

Die folgenden Angaben sind den vom Anmelder eingereichten Unterlagen entnommen

(54) Bezeichnung: Verfahren zur O-Dealkylierung von Alkylarylethern



(57) Zusammenfassung: Die Erfindung betrifft ein Verfahren zur enzymatischen, O-Dealkylierung von Alkylarylethern (Ar-O-Alkyl) der allgemeinen Formel (I) zu den entsprechenden hydroxylierten Aromaten (Ar-OH) der Formel (II) und Alkylaldehyden (Alkyl-CHO) durch Umsetzung von Alkylarylethern der Formel (I) mit einer pilzlichen Haloperoxidase-Peroxygenase [z. B. Agrocybe-aegerita-Peroxidase = AaP] in Gegenwart mindestens eines Oxidationsmittels (z. B. Wasserstoffperoxid) in einem Einstufen-Reaktionsverfahren. Die Reaktion verläuft erfindungsgemäß regioselektiv, so dass am Ende Reinheiten der Positionsisomere von mehr als 95% und Ausbeuten zwischen 20 und 90% erreicht werden. Das Verfahren kann in den verschiedensten Bereichen der Synthesechemie eingesetzt werden, u. a. zur Herstellung von Pharmaka-Vorstufen sowie zur Synthese spezieller Katalysatoren und zur selektiven Entfernung von Schutzgruppen.



DE 10 2007 058 741 A1 2009.06.04

**Beschreibung**

**[0001]** Die Erfindung betrifft ein Verfahren zur enzymatischen Spaltung von Alkylarylethern (Ar-O-Alkyl) in hydroxylierte Aromaten (Phenole; Ar-OH) und Alkylaldehyde (Alkyl-CHO).

**[0002]** Phenolische Hydroxylgruppen spielen in vielen Naturstoffen und als funktionelle Gruppe in synthetisierten organischen Chemikalien eine bedeutende Rolle (Huhn, P, 2006: Naturstoffchemie. S. Hirzel Verlag Stuttgart; Volhardt, KPC, Schore, NE, 2000: Organische Chemie. Wiley-VCH Verlag Weinheim). Es ist deshalb oftmals notwendig, an Molekülen mit phenolischen OH-Gruppen chemische Modifikationen/ Reaktionen durchzuführen. Hydroxylgruppen erhöhen generell die Reaktivität eines Aromaten gegenüber elektrophilen Substitutionen, was mit einem Verlust an Selektivität bezüglich anderer chemischer Reaktionen verbunden ist (Walter, W, Francke, W, 2004: Beyer Walter Lehrbuch der organischen Chemie. S. Hirzel Verlag Stuttgart). Zudem beeinflusst das azide Wasserstoffatom der phenolischen OH-Gruppe säureempfindliche Katalysen.

**[0003]** In der pharmazeutischen Synthesechemie, beispielsweise bei der Darstellung von biologisch aktiven, oxygenierten Verbindungen, müssen diese reaktiven phenolischen Gruppen vor unerwünschten chemischen Reaktionen geschützt werden. Dies geschieht im Allgemeinen durch eine Alkylierung der OH-Gruppe unter Bildung der korrespondierenden Alkylarylether, hauptsächlich in Form von Methyl- oder Ethylethern (Wuts, PGM 2007: Greene's protective groups in organic synthesis. 4. Ed, John Wiley & Sons; Kocienski, PJ 2005: Protecting Groups. 3. Ed. Thieme). Die Methylierung phenolischer OH-Gruppen ist chemisch relativ einfach zu realisieren und wird zumeist mittels Methyljodid, Dimethylsulfat, Diazomethan oder umweltschonend mit Dimethylcarbonat durchgeführt (Perosa, A, Selva, M, Tundo, P, Zordan F 2000: Alkyl methyl carbonates as very efficient methylating agents. The O-methylation of Phenols. Synlett, 1, 272-274). Zum Schutz phenolischer OH-Gruppen können analog auch Ether mit längeren Alkylresten synthetisiert werden.

**[0004]** Im Anschluss an die gewünschten chemischen Modifikationen des Zielmoleküls müssen die schützenden Etherbindungen gespalten werden, damit die für die Moleküleigenschaften wichtige(n) Hydroxylfunktion(en) (phenolische OH-Gruppen) wieder entstehen. Es ist allgemein bekannt, dass Alkylarylether chemisch gespalten werden können. Dies geschieht bevorzugt in Gegenwart starker, protischer Säuren mit nukleophilen Anionen (z. B. HI, HBr; Melzer, RI, Lustgarten, DM, Fischman, A 1957: Thyroxine Analogs. J Org Chem 22: 1577-1581) als nukleophiler Angriff auf das reaktivste C-Atom (Boovanahalli, SK, Kim, DW, Chioder, DY 2004: Application of io-

nic liquid halide nucleophilicity for the cleavage of ethers. A Green Protocol for the Regeneration of Phenols from Ethers. J Org Chem 69: 3340-3344) oder durch Lewis-Säuren, wie z. B. trivalente Borverbindungen, über einen elektrophilen Angriff auf den Sauerstoff des Ethers oder mittels reduktiver Spaltung (Ranu, C, Bhar, S 1996: Dealkylation of Ethers. A review. Org Prep Proc Int 28: 371-411; Claydon, J, Greeves, N, Warren, S, Wothers, P et.al. 2006: Organic Chemistry. Oxford University Press). Da die Etherbindung eine hohe Bindungsenergie (ca. 360 kJ mol<sup>-1</sup>) besitzt, gestaltet sich die chemische Dealkylierung im technischen Maßstab schwierig und kostenintensiv. So weisen die verschiedenen Möglichkeiten der chemischen Dealkylierung eine Reihe von Nachteilen auf:

- a) es sind relativ hohe Temperaturen (~50-175°C) und
- b) lange Reaktionszeiten (~1-24 h) erforderlich,
- c) meist werden nur mäßige Ausbeuten (~50-90%) erreicht,
- d) es kommt zur Entstehung unerwünschter Nebenprodukte (geringe Selektivität),
- e) es sind teure Katalysatoren erforderlich und
- f) es müssen umweltgefährdende Chemikalien eingesetzt werden.

**[0005]** (Weissmau SA, Zewge, D 2005: Recent advances in ether dealkylation. Tetrahedron 61: 7833-7863; Mejeed, M. 2007: Process for the synthesis of biologically active oxygenated compounds by dealkylation of the corresponding alkylethers. United States Patent 7253324)

**[0006]** Prozesse unter Verwendung von Iod-, Brom- und Chlorwasserstoff sowie Aluminium-(III)-chlorid und Eisen-(III)-chlorid führen zu geringen Ausbeuten und müssen meist unter strikt aziden Bedingungen ablaufen. Höhere Ausbeuten können durch kostenintensivere Bor-(III)-halogenide erzielt werden. Der Einsatz von Pyridinchlorid zur Demethylierung ist aufgrund hoher Prozess-Temperaturen (ca. 200°C) unwirtschaftlich; theoretisch geeignete phosphorhaltige Chemikalien sind wiederum unselektiv. Optimierte Verfahren zur Dealkylierung von Alkylarylethern mit Aluminium-(III)-iodid führen zu höheren Selektivitäten und Ausbeuten, sind aber, aufgrund der Verwendung von Kohlenstoffdisulfid, das toxisch und entflammbar ist, und nicht zuletzt wegen der langen Reaktionszeiten, unwirtschaftlich. Nebenprodukte bei der Anwendung von Thiolat-Katalysatoren führen zu Geruchsemissionen und hygienischen Problemen im industriellen Prozess. (Andersson, S-G B. (Malmo, SE), 1986: Method for dealkylation of alkyl-aryl ethers. United States Patent 4695659).

**[0007]** Aufgrund der bekanntermaßen hohen Selektivität und dem umweltschonenden Verlauf enzymatischer Reaktionen stellen biokatalytische Prozesse eine geeignete Alternative zu energieintensiven und

DE 10 2007 058 741 A1 2009.06.04

umweltgefährdenden chemischen Synthesen dar. Folgende enzymatische Spaltungen von Alkylarylethern sind derzeit bekannt:

a) Häm-Peroxidasen (EC 1.11.1.x): Bei dieser Enzymfamilie handelt es sich um Proteine mit einem Porphyrinringsystem und zentralem Eisen-Ion (meist  $\text{Fe}^{3+}$ ), die in Gegenwart von Wasserstoffperoxid als Elektronenakzeptor in der Lage sind, aromatische bzw. phenolische Verbindungen zu oxidieren. Das am besten untersuchte Enzym dieser Gruppe ist die Meerrettich-Peroxidase. Sie kann neben den o. g. Reaktionen verschiedene N-Dealkylierungen katalysieren, jedoch nur einige wenige O-Dealkylierungen. Im letzteren Fall handelt es sich immer um komplexe Methoxybenzol-Derivate, welche mit zusätzlichen aktivierenden Amino- und/oder anderen funktionellen Gruppen substituiert sind (Meunier, G, Meunier, B 1985: Evidences for an efficient demethylation of methoxy ellipticine catalyzed by a peroxidase. *J Am Chem Soc* 107: 2558–2560; Ross, D, Larsson, R, Norbeck, K, Ryhage, R, Moldéus, P 1985: Characterization and mechanism of formation of reactive products formed during peroxidasecatalyzed Oxidation of p-phenetidine. Trapping of reactive species by reduced glutathione and butylated hydroxyanisole. *Mol Pharmacol* 27: 277–286; Haim, N, Nemeč, J, Roman, J, Sinha, BK 1987: Peroxidase-catalyzed metabolism of etoposide (VP-16-213) and covalent binding of reactive intermediates to cellular macromolecules. *Cancer Res* 47: 5835–5840).

[0008] Des Weiteren ist bekannt, dass Lignin-Peroxidasen aus Weißfäulepilzen (z. B. *Phanerochaete chrysosporium*) befähigt sind, substituierte Alkylarylether zu spalten. Jedoch entstehen dabei stets chinonide Verbindungen als Hauptprodukte, während Phenole (z. B. Guajakol) lediglich in Spuren oder nicht nachgewiesen werden konnten. Zudem verlaufen diese Oxidationen über einen rein radikalischen Mechanismus, was eine geringe Selektivität zur Folge hat. Dies macht eine Verwendung dieser Enzyme zum Entfernen von Schutzgruppen unmöglich (Enoki, A, Goldsby, GP, Gold, MH 1981:  $\beta$ -Ether cleavage of the lignin model compound 4-ethoxy-3-methoxyphenylglycerol- $\beta$ -guaiacyl ether and derivatives by *Phanerochaete chrysosporium*. *Arch Microbiol* 129: 141–145).

[0009] Häm-basierte „Kleinstenzyme“, auch Mikroperoxidasen genannt, sind in der Lage, sowohl durch Ein-Elektron-Oxidation als auch über den intermediären Transfer von Sauerstoff, Alkylarylether zu O-dealkylieren. Doch auch in diesem Fall ist die Etherspaltung strikt an das Vorhandensein von aktivierenden Substituenten am aromatischen Ring gebunden. So kann die Mikroperoxidase 8 (MP 8) kann nur Arylether spalten, die ein Ionisierungspotential  $< 8,4$  eV besitzen. Eine Dealkylierung von stabilen Arylethern

wie 1,4-Dimethoxybenzol oder Anisol zu den entsprechenden Phenolen kann folgerichtig nicht katalysiert werden (Boersma, MG, Primus, J-L, Koerts, J, Veeger, C, Rietjens, IMCM 2000: Heme-(hydro)peroxide mediated O- and N-dealkylation. A study with microperoxidase. *Eur J Biochem* 267: 6673–6678).

[0010] Außerdem ist bekannt, dass die Chlorperoxidase (CPO) des Schlauchpilzes *Caldariomyces fumago* in Abwesenheit von Chlorid-Ionen in der Lage ist, eine Vielzahl von Verbindungen zu oxidieren und auch aromatische N-Dealkylierungen zu katalysieren (Hofrichter, M, Ullrich, R 2006: Heme-thiolate haloperoxidases: versatile biocatalysts with biological and environmental significance. *Appl Microbiol Biotechnol* 71: 276–288). Jedoch beschreibt nur eine Publikation die mögliche O-Dealkylierung eines Arylethers (p-Methylanisol) durch die CPO. Das aromatische Reaktionsprodukt (p-Cresol) konnte allerdings nicht nachgewiesen werden und die Dealkylierung wurde lediglich auf Grund des Nachweises von Formaldehyd postuliert (Miller, VP, Tschirret-Guth, RA, Ortiz de Montellano, PR 1995: Chlorperoxidase-catalyzed benzylic hydroxylation. *Arch Biochem Biophys* 319: 330–340)

b) Weiterhin ist bekannt, dass einige Cytochrom-P450-Monooxygenasen (EC 1.14.14.x) Alkylarylether O-dealkylieren können. Sie kommen ausschließlich intrazellulär vor, sind oft membranengebunden und benötigen für ihre Funktion komplexe Elektronendonatoren [NAD(P)H] sowie spezielle Elektronentransportproteine (z. B. Ferredoxin, Flavin-Reduktasen) und molekularen Sauerstoff ( $\text{O}_2$ ) als Cofaktoren. Weitere Nachteile dieser Enzyme sind ihre geringen Wechselzahlen ( $k_{\text{cat}}$ ) und katalytischen Effizienzen (Urano, Y, Higuchi, T, Hirobe, M, 1996: Substrate-dependent changes of the oxidative O-dealkylation mechanism of several chemical and biological oxidizing systems. *J. Chem. Soc.; White, GF, Russell, NJ, and Tidswell, EC, 1996: Bacterial scission of ether bonds. Microbiol.*)

c) Außerdem ist eine 4-Methoxybenzoesäure-Monooxygenase (EC 1.14.99.15) aus *Pseudomonas putida* in der Lage, mit den Cosubstraten NADH und molekularem Sauerstoff ( $\text{O}_2$ ) 4-Methoxybenzoesäure zur korrespondierenden 4-Hydroxybenzoesäure zu demethylieren. Es handelt sich dabei um eine hämfreie Monooxygenase mit einem Fe-S-Cluster (Rieske-type enzyme) im aktiven Zentrum (Bernhardt, FH, Ruf, HH and Ehrig, H, 1974: A 4-methoxybenzoate monooxygenase system from *Pseudomonas putida*. Circular dichroism studies on the iron-sulfur protei. *FERS Letters*, 43(1): 53–55; Kim, YH, Engesser, KH, 2004: Degradation of alkyl ethers, aralkyl ethers, and dibenzyl ether by *Rhodococcus* sp. strain DEE5151, isolated from diethyl ether-containing enrichment cultures. *Appl Environ Microbiol*, 70(7): 4398-401).

DE 10 2007 058 741 A1 2009.06.04

**[0011]** Die Aufgabe der vorliegenden Erfindung ist es, einen Prozess zur Dealkylierung von Arylalkylethern zu den entsprechenden Phenolen mit möglichst geringem verfahrenstechnischen und apparativen Aufwand und bei gleichzeitigem Einsatz kostengünstiger Cosubstrate durchzuführen. Die Umsetzung der Ausgangsverbindungen soll in kurzen Inkubationszeiten, bei Raumtemperatur und -druck, im wässrigen Milieu und ohne erhöhte Anforderungen an sterile bzw. semisterile Reaktionsbedingungen erfolgen. Die Reaktionsprodukte sind dabei mit möglichst geringem Aufwand zu isolieren, und eine aufwändige Trennung weiterer Reaktionsprodukte soll entfallen.

**[0012]** Das vorliegende Verfahren löst diese Aufgabe und betrifft ein Methode zur enzymatischen, O-Dealkylierung von Alkylarylethern der Formel (I) zu den entsprechenden hydroxylierten Aromaten (II) durch Umsetzung eines Alkylarylethers der Formel (I) mit einer pilzlichen Haloperoxidase-Peroxygenase („Etherase“) in Gegenwart mindestens einen Oxidationsmittels in einem Einstufen-Reaktionsverfahren.

**[0013]** Die Ausgangsverbindungen der Formel (I) werden dabei vorzugsweise mit der Haloperoxidase-Peroxygenase des Lamellenpilzes *Agrocybe aegerita* (*Agrocybe-aegerita*-Peroxidase = AaP), die eine besonders hohe Peroxygenase- und Etherase-Aktivität besitzt, und zumindest einem Oxidationsmittel zur Reaktion gebracht, wobei die Dealkylierung des Alkylarylethers erfolgt.

**[0014]** Als Oxidationsmittel werden erfindungsgemäß vorzugsweise  $H_2O_2$ , organische Peroxide oder Hydroperoxide, wie z. B. *tert*-Butylhydroperoxid, Luft oder Sauerstoff ( $O_2$ ) verwendet. Auf teure Elektronendonatoren, wie z. B. NADH oder NADPH kann bei dem vorliegenden Verfahren verzichtet werden (Konzentration des Oxidationsmittels: 0,01 bis 20 mmol/L, bevorzugt 0,1 bis 2 mmol/L  $H_2O_2$ ).

**[0015]** Dem Reaktionsgemisch können zur weiteren Beschleunigung der Umsetzung der Verbindung der Formel (I) mit dem Enzym AaP zusätzlich  $H_2O_2$ -generierende Enzyme, insbesondere Oxidasen, wie z. B. Glucose-Oxidase oder Arylalkohol-Oxidase sowie deren Substrate (Glucose bzw. Arylalkohole) zugesetzt werden.

**[0016]** Zur Erhöhung der Selektivität der Dealkylierung kann erfindungsgemäß Ascorbinsäure oder ein anderer Radikalfänger (radical scavenger, 0,1–20 mM) dem Reaktionsansatz zugesetzt werden.

**[0017]** Die Grundlage des erfindungsgemäßen enzymatischen, zellfreien Verfahrens ist eine neuartige extrazelluläre Haloperoxidase-Peroxygenase (= aromatische Peroxygenase), die über P450-ähnliche Katalyseeigenschaften verfügt und in Gegenwart eines geeigneten Oxidationsmittels (z. B. Peroxiden),

insbesondere in gepufferten wässrigen Lösungen, aromatische Alkylarylether, z. B. 1,4-Dimethoxybenzol, 1,4-Diethoxybenzol, 4-Nitroanisol, 2-Phenoxyethanol, 4-Nitrophenoxy-1-dodekansäure, 4-Methylanisol, 4-Nitrophenoxy-1-ethanol und 4-Nitrophenoxy-1-essigsäure, zu den entsprechenden hydroxylierten Aromaten O-dealkyliert und dabei mit Zusatz eines Radikalfängers (radical scavenger; z. B. Ascorbinsäure) eine hohe Selektivität erreicht wird (> 95%).

**[0018]** Bei dem eingesetzten Enzym handelt es sich um ein spezielles extrazelluläres Häm-Thiolat-Protein mit Peroxidase-, Peroxygenase- und Etherase-Funktion. Es wird von Basidiomyceten der Familien Bolbitiaceae (z. B. *Agrocybe* spp.) und Coprinaceae (z. B. *Coprinus* spp.) gebildet und zeichnet sich durch besondere katalytische Eigenschaften aus, die es von bisher beschriebenen Peroxidasen und Monooxygenasen deutlich unterscheidet. Die Enzymherstellung erfolgt vorzugsweise in Flüssigkultur, in Bioreaktoren und stickstoffreichen Medien (Ulrich, R., 2005, Dissertation, IHI Zittau; Kluge, M., 2006, Diplomarbeit, IHI Zittau).

**[0019]** Die von dem als AaP bezeichneten Enzym katalysierten Reaktionen benötigen im Unterschied zu chemischen Synthesen keine hochkonzentrierten aggressiven und umweltgefährdenden Reagenzien (< 1%  $H_2O_2$ ) und bei der Produktgewinnung kann auf chemikalien- und zeitintensive Reinigungsschritte zur Trennung der Isomerengemische verzichtet werden. Üblicherweise wird das Enzym in einer Konzentration von 0,01 U/mL bis 20 U/mL AaP, insbesondere von 0,09 bis 5 U/mL AaP, eingesetzt. Dies macht das dargestellte Reaktionsverfahren besonders umweltfreundlich.

**[0020]** Ein weiterer Vorteil gegenüber rein chemischen Synthesen besteht in der Prozessführung auf Grund der erfindungsgemäßen AaP-katalysierten Umsetzung bei Raumtemperatur und normalem Luftdruck. In einer bevorzugten Ausführungsform wird das Verfahren in wässrigen, gepufferten Lösungen durchgeführt. Dem Reaktionsgemisch können hierbei zur Stabilisierung der Reaktion im wässrigen Medium Puffer auf Basis organischer Säuren, vorzugsweise Zitronensäure, sowie Phosphate, vorzugsweise Kaliumhydrogenphosphate, zugesetzt werden (Pufferkonzentration: 5 mmol/L bis 500 mmol/L, vorzugsweise 20 bis 100 mmol/L). Weiterhin ist es möglich, die Reaktion im pH-Staten ohne Puffer unter kontinuierlicher Zusdosierung von Säuren oder Basen durchzuführen.

**[0021]** Zur Verbesserung der Löslichkeit können dem Reaktionsgemisch organische Lösungsmittel zugesetzt werden und dabei auch in einem 2-Phasensystem gearbeitet werden. Erfindungsgemäß einsetzbare Lösungsmittel sind protische Lösungsmittel, wie Methanol oder Ethanol oder aprotische polare

DE 10 2007 058 741 A1 2009.06.04

Lösungsmittel wie Ether (z. B. Diisopropylether), Aceton, Acetonitril, DMSO (Dimethylsulfoxid) sowie DMF (N,N-Dimethylformamid).

**[0022]** Als Ausgangsverbindungen der Formel (I) werden insbesondere Verbindungen aus der folgenden Gruppe eingesetzt: Alkylarylether, para-substituierte Alkylarylether (R = -X, -NO<sub>2</sub>, -Alkyl, -Phenyl, -NH<sub>2</sub>, -OH). Die Reaktion wird in einem Bereich von 5°C bis 40°C, vorzugsweise bei 20–30°C und bei pH-Werten von 3 bis 10, vorzugsweise 5 bis 8, durchgeführt. Die Reaktionszeiten liegen üblicherweise im Bereich von 0,5 bis 120 Minuten, insbesondere im Bereich von 5 bis 30 Minuten. Die erzielten Ausbeuten an Dealkylierungs-Produkten variieren zwischen 10% und 99%, vorzugsweise zwischen 20 und 90%.

**[0023]** Die Vorteile der AaP-katalysierten Umsetzung von Alkylarylether gegenüber der Katalyse mit anderen Enzymen, die Alkylarylethern spalten, liegen:

- a) in seiner höheren spezifischen Aktivität, katalytischen Effizienz und Selektivität
- b) im Einsatz preiswerter Peroxide anstelle teurer Elektronendonatoren [NAD(P)H],
- c) in der Unabhängigkeit des hydroxylierenden Enzyms von Flavin-Reduktasen, Ferredoxin und regulatorischen Proteinen,
- d) in der einfachen Enzymgewinnung ohne Zellaufschluss (extrazelluläres Protein) und
- e) in der hohen Stabilität der extrazellulären AaP und ähnlicher Peroxygenasen im Vergleich zu intrazellulären und z. T. membrangebundenen Cytochromen.
- f) im breiteren Substrat-Spektrum verglichen mit den bekannten Peroxidasen

**[0024]** Mit den AaP-katalysierten Reaktionen ist es erstmals möglich, Alkylarylether mit Hilfe eines einzelnen extrazellulären Biokatalysators, der lediglich ein Peroxid als Cosubstrat benötigt, in einem einstufigen Prozess zu den entsprechenden Hydroxyaromaten (= Phenole; z. B. 4-Methoxy-/Ethoxyphenol) umzusetzen. Das Verfahren kann in verschiedensten Bereichen der Synthesechemie eingesetzt werden, u. a. zur Herstellung von Wirkstoffen, Pharmaka-Intermediaten, speziellen Katalysatoren und Oxidationsmitteln sowie zur Entfernung von Schutzgruppen instabiler Moleküle. Die Erfindung soll nachstehend anhand von dem in der Zeichnung dargestellten Ausführungsbeispiel näher erläutert werden, wobei die Erfindung nicht auf die genannten Beispiele beschränkt ist.

#### Beispiele

**[0025]** Es zeigen:

**[0026]** Abb. 1: Allgemeines Formelschema der AaP-katalysierten Umsetzung von Alkylarylethern

**[0027]** Abb. 2: Formelschema gemäß Ausführungsbeispiel

**[0028]** Abb. 3: HPLC-Elutionsprofil (280 nm) der Umsetzung von 1,4-Diethoxybenzol durch AaP

#### Ausführungsbeispiel:

**[0029]** 500 µM 1,4-Dimethoxybenzol wurden in wässriger Kaliumphosphat-Pufferlösung (50 mM, pH = 7.0) gelöst und zusammen mit 4 mM Ascorbinsäure, 1 mM H<sub>2</sub>O<sub>2</sub> und 1 U Agrocycbe-aegerita-Peroxidase (Units bezogen auf die Oxidation von Veratrylalkohol zu Veratrylaldehyd; Ullrich et al. 2004, Appl. Environ. Microbiol.: 70, 4575-81) in einem Gesamtvolumen von 1 ml bei 24 °C in einem verschlossenen Glasgefäß gerührt. Die Reaktionszeit betrug insgesamt 30 min. Als einziges Produkt dieser Reaktion (Ausbeute 45%) wurde 4-Methoxyphenol anhand eines authentischen Standards (Sigma) über die Retentionszeit sowie UV-Spektrum detektiert. Die chromatographische Trennung und Produkt-Identifizierung erfolgte unter Verwendung einer speziellen HPLC-Säule (Phenomex synergi 4 µm Fusion-RP 80A, 150 × 2 mm) und eines HPLC-DAD Systems der Firma AGILENT.



DE 10 2007 058 741 A1 2009.06.04

**ZITATE ENHALTEN IN DER BESCHREIBUNG**

*Diese Liste der vom Anmelder aufgeführten Dokumente wurde automatisiert erzeugt und ist ausschließlich zur besseren Information des Lesers aufgenommen. Die Liste ist nicht Bestandteil der deutschen Patent- bzw. Gebrauchsmusteranmeldung. Das DPMA übernimmt keinerlei Haftung für etwaige Fehler oder Auslassungen.*

**Zitierte Patentliteratur**

- US 7253324 [0005]
- US 4695659 [0006]

**Zitierte Nicht-Patentliteratur**

- Huhn, P, 2006: Naturstoffchemie. S. Hirzel Verlag Stuttgart; Volhardt, KPC, Schore, NE, 2000: Organische Chemie. Wiley-VCH Verlag Weinheim [0002]
- Walter, W, Francke, W, 2004: Beyer Walter Lehrbuch der organischen Chemie. S. Hirzel Verlag Stuttgart [0002]
- Wuts, PGM 2007: Greene's protective groups in organic synthesis. 4. Ed, John Wiley & Sons; Kocienski, PJ 2005: Protecting Groups. 3. Ed. Thieme [0003]
- Perosa, A, Selva, M, Tundo, P, Zordan F 2000: Alkyl methyl carbonates as very efficient methylating agents. The O-methylation of Phenols. Synlett, 1, 272-274 [0003]
- HI, HBr; Meltzer, RI, Lustgarten, DM, Fischman, A 1957: Thyroxine Analogs. J Org Chem 22: 1577-1581 [0004]
- Boovannahalli, SK, Kim, DW, Chioder, DY 2004: Application of ionic liquid halide nucleophilicity for the cleavage of ethers. A Green Protocol for the Regeneration of Phenols from Ethers. J Org Chem 69: 3340-3344 [0004]
- Ranu, C, Bhar, S 1996: Dealkylation of Ethers. A review. Org Prep Proc Int 28: 371-411; Claydon, J, Greeves, N, Warren, S, Wothers, P et.al. 2006: Organic Chemistry. Oxford University Press [0004]
- Weissmau SA, Zewge, D 2005: Recent advances in ether dealkylation. Tetrahedron 61: 7833-7863; Mejeed, M. 2007: Process for the synthesis of biologically active oxygenated compounds by dealkylation of the corresponding alkyl ethers [0005]
- Andersson, S-G B. (Malmo, SE), 1986: Method for dealkylation of alkyl-aryl ethers [0006]
- Meunier, G, Meunier, B 1985: Evidences for an efficient demethylation of methoxy ellipticine catalyzed by a peroxidase. J Am Chem Soc 107: 2558-2560 [0007]
- Ross, D, Larsson, R, Norbeck, K, Ryhage, R, Moldéus, P 1985: Characterization and mechanism of formation of reactive products formed du-

- ring peroxidase-catalyzed Oxidation of p-phenetidine. Trapping of reactive species by reduced glutathione and butylated hydroxyanisole. Mol Pharmacol 27: 277-286 [0007]
- Haim, N, Nemeč, J, Roman, J, Sinha, BK 1987: Peroxidase-catalyzed metabolism of etoposide (VP-16-213) and covalent binding of reactive intermediates to cellular macromolecules. Cancer Res 47: 5835-5840 [0007]
- Enoki, A, Goldsby, GP, Gold, MH 1981:  $\beta$ -Ether cleavage of the lignin model compound 4-ethoxy-3-methoxyphenylglycerol- $\beta$ -guaiacyl ether and derivatives by Phanerochaete chrysosporium. Arch Microbiol 129: 141-145 [0008]
- Boersma, MG, Primus, J-L, Koerts, J, Veeger, C, Rietjens, IMCM 2000: Heme-(hydro)peroxide mediated O- and N-dealkylation. A study with microperoxidase. Eur J Biochem 267: 6673-6678 [0009]
- Hofrichter, M, Ullrich, R 2006: Heme-thiolate haloperoxidases: versatile biocatalysts with biological and environmental significance. Appl Microbiol Biotechnol 71: 276-288 [0010]
- Miller, VP, Tschirret-Guth, RA, Ortiz de Montellano, PR 1995: Chloroperoxidase-catalyzed benzylic hydroxylation. Arch Biochem Biophys 319: 330-340 [0010]
- Urano, Y, Higuchi, T, Hirobe, M, 1996: Substrate-dependent changes of the oxidative O-dealkylation mechanism of several chemical and biological oxidizing systems. J. Chem. Soc.; White, GF, Russell, NJ, and Tidswell, EC, 1996: Bacterial scission of ether bonds. Microbiol. [0010]
- Bernhardt, FH, Ruf, HH and Ehrig, H, 1974: A 4-methoxybenzoate monooxygenase system from Pseudomonas putida. Circular dichroism studies on the iron-sulfur protei. FERS Letters, 43(1): 53-55 [0010]
- Kim, YH, Engesser, KH, 2004: Degradation of alkyl ethers, aralkyl ethers, and dibenzyl ether by Rhodococcus sp. strain DEE5151, isolated from diethyl ether-containing enrichment cultures. Appl Environ Microbiol, 70(7): 4398-401 [0010]
- Ullrich, R., 2005, Dissertation, IHI Zittau; Kluge, M., 2006, Diplomarbeit, IHI Zittau [0018]
- Ullrich et al. 2004, Appl. Environ. Microbiol.: 70, 4575-81 [0029]

DE 10 2007 058 741 A1 2009.06.04

**Patentansprüche**

1. Verfahren zur enzymatischen O-Dealkylierung von Alkylarylethern der Formel (I) zu entsprechenden hydroxylierten Aromaten (Phenole) der Formel (II), durch Umsetzung von Alkylarylethern der Formel (I) mit einer pilzlichen aromatischen Haloperoxidase-Peroxygenase [Agrocybe-aegerita-Peroxidase = AaP] in Gegenwart mindestens eines Oxidationsmittels in einem Einstufen-Reaktionsverfahren.

2. Verfahren nach Anspruch 1, dadurch gekennzeichnet, dass als Alkylarylether 1,4-Dimethoxybenzol eingesetzt wird.

3. Verfahren nach Anspruch 1, dadurch gekennzeichnet, dass als Alkylarylether 1,4-Diethoxybenzol eingesetzt wird.

4. Verfahren nach Anspruch 1, dadurch gekennzeichnet, dass als Alkylarylether 4-Nitroanisol eingesetzt wird.

5. Verfahren nach Anspruch 1, 2, 3 und/oder 4, dadurch gekennzeichnet, dass als Haloperoxidase-Peroxygenase die Enzyme aus *Agrocybe aegerita*, *Agrocybe chaxingu*, *Coprinus radians* oder *Coprinus verticillatus* verwendet werden.

6. Verfahren nach Anspruch 1, 2, 3 und/oder 3, dadurch gekennzeichnet, dass als Haloperoxidase-Peroxygenase die Enzyme aus Vertretern der Familien *Bolbitiaceae*, *Coprinaceae* und *Tricholomataceae* verwendet werden.

7. Verfahren nach mindestens einem der vorhergehenden Ansprüche, dadurch gekennzeichnet, dass als Oxidationsmittel Wasserstoffperoxid, organische Peroxide oder Hydroperoxide, Luft oder Sauerstoff eingesetzt werden.

8. Verfahren nach mindestens einem der vorhergehenden Ansprüche, dadurch gekennzeichnet, dass das Oxidationsmittel in katalytischen Mengen, vorzugsweise in Mengen von < 0,01% bezogen auf die Konzentration der Verbindung der Formel (I) eingesetzt wird.

9. Verfahren nach mindestens einem der vorhergehenden Ansprüche, dadurch gekennzeichnet, dass dem Reaktionsgemisch zur weiteren Beschleunigung der Umsetzung der Verbindung der Formel (I) mit dem Enzym AaP weitere Enzyme, die H<sub>2</sub>O<sub>2</sub> generieren, zugesetzt werden.

10. Verfahren nach mindestens einem der vorgenannten Ansprüche, dadurch gekennzeichnet, dass dem Reaktionsmedium zur Stabilisierung der Reaktion im wässrigen Medium Puffer auf Basis organischer Säuren und/oder Phosphate zugesetzt werden.

den.

11. Verfahren nach mindestens einem der vorhergehenden Ansprüche, dadurch gekennzeichnet, dass die Reaktion in einem Temperaturbereich zwischen 10°C bis 40°C durchgeführt wird.

12. Verfahren nach mindestens einem der vorgenannten Ansprüche, dadurch gekennzeichnet, dass zur Verbesserung der Substrat-Löslichkeit organische Lösungsmittel zugesetzt werden können.

13. Verfahren nach mindestens einem der vorgenannten Ansprüche, dadurch gekennzeichnet, dass zur Erhöhung von Selektivität und Produktausbeute Ascorbinsäure oder andere Radikalfänger zugesetzt werden.

Es folgen 2 Blatt Zeichnungen

DE 10 2007 058 741 A1 2009.06.04

## Anhängende Zeichnungen

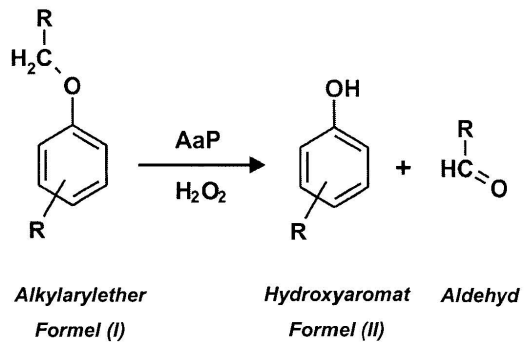


**Abb. 1** Allgemeines Formelschema der AaP-katalysierten Umsetzung von Alkylarylethern zu den entsprechenden hydroxylierten Aromaten (Phenole) und Alkylaldehyden (z. B. Acetaldehyd)

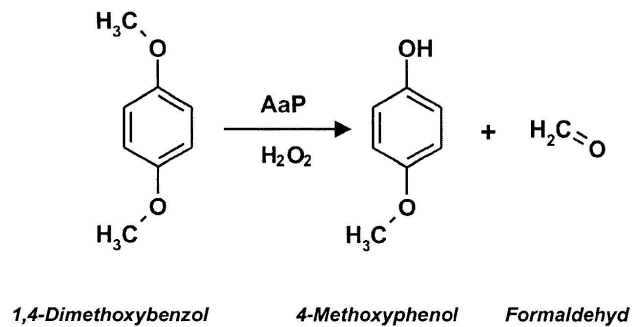


**Abb. 2** Formelschema gemäß Ausführungsbeispiel

DE 10 2007 058 741 A1 2009.06.04

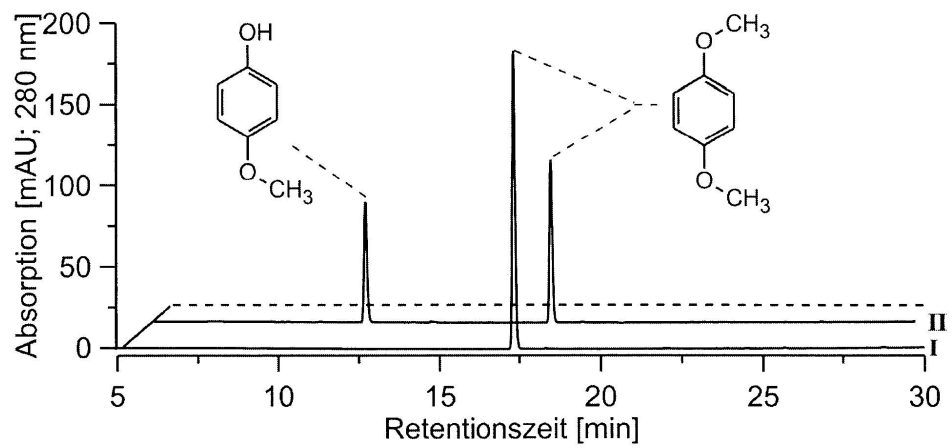


Abb. 3 HPLC-Elutionsprofil (280 nm) der Umsetzung von 1,4-Dimethoxybenzol (I = Standard) durch AaP zu 4-Methoxyphenol (II)



(19) Bundesrepublik Deutschland  
Deutsches Patent- und Markenamt

(10) DE 10 2008 034 829 A1 2010.02.04

(12)

## Offenlegungsschrift

(21) Aktenzeichen: 10 2008 034 829.5  
(22) Anmeldetag: 23.07.2008  
(43) Offenlegungstag: 04.02.2010

(51) Int Cl.<sup>8</sup>: **C07C 59/52** (2006.01)  
C07C 57/30 (2006.01)  
C07C 51/367 (2006.01)  
C07C 41/26 (2006.01)  
C07C 39/08 (2006.01)  
C07C 37/60 (2006.01)

(71) Anmelder:  
JenaBios GmbH, 07749 Jena, DE

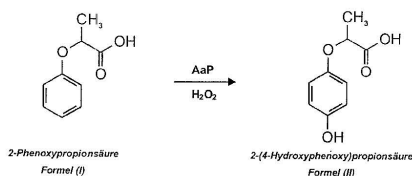
(74) Vertreter:  
Sonnefeld, Teichmann, Rechtsanwälte, 07743  
Jena

(72) Erfinder:  
Kinne, Matthias, 02827 Görlitz, DE; Ullrich, Rene,  
Dr.rer.nat., 02763 Zittau, DE; Hofrichter, Martin,  
Prof.Dr.rer.nat.habil., 02763 Zittau, DE; Scheibner,  
Katrin, Prof.Dr.rer.nat., 07745 Jena, DE

Die folgenden Angaben sind den vom Anmelder eingereichten Unterlagen entnommen

(54) Bezeichnung: Verfahren zur Herstellung von 2-(4-Hydroxyphenoxy)propionsäure

(57) Zusammenfassung: Die Erfindung betrifft ein Verfahren zur enzymatischen, Hydroxylierung von 2-Phenoxypropionsäure (Formel I) zu 2-(4-Hydroxyphenoxy)propionsäure (Formel II) durch die Umsetzung von 2-Phenoxypropionsäure (Formel I) mit einer pilzlichen Peroxygenase (z. B. Agrocybe-aegerita-Peroxidase, AaP) in Gegenwart mindestens eines Oxidationsmittels (z. B. Wasserstoffperoxid) in einem Einstufen-Reaktionsverfahren. Die Reaktion verläuft erfindungsgemäß regioselektiv und enantioselektiv, so dass am Ende Reinheiten der Positionsisomere von mehr als 98% mit einem Enantiomerenüberschuss an (R)-2-(4-Hydroxyphenoxy)propionsäure von ee > 60% und Ausbeuten zwischen 20 und 90% erreicht werden. Das Verfahren kann in den verschiedenen Bereichen der Synthesechemie eingesetzt werden.



DE 10 2008 034 829 A1 2010.02.04

**Beschreibung**

**[0001]** Die Erfindung betrifft ein einstufiges, enzymatisches Verfahren zur regioselektiven Hydroxylierung von 2-Phenoxypropionsäure zu 2-(4-Hydroxyphenoxy)propionsäure in einem einstufigen Verfahren.

**[0002]** 2-(4-Hydroxyphenoxy)propionsäure ist ein häufig eingesetztes Zwischenprodukt bei der Herstellung enantiomerenreiner Herbizide. Chemische Verfahren zur Herstellung von racemischen, sowie von enantiomerenreinen Formen von 2-(4-Hydroxyphenoxy)propionsäure sind bekannt. Der Nachteil dieser, auf der Umsetzung von Hydrochinon basierenden Verfahren besteht in der aufwendigen Abtrennung unerwünschter Nebenprodukte. Eine wirtschaftliche Produktion dieser Verbindungen ist deshalb nicht möglich (Cooper, B; Ladner, W; Hauer, B; Siegel, H 1992: Process for fermentative production of 2-(4-Hydroxyphenoxy)propionic acid; European Patent EP 0465494). Mikroorganismen sind in der Lage, verschiedene aromatische Verbindungen zu hydroxylieren. Dabei entstehen überwiegend bishydroxylierte Verbindungen oder Gemische verschiedener Regioisomere (Byrde, R, J, W; Woodcook, D 1957: Fungal detoxication. 2. The metabolism of some phenoxy-n-alkylcarboxylic acids by *Aspergillus niger*, Biochem. J., 65, 682). Die regioselektive mikrobielle in-vivo Monohydroxylierung von 2-Phenoxypropionsäure zu 2-(4-Hydroxyphenoxy)propionsäure durch den insektenpathogenen Schimmelpilz *Beauveria bassiana* ist in einer Arbeit beschrieben worden (Dingler, C; Ladner, W; Krei, G, A; Cooper, B und Hauer, B 1996: Preparation of (R)-2-(4-Hydroxyphenoxy)propionic acid by Biotransformation; Pestic. Sci., 46, 33–35). Auf dieser Grundlage werden in Deutschland derzeit etwa 1.000 Tonnen (R)-2-(4-Hydroxyphenoxy)propionsäure pro Jahr durch die Firma BASF mittels Ganzzell-Biotransformation hergestellt (Positionspapier der Dechema e. V. 2004: Weiße Biotechnologie: Chancen für Deutschland). Das dafür benötigte Substrat (R)-2-Phenoxypropionsäure wird aus den umweltrelevanten Chemikalien (S)-2-Chlorpropionsäureisobutylester und Phenol synthetisiert (Liese, A; Seelbach, K; Wandrey, C 2006: Industrial Biotransformation; Wiley-VCH-Verlag, Weinheim).

**[0003]** Intrazelluläre Monooxygenasen vom P450- und Rieske-Typ sind in der Lage, Sauerstoff in Substratmoleküle einzuführen (Bernhardt, R 2004: Cytochrome P450: Versatile Enzymsysteme mit Anwendung in der Biotechnologie und Medizin, Magazin Forschung 1; Ullrich, R & Hofrichter M 2007: Enzymatic hydroxylation of aromatic compounds. Cellular and Molecular Life Sciences 64: 271–293). Der derzeitige Einsatz von Monooxygenasen in industriellen Prozessen bleibt jedoch wiederum auf Ganzzell-Biotransformationen beschränkt (Urlacher, V, B; Lutz-Wahl, S; Schmid., R, D 2004: Microbial P450 en-

zymes in biotechnology, Applied Microbiology and Biotechnology, 64, 3, 317–325), da eine Langzeitstabilität der Enzyme nicht gegeben ist und teure Cofaktoren (NADH) eingesetzt werden müssen (Eiben, S; Kaysser, L; Maurer, S; Kühnel, K; Urlacher, V, B; Schmid, R, D; 2006: Preparative use of isolated CYP102 monooxygenases-A critical appraisal, Journal of Biotechnology, 124, 662–669).

**[0004]** Die enantioselektive und regioselektive Monohydroxylierung von 2-Phenoxypropionsäure zu 2-(4-Hydroxyphenoxy)propionsäure durch isolierte Biokatalysatoren (in vitro) ist bisher nicht beschrieben worden. Es wurde jedoch kürzlich gefunden, dass ein stabiles extrazelluläres Pilzenzym, die *Agroclybe-aegerita*-Peroxygenase (AaP), 2-Phenoxypropionsäure hoch regioselektiv zu 2-(4-Hydroxyphenoxy)propionsäure und bevorzugt zu dessen (R)-Enantiomer umzusetzen vermag.

**[0005]** Gegenstand der vorliegenden Erfindung ist ein Verfahren zur enzymatischen Herstellung von 2-(4-Hydroxyphenoxy)propionsäure, das dadurch gekennzeichnet ist, dass man 2-Phenoxypropionsäure oder deren Salze in Gegenwart äquimolarer Konzentrationen an  $H_2O_2$  und dem isolierten extrazellulären Peroxygenase-Biokatalysator hydroxyliert. Die Aufgabe der vorliegenden Erfindung ist es, einen Prozess zur Hydroxylierung von 2-Phenoxypropionsäure zu 2-(4-Hydroxyphenoxy)propionsäure mit möglichst geringem verfahrenstechnischen und apparativen Aufwand und bei gleichzeitigem Einsatz kostengünstiger Cosubstrate durchzuführen. Die Umsetzung der Ausgangsverbindungen soll in kurzen Inkubationszeiten, bei Raumtemperatur und -druck, im wässrigen Milieu sowie ohne erhöhte Anforderungen an sterile bzw. semisterile Reaktionsbedingungen in einem einstufigen Verfahren erfolgen. Die Reaktionsprodukte sind dabei mit möglichst geringem Aufwand zu isolieren, und eine aufwändige Abtrennung weiterer Reaktionsprodukte soll entfallen.

**[0006]** Das vorliegende Verfahren löst diese Aufgabe und betrifft ein Methode zur enzymatischen, Hydroxylierung von 2-Phenoxypropionsäure (Formel I) zu 2-(4-Hydroxyphenoxy)propionsäure (Formel II) durch Umsetzung von 2-Phenoxypropionsäure (Formel I) mit einer pilzlichen Peroxygenase in Gegenwart mindestens einen Oxidationsmittels in einem Einstufen-Reaktionsverfahren.

**[0007]** Die Ausgangsverbindungen der Formel (I) werden dabei vorzugsweise mit der Peroxygenase des Lamellenpilzes *Agroclybe aegerita* (*Agroclybe-aegerita*-Peroxygenase = AaP; Synonyme: *Agroclybe-aegerita*-Peroxidase, Haloperoxidase-Peroxygenase), die eine besonders hohe Peroxygenase-Aktivität besitzt, und zumindest einem Oxidationsmittel zur Reaktion gebracht, wobei die Hydroxylierung von

DE 10 2008 034 829 A1 2010.02.04

2-Phenoxypropionsäure erfolgt.

**[0008]** Als Oxidationsmittel werden erfindungsgemäß vorzugsweise  $H_2O_2$ , organische Peroxide oder Hydroperoxide, wie z. B. tert-Butylhydroperoxid, Luft oder Sauerstoff ( $O_2$ ) verwendet. Auf teure Elektronendonatoren, wie z. B. NADH oder NADPH kann bei dem vorliegenden Verfahren verzichtet werden (Konzentration des Oxidationsmittels: 0,01 bis 20 mmol/L, bevorzugt 0,1 bis 2 mmol/L  $H_2O_2$ ).

**[0009]** Dem Reaktionsgemisch können zur weiteren Beschleunigung der Umsetzung der Verbindung der Formel (I) mit dem Enzym AaP zusätzlich  $H_2O_2$ -generierende Enzyme, insbesondere Oxidasen, wie z. B. Glucose-Oxidase oder Arylalkohol-Oxidase sowie deren Substrate (Glucose bzw. Arylalkohole) zugesetzt werden.

**[0010]** Zur Erhöhung der Regioselektivität der Hydroxylierung kann erfindungsgemäß Ascorbinsäure oder ein anderer Radikalfänger (0,1–20 mM) dem Reaktionsansatz zugesetzt werden.

**[0011]** Die Grundlage des erfindungsgemäßen enzymatischen, zellfreien Verfahrens ist eine spezielle extrazelluläre Peroxygenase, die über P450-ähnliche Katalyseeigenschaften verfügt und in Gegenwart eines geeigneten Oxidationsmittels (z. B. Peroxiden), insbesondere in gepufferten wässrigen Lösungen, 2-Phenoxypropionsäure zur 2-(4-Hydroxyphenoxy)propionsäure hydroxyliert und dabei mit Zusatz eines Radikalfängers (radical scavenger; z. B. Ascorbinsäure) eine hohe Stereo-(ee > 60%) und Regioselektivität (> 98%) erreicht.

**[0012]** Bei dem eingesetzten Enzym handelt es sich um ein Häm-Thiolat-Protein mit Peroxidase- und Peroxygenase-Funktionen. Es wird von Basidiomyceten der Familien Bolbitiaceae (z. B. *Agrocybe* spp.) Agaricaceae, (z. B. *Coprinus coprinellus* oder *Coprinus coprinopsis*) sowie Psatyrellaceae gebildet und zeichnet sich durch besondere katalytische Eigenschaften aus, die es von bisher beschriebenen Peroxidasen und Monoxygenasen deutlich unterscheidet. Die Enzymherstellung erfolgt vorzugsweise in Flüssigkultur, in Bioreaktoren und stickstoffreichen Medien (Ullrich, R 2005: Dissertation, IHI Zittau; Kluge, M 2006: Diplomarbeit, IHI Zittau).

**[0013]** Die von dem als AaP bezeichneten Enzym katalysierten Reaktionen benötigen im Unterschied zu chemischen Synthesen keine hochkonzentrierten aggressiven und umweltgefährdenden Reagenzien (< 1%  $H_2O_2$ ) und bei der Produktgewinnung kann auf chemikalien- und zeitintensive Reinigungsschritte zur Trennung der Isomerengemische verzichtet werden. Üblicherweise wird das Enzym in einer Konzentration von 0,01 U/mL bis 20 U/mL AaP, insbesondere von 0,09 bis 5 U/mL AaP, eingesetzt (1 Unit setzt 1  $\mu$ mol

Substrat pro Minute um). Dies macht das dargestellte Reaktionsverfahren besonders umweltfreundlich.

**[0014]** Ein weiterer Vorteil gegenüber rein chemischen Synthesen besteht in der Prozessführung auf Grund der erfindungsgemäßen AaP-katalysierten Umsetzung bei Raumtemperatur und normalem Luftdruck. In einer bevorzugten Ausführungsform wird das Verfahren in wässrigen, gepufferten Lösungen durchgeführt. Dem Reaktionsgemisch können hierbei zur Stabilisierung der Reaktion im wässrigen Medium Puffer auf Basis organischer Säuren, vorzugsweise Zitronensäure, sowie Phosphate, vorzugsweise Kaliumhydrogenphosphate, zugesetzt werden (Pufferkonzentration: 5 mmol/L bis 500 mmol/L, vorzugsweise 20 bis 100 mmol/L). Weiterhin ist es möglich, die Reaktion im pH-Staten ohne Puffer unter kontinuierlicher Zudosierung von Säuren oder Basen durchzuführen.

**[0015]** Zur Verbesserung der Löslichkeit können dem Reaktionsgemisch organische Lösungsmittel zugesetzt und in einem 2-Phasensystem gearbeitet werden. Erfindungsgemäß einsetzbare Lösungsmittel sind protische Lösungsmittel, wie Methanol oder Ethanol oder aprotische polare Lösungsmittel wie Ether (z. B. Diisopropylether), Aceton, Acetonitril, DMSO (Dimethylsulfoxid) sowie DMF (N,N-Dimethylformamid).

**[0016]** Die Reaktion wird in einem Bereich von 5°C bis 40°C, vorzugsweise bei 20–30°C und bei pH-Werten von 3 bis 10, vorzugsweise 5 bis 8, durchgeführt. Die Reaktionszeiten liegen üblicherweise im Bereich von 0,5 bis 120 Minuten, insbesondere im Bereich von 5 bis 30 Minuten. Die erzielten Ausbeuten an 2-(4-Hydroxyphenoxy)propionsäuren variieren zwischen 10% und 99%, vorzugsweise zwischen 20% und 90%.

**[0017]** Die Vorteile der AaP-katalysierten Hydroxylierung von 2-Phenoxypropionsäure gegenüber der Biotransformation und anderen Enzymen die zur selektiven Hydroxylierung befähigt sind, liegen:

- a) in einer höheren spezifischen Aktivität, katalytischen Effizienz und Selektivität,
- b) im Einsatz preiswerter Peroxide als Cosubstrate anstelle teurer Elektronendonatoren (NADH, NADPH),
- c) in der Unabhängigkeit des hydroxylierenden Enzyms von Flavin-Reduktasen, Ferredoxin und regulatorischen Proteinen,
- d) in der einfachen Enzymgewinnung ohne Zellaufschluss (extrazelluläres Protein) und
- e) in der hohen Stabilität der extrazellulären AaP und ähnlicher Peroxygenasen im Vergleich zu intrazellulären, löslichen oder membrangebundenen Oxygenasen.

**[0018]** Mit den AaP-katalysierten Reaktionen ist es

DE 10 2008 034 829 A1 2010.02.04

erstmalig möglich, 2-Phenoxypropionsäure mit Hilfe eines einzelnen extrazellulären Biokatalysators, der lediglich Peroxide als Cosubstrat benötigt, in einem einstufigen Prozess zur entsprechenden 2-(4-Hydroxyphenoxy)propionsäure umzusetzen. Das Verfahren kann in verschiedensten Bereichen der Synthesechemie eingesetzt werden. Die Erfindung soll nachstehend anhand von dem in der Zeichnung dargestellten Ausführungsbeispiel näher erläutert werden, wobei die Erfindung allerdings nicht auf die genannten Beispiele beschränkt ist.

## Beispiele

[0019] Es zeigen:

[0020] Abb. 1: Formelschema der Peroxygenase katalysierten Umsetzung von 2-Phenoxypropionsäure

[0021] Abb. 2: HPLC-Elutionsprofil (aufgenommen bei einer Wellenlänge von 220 nm) der Umsetzung von 2-Phenoxypropionsäure durch die *Agrocybe-aegerita*-Peroxygenase (AaP)

[0022] Abb. 3: HPLC-Elutionsprofil (bei 270 nm) der enantioselektiven Umsetzung von 2-Phenoxypropionsäure durch die AaP (chirale Trennung);

## Ausführungsbeispiele:

[0023] 500 µM 2-Phenoxypropionsäure wurden in wässriger Kaliumphosphat-Pufferlösung (50 mM, pH = 7.0) gelöst und zusammen mit 4 mM Ascorbinsäure, 1 mM H<sub>2</sub>O<sub>2</sub> und 1 U *Agrocybe-aegerita*-Peroxygenase (Units bezogen auf die Oxidation von Veratrylalkohol zu Veratrylaldehyd; Ullrich et al. 2004: Novel haloperoxidase from the agaric basidiomycete *Agrocybe aegerita* oxidizes aryl alcohols and aldehydes, Appl. Environ. Microbiol., 70, 4575–81) in einem Gesamtvolumen von 1 ml bei 23°C in einem verschlossenen Glasgefäß gerührt. Die Reaktionszeit betrug insgesamt 30 Sekunden. Als einziges Produkt dieser Reaktion wurde 2-(4-Hydroxyphenoxy)propionsäure anhand eines authentischen Standards (Sigma) über die Retentionszeit sowie UV-Spektrum detektiert. Die chromatographische Trennung und Produkt-Identifizierung erfolgte unter Verwendung einer speziellen HPLC-Säule (Phenomex synerg 4 µm Fusion-RP 80A, 150 × 2 mm,) und eines HPLC-DAD Systems der Firma AGILENT. Die chirale Trennung erfolgte mit Hilfe einer Säulenkombination (Agilent Zorbax SB-C18 Rapid Resolution Cartridge 30 × 2.1 mm 3,5 µm; ORpak CDBS-453 150 × 4,6 mm).



DE 10 2008 034 829 A1 2010.02.04

**ZITATE ENTHALTEN IN DER BESCHREIBUNG**

*Diese Liste der vom Anmelder aufgeführten Dokumente wurde automatisiert erzeugt und ist ausschließlich zur besseren Information des Lesers aufgenommen. Die Liste ist nicht Bestandteil der deutschen Patent- bzw. Gebrauchsmusteranmeldung. Das DPMA übernimmt keinerlei Haftung für etwaige Fehler oder Auslassungen.*

**Zitierte Patentliteratur**

- EP 0465494 [0002]

**Zitierte Nicht-Patentliteratur**

- Cooper, B; Ladner, W; Hauer, B; Siegel, H 1992: Process for fermentative production of 2-(4-Hydroxyphenoxy)propionic acid [0002]
- Byrde, R, J, W; Woodcook, D 1957: Fungal detoxication. 2. The metabolism of some phenoxy-n-alkylcarboxylic acids by *Aspergillus niger*, Biochem. J., 65, 682 [0002]
- Dingler, C; Ladner, W; Krei, G, A; Cooper, B und Hauer, B 1996: Preparation of (R)-2-(4-Hydroxyphenoxy)propionic acid by Biotransformation; Pestic. Sci., 46, 33–35 [0002]
- Positionspapier der Dechema e. V. 2004: Weiße Biotechnologie: Chancen für Deutschland [0002]
- Liese, A; Seelbach, K; Wandrey, C 2006: Industrial Biotransformation; Wiley-VCH-Verlag, Weinheim [0002]
- Bernhardt, R 2004: Cytochrome P450: Versatile Enzymsysteme mit Anwendung in der Biotechnologie und Medizin, Magazin Forschung 1 [0003]
- Ullrich, R & Hofrichter M 2007: Enzymatic hydroxylation of aromatic compounds. Cellular and Molecular Life Sciences 64: 271–293 [0003]
- Urlacher, V, B; Lutz-Wahl, S; Schmid., R, D 2004: Microbial P450 enzymes in biotechnology, Applied Microbiology and Biotechnology, 64, 3, 317–325 [0003]
- Eiben, S; Kaysser, L; Maurer, S; Kühnel, K; Urlacher, V, B; Schmid, R, D; 2006: Preparative use of isolated CYP102 monooxygenases-A critical appraisal, Journal of Biotechnology, 124, 662–669 [0003]
- Ullrich, R 2005: Dissertation, IHI Zittau [0012]
- Kluge, M 2006: Diplomarbeit, IHI Zittau [0012]
- Ullrich et al. 2004: Novel haloperoxidase from the agaric basidiomycete *Agrocybe aegerita* oxidizes aryl alcohols and aldehydes, Appl. Environ. Microbiol., 70, 4575–81 [0023]

DE 10 2008 034 829 A1 2010.02.04

**Patentansprüche**

1. Verfahren zur enzymatischen Hydroxylierung von 2-Phenoxypropionsäure (Formel I) zur 2-(4-Hydroxyphenoxy)propionsäure (Formel II), durch Umsetzung von 2-Phenoxypropionsäure (Formel I) mit einer pilzlichen Peroxygenase in Gegenwart mindestens eines Oxidationsmittels in einem Einstufen-Reaktionsverfahren.

2. Verfahren nach Anspruch 1 dadurch gekennzeichnet, dass als Peroxygenase die Enzyme aus *Agrocybe aegerita*, *Agrocybe chaxingu*, *Coprinus coprinellus* oder *Coprinus coprinopsis* verwendet werden (Synonyme: *Agrocybe-aegerita*-Peroxygenase, *Agrocybe-aegerita*-Peroxidase, AaP, Haloperoxidase-Peroxygenase).

3. Verfahren nach Anspruch 1 dadurch gekennzeichnet, dass als Peroxygenase die Enzyme aus Vertretern der Familien *Bolbitiaceae*, *Agaricaceae*, *Psatyrellaceae* und *Tricholomataceae* verwendet werden.

4. Verfahren nach mindestens einem der vorhergehenden Ansprüche, dadurch gekennzeichnet, dass als Oxidationsmittel Wasserstoffperoxid, organische Peroxide oder Hydroperoxide, Luft oder Sauerstoff eingesetzt werden.

5. Verfahren nach mindestens einem der vorhergehenden Ansprüche, dadurch gekennzeichnet, dass das Oxidationsmittel in äquimolarer Menge bezogen auf die Konzentration der Verbindung der Formel (I) eingesetzt wird.

6. Verfahren nach mindestens einem der vorhergehenden Ansprüche, dadurch gekennzeichnet, dass dem Reaktionsgemisch zur weiteren Beschleunigung der Umsetzung der Verbindung der Formel (I) mit dem Enzym AaP weitere Enzyme, die  $H_2O_2$  generieren, zugesetzt werden.

7. Verfahren nach mindestens einem der vorgenannten Ansprüche, dadurch gekennzeichnet, dass dem Reaktionsmedium zur Stabilisierung der Reaktion im wässrigen Medium Puffer auf Basis organischer Säuren und/oder Phosphate zugesetzt werden.

8. Verfahren nach mindestens einem der vorhergehenden Ansprüche, dadurch gekennzeichnet, dass die Reaktion in einem Temperaturbereich zwischen 10°C bis 40°C durchgeführt wird.

9. Verfahren nach mindestens einem der vorgenannten Ansprüche, dadurch gekennzeichnet, dass zur Verbesserung der Substrat-Löslichkeit organische Lösungsmittel zugesetzt werden können.

10. Verfahren nach mindestens einem der vorgenannten Ansprüche, dadurch gekennzeichnet, dass zur Erhöhung von Selektivität und Produktausbeute Ascorbinsäure oder andere Radikalfänger zugesetzt werden.

Es folgen 2 Blatt Zeichnungen

DE 10 2008 034 829 A1 2010.02.04

## Anhängende Zeichnungen

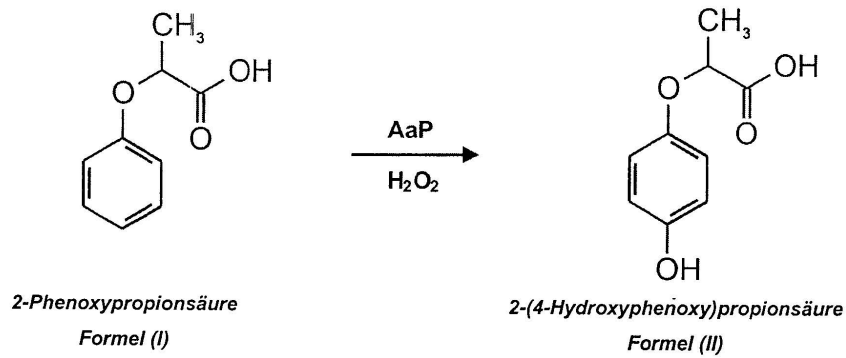


**Abb. 1** Formelschema der AaP-katalysierten Umsetzung von 2-Phenoxypropionsäure (Formel I) zur 2-(4-Hydroxyphenoxy)propionsäure (Formel II)

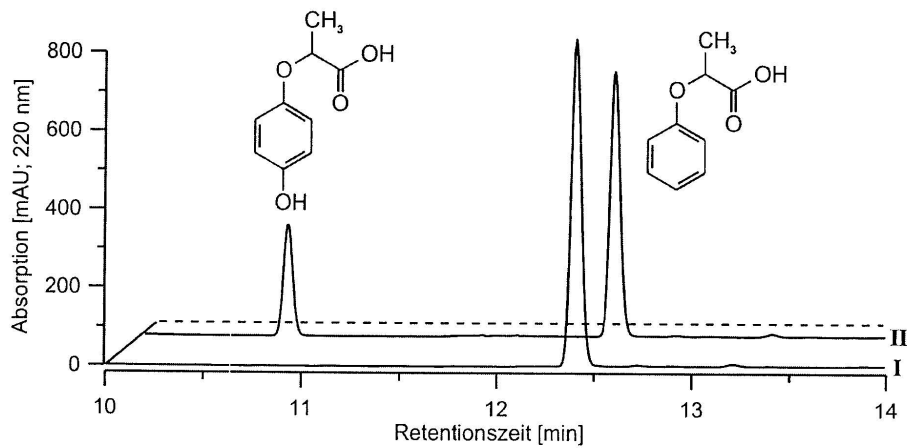


**Abb. 2** HPLC-Elutionsprofil (220 nm) der Umsetzung von 2-Phenoxypropionsäure (Formel I) zur 2-(4-Hydroxyphenoxy)propionsäure (Formel II). I Kontrolle ohne Enzym; II Umsetzung nach Zugabe von AaP.

DE 10 2008 034 829 A1 2010.02.04

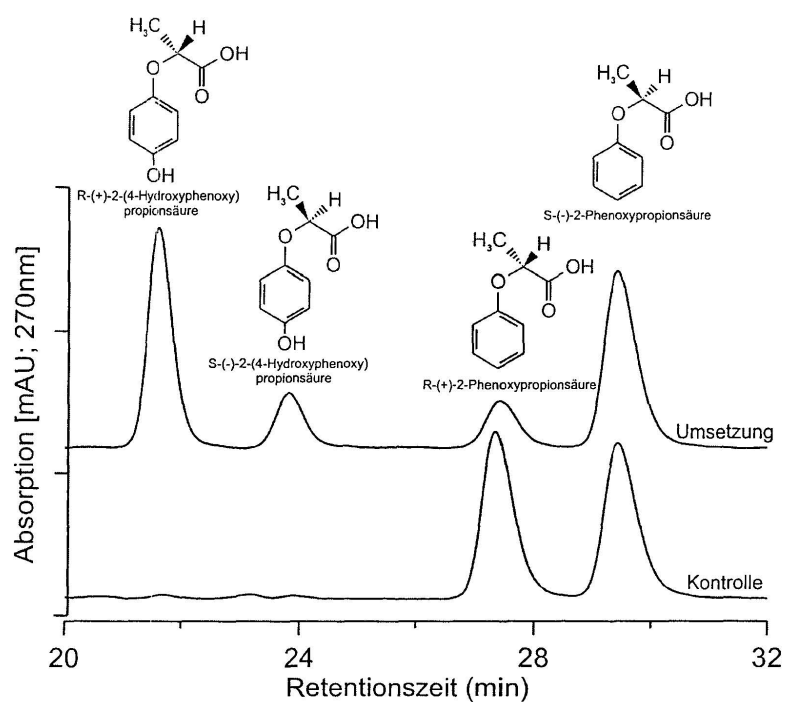


**Abb. 3** HPLC-Elutionsprofil (270 nm) der Umsetzung von racemischer 2-Phenoxypropionsäure (Formel I) zur (*R*)- und (*S*)-2-(4-Hydroxyphenoxy)propionsäure (Formel II). Kontrolle ohne Enzym (unten); Umsetzung nach Zugabe von AaP (oben). Der Enantiomerenüberschuss von (*R*)-2-(4-Hydroxyphenoxy)propionsäure versus (*S*)-2-(4-Hydroxyphenoxy)propionsäure beträgt ca. 60%.



## Regioselective preparation of (*R*)-2-(4-hydroxyphenoxy)propionic acid with a fungal peroxygenase

Matthias Kinne<sup>a,\*</sup>, René Ullrich<sup>a</sup>, Kenneth E. Hammel<sup>b</sup>, Katrin Scheibner<sup>c</sup>, Martin Hofrichter<sup>a</sup>

<sup>a</sup> Unit of Environmental Biotechnology, International Graduate School of Zittau, Markt 23, 02763 Zittau, Germany

<sup>b</sup> USDA Forest Products Laboratory, Madison, WI 53726, USA

<sup>c</sup> University of Applied Sciences Lausitz, 01968 Senftenberg, Germany

### ARTICLE INFO

#### Article history:

Received 30 June 2008

Revised 22 July 2008

Accepted 29 July 2008

Available online 31 July 2008

#### Keywords:

Peroxidase

Peroxygenase

Oxygenase

Cytochrome P450

Hydroxylation

2-(4-Hydroxyphenoxy)propionic acid

Ascorbic acid

### ABSTRACT

The extracellular heme-thiolate peroxygenase of *Agrocybe aegerita* catalyzed the H<sub>2</sub>O<sub>2</sub>-dependent hydroxylation of 2-phenoxypropionic acid (POPA) to give the herbicide precursor 2-(4-hydroxyphenoxy)propionic acid (HPOPA). The reaction proceeded regioselectively with an isomeric purity near 98%, and yielded the desired *R*-isomer of HPOPA with an enantiomeric excess of 60%. <sup>18</sup>O-labeling experiments showed that the phenolic hydroxyl in HPOPA originated from H<sub>2</sub>O<sub>2</sub>, which establishes that the reaction is mechanistically a peroxygenation. Our results raise the possibility that fungal peroxygenases may be useful for a variety of organic oxidations.

© 2008 Elsevier Ltd. All rights reserved.

Selective hydroxylations of aromatic compounds are among the most challenging reactions in synthetic chemistry and have gained steadily increasing attention during recent years because hydroxylated aromatic precursors are used extensively in the chemical industry.<sup>1</sup> For example, (*R*)-2-(4-hydroxyphenoxy)propionic acid [(*R*)-HPOPA] is an intermediate in the synthesis of enantiomerically pure aryloxyphenoxypropionic acid-type herbicides, in which the crop protection activity normally derives from one enantiomer.<sup>2</sup> Although chemical syntheses of (*R*)-HPOPA from hydroquinone and an (*S*)-2-halopropionic acid are available, problems with the removal of byproducts prevent the cost-effective use of this approach.<sup>3,4</sup> Instead, (*R*)-HPOPA is currently prepared from (*R*)-2-phenoxypropionic [(*R*)-POPA] with whole cells of the ascomycete *Beauveria bassiana*, which produces regioselective oxidases that catalyze this hydroxylation.<sup>5,6</sup> The company BASF currently produces about 1000 tons per year of (*R*)-HPOPA in this way.<sup>7–9</sup> The required feedstock, (*R*)-POPA, is synthesized from (*S*)-2-chloropropionic acid isobutylester and phenol.<sup>8</sup>

A similar but simpler approach is to use purified microbial enzymes to hydroxylate POPA in one step. One possibility would be to use intracellular monooxygenases such as cytochrome P450 (cytP450),<sup>10,11</sup> but current applications of these enzymes are restricted to whole-cell biotransformations because cytP450s are not highly stable and their intracellular location makes them hard to produce in quantity.<sup>12,13</sup> Alternatively, modified hemoproteins such as microperoxidases might be used to catalyze aromatic hydroxylations by a cytP450-like oxygen transfer mechanism, but more research is needed to improve the performance of these catalysts.<sup>14–19</sup> We have taken a new approach by using a recently discovered heme-thiolate enzyme from the basidiomycete *Agrocybe aegerita*. This highly stable, secreted *A. aegerita* peroxidase/peroxygenase (AaP) has already been shown to oxidize a wide range of aromatic substrates and appears to be an unusually versatile oxidoreductase for biotechnological applications.<sup>20,21</sup> Here, we show that AaP hydroxylates POPA to HPOPA with complete regioselectivity and significant enantioselectivity.

The major isoform of AaP was produced in a 5-l stirred-tank bioreactor and purified by several steps of fast protein liquid chromatography (FPLC) as described previously.<sup>20,21</sup> The final enzyme preparations had a specific activity of around 60 U mg<sup>-1</sup> with 3,4-dimethoxybenzyl alcohol as the substrate and an RZ ( $A_{418 \text{ nm}}/A_{280 \text{ nm}}$ ) value near 1.7. Chemicals including racemic POPA and

Abbreviations: AaP, *Agrocybe aegerita* peroxygenase; cytP450, cytochrome P450; POPA, 2-phenoxypropionic acid; HPOPA, 2-(4-hydroxyphenoxy)propionic acid.

\* Corresponding author. Tel.: +49 3583 612723; fax: +49 3583 612734.

E-mail address: Kinne@ihi-zittau.de (M. Kinne).

HPOPA,  $^{18}\text{O}$ -labeled  $\text{H}_2\text{O}$ , and ascorbic acid were purchased from Sigma–Aldrich. Separate enantiomers of POPA and HPOPA were purchased from Chemos.  $^{18}\text{O}$ -labeled  $\text{H}_2\text{O}_2$  (2% wt/vol) was obtained from Icon Isotopes.

The reaction mixtures (1 ml) contained various amounts of purified AaP, 50 mM potassium phosphate buffer (pH 3–10), and 0.5–2 mM of the substrate. The reactions were started by the addition of  $\text{H}_2\text{O}_2$  (1 mM) and mixtures were stirred at room temperature. When indicated, ascorbic acid was added to a final concentration of 4 mM. The reactions were stopped with 0.1 ml of 50% wt/vol trichloroacetic acid. Products were identified and quantified against authentic standards.

Products were analyzed using high performance liquid chromatography (HPLC) on a Hewlett Packard HP Series 1100 instrument equipped with an Agilent 1100 Series DAD G1 diode array detector (DAD) and an Agilent LC/MSD VC electrospray ionization mass spectrometer (ESI-MS).

For routine nonenantioselective separations, the instrument was fitted with a Phenomenex Synergi 4u Fusion RP-80A reversed phase column (4.6 by 150 mm, 4  $\mu\text{m}$  particle size). The column was eluted at 40  $^\circ\text{C}$  and 1 ml  $\text{min}^{-1}$  with aqueous phosphoric acid solution (15 mM, pH 3)/acetonitrile, 95:5, for 5 min, followed by a 10-min linear gradient to 100% acetonitrile.

Chiral separations were performed using an Agilent Zorbax SB-C18 Rapid Resolution Cartridge (2.1 by 30 mm, 3.5  $\mu\text{m}$  particle size) connected in series with an Shodex CDBS-453 column (4.6 by 150 mm, 3  $\mu\text{m}$  particle size). The isocratic mobile phase consisted of 10% acetonitrile and 90% aqueous 0.2 mM sodium chloride that contained 1% vol/vol acetic acid. The columns were operated at 10  $^\circ\text{C}$  and 0.5 ml  $\text{min}^{-1}$  for 35 min.

Liquid chromatography/mass spectroscopic (LC/MS) analyses were performed using a reversed phase Phenomenex Gemini 5u C6 Phenyl 110A column (4.6 by 150 mm, 5  $\mu\text{m}$  particle size). The isocratic mobile phase consisted of 5% vol/vol acetonitrile and 95% aqueous 0.1% vol/vol ammonium formate that had been adjusted to pH 10 beforehand with NaOH. The column was operated at 40  $^\circ\text{C}$  and 1 ml  $\text{min}^{-1}$  for 5 min. Electrospray ionization was performed in the negative ionization mode.

To assess POPA hydroxylation, we treated a racemic mixture of POPA with purified AaP and two equivalents of  $\text{H}_2\text{O}_2$  in the presence of ascorbic acid. This last ingredient was included to prevent HPOPA polymerization, an undesirable side reaction attributable to the general peroxidase activity of AaP.<sup>22</sup> The results showed that the reaction proceeded rapidly and regioselectively, giving HPOPA as the sole detectable product (Fig. 1, left; calculated isomeric purity was 98%), and that 27% conversion of the POPA occurred under these conditions (Fig. 1, right). Alternatively, the conversion could

be increased to 43% by retaining the original stoichiometry, but by adding the  $\text{H}_2\text{O}_2$  slowly via a syringe pump (Table 1). We found that the minimum molar ratio of ascorbic acid to HPOPA needed to prevent product polymerization was 3.25 to 1. Further work showed that HPOPA production occurred from pH 3 to 10, with a broad maximum between pH 5 and 8 (data not shown). Control reactions without AaP or with heat-inactivated AaP gave no conversion of POPA.

Chiral HPLC analyses after AaP-catalyzed oxidations of racemic POPA showed that both enantiomers were hydroxylated, but that (*R*)-POPA was clearly the preferred substrate. The resulting HPOPA contained a 60% enantiomeric excess (ee) of the *R*-enantiomer (Fig. 2). When the oxidations were performed on either of the pure POPA enantiomers, the corresponding HPOPA enantiomer was obtained as the sole detectable product in each case (data not shown).

The origin of the phenolic oxygen that results from AaP-catalyzed aromatic hydroxylation has until now remained unclear. To clarify this point, we compared natural abundance  $\text{H}_2\text{O}_2$  with  $\text{H}_2^{18}\text{O}_2$  as the oxidant (oxygen donor) in AaP-catalyzed hydroxylations of POPA to HPOPA. The mass spectra of the products (Fig. 3) show that the principal  $[\text{M}-\text{H}]^-$  ion had an  $m/z$  of 181, as expected for the reaction with natural abundance  $\text{H}_2\text{O}_2$ , but shifted to  $m/z$  183 with almost complete disappearance of the  $m/z$  181 ion when  $\text{H}_2^{18}\text{O}_2$  was used. A similar experiment using  $\text{H}_2^{18}\text{O}$  gave no detectable  $^{18}\text{O}$  incorporation (data not shown), as expected because phenolic oxygens are not readily exchangeable with water under our reaction conditions.<sup>23</sup> An additional experiment with natural abundance  $\text{H}_2\text{O}_2$  in a  $\text{N}_2$ -purged reaction mixture showed that HPOPA production was not inhibited by depletion of  $\text{O}_2$  (data not shown), and therefore molecular oxygen did not contribute significantly as an electron acceptor. These results show that the new phenolic oxygen in HPOPA originated from  $\text{H}_2\text{O}_2$ .

Our results show that AaP hydroxylates POPA regioselectively at the *para*-position to give HPOPA and that the reaction has a per-oxygenative mechanism, that is, the transferred oxygen originates from peroxide and does not come from dioxygen ( $\text{O}_2$ ) or water ( $\text{H}_2\text{O}$ ) as usually occurs in oxygenation reactions. Some intracellular cytp450s perform similar oxidations when given  $\text{H}_2\text{O}_2$  as an

**Table 1**  
Conversion of racemic mixture of POPA (500  $\mu\text{M}$ ) to HPOPA by AaP (1 U  $\text{ml}^{-1}$ , 1.8  $\mu\text{M}$ ) in the presence of ascorbic acid and a final concentration of 1 mM  $\text{H}_2\text{O}_2$

$\text{H}_2\text{O}_2$ -addition	C ( $\mu\text{M}$ ) rac. POPA	C ( $\mu\text{M}$ ) rac. HPOPA	$\Sigma$ ( $\mu\text{M}$ )
Direct	369	134	503
Syringe pump (0.5 $\text{mM h}^{-1}$ )	292	220	512

Reaction products were analyzed as described before.

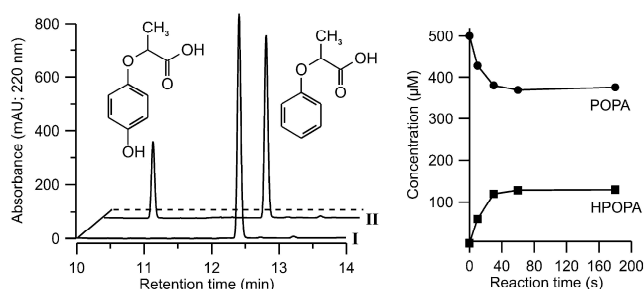


**Figure 1.** HPLC elution profile (left) of products formed by AaP (1 U  $\text{ml}^{-1}$ , 0.5  $\mu\text{M}$ ) during the conversion of POPA (500  $\mu\text{M}$ ) to HPOPA in the presence of ascorbic acid. Control without enzyme (I); complete reaction (II). The reaction was started by addition of  $\text{H}_2\text{O}_2$  (1 mM) at pH 7.0. Time course of AaP-catalyzed hydroxylation of POPA (500  $\mu\text{M}$ ) to HPOPA (right).

5952

M. Kinne et al./Tetrahedron Letters 49 (2008) 5950–5953

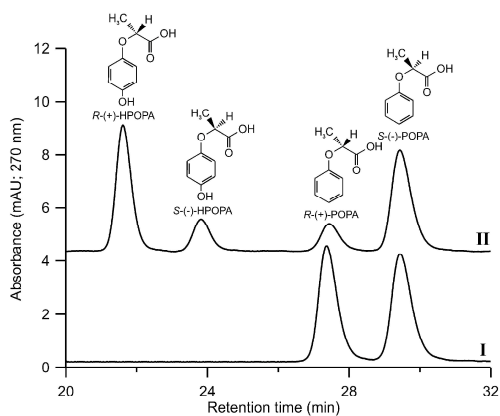


**Figure 2.** HPLC elution profile of products formed by AaP ( $1 \text{ U ml}^{-1}$ ,  $0.5 \text{ }\mu\text{M}$ ) during the conversion of racemic POPA ( $1 \text{ mM}$ ) to HPOPA in the presence of ascorbic acid. Control without enzyme (I); complete reaction (II). The reaction was started by the addition of  $\text{H}_2\text{O}_2$  ( $10 \times 0.1 \text{ mM}$ ) at pH 7.0.

artificial oxidant.<sup>24</sup> This so-called 'shunt' pathway is a remarkable side reaction of a few cytP450s, in the course of which the substrate is directly oxidized by  $\text{H}_2\text{O}_2$  to the hydroperoxy-ferryl state of the heme, requiring neither the stepwise activation of dioxygen nor an electron requirement from NAD(P)H.<sup>1</sup> Since cytP450 and AaP are both heme-thiolate enzymes, the catalytic cycle of AaP probably resembles the cytP450-catalyzed 'peroxidase shunt' pathway. However, AaP appears to be the better choice as a biocatalyst, because it not only performs diverse oxidations,<sup>20</sup> but is easier to produce and more stable than currently available cytP450s.

The data also show that AaP exhibits significant enantioselectivity toward POPA, with the industrially more important *R*-enantiomer reacting more rapidly. This property of AaP could be exploited

to improve the yield of *R*-HPOPA from the POPA feedstock currently used, which although enriched in *R*-POPA is not enantiopure.<sup>8,25</sup> Further work is needed to ascertain how AaP recognizes the asymmetric center in POPA, but we surmise that a structural interaction between the enzyme's active site and the carboxylic acid moiety of the substrate may be important. We are currently investigating the possibility that the enantioselectivity of AaP may be useful with other aromatic substrates as well.

#### Acknowledgments

We thank Ulrike Schneider and Monika Brandt for technical assistance and Martin Kluge (Inge), Christiane Liers and Marzena Poraj-Kobielska (Magda) for useful discussions. Financial support by the Konrad Adenauer Foundation is gratefully acknowledged.

#### References and notes

- Ullrich, R.; Hofrichter, M. *Cell Mol. Life Sci.* **2007**, *64*, 271–293.
- Siegel, W.; Sauter, H.; Schaefer, G. U.S. Patent 5,801,272, 1998.
- Cleugh, E. S. U.S. Patent 7,268,249, 2007.
- Cooper, B.; Ladner, W.; Hauer, B.; Siegel, H. European Patent EP0465494, 1992.
- Dingler, C.; Ladner, W.; Krei, G. A.; Cooper, B. S.; Hauer, B. *Pestic. Sci.* **1996**, *46*, 33–53.
- Ladner, W.; Staudenmaier, H. R.; Hauer, B.; Müller, U.; Pressler, U.; Meyer, J.; Siegel, H. U.S. Patent 5,928,912, 1999.
- Schmid, A.; Hollmann, F.; Park, J. B.; Buhler, B. *Curr. Opin. Biotechnol.* **2002**, *13*, 359–366.
- Liese, A.; Seelbach, K.; Wandrey, C. *Industrial Biotransformations*; Wiley-VCH Verlag GmbH & Co KGaA: Weinheim, 2006.
- van Beilen, J. B.; Duetz, W. A.; Schmid, A.; Witholt, B. *Trends Biotechnol.* **2003**, *21*, 170–177.
- Urlacher, V. B.; Eiben, S. *Trends Biotechnol.* **2006**, *24*, 324–330.
- van Beilen, J. B.; Duetz, W. A.; Schmid, A.; Witholt, B. *Trends Biotechnol.* **2003**, *21*, 170–177.
- Urlacher, V. B.; Lutz-Wahl, S.; Schmid, R. D. *Appl. Microb. Biotechnol.* **2004**, *64*, 317–325.
- Eiben, S.; Kaysser, L.; Maurer, S.; Kuhnel, K.; Urlacher, V. B.; Schmid, R. D. *J. Biotechnol.* **2006**, *124*, 662–669.
- Osman, A. M.; Koerts, J.; Boersma, M. G.; Boeren, S.; Veeger, C.; Rietjens, I. M. *Eur. J. Biochem.* **1996**, *240*, 232–238.
- Veeger, C. *J. Inorg. Biochem.* **2002**, *91*, 35–45.
- Caputi, L.; Di Tullio, A.; Di Leandro, L.; De Angelis, F.; Malatesta, F. *Biochim. Biophys. Acta* **2005**, *1725*, 71–80.

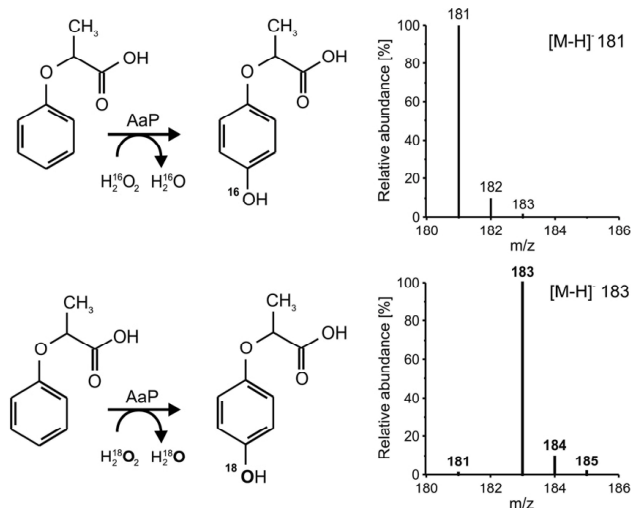


**Figure 3.** Mass spectra showing molecular ions of HPOPA obtained from the oxidation of POPA with AaP ( $2 \text{ U ml}^{-1}$ ,  $0.9 \text{ }\mu\text{M}$ ) in the presence of natural abundance  $\text{H}_2\text{O}_2$  (top) or  $\text{H}_2^{18}\text{O}_2$  (bottom). Ascorbic acid was included in the reactions.

## APPENDIX

### Author's personal copy

M. Kinne et al./Tetrahedron Letters 49 (2008) 5950–5953

5953

17. Prieto, T.; Marcon, R. O.; Prado, F. M.; Caires, A. C.; Di Mascio, P.; Brochsztain, S.; Nascimento, O. R.; Nantes, I. L. *Phys. Chem. Chem. Phys.* **2006**, *8*, 1963–1973.
18. Dorovska-Taran, V.; Posthumus, M. A.; Boeren, S.; Boersma, M. G.; Teunis, C. J.; Rietjens, I. M.; Veeger, C. *Eur. J. Biochem.* **1998**, *253*, 659–668.
19. Dallacosta, C.; Monzani, E.; Casella, L. *J. Biol. Inorg. Chem.* **2003**, *8*, 770–776.
20. Ullrich, R.; Nuske, J.; Scheibner, K.; Spantzel, J.; Hofrichter, M. *Appl. Environ. Microbiol.* **2004**, *70*, 4575–4581.
21. Ullrich, R.; Hofrichter, M. *FEBS Lett.* **2005**, *579*, 6247–6250.
22. Hofrichter, M.; Ullrich, R. *Appl. Microbiol. Biotechnol.* **2006**, *71*, 276–288.
23. Koizumi, M.; Titani, T. *Bull. Chem. Soc. Jpn.* **1938**, *13*, 607.
24. Joe, H.; Lin, Z.; Arnold, F. H. *Nature* **1999**, *399*, 670–673.
25. Schmid, R. D.; Urlacher, V. B. *Modern Biooxidation Enzymes*; Wiley-VCH Verlag GmbH & Co KGaA: Weinheim, 2007.





Contents lists available at ScienceDirect

Bioorganic &amp; Medicinal Chemistry Letters

journal homepage: [www.elsevier.com/locate/bmcl](http://www.elsevier.com/locate/bmcl)

## Regioselective preparation of 5-hydroxypropranolol and 4'-hydroxydiclofenac with a fungal peroxygenase

Matthias Kinne<sup>a,\*</sup>, Marzena Poraj-Kobielska<sup>a</sup>, Elisabet Aranda<sup>a</sup>, René Ullrich<sup>a</sup>, Kenneth E. Hammel<sup>b</sup>, Katrin Scheibner<sup>c</sup>, Martin Hofrichter<sup>a</sup>

<sup>a</sup> Unit of Environmental Biotechnology, International Graduate School of Zittau, Markt 23, 02763 Zittau, Germany

<sup>b</sup> USDA Forest Products Laboratory, Madison, WI 53726, USA

<sup>c</sup> University of Applied Sciences Lausitz, 01968 Senftenberg, Germany

### ARTICLE INFO

#### Article history:

Received 30 January 2009  
Revised 1 April 2009  
Accepted 2 April 2009  
Available online 9 April 2009

#### Keywords:

Peroxidase  
Peroxygenase  
Oxygenase  
Cytochrome P450  
Hydroxylation  
5-Hydroxypropranolol  
Propranolol  
4'-Hydroxydiclofenac  
Diclofenac  
Ascorbic acid

### ABSTRACT

An extracellular peroxygenase of *Agrocybe aegerita* catalyzed the H<sub>2</sub>O<sub>2</sub>-dependent hydroxylation of the multi-function beta-adrenergic blocker propranolol (1-naphthalen-1-yloxy-3-(propan-2-ylamino)propan-2-ol) and the non-steroidal anti-inflammatory drug diclofenac (2-[2-[(2,6-dichlorophenyl)amino]phenyl]acetic acid) to give the human drug metabolites 5-hydroxypropranolol (5-OHP) and 4'-hydroxydiclofenac (4'-OHD). The reactions proceeded regioselectively with high isomeric purity and gave the desired 5-OHP and 4'-OHD in yields up to 20% and 65%, respectively. <sup>18</sup>O-labeling experiments showed that the phenolic hydroxyl groups in 5-OHP and 4'-OHD originated from H<sub>2</sub>O<sub>2</sub>, which establishes that the reaction is mechanistically a peroxygenation. Our results raise the possibility that fungal peroxygenases may be useful for versatile, cost-effective, and scalable syntheses of drug metabolites.

© 2009 Elsevier Ltd. All rights reserved.

Selective hydroxylations of aromatic compounds are among the most challenging reactions in synthetic chemistry and have gained steadily increasing attention during the last decade because hydroxylated aromatics are important precursors and products in the pharmaceutical industry.<sup>1</sup> For example, 5-hydroxypropranolol (5-OHP), a human metabolite of the beta blocker propranolol (1-naphthalen-1-yloxy-3-(propan-2-ylamino)propan-2-ol), is of pharmacological interest as it is frequently used in metabolic studies and has been demonstrated to be equipotent to propranolol as a  $\beta$ -receptor antagonist.<sup>2</sup> Another important human drug metabolite is 4'-hydroxydiclofenac (4'-OHD), a major metabolite of the anti-inflammatory drug diclofenac (2-[2-[(2,6-dichlorophenyl)amino]phenyl]acetic acid) in humans.<sup>3</sup>

Although a four-step chemical synthesis of 5-OHP from 1,5-naphthalenediol is available, a low overall yield (<5%)<sup>4</sup> and problems with the removal of byproducts have prevented the

cost-effective use of this approach. The chemical synthesis of 4'-OHD has likewise proved difficult.<sup>3</sup> A simpler approach would be to use an enzyme to hydroxylate these drugs in one step. One possibility would be the use of monooxygenases such as cytochrome P450s (cytP450s). This approach has been shown to work for 4'-OHD synthesis,<sup>3,5,6</sup> but is currently restricted to whole-cell biotransformations because cytP450s are poorly stable and catalytically slow. Moreover, their intracellular location makes them difficult to produce in quantity.<sup>7,8</sup> Another approach, the use of laboratory-evolved, engineered cytP450s for H<sub>2</sub>O<sub>2</sub>-dependent hydroxylation of propranolol to 5-OHP via the so-called 'peroxide shunt', has been demonstrated but needs further optimization.<sup>9</sup>

We used a recently discovered heme-thiolate enzyme from the basidiomycete *Agrocybe aegerita* to hydroxylate propranolol and diclofenac. This stable, secreted peroxygenase (AaP) oxidizes a wide range of aromatic substrates and appears to be a versatile oxidoreductase for biotechnological applications.<sup>10–15</sup> We treated each of the compounds (0.5 mM) with purified AaP (0.4  $\mu$ M) and four equivalents of H<sub>2</sub>O<sub>2</sub> (2 mM) in the presence of ascorbic acid (4 mM). The last ingredient was added to prevent polymerization

**Abbreviations:** AaP, *Agrocybe aegerita* peroxygenase; cytP450, cytochrome P450; 4'-OHD, 4'-hydroxydiclofenac; 5-OHD, 5-hydroxydiclofenac; 4-OHP, 4-hydroxypropranolol; 5-OHP, 5-hydroxypropranolol.

\* Corresponding author. Tel.: +49 3583 612723; fax: +49 3583 612734.

E-mail address: [kinne@ihi-zittau.de](mailto:kinne@ihi-zittau.de) (M. Kinne).

0960-894X/\$ - see front matter © 2009 Elsevier Ltd. All rights reserved.  
doi:10.1016/j.bmcl.2009.04.015

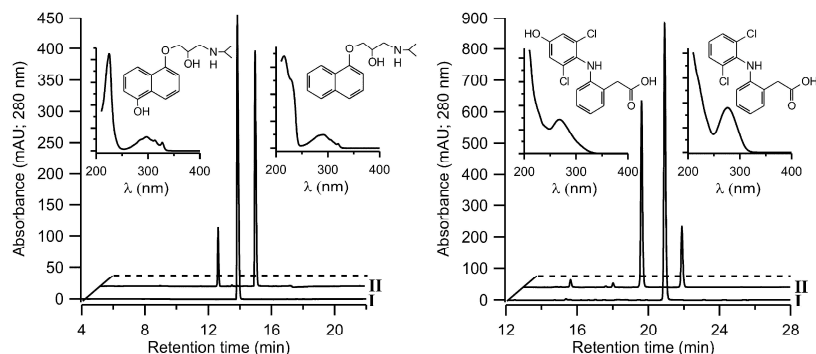


**Figure 1.** HPLC elution profiles showing products formed by AaP ( $2 \text{ U ml}^{-1}$ ,  $0.4 \mu\text{M}$ ) after conversion of propranolol ( $500 \mu\text{M}$ , left) and diclofenac ( $500 \mu\text{M}$ , right) in the presence of ascorbic acid ( $4 \text{ mM}$ ). Controls without enzyme (I). Complete reactions (II). The reactions (pH 7) were started by addition of  $\text{H}_2\text{O}_2$  ( $2 \text{ mM}$ ). Insets show UV/visible absorption spectra of the reactant (right) and major product (left) in each chromatogram.<sup>18</sup>

of 5-OHP or 4'-OHD, an undesirable side reaction attributable to the general peroxidase activity of AaP.<sup>16</sup> The mixtures were stirred at room temperature for 3 min and stopped with  $0.1 \text{ ml}$  of  $50\% \text{ wt/vol}$  trichloroacetic acid, after which products were identified and quantified against authentic standards by HPLC.<sup>17</sup>

The reactions proceeded rapidly and regioselectively, converting about 20% of racemic propranolol to 5-OHP and about 65% of diclofenac to 4'-OHD (Figs. 1 and 2). For propranolol oxidation, the formation of byproducts previously reported for the cytP450-catalyzed reaction<sup>9</sup> was insignificant: 4-hydroxypropranolol and 1-naphthol occurred only in trace quantities, and *N*-desisopropylpropranolol was not found. The enantiomeric excess of *S*-5-OHP during AaP-catalyzed hydroxylation of propranolol was less than 2% (data not shown), that is, the reaction was not enantioselective. For diclofenac oxidation, the human drug metabolite 5-OHD<sup>3</sup> was not formed, but traces of several other unidentified byproducts were detected. Control reactions without AaP or with heat-inactivated enzyme gave no conversion of propranolol or diclofenac.

The failure of the reactions to proceed to completion was probably not a consequence of enzyme inactivation, because reac-

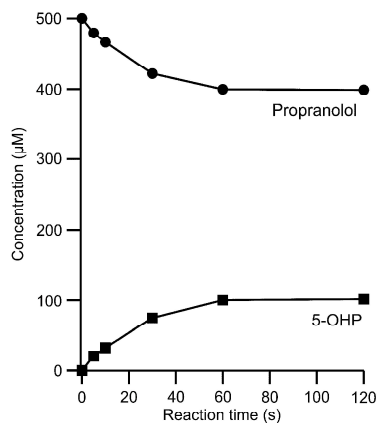


**Figure 2.** Time course of AaP-catalyzed 5-hydroxylation of propranolol (reaction conditions are the same as in Figure 1, standard deviation  $<5\%$ ).

tions conducted with more AaP did not give significantly higher yields (data not shown). It appears more likely that the phenolic products 5-OHP and 4'-OHD prevented further oxidation of the parent compounds because they also are AaP substrates. Under our reaction conditions, these phenols probably consumed some of the  $\text{H}_2\text{O}_2$  by undergoing continuous, competitive AaP-catalyzed oxidation to the 5-OHP and 4'-OHD phenoxy radicals, which in turn were continuously re-reduced to 5-OHP and 4'-OHD by the excess ascorbate we included. This conclusion is supported by our observation that propranolol was rapidly polymerized when the reactions were conducted in the absence of ascorbate (data not shown).

When we conducted the AaP-catalyzed oxidation of propranolol with  $\text{H}_2^{18}\text{O}_2$  in place of  $\text{H}_2\text{O}_2$ , mass spectral analysis<sup>18</sup> of the resulting 5-OHP (Fig. 3) showed that the principal  $[\text{M}-\text{H}]^-$  ion had shifted from the natural abundance  $m/z$  of 274 to  $m/z$  276 for propranolol. Similarly, the analogous experiment with diclofenac showed that the principal ion of 4'-OHD shifted from an  $m/z$  of 310 to an  $m/z$  of 312 (data not shown). Experiments using  $\text{H}_2^{18}\text{O}$  gave no detectable  $^{18}\text{O}$  incorporation (data not shown), as expected because phenolic oxygens are not readily exchangeable with water under our reaction conditions.<sup>19</sup> An additional experiment with natural abundance  $\text{H}_2\text{O}_2$  in an  $\text{N}_2$ -purged reaction mixture showed that propranolol production was not inhibited by depletion of  $\text{O}_2$  (data not shown), and therefore  $\text{O}_2$  did not contribute significantly as an electron acceptor. These results show that the new phenolic oxygens in 5-OHP and 4'-OHD originated from  $\text{H}_2\text{O}_2$ .

Since cytP450s and AaP are both heme-thiolate enzymes, the catalytic cycle of AaP probably resembles the 'peroxide shunt' that is responsible for the hydroxylation of propranolol by some engineered cytP450s.<sup>9</sup> However, AaP appears to be the better choice as a biocatalyst because it is easier to produce, is more efficient, is more stable to  $\text{H}_2\text{O}_2$ , and in the case of propranolol exhibits higher regioselectivity (Table 1). On the other hand, although AaP regioselectively hydroxylates other precursors as well,<sup>14</sup> it has some limitations. For example, we have observed that, although AaP efficiently hydroxylates *N*-phenylacetamide to acetaminophen (yields up to 80%, unpublished results), it very poorly adds the second 3-hydroxyl needed to produce the human drug metabolite 3-hydroxyacetaminophen. We are currently exploring the possibility that AaP may catalyze useful one-step monooxygenations of other pharmaceutically relevant aromatics.

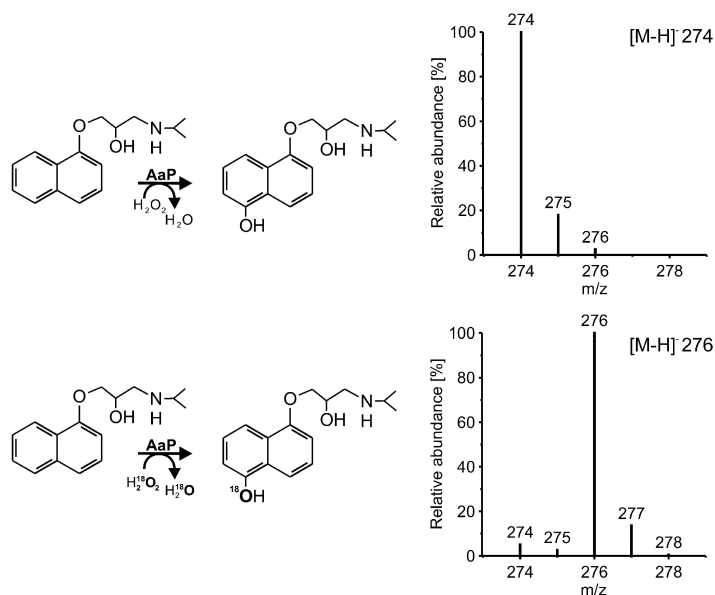


**Figure 3.** Mass spectra showing molecular ions of 5-OHP obtained from the oxidation of propranolol with AaP ( $1 \text{ U ml}^{-1}$ ,  $0.2 \text{ }\mu\text{M}$ ) in the presence of natural abundance  $\text{H}_2\text{O}_2$  (top) or  $\text{H}_2^{18}\text{O}_2$  (bottom).<sup>19</sup>

**Table 1**  
Conversion of propranolol (5 mM) to 5-OHP by AaP and cytP450.<sup>c</sup>

Enzyme in reaction ( $\mu\text{M}$ )	Conversion of propranolol to 5-OHP (%)	Reaction time (min)	Products formed
AaP <sup>a</sup> (0.6)	13.6	2	1
CytP450 <sup>b</sup> (5.0)	0.5	180	4

<sup>a</sup>  $\text{H}_2\text{O}_2$  concentration was 5 mM.

<sup>b</sup>  $\text{H}_2\text{O}_2$  concentration was 1 mM. Data are for mutant D6H10 in Ref. 9.

<sup>c</sup> Conversion of diclofenac to 4'-OHD under these reaction conditions was 30%.

### Acknowledgments

We thank Ulrike Schneider and Monika Brandt for technical assistance, and Martin Kluge (Inge) and Christiane Liers for useful discussions. This work was supported by the Konrad Adenauer Foundation (M.K.), the Fulbright Foundation (K.E.H.) and the Deutsche Bundesstiftung Umwelt (M.H. and K.S., Project Number 13225–32).

### References and notes

- Ullrich, R.; Hofrichter, M. *Cell. Mol. Life. Sci.* **2007**, *64*, 271.
- Greenslade, F. C.; Newquist, K. L. *Arch. Int. Pharmacodyn. Ther.* **1978**, *233*, 270.
- Webster, R.; Pacey, M.; Winchester, T.; Johnson, P.; Jezequel, S. *Appl. Microbiol. Biotechnol.* **1998**, *49*, 371.
- Oatis, J. E., Jr.; Russell, M. P.; Knapp, D. R.; Walle, T. J. *Med. Chem.* **1981**, *24*, 309.
- Vail, R. B.; Homann, M. J.; Hanna, I.; Zaks, A. *J. Ind. Microbiol. Biotechnol.* **2005**, *32*, 67.

- Rushmore, T. H.; Reider, P. J.; Slaughter, D.; Assang, C.; Shou, M. *Metab. Eng.* **2000**, *2*, 115.
- Urlacher, V. B.; Lutz-Wahl, S.; Schmid, R. D. *Appl. Microb. Biotechnol.* **2004**, *64*, 317.
- Eiben, S.; Kaysser, L.; Maurer, S.; Kuhnel, K.; Urlacher, V. B.; Schmid, R. D. *J. Biotechnol.* **2006**, *124*, 662.
- Otey, C. R.; Bandara, G.; Lalonde, J.; Takahashi, K.; Arnold, F. H. *Biotechnol. Bioeng.* **2006**, *93*, 494.
- Ullrich, R.; Nuske, J.; Scheibner, K.; Spantzel, J.; Hofrichter, M. *Appl. Environ. Microbiol.* **2004**, *70*, 4575.
- Ullrich, R.; Hofrichter, M. *FEBS Lett.* **2005**, *579*, 6247.
- Aranda, E.; Kinne, M.; Kluge, M.; Ullrich, R.; Hofrichter, M. *Appl. Microbiol. Biotechnol.* **2009**, *82*, 1057.
- Kluge, M.; Ullrich, R.; Dolge, C.; Scheibner, K.; Hofrichter, M. *Appl. Microbiol. Biotechnol.* **2009**, *81*, 1071.
- Kinne, M.; Ullrich, R.; Hammel, K. E.; Scheibner, K.; Hofrichter, M. *Tetrahedron Lett.* **2008**, *49*, 5950.
- Ullrich, R.; Dolge, C.; Kluge, M.; Hofrichter, M. *FEBS Lett.* **2008**, *582*, 4100.
- Hofrichter, M.; Ullrich, R. *Appl. Microbiol. Biotechnol.* **2006**, *71*, 276.
- HPLC was done on a Phenomenex Synergi Fusion RP-80A reverse phase column (4.6 by 150 mm, 4  $\mu\text{m}$  particle size). The column was eluted at  $40^\circ\text{C}$  and a flow rate of  $1 \text{ ml min}^{-1}$  with a mixture of aqueous phosphoric acid solution (15 mM, pH 3) and acetonitrile, 95:5, for 5 min, followed by a 25-min linear gradient to 100% acetonitrile. Elution times of propranolol, 5-OHP, 4-OHP, 1-naphthol, *N*-desisopropylpropranolol, diclofenac, 5-OHD and 4'-OHD were checked against authentic standards.
- Liquid chromatography/mass spectroscopic (LC/MS) analyses were performed using a reversed phase Synergi Gemini C6-Phenyl 110A column (4.6 by 150 mm, 5  $\mu\text{m}$  particle size). The isocratic mobile phase consisted of 5% vol/vol acetonitrile and 95% aqueous 0.1% vol/vol ammonium formate that had been adjusted to pH 10 beforehand with NaOH. The column was operated at  $40^\circ\text{C}$  and  $1 \text{ ml min}^{-1}$  for 5 min. Electrospray ionization was performed in the negative ionization mode.
- Koizumi, M.; Titani, T. *Bull. Chem. Soc. Jpn.* **1938**, *13*, 607.

## Oxidative Cleavage of Diverse Ethers by an Extracellular Fungal Peroxygenase\*

Received for publication, July 9, 2009, and in revised form, August 19, 2009. Published, JBC Papers in Press, August 27, 2009, DOI 10.1074/jbc.M109.040857

Matthias Kinne<sup>†1</sup>, Marzena Poraj-Kobielska<sup>‡</sup>, Sally A. Ralph<sup>§</sup>, René Ullrich<sup>‡</sup>, Martin Hofrichter<sup>‡</sup>, and Kenneth E. Hammel<sup>§¶1,2</sup>

From the <sup>†</sup>Unit of Environmental Biotechnology, International Graduate School of Zittau, 02763 Zittau, Germany, the <sup>‡</sup>United States Department of Agriculture Forest Products Laboratory, Madison, Wisconsin 53726, and the <sup>§</sup>Department of Bacteriology, University of Wisconsin, Madison, Wisconsin 53706

Many litter-decay fungi secrete heme-thiolate peroxxygenases that oxidize various organic chemicals, but little is known about the role or mechanism of these enzymes. We found that the extracellular peroxxygenase of *Agrocybe aegerita* catalyzed the H<sub>2</sub>O<sub>2</sub>-dependent cleavage of environmentally significant ethers, including methyl *t*-butyl ether, tetrahydrofuran, and 1,4-dioxane. Experiments with tetrahydrofuran showed the reaction was a two-electron oxidation that generated one aldehyde group and one alcohol group, yielding the ring-opened product 4-hydroxybutanal. Investigations with several model substrates provided information about the route for ether cleavage: (a) steady-state kinetics results with methyl 3,4-dimethoxybenzyl ether, which was oxidized to 3,4-dimethoxybenzaldehyde, gave parallel double reciprocal plots suggestive of a ping-pong mechanism ( $K_{m(\text{peroxide})}$  1.99 ± 0.25 mM;  $K_{m(\text{ether})}$  1.43 ± 0.23 mM;  $k_{\text{cat}}$  720 ± 87 s<sup>-1</sup>), (b) the cleavage of methyl 4-nitrobenzyl ether in the presence of H<sub>2</sub><sup>18</sup>O<sub>2</sub> resulted in incorporation of <sup>18</sup>O into the carbonyl group of the resulting 4-nitrobenzaldehyde, and (c) the demethylation of 1-methoxy-4-trideuteromethoxybenzene showed an observed intramolecular deuterium isotope effect [( $k_{\text{H}}/k_{\text{D}}$ )<sub>obs</sub>] of 11.9 ± 0.4. These results suggest a hydrogen abstraction and oxygen rebound mechanism that oxidizes ethers to hemiacetals, which subsequently hydrolyze. The peroxxygenase appeared to lack activity on macromolecular ethers, but otherwise exhibited a broad substrate range. It may accordingly have a role in the biodegradation of natural and anthropogenic low molecular weight ethers in soils and plant litter.

Recently, a new group of extracellular peroxxygenases was described in agaric fungi that are ubiquitous biodegraders of lignocellulose in soils and plant litter. These heme-thiolate enzymes catalyze H<sub>2</sub>O<sub>2</sub>-dependent halogenations and hydroxylations of numerous aromatic substrates, and thus show some functional similarity to heme chloroperoxidase and to

cytochromes P450 (P450s),<sup>3</sup> which are also heme-thiolate proteins (1–4). However, the best-characterized fungal peroxxygenase, from *Agrocybe aegerita*, exhibits low sequence identity (~25%) with heme chloroperoxidase and no significant sequence identity with the P450s (5). On the other hand, the absorption spectrum of the native peroxxygenase and of its carbon monoxide adduct closely resemble those of P450s (6). So far, little is known about the catalytic cycle of the *A. aegerita* peroxxygenase.

The physiological function of these peroxxygenases is also unclear, but their extracellular location suggests a role in the biodegradation or detoxification of organic chemicals encountered by the fungi. Ethers stand out as potential substrates for several reasons. First, ether linkages are widespread in soils and litter, not only in abundant natural substances such as lignin, flavonoids, and lignans, but also in anthropogenic compounds that include many solvents, biocides, and surfactants (7–11). Second, an oxidative mechanism is required for the biodegradation of ethers, which are relatively recalcitrant because they do not hydrolyze at physiological pH values (7). Finally, it is already known that functionally similar monooxygenases, including P450s, are capable of ether scission and have a role in the intracellular metabolism of these compounds by some organisms (7, 12–15).

Here we show that the extracellular peroxxygenase from *A. aegerita* cleaves many ethers, including some significant environmental pollutants, and we evaluate some limitations on the etherolytic reactions that the enzyme can accomplish. In addition, we report data from stoichiometrical analyses, steady-state kinetics experiments, an H<sub>2</sub><sup>18</sup>O<sub>2</sub>-labeling study, and intramolecular deuterium isotope effect determinations. These results provide insights into the enzymatic mechanism for ether cleavage.

### EXPERIMENTAL PROCEDURES

**Reagents**—Commercially available chemicals were purchased from Sigma-Aldrich, except for H<sub>2</sub><sup>18</sup>O<sub>2</sub> (90 atom %, 2% w/v), which was obtained from Icon Isotopes, and terminally brominated polyethylene glycol (PEG, ~2 kDa), which was purchased from Iris Biotech GmbH. All of the aliphatic ethers used as substrates were the highest grade available, contained no antioxidant, and were received from the manufacturer under

\* This work was supported in part by Deutsche Bundesstiftung Umwelt Project Number 13225-32 (to M. H.), European Union Integrated Project Biorenew (to M. H.), and Grant DE-A102-07ER64480 from the Office of Biological and Environmental Research, United States Dept. of Energy (to K. E. H.).

<sup>1</sup> Supported by the Konrad Adenauer Foundation.

<sup>2</sup> Supported by the German-American Fulbright Commission. To whom correspondence should be addressed: USDA Forest Products Laboratory, 1 Gifford Pinchot Dr., Madison, WI 53726. Tel.: 608-231-9528; Fax: 608-231-9262; E-mail: kehammel@wisc.edu.

<sup>3</sup> The abbreviations used are: P450, cytochrome P450; PEG, polyethylene glycol; GC/MS, gas chromatography/mass spectrometry.

## Ether Cleavage by an Extracellular Peroxygenase

nitrogen in small bottles. A new bottle of each aliphatic ether was opened for each experiment and analyzed beforehand by gas chromatography/mass spectrometry (GC/MS). The results showed that none of these ethers contained detectable levels of the alcohols, aldehydes, or ketones that we detected as reaction products in the experiments described below.

Methyl 3,4-dimethoxybenzyl ether was prepared by reacting 3,4-dimethoxybenzyl alcohol in methanol containing *p*-toluenesulfonic acid as previously described (16), but with modified product purification. At the conclusion of the reaction, the mixture was extracted with several portions of cyclohexane, which were dried over  $\text{MgSO}_4$  and concentrated on a rotary evaporator to produce a thick syrup. This crude product was fractionated by vacuum column chromatography on silica gel with cyclohexane as the eluant (17). Fractions were analyzed by thin layer chromatography and by  $^1\text{H}$  NMR analysis, and those showing no detectable impurities were pooled for solvent removal. MS  $m/z$  (%) 182 ( $\text{M}^+$ , 44), 166 (3), 151 (100), 139 (7), 124 (4), 107 (14), 91 (9), 77 (12), 65 (5), 51 (4).  $^1\text{H}$  NMR ( $\text{CDCl}_3$ )  $\delta$  (ppm) 3.35 (s, 3H,  $-\text{CH}_2\text{OCH}_3$ ), 3.86 (s, 3H,  $-\text{OCH}_3$ ), 3.87 (s, 3H,  $-\text{OCH}_3$ ), 4.37 (s, 2H,  $-\text{CH}_2\text{O}-$ ), 6.81 (d,  $J = 8.1$  Hz, 1H,  $-\text{ArC}_5\text{H}$ ), 6.85 (dd,  $J = 8.1$  Hz, 2.0 Hz, 1H,  $-\text{ArC}_6\text{H}$ ), 6.87 (d,  $J = 2.0$  Hz,  $-\text{ArC}_2\text{H}$ ).

Methyl 4-nitrobenzyl ether was prepared from 4-nitrobenzyl alcohol and  $\text{CH}_3\text{I}$  as described previously (18) and recrystallized twice at  $4^\circ\text{C}$ , first from petroleum ether and then from water. MS  $m/z$  (%) 167 ( $\text{M}^+$ , 4), 166 (11), 136 (11), 121 (14), 120 (35), 108 (13), 107 (100), 106 (14), 105 (13), 91 (27), 90 (25), 89 (85), 78 (47), 77 (81), 65 (11), 63 (27), 51 (28), 50 (16).  $^1\text{H}$  NMR ( $\text{CDCl}_3$ )  $\delta$  (ppm) 3.48 (s, 3H,  $-\text{OCH}_3$ ), 4.59 (s, 2H,  $-\text{CH}_2\text{O}-$ ), 7.53 (d,  $J = 8.6$  Hz, 2H,  $-\text{ArC}_{2,6}\text{H}$ ), 8.24 (d,  $J = 8.6$  Hz, 2H,  $-\text{ArC}_{3,5}\text{H}$ ).

1-Methoxy-4-trideuteromethoxybenzene was prepared from 4-methoxyphenol and  $\text{CD}_3\text{I}$  (99.5 atom % D) as described previously (19) and recrystallized twice from aqueous ethanol. MS  $m/z$  (%) 141 ( $\text{M}^+$ , 100), 126 (70,  $-\text{CH}_3$ ), 123 (62,  $-\text{CD}_3$ ), 98 (34,  $-\text{CH}_3$ ,  $-\text{CO}$ ), 95 (31,  $-\text{CD}_3$ ,  $-\text{CO}$ ).  $^1\text{H}$  NMR (360 MHz,  $\text{CDCl}_3$ )  $\delta$  6.84 (s, 4H,  $-\text{ArC}_{2,3,5,6}\text{H}$ ), 3.77 (s, 3H,  $-\text{OCH}_3$ ).

PEG terminated with 4-nitrophenyl ethers was prepared by stirring 1 g of dibromo-PEG ( $\sim 0.5$  mmol) overnight in acetone that contained 10 mmol each of 4-nitrophenol and powdered  $\text{K}_2\text{CO}_3$ . The acetone was then removed by rotary evaporation, and the product was redissolved in water, after which it was dialyzed twice against 100 mM  $\text{NaHCO}_3$  and twice against distilled water, using a 1-kDa cutoff bag, and finally lyophilized. Approximately 60% of the PEG end groups were 4-nitrophenyl-substituted by this method, as shown by integration of the  $^1\text{H}$  NMR signals (in  $\text{CDCl}_3$ ) for the aromatic protons (6.99 and 8.20 ppm) and the internal polyoxyethylene protons (3.65 ppm).

The extracellular peroxygenase of *A. aegerita* (isoform II, 44 kDa) was produced and purified as described previously (2). The enzyme preparation was homogeneous by SDS-polyacrylamide gel electrophoresis and exhibited an  $A_{418}/A_{280}$  ratio of 1.75. The specific activity of the peroxygenase was 117 units  $\text{mg}^{-1}$ , where 1 unit represents the oxidation of 1  $\mu\text{mol}$  of 3,4-dimethoxybenzyl alcohol to 3,4-dimethoxybenzaldehyde in 1 min at  $23^\circ\text{C}$  (2).

**Product Identification**—Typical reaction mixtures (0.2–1.0 ml) contained purified peroxygenase (1–2 units  $\text{ml}^{-1}$ ), potas-

sium phosphate buffer (50 mM, pH 7.0), and the ether substrate (1–10 mM). When alkyl aryl ethers were used as substrates, the reactions also contained ascorbic acid (4 mM) to inhibit further oxidation of the phenolic products that were released (20, 21). The reactions were started by the addition of limiting  $\text{H}_2\text{O}_2$  (0.1–0.5 mM) and stirred at room temperature for 3 min, at which time chromatographic analyses showed that product formation was complete.

The reaction products 3,4-dimethoxybenzaldehyde and 4-nitrophenol were analyzed by high performance liquid chromatography (HPLC) using an Agilent Series 1100 instrument equipped with a diode array detector and an electrospray ionization mass spectrometer. Reverse phase chromatography was performed on a Luna C18 column (4.6-mm diameter by 150-mm length, 5- $\mu\text{m}$  particle size, Phenomenex), which was eluted at 0.35  $\text{ml min}^{-1}$  and  $40^\circ\text{C}$  with aqueous 0.1% v/v ammonium formate (pH 3.5)/acetonitrile, 95:5 for 5 min, followed by a 25-min linear gradient to 100% acetonitrile. Products were identified relative to authentic standards, based on their retention times, UV absorption spectra, and  $[\text{M} + \text{H}]^+$  or  $[\text{M} - \text{H}]^-$  ions.

Aliphatic aldehydes or ketones produced from the ethers were analyzed as their 2,4-dinitrophenylhydrazones after addition of 0.2 volume of 0.1% 2,4-dinitrophenylhydrazine solution in 0.6 N HCl to each reaction mixture. The derivatized products were analyzed using the same HPLC apparatus as above, but the Luna C18 column was eluted with aqueous 0.1% (v/v) ammonium formate (pH 3.5)/acetonitrile, 70:30 for 5 min, followed by a 25-min linear gradient to 100% acetonitrile. With two exceptions, the dinitrophenylhydrazones were identified relative to authentic standards, based on their retention times, UV absorption spectra, and  $[\text{M} - \text{H}]^-$  ions. As no standards of the 5-hydroxypentanal or 2-(2-hydroxyethoxy)acetaldehyde derivatives were available, they were tentatively identified based on their  $[\text{M} - \text{H}]^-$  ions.

The reaction product 4-methoxyphenol was analyzed by reverse phase HPLC using the above apparatus but with a Gemini Phenyl column (4.6-mm diameter by 150-mm length, 5- $\mu\text{m}$  particle size, Phenomenex). The column was eluted at 1  $\text{ml min}^{-1}$  and  $40^\circ\text{C}$  with aqueous 0.1% (v/v) ammonium formate (pH 10)/acetonitrile, 95:5 for 5 min, followed by a 20-min linear gradient to 100% acetonitrile. The product was identified relative to an authentic standard, based on its retention time and  $[\text{M} - \text{H}]^-$  ion.

The reaction product 4-nitrobenzaldehyde was analyzed by GC of a benzene extract, using a Hewlett Packard 6890 chromatograph equipped with a Hewlett Packard 5973 mass spectrometer. GC was performed isothermally at  $150^\circ\text{C}$ , using helium as the carrier gas at a column flow rate of 1  $\text{ml min}^{-1}$  on a 5% polysiloxane column (Zebron ZB-5, 250  $\mu\text{m}$  diameter by 30 m length, 0.25  $\mu\text{m}$  film thickness, Phenomenex). The product was identified relative to an authentic standard by its retention time and by electron impact MS at 70 eV.

The products ethanol, 2-propanol, and *t*-butanol were detected by subjecting dichloromethane extracts of the aqueous reaction mixtures to GC/MS analysis using the equipment just described. GC was performed using a linear temperature program from  $40$  to  $150^\circ\text{C}$  ( $10^\circ\text{C min}^{-1}$ ), using helium as the carrier gas at a column flow rate of 1  $\text{ml min}^{-1}$ , on a 5% phenyl-

methylpolysiloxane column (DB-5MS, 250- $\mu$ m diameter by 30-m length, 0.25- $\mu$ m film thickness, J&W Scientific). The products were identified relative to authentic standards by their retention times and by electron impact MS at 70 eV.

The reaction product methanol was analyzed by GC/MS as described previously (22) using the equipment just described plus a Hewlett Packard 7694 headspace sampler. The aqueous sample solutions (2 ml) were equilibrated at 90 °C in the headspace oven, after which GC was performed isothermally at 45 °C, using helium as the carrier gas at a column flow rate of 1 ml min<sup>-1</sup>, on the DB-5MS column described above. The methanol was identified relative to an authentic standard by its retention time and by electron impact MS at 70 eV.

To look for evidence that the peroxygenase cleaved ether bonds in 4-nitrophenyl-terminated PEG, we analyzed reaction mixtures by gel permeation chromatography on a column of Sephadex G-25 superfine (1.5-cm diameter, 30-cm length, GE Healthcare) in aqueous Na<sub>2</sub>SO<sub>4</sub> (0.35 M, adjusted to pH 3.5) at room temperature (23). The UV absorbance of the eluant was monitored with a diode array detector to determine whether a shift in the polymer molecular weight distribution had occurred (24).

**Product Quantification**—Stoichiometrical analyses of tetrahydrofuran cleavage were performed by HPLC as described above, using an external standard curve of 4-hydroxybutanal 2,4-dinitrophenylhydrazone for quantification of UV absorbance at 360 nm. 4-Hydroxybutanal 2,4-dinitrophenylhydrazone standards were prepared by adding aliquot portions of 2-ethoxytetrahydrofuran to excess 0.1% 2,4-dinitrophenylhydrazine solution in 0.6 N HCl. Stoichiometrical analyses of methyl 3,4-dimethoxybenzyl ether cleavage were also performed by HPLC as described above, using an external standard curve of 3,4-dimethoxybenzaldehyde for quantification of UV absorbance at 310 nm. Both standard curves had linear regression values with  $R^2 > 0.99$ .

**Enzyme Kinetics**—The kinetics of tetrahydrofuran cleavage were analyzed in stirred reactions (0.20 ml, 23 °C) that contained 0.193  $\mu$ M of the peroxygenase, potassium phosphate buffer (50 mM, pH 7.0), and 0.060–2.500 mM of the ether. The reactions were initiated with 2.00 mM H<sub>2</sub>O<sub>2</sub> and stopped with 0.400 ml of 0.1% 2,4-dinitrophenylhydrazine solution in 0.6 N HCl after 10 s, at which time less than 6% of the tetrahydrofuran had been consumed. The resulting 4-hydroxybutanal-2,4-dinitrophenylhydrazone was quantified by HPLC as described above, and an apparent value of the  $K_m$  for tetrahydrofuran was obtained by nonlinear regression using the Michaelis-Menten model in the ANEMONA program (25).

The kinetics of methyl 3,4-dimethoxybenzyl ether cleavage were analyzed in stirred reactions (2.00 ml, 23 °C) that contained 0.098  $\mu$ M of the peroxygenase, potassium phosphate buffer (25 mM, pH 7.0), and 0.500–2.000 mM of the ether. The reactions were initiated with 0.067–0.200 mM H<sub>2</sub>O<sub>2</sub>, and the initial velocity of 3,4-dimethoxybenzaldehyde formation was measured by the increase in absorbance at 310 nm ( $\epsilon = 9300$  M<sup>-1</sup> cm<sup>-1</sup>) (26) using a Cary 50 UV/visible spectrophotometer. Three kinetic traces were obtained for each pair of substrate concentrations. Kinetic parameters were determined by non-

### Ether Cleavage by an Extracellular Peroxygenase

linear regression using the ping-pong model in the ANEMONA program (25).

**<sup>18</sup>O Labeling Experiment**—The reaction mixture (0.50 ml, stirred at room temperature) contained 2 units of the peroxygenase, potassium phosphate buffer (50 mM, pH 7.0), and 0.5 mM methyl 4-nitrobenzyl ether. The reaction was initiated with 2.0 mM H<sub>2</sub><sup>18</sup>O<sub>2</sub> and stopped after 5 s by rapid mixing with 0.50 ml of benzene. A portion of the upper organic phase was immediately removed with a pipette and analyzed by GC/MS as described above. For each  $m/z$  value, the average total ion count within the 4-nitrobenzaldehyde peak was used after background correction to generate the ion count used for mass abundance calculations.

**Deuterium Isotope Effect Experiments**—The reaction mixtures (0.20 ml, stirred at room temperature) contained 0.4 units of the peroxygenase, potassium phosphate buffer (50 mM, pH 7.0), 4 mM ascorbate, and 0.5 mM 1-methoxy-4-trideuteriomethoxybenzene. The reaction was initiated with 2.0 mM H<sub>2</sub>O<sub>2</sub>, and 10 s later, a portion was analyzed by LC/MS as described above. For each  $m/z$  value, the average total ion count within the 4-methoxyphenol peak was used after background correction to generate the ion count used for mass abundance calculations.

## RESULTS AND DISCUSSION

**Cleavage of Environmentally Significant Ethers**—In qualitative experiments done with limiting H<sub>2</sub>O<sub>2</sub>, we found that the *A. aegerita* peroxygenase cleaved alkyl ethers (I–VI, Table 1). The products were carbonyl compounds, which we identified by HPLC/MS as their 2,4-dinitrophenylhydrazones, and alcohols, which we identified directly by GC/MS. Notably, the gasoline additive methyl *t*-butyl ether (III) yielded formaldehyde and *t*-butanol, and the widely used solvent tetrahydrofuran (IV) gave the ring-opened product 4-hydroxybutanal. The solvent 1,4-dioxane (VI) was also oxidized, and although in this case no authentic standard was available, the  $m/z$  value for the derivatized product was the same as that expected for the 2,4-dinitrophenylhydrazone of the ring-opened product 2-(2-hydroxyethoxy)acetaldehyde. When these reactions were conducted with nonlimiting H<sub>2</sub>O<sub>2</sub>, oxidation of the resulting alcohol moieties also occurred, thus generating additional carbonyl groups. For example, 1,4-dioxane was cleaved at both ether linkages and then further oxidized to glyoxal under these conditions (data not shown).

A quantitative analysis of tetrahydrofuran cleavage in the presence of limiting oxidant showed that one equivalent of 4-hydroxybutanal was formed per equivalent of H<sub>2</sub>O<sub>2</sub> supplied (Table 2), thus identifying the catalyzed reaction as a two-electron oxidation that splits this ether into one aldehyde and one alcohol. The apparent  $K_m$  of the peroxygenase for tetrahydrofuran was 2.1 mM, and the initial turnover rate of the enzyme with 2.5 mM of this ether and 2.0 mM H<sub>2</sub>O<sub>2</sub> was 33 s<sup>-1</sup> (data not shown). We did not attempt a more complete analysis of tetrahydrofuran oxidation kinetics at a saturating H<sub>2</sub>O<sub>2</sub> concentration, because under these conditions the peroxygenase exhibits an interfering catalase activity.<sup>4</sup> More-

<sup>4</sup> R. Ullrich, M. Pecyna, M. Kluge, M. Kinne, C. Liers, and M. Hofrichter, Proceedings of the 8th International Peroxidase Symposium, Tampere, Finland, 20–24 August 2008, page 48.

## Ether Cleavage by an Extracellular Peroxygenase

TABLE 1

Products identified by mass spectroscopy after cleavage of ethers by *A. aegerita* peroxygenase in the presence of limiting  $H_2O_2$

The  $m/z$  value for the major observed diagnostic ion is shown in each case.

	Substrate	Carbonyl product	Alcohol product
I		$\text{CH}_2=\text{O}$ [M-H] <sup>-</sup> 223 <sup>a</sup>	$\text{CH}_3\text{OH}$ [M] <sup>+</sup> 46
II		$\text{CH}_3\text{C}=\text{O}$ [M-H] <sup>-</sup> 237 <sup>a</sup>	$\text{CH}_3\text{CH}_2\text{OH}$ [M-CH <sub>3</sub> ] <sup>+</sup> 45
III		$\text{H}_2\text{C}=\text{O}$ [M-H] <sup>-</sup> 209 <sup>a</sup>	$\text{CH}_3\text{CH}_2\text{CH}_2\text{OH}$ [M-CH <sub>3</sub> ] <sup>+</sup> 59
IV		$\text{O}=\text{CHCH}_2\text{CH}_2\text{CH}_2\text{OH}$ [M-H] <sup>-</sup> 267 <sup>a</sup>	
V		$\text{O}=\text{CHCH}_2\text{CH}_2\text{CH}_2\text{CH}_2\text{OH}$ [M-H] <sup>-</sup> 281 <sup>a,b</sup>	
VI		$\text{O}=\text{CHCH}_2\text{CH}_2\text{CH}_2\text{OH}$ [M-H] <sup>-</sup> 283 <sup>a,b</sup>	
VII		$\text{H}_3\text{C}-\text{C}=\text{O}$ [M+H] <sup>+</sup> 167	$\text{H}_3\text{C}-\text{OH}$ [M-H] <sup>+</sup> 31
VIII		$\text{H}_3\text{C}-\text{C}=\text{O}$ [M] <sup>+</sup> 151	$\text{H}_3\text{C}-\text{OH}$ [M-H] <sup>+</sup> 31
IX		$\text{H}_2\text{C}=\text{O}$ [M-H] <sup>-</sup> 209 <sup>a</sup>	[M-H] <sup>-</sup> 123
X		$\text{H}_2\text{C}=\text{O}$ [M-H] <sup>-</sup> 209 <sup>a</sup>	[M-H] <sup>-</sup> 138 <sup>c</sup>
XI			No reaction <sup>d</sup>

<sup>a</sup> MS of the 2,4-dinitrophenylhydrazone.

<sup>b</sup> No authentic standard was available.

<sup>c</sup> 4-Nitrocatechol was also produced.

<sup>d</sup>  $n \approx 45$ .

over, the cumbersome nature of our HPLC assay for 4-hydroxybutanal formation made initial rate determinations difficult. Instead, we sought an alternative substrate that would provide a more convenient assay.

**Bisubstrate Kinetics**—We found that the peroxygenase cleaved methyl benzyl ethers such as VII and VIII (Table 1),

TABLE 2

Stoichiometry of tetrahydrofuran oxidation by *A. aegerita* peroxygenase

The initial tetrahydrofuran concentration was 10 mM.

$H_2O_2$ added $\mu\text{M}$	4-Hydroxybutanal produced $\mu\text{M}$	4-Hydroxybutanal/ $H_2O_2$
100	101	1.01
200	194	0.97
300	292	0.97
400	375	0.94
500	489	0.98

TABLE 3

Stoichiometry of methyl 3,4-dimethoxybenzyl ether oxidation by *A. aegerita* peroxygenase

The initial methyl 3,4-dimethoxybenzyl ether concentration was 1.0 mM.

$H_2O_2$ added $\mu\text{M}$	3,4-Dimethoxybenzaldehyde produced $\mu\text{M}$	3,4-Dimethoxybenzaldehyde/ $H_2O_2$
11	12	1.09
22	23	1.05
33	33	1.00
44	43	0.98
55	54	0.98
110	105	0.95

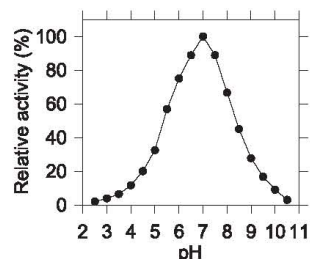


FIGURE 1. Relative rates of methyl 3,4-dimethoxybenzyl ether cleavage by the *A. aegerita* peroxygenase at various pH values.

yielding benzaldehydes and methanol, which we identified by HPLC and GC/MS without derivatization. The benzyl alcohols were not detectable as products, even when  $H_2O_2$  was limiting, and formaldehyde was found only in extended reactions with excess  $H_2O_2$ . These results implied that the benzyl and not the methyl moiety was selectively oxidized during cleavage, the formaldehyde arising only later via oxidation of the released methanol.

The HPLC/MS results obtained with methyl 3,4-dimethoxybenzyl ether (VII, Table 1) showed in addition that its benzyl ether linkage was cleaved exclusively, with no discernible attack on its methoxyl groups (data not shown). Quantitative analyses of methyl 3,4-dimethoxybenzyl ether cleavage in the presence of limiting  $H_2O_2$  were consistent with this picture, showing that one equivalent of 3,4-dimethoxybenzaldehyde was produced per equivalent of oxidant supplied (Table 3). The pH optimum for the reaction was 7.0, with 50% activity occurring at pH 5.4 and pH 8.4 (Fig. 1).

Because a direct spectrophotometric assay is available to monitor the production of 3,4-dimethoxybenzaldehyde (26), we selected methyl 3,4-dimethoxybenzyl ether for initial rate kinetics experiments at pH 7.0, assuming steady-state conditions and using a nonlinear regression method to calculate the

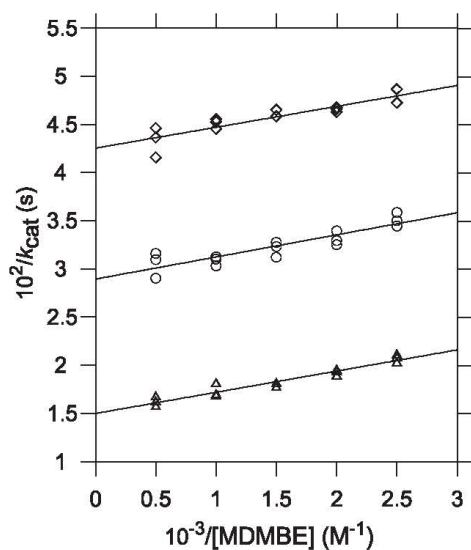


FIGURE 2. Double reciprocal plots of the kinetics data for methyl 3,4-dimethoxybenzyl ether (MDMBE) cleavage by *A. aegerita* peroxygenase. The  $\text{H}_2\text{O}_2$  concentrations used were 0.067 mM ( $\diamond$ ), 0.100 mM ( $\circ$ ), and 0.200 mM ( $\triangle$ ). The kinetic parameters reported in the text were calculated by a nonlinear regression method (25).

kinetic parameters (25). The results gave a  $k_{\text{cat}}$  of  $720 \pm 87 \text{ s}^{-1}$ , a  $K_m$  for  $\text{H}_2\text{O}_2$  of  $1.99 \pm 0.25 \text{ mM}$  ( $k_{\text{cat}}/K_m = 3.6 \times 10^5 \text{ M}^{-1} \text{ s}^{-1}$ ), and a  $K_m$  for methyl 3,4-dimethoxybenzyl ether of  $1.43 \pm 0.23 \text{ mM}$  ( $k_{\text{cat}}/K_m = 5.0 \times 10^5 \text{ M}^{-1} \text{ s}^{-1}$ ). Double reciprocal plots of the same data gave parallel lines (Fig. 2), which is consistent with a ping-pong enzymatic mechanism.

It is interesting to compare the above values with those obtained for functionally similar enzymes. Some P450s that cleave aromatic ethers such as alkoxycoumarins bind them more strongly with  $K_m$  values around 1–10  $\mu\text{M}$ , but have much lower  $k_{\text{cat}}$  values in the vicinity of  $0.1 \text{ s}^{-1}$  or less (27, 28). Similarly, fungal lignin peroxidases have relatively low  $K_m$  values around 10–100  $\mu\text{M}$  for  $\text{H}_2\text{O}_2$  and for simple aromatic substrates such as 3,4-dimethoxybenzyl alcohol, but also exhibit low  $k_{\text{cat}}$  values on the order of 1–10  $\text{s}^{-1}$  (26). As a result, the  $k_{\text{cat}}/K_m$  ratios for methyl 3,4-dimethoxybenzyl ether cleavage by the *A. aegerita* peroxygenase are somewhat higher than those for lignin peroxidase-catalyzed benzyl alcohol oxidations and are much higher than those for P450-catalyzed ether oxidations.

**Source of the Oxygen Introduced during Ether Cleavage**—We showed previously by  $^{18}\text{O}$  labeling that  $\text{H}_2\text{O}_2$  supplies the oxygen atom that the *A. aegerita* peroxygenase introduces when it hydroxylates aromatic rings (20, 21). The analogous experiment is difficult with alkyl ethers, because the oxygen on the resulting aliphatic aldehyde exchanges rapidly in water. However, benzaldehyde oxygens exchange less rapidly, making the assay feasible with benzyl ethers if a short reaction time is employed (29). We selected methyl 4-nitrobenzyl ether (VIII, Table 1) as the substrate because the nitro substituent in the

### Ether Cleavage by an Extracellular Peroxygenase

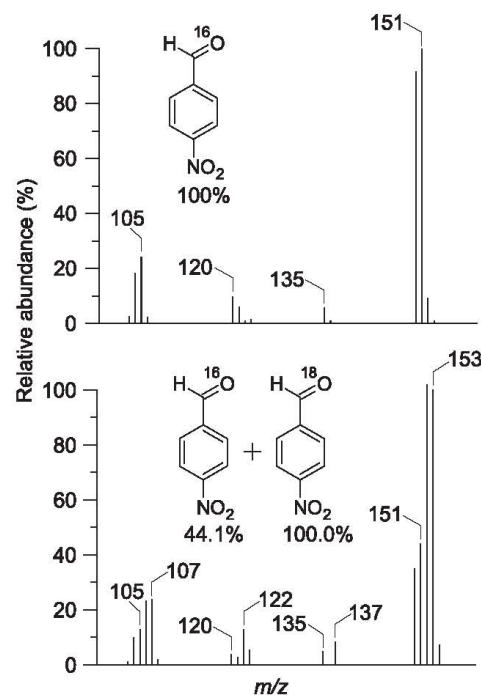


FIGURE 3. Incorporation of  $^{18}\text{O}$  from  $\text{H}_2\text{}^{18}\text{O}_2$  into the carbonyl group of 4-nitrobenzaldehyde after cleavage of methyl 4-nitrobenzyl ether by *A. aegerita* peroxygenase. Upper, MS of the product obtained with natural abundance  $\text{H}_2\text{O}_2$ . Structural assignments (37) for  $m/z$  values are as follows:  $[\text{M}]^+$ , 151;  $[\text{M} - \text{O}]^+$ , 135;  $[\text{M} - \text{NO} - \text{H}]^+$ , 120;  $[\text{M} - \text{NO}_2]^+$ , 105. Lower, MS of the product obtained with 90 atom %  $\text{H}_2\text{}^{18}\text{O}_2$ .

resulting benzaldehyde has been reported to slow the exchange additionally (30). GC/MS analysis showed that the peroxygenase-catalyzed cleavage of this ether in the presence of 90 atom %  $\text{H}_2\text{}^{18}\text{O}_2$  resulted in 69%  $^{18}\text{O}$  incorporation into the carbonyl group of the resulting 4-nitrobenzaldehyde, as evidenced by the shift of the principal molecular ion from  $m/z$  151 to  $m/z$  153 (Fig. 3).

**Evidence for a Hydrogen Abstraction Mechanism**—Additional work showed that the *A. aegerita* peroxygenase cleaved alkyl aryl ethers, yielding aliphatic aldehydes and phenols. The phenols tended to undergo further oxidation to polymeric products and 1,4-benzoquinone because this enzyme exhibits general peroxidase activity (31). However, the phenolic products were readily detectable when ascorbate was included in the assay to suppress their further oxidation (20, 21). By this method we found, for example, that 1,4-dimethoxybenzene (IX, Table 1) was oxidized to 4-methoxyphenol. Because 1,4-dimethoxybenzene is symmetrical and its methoxyl carbons are not prochiral, it is a suitable substrate to determine whether a catalyzed etherolytic reaction exhibits an intramolecular deuterium isotope effect, which gives an approximate value for the intrinsic deuterium isotope effect on cleavage of the ether bond (19, 27, 32).



## Ether Cleavage by an Extracellular Peroxygenase

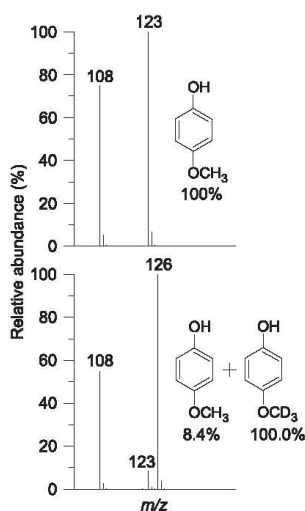


FIGURE 4. Preferential cleavage by *A. aegerita* peroxygenase of the non-deuterated methoxyl group in 1-methoxy-4-trideuteromethoxybenzene. Upper, MS of 4-methoxyphenol- $h_3$  obtained from the oxidation of natural abundance 1,4-dimethoxybenzene. Structural assignments for  $m/z$  values are as follows:  $[M - H]^-$ , 123;  $[M - CH_3 - H]^-$ , 108. Lower, MS of the 4-methoxyphenol- $h_3$ /4-methoxyphenol- $d_3$  mixture obtained from the oxidation of 1-methoxy-4-trideuteromethoxybenzene. The lower MS shown is one of three used to calculate the observed mean intramolecular isotope effect.

HPLC/MS analysis showed that the peroxygenase-catalyzed cleavage of 1-methoxy-4-trideuteromethoxybenzene resulted in a marked preponderance of 4-methoxyphenol- $d_3$  ( $m/z$  126,  $[M - H]^-$ ) over 4-methoxyphenol- $h_3$  ( $m/z$  123,  $[M - H]^-$ ) (Fig. 4). The observed mean intramolecular isotope effect  $[(k_H/k_D)_{obs}]$  from three experiments was  $11.9 \pm 0.4$ . In general, oxidations that occur via hydrogen abstraction exhibit intrinsic deuterium isotope effects of this magnitude, whereas those that occur via insertion of an oxygen atom show much lower isotope effects with  $(k_H/k_D)_{obs} \approx 2$  (27, 32).

**Hypothetical Reaction Mechanism**—In summary, our data show that ether cleavage by the *A. aegerita* peroxygenase exhibits (a) kinetics that are consistent with a ping-pong reaction mechanism, (b) incorporation of  $H_2O_2$ -derived oxygen into the oxidized product, and (c) a high intramolecular deuterium isotope effect that suggests abstraction of an ether  $\beta$ -hydrogen by the enzyme. These results support a mechanism similar to that envisaged for the peroxygenase activity of P450 (12, 13), in which the enzyme heme is oxidized by  $H_2O_2$  to give an iron species that carries one of the peroxide oxygens and can be depicted formally as  $FeO^{3+}$ . This intermediate then abstracts a hydrogen located beta to the ether oxygen, which is followed by rebound of an  $\cdot OH$  equivalent to produce a hemiacetal that subsequently hydrolyzes (Fig. 5).

This working model obviously needs refinement, especially regarding the structure of the oxidized heme. Our attempts to observe oxidized intermediates after titration of the enzyme with  $H_2O_2$  have been unsuccessful because they result in bleaching of the heme, and further progress will probably require a rapid transient-state kinetics approach. The sequence

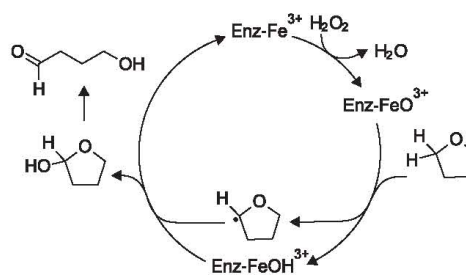


FIGURE 5. Hypothetical reaction mechanism for ether cleavage by *A. aegerita* peroxygenase, with tetrahydrofuran shown as the oxidized substrate.

of substrate binding to the peroxygenase also remains to be established, and additional experiments with molecular clock substrates would be advisable to check whether they yield data consistent with the radical rebound mechanism we have proposed (13).

**Scope of Ether Cleavage**—We noted some apparent size limitations on ether substrates for the *A. aegerita* peroxygenase. For example, although the enzyme cleaved 4-nitroanisole (X, Table 1) to 4-nitrophenol, it failed to cleave a 4-nitrophenyl-terminated PEG (XI). The gel permeation chromatography method we used to assess cleavage provides a sensitive assay for random *endo* scissions of the polyoxyethylene ethers in PEG (24), yet we observed no shift in the molecular weight distribution of the polymer after enzymatic treatment. Moreover, we found no evidence for *exo* cleavage of model XI, which would have released 4-nitrophenol if it had occurred. In additional experiments, we found that the peroxygenase released *n*-propanal efficiently from 1,4-di-*n*-propoxybenzene, but released only traces of *n*-butanal from 1,4-di-*n*-butoxybenzene (data not shown). These results suggest that the active site of the *A. aegerita* peroxygenase is unlikely to accommodate macromolecular ethers such as lignin or polyoxyethylene surfactants.

However, our results indicate a likely role for fungal peroxygenases in the extracellular breakdown of natural and anthropogenic low molecular weight ethers. Some of these reactions are probably fortuitous, as are many of the extracellular xenobiotic oxidations carried out by lignocellulolytic fungi (33). In other cases, ether cleavage may have a physiological function, for example in the biodegradation of lignin fragments, or in the detoxification of fungicidal methoxyaromatic phytotoxins via demethylation and subsequent polymerization (34). It is pertinent that many lignocellulolytic fungi produce the necessary extracellular  $H_2O_2$  (35), and that this oxidant is also deposited in soils from rainwater (36).

**Acknowledgment**—We thank Kolby Hirth for spectroscopic analyses of the synthesized peroxygenase substrates.

## REFERENCES

- Hofrichter, M., and Ullrich, R. (2006) *Appl. Microbiol. Biotechnol.* **71**, 276–288
- Ullrich, R., Nüske, J., Scheibner, K., Spantzel, J., and Hofrichter, M. (2004) *Appl. Environ. Microbiol.* **70**, 4575–4581



3. Kluge, M., Ullrich, R., Dolge, C., Scheibner, K., and Hofrichter, M. (2009) *Appl. Microbiol. Biotechnol.* **81**, 1071–1076
4. Anh, D. H., Ullrich, R., Benndorf, D., Svatos, A., Muck, A., and Hofrichter, M. (2007) *Appl. Environ. Microbiol.* **73**, 5477–5485
5. Pecyna, M. J., Ullrich, R., Bittner, B., Clemens, A., Scheibner, K., Schubert, R., and Hofrichter, M. (2009) *Appl. Microbiol. Biotechnol.*, in press
6. Ullrich, R., and Hofrichter, M. (2005) *FEBS Lett.* **579**, 6247–6250
7. White, G. F., Russell, N. J., and Tidswell, E. C. (1996) *Microbiol. Rev.* **60**, 216–232
8. Boerjan, W., Ralph, J., and Baucher, M. (2003) *Annu. Rev. Plant Biol.* **54**, 519–546
9. Whiting, D. A. (2001) *Nat. Prod. Rep.* **18**, 583–606
10. Isaacson, C., Mohr, T. K., and Field, J. A. (2006) *Environ. Sci. Technol.* **40**, 7305–7311
11. Scow, K. M., and Hicks, K. A. (2005) *Curr. Opin. Biotechnol.* **16**, 246–253
12. Guengerich, F. P. (2001) *Chem. Res. Toxicol.* **14**, 611–650
13. Ortiz de Montellano, P. R., and de Voss, J. J. (2005) in *Cytochrome P450. Structure, Mechanism, and Biochemistry* (Ortiz de Montellano, P. R., ed), 3rd Ed., pp. 183–245, Kluwer Academic/Plenum Publishers, New York, NY
14. Lopes Ferreira, N. L., Malandain, C., and Fayolle-Guichard, F. (2006) *Appl. Microbiol. Biotechnol.* **72**, 252–262
15. Mahendra, S., Petzold, C. J., Baidoo, E. E., Keasling, J. D., and Alvarez-Cohen, L. (2007) *Environ. Sci. Technol.* **41**, 7330–7336
16. Schmidt, H. W., Haemmerli, S. D., Schoemaker, H. E., and Leisola, M. S. (1989) *Biochemistry* **28**, 1776–1783
17. Pedersen, D. S., and Rosenbohm, C. (2001) *Synthesis*, 2431–2434
18. Lawson, T., Gannett, P. M., Yau, W. M., Dalal, N. S., and Toth, B. (1995) *J. Agric. Food Chem.* **43**, 2627–2635
19. Foster, A. B., Jarman, M., Stevens, J. D., Thomas, P., and Westwood, J. H. (1974) *Chem.-Biol. Interact.* **9**, 327–340
20. Kinne, M., Poraj-Kobielska, M., Aranda, E., Ullrich, R., Hammel, K. E., Scheibner, K., and Hofrichter, M. (2009) *Bioorg. Med. Chem. Lett.* **19**, 3085–3087
21. Kinne, M., Ullrich, R., Hammel, K. E., Scheibner, K., and Hofrichter, M. (2008) *Tetrahedron Lett.* **49**, 5950–5953
22. Li, H., Zhan, H., Fu, S., Liu, M., and Chai, X. S. (2007) *J. Chromatogr. A* **1175**, 133–136
23. Cooke, M. P., Archer, B. G., and Krakauer, H. (1974) *Biochem. Biophys. Res. Commun.* **57**, 1032–1037
24. Kerem, Z., Jensen, K. A., and Hammel, K. E. (1999) *FEBS Lett.* **446**, 49–54
25. Hernández, A., and Ruiz, M. T. (1998) *Bioinformatics* **14**, 227–228
26. Tien, M., Kirk, T. K., Bull, C., and Fee, J. A. (1986) *J. Biol. Chem.* **261**, 1687–1693
27. Yun, C. H., Kim, K. H., Calcutt, M. W., and Guengerich, F. P. (2005) *J. Biol. Chem.* **280**, 12279–12291
28. Kim, D., and Guengerich, F. P. (2004) *Arch. Biochem. Biophys.* **432**, 102–108
29. Tien, M., and Kirk, T. K. (1984) *Proc. Natl. Acad. Sci. U.S.A.* **81**, 2280–2284
30. Samuel, D., and Silver, B. L. (1965) *Adv. Phys. Org. Chem.* **3**, 121–186
31. Ullrich, R., and Hofrichter, M. (2007) *Cell. Mol. Life Sci.* **64**, 271–293
32. Nelson, S. D., and Trager, W. F. (2003) *Drug Metab. Dispos.* **31**, 1481–1498
33. Tortella, G. R., Diez, M. C., and Duran, N. (2005) *Crit. Rev. Microbiol.* **31**, 197–212
34. Delslerone, L. M., McCluskey, K., Matthews, D. E., and Vanetten, H. D. (1999) *Phys. Mol. Plant Pathol.* **55**, 317–326
35. Leonowicz, A., Matuszewska, A., Luterek, J., Ziegenhagen, D., Wojtaś-Wasilewska, M., Cho, N. S., Hofrichter, M., and Rogalski, J. (1999) *Fungal Genet. Biol.* **27**, 175–185
36. Kok, G. L. (1980) *Atmos. Environ.* **14**, 653–656
37. McLafferty, F. W., and Tureček, F. (1993) *Interpretation of Mass Spectra*, 4th Ed., University Science Books, Sausalito, CA



Contents lists available at ScienceDirect

Biochemical and Biophysical Research Communications

journal homepage: [www.elsevier.com/locate/ybbrc](http://www.elsevier.com/locate/ybbrc)

## Stepwise oxygenations of toluene and 4-nitrotoluene by a fungal peroxygenase

Matthias Kinne<sup>a,\*</sup>, Christian Zeisig<sup>a</sup>, René Ullrich<sup>a</sup>, Gernot Kayser<sup>a</sup>, Kenneth E. Hammel<sup>b</sup>, Martin Hofrichter<sup>a</sup><sup>a</sup> Unit of Environmental Biotechnology, International Graduate School of Zittau, Markt 23, 02763 Zittau, Germany<sup>b</sup> USDA Forest Products Laboratory, Madison, WI 53726, USA

## ARTICLE INFO

## Article history:

Received 27 April 2010

Available online xxxxx

## Keywords:

Oxygenase

Peroxidase

Peroxygenase

P450

Toluene

4-Nitrotoluene

Benzylic hydroxylation

Benzaldehyde

Oxidation

## ABSTRACT

Fungal peroxygenases have recently been shown to catalyze remarkable oxidation reactions. The present study addresses the mechanism of benzylic oxygenations catalyzed by the extracellular peroxygenase of the agaric basidiomycete *Agrocybe aegerita*. The peroxygenase oxidized toluene and 4-nitrotoluene via the corresponding alcohols and aldehydes to give benzoic acids. The reactions proceeded stepwise with total conversions of 93% for toluene and 12% for 4-nitrotoluene. Using H<sub>2</sub><sup>18</sup>O<sub>2</sub> as the co-substrate, we show here that H<sub>2</sub>O<sub>2</sub> is the source of the oxygen introduced at each reaction step. *A. aegerita* peroxygenase resembles cytochromes P450 and heme chloroperoxidase in catalyzing benzylic hydroxylations.

© 2010 Elsevier Inc. All rights reserved.

## 1. Introduction

Selective C–H oxidations occur in a wide range of biological transformations and are one of the most challenging reactions in organic chemistry. Therefore, it is of interest to understand the reaction mechanisms of enzymes that are capable of these reactions, and to apply these biocatalysts as tools for organic synthesis.

Recently a new group of extracellular fungal heme biocatalysts, the aromatic peroxygenases (APOs), was found in agaric basidiomycetes. These heme-thiolate enzymes may represent a new superfamily of heme peroxidases [1,2], and show some functional similarities with the latter enzymes in catalyzing the H<sub>2</sub>O<sub>2</sub>-dependent oxidation of substrates such as phenols and halide ions (e.g. Br<sup>-</sup>), but also resemble cytochrome P450-dependent monooxygenases (P450s) in mediating selective epoxidations/hydroxylations of numerous aromatic and aliphatic substrates. <sup>18</sup>O-Labeling studies have established that H<sub>2</sub>O<sub>2</sub> is the source of oxygen introduced during a variety of peroxygenase-catalyzed oxidations, including the epoxidation and hydroxylation of aromatics [3–6], the sulfoxi-

dation of dibenzothiophene [4], the *N*-oxidation of pyridine derivatives [7] and the cleavage of diverse ethers to produce aldehydes and ketones [8].

Previous work has shown that the best-characterized fungal peroxygenase, from *Agrocybe aegerita*, can oxidize toluene to form benzyl alcohol, benzaldehyde, and benzoic acid [9]. However, the mechanism of the benzylic oxidations catalyzed by *A. aegerita* aromatic peroxygenase (*Aae*APO) remains unclear. The work we report here suggests that *Aae*APO-catalyzed reactions resemble the benzylic hydroxylations catalyzed by P450s via their H<sub>2</sub>O<sub>2</sub>-dependent “peroxide shunt” mechanism.

## 2. Materials and methods

## 2.1. Chemicals and enzyme preparation

All chemicals used were purchased from Sigma–Aldrich except H<sub>2</sub><sup>18</sup>O<sub>2</sub> (90 atom%, 2% wt/vol), which was obtained from Icon Isotopes. *Aae*APO (isoform II, pl 5.6) was produced and purified as described previously [10,11]. The enzyme preparation was homogeneous by SDS polyacrylamide gel electrophoresis and exhibited an A<sub>418</sub>/A<sub>280</sub> ratio of 1.75. The specific activity of the peroxygenase was 117 U mg<sup>-1</sup>, where 1 U represents the oxidation of 1 μmol of 3,4-dimethoxybenzyl alcohol to 3,4-dimethoxybenzaldehyde in 1 min at 23 °C [10].

Abbreviations: *Aae*APO, aromatic peroxygenase from *Agrocybe aegerita*; P450, cytochrome P450.

\* Corresponding author. Fax: +49 3583 612734.

E-mail address: kinne@ihi-zittau.de (M. Kinne).

0006-291X/\$ - see front matter © 2010 Elsevier Inc. All rights reserved.  
doi:10.1016/j.bbrc.2010.05.036

Please cite this article in press as: M. Kinne et al., Stepwise oxygenations of toluene and 4-nitrotoluene by a fungal peroxygenase, *Biochem. Biophys. Res. Commun.* (2010), doi:10.1016/j.bbrc.2010.05.036

## 2.2. Reaction conditions

Typical reaction mixtures (0.5 ml) contained purified peroxygenase (4 U ml<sup>-1</sup>), potassium phosphate buffer (50 mM, pH 7.0), acetonitrile (5% vol/vol) and the substrate (0.5 mM). The reactions were started by the addition of H<sub>2</sub>O<sub>2</sub> (1 mM).

## 2.3. Product identification

The reaction products benzoic acid and 4-nitrobenzoic acid were analyzed by high performance liquid chromatography (HPLC) using an Agilent Series 1100 instrument equipped with a diode array detector and an electrospray ionization mass spectrometer on a Luna 5- $\mu$ m-pore-size C18 column (Phenomenex). The column was eluted at 40 °C and 0.35 ml min<sup>-1</sup> with an aqueous ammonium formate solution (0.1% vol/vol, pH 3.5)/acetonitrile, 95:5 (70:30 for nitro-substituted compounds), for 5 min, followed by a 25-min linear gradient to 100% acetonitrile. Products were identified relative to authentic standards, based on their retention times, UV absorption spectra, and [M-H]<sup>-</sup> ions.

The reaction products benzyl alcohol, 4-nitrobenzyl alcohol, benzaldehyde and 4-nitrobenzaldehyde were analyzed by gas chromatography (GC) of benzene extracts, using a Hewlett Packard 6890 chromatograph equipped with a Hewlett Packard 5973 mass spectrometer. GC was performed with a temperature program starting at 40 °C for 2 min and then increasing at 15 °C min<sup>-1</sup> to 220 °C, using helium as the carrier gas at a column flow rate of 1 ml min<sup>-1</sup> on a 5% polysiloxane column (Zebron ZB-5, 250  $\mu$ m diameter by 30 m length, 0.25  $\mu$ m film thickness, Phenomenex). The products were identified relative to authentic standards by their retention times and by electron impact MS at 70 eV. For each *m/z* value, the average total ion count within the product peak was used after background correction to generate the ion count used for mass abundance calculations. Calculation of <sup>18</sup>O-incorporation was performed by dividing the sum of the natural species abundance and the isotope abundance with the isotope abundance. The 10% of natural abundance H<sub>2</sub>O<sub>2</sub> in the H<sub>2</sub><sup>18</sup>O<sub>2</sub> preparation was taken into account in these calculations.

## 2.4. Kinetics experiments

The time course of product release during *Aae*APO-catalyzed hydroxylation of toluene and 4-nitrotoluene was analyzed in stirred reactions (0.20 ml, 23 °C) that contained 1 U ml<sup>-1</sup> of the peroxygenase, potassium phosphate buffer (50 mM, pH 7.0), and 0.50 mM of the substrate. The reactions were initiated with 1 mM H<sub>2</sub>O<sub>2</sub> and stopped with 0.02 ml of 50% (w/vol) trichloroacetic acid after 5, 10, 30, 60 and 120 s. The reaction products were quantified by HPLC as described above.

## 3. Results

*Aae*APO hydroxylated toluene and 4-nitrotoluene to give the corresponding benzyl alcohols, benzaldehydes and benzoic acids. The reactions proceeded rapidly with total conversions of 93% for toluene and 12% for 4-nitrotoluene (Fig. 1). The low extent of 4-nitrotoluene oxidation is attributable to inhibition of the enzyme by the substrate, which has also been observed during P450-catalyzed oxidations of nitroaromatics [12,13]. The initial product of toluene oxidation was benzyl alcohol, which then declined with concomitant production of benzaldehyde, which in turn declined with concomitant production of benzoic acid. When benzyl alcohol was used instead of toluene as the starting substrate, the products were benzaldehyde and benzoic acid (Supplementary Fig. 1A), whereas with benzaldehyde as the starting material, only benzoic

acid was formed (Supplementary Fig. 1B). In reactions with 4-nitrotoluene as the starting substrate, the reaction sequence was not as apparent (Fig. 1), but other experiments with 4-nitrobenzyl alcohol or 4-nitrobenzaldehyde as starting substrates showed the same precursor-product relationships as in the experiments with toluene (Supplementary Fig. 1C and D).

An <sup>18</sup>O-labeling study established that H<sub>2</sub>O<sub>2</sub> supplied the oxygen incorporated during *Aae*APO-catalyzed oxidation of the two toluenes. (Fig. 2). When we conducted the reaction with toluene and H<sub>2</sub><sup>18</sup>O<sub>2</sub>, mass spectral analysis of the resulting benzyl alcohol showed that its principal ion had shifted from the natural abundance *m/z* of 108 to *m/z* 110. Similarly, the reaction with 4-nitrotoluene and H<sub>2</sub><sup>18</sup>O<sub>2</sub> yielded 4-nitrobenzyl alcohol in which the principal ion had shifted from *m/z* 153 to *m/z* 155.

We also observed incorporation of <sup>18</sup>O from H<sub>2</sub><sup>18</sup>O<sub>2</sub> in the benzaldehyde and benzoic acid formed from toluene in these experiments. To clarify this finding, we performed labeling experiments using each of the intermediate products as *Aae*APO substrates, and thus showed that <sup>18</sup>O was incorporated from H<sub>2</sub><sup>18</sup>O<sub>2</sub> at each oxidation step. With benzyl alcohol as the substrate, some of the resulting benzaldehyde shifted from its natural abundance *m/z* of 106 (100%) to *m/z* 108 (22%), which indicates 18% incorporation of <sup>18</sup>O from H<sub>2</sub><sup>18</sup>O<sub>2</sub>. The *m/z* values for the benzoic acid formed in this experiment also shifted, in this case from *m/z* 121 to *m/z* 123 (100%) and *m/z* 125 (9.5%). When benzaldehyde was used as the substrate instead, the resulting benzoic acid shifted quantitatively from its natural abundance *m/z* of 121 to *m/z* 123 (Fig. 3).

The same trend was apparent with 4-nitro-substituted substrates. In reactions started from 4-nitrobenzyl alcohol, some of the resulting 4-nitrobenzaldehyde shifted from the natural abundance *m/z* of 151 (100%) to *m/z* 153 (15.5%), thus indicating 13% incorporation of <sup>18</sup>O from H<sub>2</sub><sup>18</sup>O<sub>2</sub>. The *m/z* values for the 4-nitrobenzoic acid formed in this experiment also shifted, in this case from *m/z* 166 to *m/z* 168 (100%) and *m/z* 170 (9.5%). The shift from the natural abundance *m/z* of 166 to *m/z* 168 was quantitative for 4-nitrobenzoic acid when 4-nitrobenzaldehyde was used instead as the starting substrate (Fig. 3).

## 4. Discussion

Our results show that *Aae*APO can convert toluenes to benzoic acids via sequential two-electron oxidations, and that the intermediate benzyl alcohols and benzaldehydes are released from the enzyme active site. In addition to side chain oxidation, *Aae*APO also catalyzes the oxygenation of the aromatic ring of toluene (but not of 4-nitrotoluene) leading to mixtures of *p*- and *o*-cresol and their oxidation products [9]. As reported earlier, these reactions may compete with side chain oxidation. In the present study, where the focus has been on side chain oxidations, ring oxygenation of toluene was ignored.

The <sup>18</sup>O-labeling experiments establish that the oxygens introduced during oxidations originate from H<sub>2</sub>O<sub>2</sub>. The results support a mechanism similar to that envisaged for the peroxygenase activity of P450s [14,15] and for ether cleavage catalyzed by *Aae*APO [8], in which the enzyme heme is oxidized by H<sub>2</sub>O<sub>2</sub> to give a ferryl oxygen intermediate [16] that carries one of the peroxide oxygens and can be depicted formally as (FeO)<sup>3+</sup>. The latter (very probably a Compound I-type intermediate) abstracts a hydrogen from the benzylic carbon to give an enzyme-bound benzylic radical, after which rebound of an  $\bullet$ OH equivalent occurs to introduce a new hydroxyl group on the same carbon (Fig. 4).

According to this model, oxygen incorporation from H<sub>2</sub>O<sub>2</sub> should be quantitative when a toluene is oxidized to a benzyl alcohol, and our data agree with this picture. When the substrate is a benzyl alcohol instead, the enzyme-bound intermediate will be

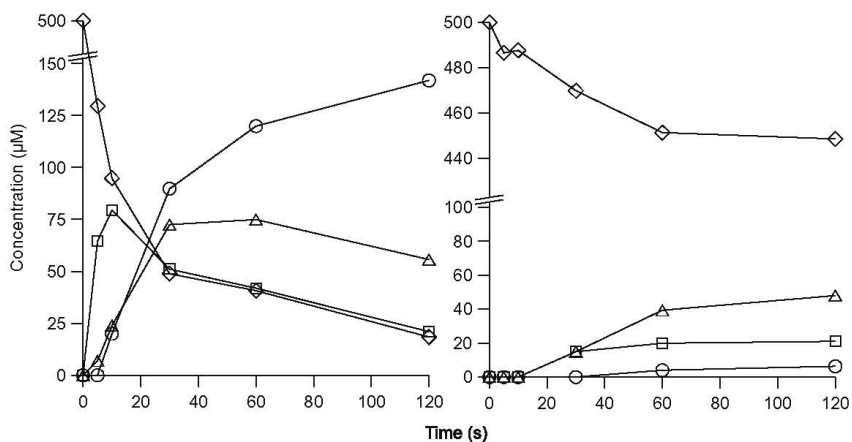


Fig. 1. Time course of *AaeAPO*-catalyzed oxidation of toluene (left) and 4-nitrotoluene (right). Toluenes ( $\diamond$ ), benzyl alcohols ( $\square$ ), benzaldehydes ( $\Delta$ ), benzoic acids ( $\circ$ ).

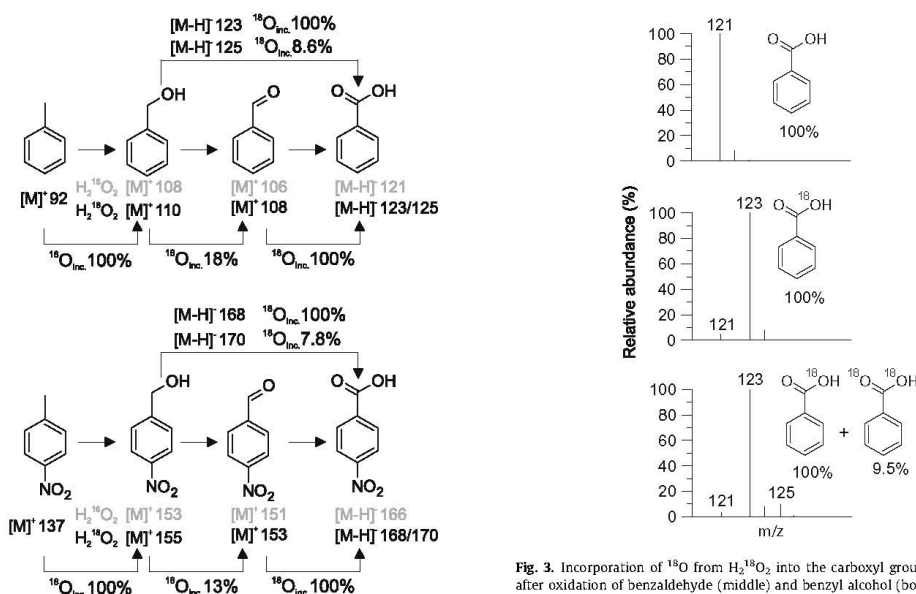


Fig. 2. Reaction scheme showing the yields of  $^{18}\text{O}$ -incorporation into reaction products during *AaeAPO*-catalyzed oxidation of toluene (top) and 4-nitrotoluene (bottom) in the presence of  $\text{H}_2^{18}\text{O}_2$ .

an  $\alpha$ -hydroxybenzylic radical and the resulting initial product will be a *gem*-diol in equilibrium with the benzaldehyde. Consequently, some of the oxygens introduced from  $\text{H}_2\text{O}_2$  will be lost via non-stereospecific exchange with water, again in accord with our results. Finally, when the substrate is a benzaldehyde, the enzyme-bound intermediate will be an  $\alpha$ -oxobenzylic radical, oxygen incorporation from  $\text{H}_2\text{O}_2$  will be quantitative, and the resulting product will be the benzoic acid, once more in agreement with our data. In theory, this last oxidation could proceed via the *gem*-triol, but this

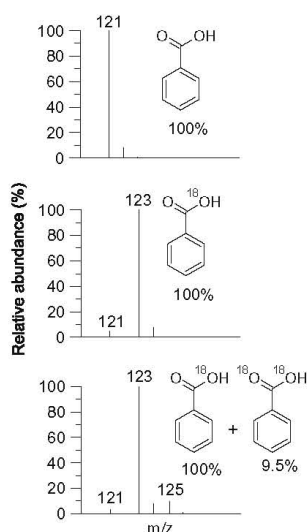


Fig. 3. Incorporation of  $^{18}\text{O}$  from  $\text{H}_2^{18}\text{O}_2$  into the carboxyl group of benzoic acid after oxidation of benzaldehyde (middle) and benzyl alcohol (bottom) by *AaeAPO*. MS of the product obtained with natural abundance  $\text{H}_2\text{O}_2$  (top).

intermediate can be ruled out because we found that no exchange of incorporated oxygen occurred during the oxidation of either benzaldehyde (Fig. 4).

The sequential *AaeAPO*-catalyzed oxidations we have described here are also typical of P450s [17,18], but the latter enzymes are intracellular, whereas *AaeAPO* is secreted into the surrounding environment by the fungal hyphae. Some other oxidative fungal enzymes such as lignin peroxidases and chloroperoxidases also have an extracellular location, but are more limited than *AaeAPO* in the variety of compounds they can utilize as electron donors. For example, lignin peroxidase does not oxidize benzyl alcohol, and neither of these peroxidases is able to oxidize 4-nitrotoluene

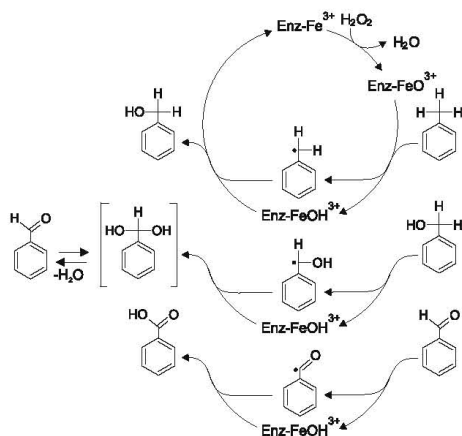


Fig. 4. Proposed reaction mechanism for benzylic oxidation by *AaeAPO*.

[17,19,20]. The broad substrate range and ubiquitous distribution of extracellular APOs may indicate an important environmental role for them in the oxidation of both natural and anthropogenic aromatics.

#### Acknowledgments

We thank Martin Kluge (Inge) and Marzena Poraj-Kobielska for fruitful discussions. This work was supported by the Konrad Adenauer Foundation, the Fulbright Foundation, the Deutsche Bundesstiftung Umwelt (Project No. 13225-32) and the European Union (integrated project "BIORENEW", European Social Fund project number 609910).

#### Appendix A. Supplementary data

Supplementary data associated with this article can be found, in the online version, at doi:10.1016/j.bbrc.2010.05.036.

#### References

- [1] M.J. Pecyna, R. Ullrich, B. Bittner, A. Clemens, K. Scheibner, R. Schubert, M. Hofrichter, Molecular characterization of aromatic peroxxygenase from *Agrocybe aegerita*, *Appl. Microbiol. Biotechnol.* 84 (2009) 885–897.

- [2] M. Hofrichter, R. Ullrich, M. Pecyna, C. Liers, T. Lundell, New and classic families of secreted fungal heme peroxidases, *Appl. Microbiol. Biotechnol.* Doi: 10.1007/s00253-010-2633-0 (2010).
- [3] M. Kinne, R. Ullrich, K.E. Hammel, K. Scheibner, M. Hofrichter, Regioselective preparation of (*R*)-2-(4-hydroxyphenoxy)propionic acid with a fungal peroxxygenase, *Tetrahedron Lett.* 49 (2008) 5950–5953.
- [4] E. Aranda, M. Kinne, M. Kluge, R. Ullrich, M. Hofrichter, Conversion of dibenzothiophene by the mushrooms *Agrocybe aegerita* and *Coprinellus radians* and their extracellular peroxxygenases, *Appl. Microbiol. Biotechnol.* 82 (2008) 1057–1066.
- [5] M. Kinne, M. Poraj-Kobielska, E. Aranda, R. Ullrich, K.E. Hammel, K. Scheibner, M. Hofrichter, Regioselective preparation of 5-hydroxypropranolol and 4'-hydroxydiclofenac with a fungal peroxxygenase, *Bioorg. Med. Chem. Lett.* 19 (2009) 3085–3087.
- [6] M. Kluge, R. Ullrich, C. Dolge, K. Scheibner, M. Hofrichter, Hydroxylation of naphthalene by aromatic peroxxygenase from *Agrocybe aegerita* proceeds via oxygen transfer from H<sub>2</sub>O<sub>2</sub> and intermediary epoxidation, *Appl. Microbiol. Biotechnol.* 81 (2009) 1071–1076.
- [7] R. Ullrich, C. Dolge, M. Kluge, M. Hofrichter, Pyridine as novel substrate for regioselective oxygenation with aromatic peroxxygenase from *Agrocybe aegerita*, *FEBS Lett.* 582 (2008) 4100–4106.
- [8] M. Kinne, M. Poraj-Kobielska, S.A. Ralph, R. Ullrich, M. Hofrichter, K.E. Hammel, Oxidative cleavage of diverse ethers by an extracellular fungal peroxxygenase, *J. Biol. Chem.* 284 (2009) 29343–29349.
- [9] R. Ullrich, M. Hofrichter, The haloperoxidase of the agaric fungus *Agrocybe aegerita* hydroxylates toluene and naphthalene, *FEBS Lett.* 579 (2005) 6247–6250.
- [10] R. Ullrich, J. Nüske, K. Scheibner, J. Spantzel, M. Hofrichter, Novel haloperoxidase from the agaric basidiomycete *Agrocybe aegerita* oxidizes aryl alcohols and aldehydes, *Appl. Environ. Microbiol.* 70 (2004) 4575–4581.
- [11] R. Ullrich, C. Liers, S. Schimpke, M. Hofrichter, Purification of homogeneous forms of fungal peroxxygenase, *Biotechnol. J.* 4 (2009) 1619–1626.
- [12] L.A. Sternson, R.E. Gammans, Interaction of aromatic nitro compounds with reduced hepatic microsomal cytochrome P-450, *Drug. Metab. Dispos.* 3 (1975) 266–274.
- [13] Z.V. Kuropteva, M.E. Kudriavtsev, Inhibition of cytochrome P-450 when exposed to nitro-compounds, *Biofizika* 42 (1997) 484–489.
- [14] F.P. Guengerich, Common and uncommon cytochrome P450 reactions related to metabolism and chemical toxicity, *Chem. Res. Toxicol.* 14 (2001) 611–650.
- [15] P.R. Ortiz de Montellano, J.J. de Voss, *Substrate Oxidation by Cytochrome P450 Enzymes*, third ed. Kluwer Academic/Plenum Publishers, New York, 2005.
- [16] R.P. Hanzlik, K.H.J. Ling, Active site dynamics of toluene hydroxylation by cytochrome P-450, *J. Org. Chem.* 55 (1990) 3992–3997.
- [17] U. Scheller, T. Zimmer, D. Becher, F. Schauer, W.H. Schunck, Oxygenation cascade in conversion of *n*-alkanes to alpha, omega-dioic acids catalyzed by cytochrome P450 52A3, *J. Biol. Chem.* 273 (1998) 32528–32534.
- [18] H. Teramoto, H. Tanaka, H. Wariishi, Fungal cytochrome P450s catalyzing hydroxylation of substituted toluenes to form their hydroxymethyl derivatives, *FEMS Microbiol. Lett.* 234 (2004) 255–260.
- [19] V.P. Miller, R.A. Tschirret-Guth, P.R. Ortiz de Montellano, Chloroperoxidase-catalyzed benzylic hydroxylation, *Arch. Biochem. Biophys.* (319) (1995) 333–340.
- [20] R. Russ, T. Zelinski, T. Anke, Benzylic biooxidation of various toluenes to aldehydes by peroxidase, *Tetrahedron Lett.* 43 (2002) 791–793.

# ACKNOWLEDGEMENT

This research project would not have been possible without the support of many people.

Foremost, I want to express my special gratitude to my supervisors professor Martin Hofrichter and professor Kenneth E. Hammel for their encouragement, persistence, and patience. Professor Hofrichter not only gave me the opportunity to work in such a stimulating research context and laid out the theoretical and methodological basics of my research; he was also a constructive critic in the best sense and continuous supporter of my work. I am very grateful to him for all the knowledge he shared with me. Professor Hammel broadened my perspective of development by letting me participate from his impressive theoretical, methodological, and empirical knowledge on numerous aspects of biochemical research. I am heartily thankful for his tremendous support in all other aspects that are involved in writing of publications.

I would like to thank professor Katrin Scheibner, who supports me in writing of patents and for giving me the opportunity to have a look behind the scenes of applied biotechnology.

Special thanks also to my laboratory advisor Dr. Renè Ullrich for his guidance, assistance, and advice regarding the selection and operation of research methods and ideas.

I want to express my gratitude to Martin Kluge, for his assistance with the analytical instrumentation as well as to Dr. Christiane Liers for fruitful discussions.

I would like to thank my laboratory colleagues Marzena Poraj-Kobielska, Mandy Starke, and Christian Zeisig and the laboratory technicians Sally Ralph, Ulrike Schneider, Monika Brandt and Andreas Elsner for their technical and scientific assistance.

Lastly, I offer my regards and blessings to all of those who supported me in any respect during the completion of the project, especially my family for their encouragement.

I would like to thank the Konrad Adenauer Foundation for the financial support.

## Versicherung an Eides statt

Hiermit versichere ich, dass ich die vorliegende Arbeit ohne unzulässige Hilfe Dritter und ohne Benutzung anderer als der angegebenen Hilfsmittel angefertigt habe; die aus fremden Quellen direkt oder indirekt übernommenen Gedanken sind als solche kenntlich gemacht.

Bei der Auswahl und Auswertung des Materials sowie bei der Herstellung des Manuskripts habe ich keine Unterstützungsleistungen erhalten.

Weitere Personen waren an der Abfassung der vorliegenden Arbeit nicht beteiligt. Die Hilfe eines Promotionsberaters habe ich nicht in Anspruch genommen. Weitere Personen haben von mir keine geldwerten Leistungen für Arbeit erhalten, die nicht als solche kenntlich gemacht worden sind.

Die Arbeit wurde bisher weder im Inland noch im Ausland in gleicher oder ähnlicher Form einer anderen Prüfungsbehörde vorgelegt.

Zittau, den 23. April 2010

Matthias Kinne